Geological and Petrological Studies on the Hiroshima Granite in the Togouchi–Yuu–Takehara District Southwest Japan

by

Takehiro HAYASHI

to be published in Bull. Fac. Sch. Educ. Hiroshima Univ., Part II, vol. 16, 1994

CONTENTS

I INTRODUCTION

Late Cretaceous to Palaeogene igneous rocks as acidic volcano–plutonic association are widely developed in the Inner Zone of Southwest Japan (Fig. 1). They in Chugoku Province have been classified into three E–W trending zones, based on ages of activity and modes of occurrence: Ryoke zone, San–yo zone and San–in zone from south to north (Fig. 2).

Radiometric ages of the granitic rocks in the San–yo zone widely range from 70Ma to 103Ma showing a cluster around 85Ma (Fig. 3) (Geological Survey of Japan, 1982; Higashimoto et al., 1983, 1985, 1986). Such an age variation may show that in the San–yo zone there are many masses with different intrusion ages, but it is also found even within a small mass. There is little difference in radiometric ages between the granitic rocks of the San–yo zone and those of the Ryoke zone but radiometric ages of the granitic rocks of the San–in zone are clearly younger than those of the other zones. According to Ishihara (1977), the granites in the San–yo zone and the Ryoke zone are largely of ilmenite–series, and those in the San–in zone commonly of magnetite–series.

Since Kojima et al. (1959) called medium–grained to coarse–grained granitic rocks developed in the southern halves of Hiroshima Prefecture and Okayama Prefecture the Hiroshima granitic complex, the granitic rocks in the San–yo zone have been called as a whole the Hiroshima Granite. On the other hand, granitic rocks in the Ryoke zone have been called the Ryoke Granite (younger and older), and those in the San–in zone the San–in Granite.

As summarized by Murakami and Imaoka (1986), studies on volcanic and granitic rocks in the San–yo zone have been done, in attempting to clarify their magma types and petrological characteristics based mainly on their mineralogy and petrochemistry and the history of volcano–plutonic activities. The intrusion and emplacement mechanisms of the granitic rocks have so far scarcely been analyzed. The main purpose of this paper is throwing light on the mechanism of emplacement of the Hiroshima Granite and on the space problem of volcano–plutonism in the Inner Zone of Southwest Japan during the late Cretaceous.

Because the way of intrusion of a granite mass and its lithology are closely reflected on the formation history of the mass, it is considered to be essentially important for the present author's purpose to clarify not only geological and structural features but also lithological and mineralogical changes within the mass. Therefore, the author believes that the accumulation of detailed geological data as well as petrological and mineralogical data must give a first step to the success in solution of above-mentioned problems. In order to analyze the problems the author has selected the Togouchi-Yuu-Takehara district as a granite field (here called T-Y-T district) to study. The T-Y-T district is situated around Hiroshima City, extending about 91km from south to north, and about 74km from east to west, in the central Chugoku Province (Fig. 2).

Pre-Cretaceous formations and late Cretaceous to Paleogene igneous rocks of the San-yo zone are widely developed in the T-Y-T district as shown in Fig. 4. In the southern margin of the district occur the Ryoke metamorphic rocks and the Ryoke Granite. The Cretaceous to Paleogene igneous rocks of this district consist mainly of rhyolitic and granitic rocks. The latter show commonly a disconcordant relation to the country rocks such as pre-Cretaceous formations and Cretaceous volcanic rocks (Fig. 5). Yoshino and Hayashi (1979) reported that the boundary surface between a granite and its host rocks in the Ozegawa area situated in the southern part of the T-Y-T district is also disconcordant, showing "step-like structure" characterized by the repetition of a steep wall contact and a nearly horizontal roof contact.

Such a step-like structure has been reported in the other areas in the world, for example, Myers (1975) showed in the Coastal Batholith (Mesozoic to Tertiary) in Peru that granitic bodies are characterized by a steep wall contact and a gentle roof contact. Takahashi, M (1985) also reported that Miocene Okueyama pluton in Kyushu Province has the similar boundary with rhyolitic host rock to that in the Coastal Batholith.

In order to discuss the intrusion mechanism of granite, it is necessary to begin with the clarification of the structural relationship between granite and its country rocks in the T-Y-T district. Next, as for the internal structure of the granitic rocks of the T-Y-T district, some

authors have suggested that the granitic rocks do not occur as a uniform mass, but are consisted of several granitic rock bodies which vary in lithology and activity stages.

Tomonari (1984) subdivided the granitic rocks cropping out in the Middle Belt of Palaeozoic Terrane in Hiroshima Pref. (equivalent to Maizuru Terrane) into four different types of Mannari, Asida, Mikawa and Hirotani, based mainly on lithological difference. Suzuki, T (1986) subdivided the granitic rocks in the northwestern area of the T–Y–T district into Kake granite, Mugitani granodiorite and Togouchi granodiorites, each of which was subdivided further into two or three facies based on lithological characteristics. Yoshino and Hayashi (1989) clarified that the Togouchi granodiorites (Suzuki, T., 1986) is composed of six different facies which are diorite porphyry, granodiorite porphyry, granite porphyry, quartz diorite, granodiorite and granite.

As for the relationship among each rock body constituting a granitic mass, the following studies have been done. Hara (1955) showed that granite in the Hata area is composed of fine–grained facies, medium– to coarse–grained facies, and that each of which occurs as a layered body. Yoshida et al. (1985) reported that granite in the Takehara area is consisted of coarse–grained facies, medium–grained facies and fine–grained facies, and that each of which occurs as layered body. In the Tsuta area of the district, Takahashi,Y et al. (1989) showed that granite is constructed by six different types of granitic rocks which are granophyric granite, fine–grained biotite granite, fine– to medium–grained biotite granite, medium– to coarse–grained biotite granite, medium–grained hornblende–biotite granite and quartz diorite, and that each of which occurs as a layered body. Takahashi,Y (1991) also showed that granite in the Hiroshima area situated on the east of the Tsuta area is constructed by three different granitic rocks which are fine–grained biotite granite, medium– to coarse–grained biotite granite and medium–grained hornblende biotite granite, and showed that each of which occurs as a layered body. In an every study mentioned above, it has been clearly shown that a coarse–grained granitic rock body tends to occupy lowermost level of a large mass, and a fine–grained one the uppermost level. Furthermore, it is notable that the hornblende biotite granite formed in earlier

stage occupies relatively upper level of a large mass.

In the problem of intrusion mechanism of granite, it is more necessary to understand tectonic significance of such layered structure of a granitic mass as mentioned above, which can be attributed to results of either fractionation of a single magma within a pluton or accumulation of several plutons individually intruded. Therefore, it is the most important theme to clarify features of the layered structure of the granitic mass (Hiroshima Granite) in the T–Y–T district.

In the northwestern area of the T–Y–T district, many faults are developed in NE–SW trend (Yamada et al., 1986) (Fig. 1). Such NE–SW trending faults distinctively appear in pre–Cretaceous formations and Cretaceous volcanic rocks, but they are obscure in the granitic rocks in some places. It is noticeable that the dominant boundaries between the granitic rocks and their country rocks which are regarded as intrusion contact, are sometimes in NE–SW trend and placed in the extension of such NE–SW trending faults, e.g. near Kabe, in the west of Saeki. It has been suggested by some authors that fault or faulting played an important role in the intrusion processes of granitic rocks as, for example, the Coastal Batholith in Peru (Pitcher and Bussell, 1977), the Main Donegal Granite in Ireland (Hutton 1982), the Central Extremadura batholith in Spain (Castro, 1985) and the biotite granite at Strontian in Scotland (Hutton, 1988).

Therefore, in the district it becomes also to be a more important theme to clarify relation not only between geological structure and shape of a granitic mass, but also between the shape and internal structure of the mass.

For the purpose mentioned above, the author selected the Togouchi area situated in the northwestern margin of the T–Y–T district to study further in detail, in which a northern limit of the granitic mass exists, and the granitic rocks are in contact with either pre–Cretaceous formations or Cretaceous volcanic rocks.

In the area, geological structure, lithological feature and mineralogy, internal structure and shape of the granite mass have been investigated. The area is considered to be situated near the boundary between the San–yo zone and the San–in zone (Ishihara, 1977). Suzuki,M. (1987) stated that the Togouchi granodiorites belongs to magnetite–series granite. Therefore,

these studies in the area are also helpful for understanding the zonal arrangement of granitic rocks in Chugoku Province.

With reference to the study of the area, the granitic rocks in the other six areas in the T–Y–T district than the Togouchi area have been investigated and reviewed (Fig. 2). As a result, the megascopical shape and internal structure of the granitic rocks and structural relationship between the granitic rocks and country rocks throughout the T–Y–T district will be clarified (Figs. 4 and 5). Additionally, the fabrics of fluid inclusion planes in quartz grains will be also analyzed to clarify the deformation history of the granitic rocks during cooling.

Based on the results from the studies mentioned above, the problem on the emplacement mechanism of the granitic rocks will be discussed.

ACKNOWLEDGEMENT

The author wishes to express his sincerest gratitude to Prof. Ikuo Hara of Hiroshima University for valuable instruction, constant encouragement and critical reading of the manuscript. He is much indebted to Assoc. Prof. Morihisa Suzuki of the same university for valuable advice in both field and laboratory, and constant support and encouragement. He is also indebted to Prof. Yuji Okimura, Prof. Setsuo Takeno, Prof. Satoru Honda and Prof. Yuji Sano of the same university for their guidance and critical advice. He is much obliged to *ex*–Prof. Hisashi Kusumi, Emeritus Prof. Gensei Yoshino, *ex*–Prof. Norihisa Yoshimura and Prof. Yoji Teraoka of the same university for their guidance and constant encouragement. He is also obliged to Assoc. Prof. Makoto Watanabe, Assoc. Prof. Ryuji Kitagawa, Assit. Prof. Takami Miyamoto, Dr. Yasutaka Hayasaka, Dr. Kenichi Hoshino and Dr. Takao Yano of the same university for their kind advice on laboratory technics and constant encouragement. His thanks is also due to Assoc. Prof. Tohru Sakiyama of Himeji Institute of Technology, Dr. Ryozo Tominaga of Misuzugaoka Senior High School and Dr. Yukiko Ohtomo of Universitat Autonoma de Barcelona for their advice and discussions. He is grateful to Mr. Asao Minami for chemical

analysis and to Mr. Akito Magai for preparing thin sections. His thanks are also extended to the graduates of Earth Science Lab., Faculty of School Education, Hiroshima University, who assisted the author both in field research and laboratory analysis.

II OUTLINE OF GEOLOGICAL FRAMEWORK

The pre-Cretaceous rocks as country rocks for Cretaceous igneous rocks in the T-Y-T districts have been classified into five units with reference to age and lithology (Fig. 6). Akiyoshi Terrane rocks as a Permian accretionary complex, Maizuru Terrane rocks as a latest Permian accretionary complex, Suo Tarrane rocks as a high P/T rocks of Triassic age and upper unit Mikawa Group and lower unit Kuga Group of the Kuga-Tamba-Mino-Ashio Tarrane rocks as Jurassic accretionary complex (cf. Ichikawa, 1990). These units are respectively developed as flat-lying nappes, which are folded in upright fashion and gentle form with E-W trending axes (Kojima, 1953; Hara et al., 1979; Nishimura, 1990). The upper members of nappes such as Akiyoshi Tarrane nappe and Maizuru Tarrane nappe are distributed in the northwestern and southeastern part of this district, while the lower member such as Mikawa nappe and Kuga nappe in the southern part and central part along the River Ohta (Fig. 4). The southern extension of the Kuga nappe corresponds to the metamorphic rocks of the Ryoke zone (Higashimoto et al., 1983).

Volcanic rocks in San-yo zone which consist of andesite, dacite, rhyolite and their tuffaceous equivalents, are widely distributed in the San-yo zone as shown in Fig. 1. They are divided into four groups formed by a series of Cretaceous to Paleogene igneous activity, Kanmon, Shunan, Hikimi and Abu Groups in the order of younging. Their distribution areas are roughly arranged in to two E-W trending zones as shown in Fig. 1. The one (northern volcanic zone) is placed along the Chugoku Mountains, being in the northern outside of the distribution zone of Cretaceous granitic rocks mentioned above. The other (southern volcanic zone) is placed along northern coast of Seto inland sea on the east of Hiroshima City. The northern volcanic zone contains the Sandan-kyo block and Takada block after Yoshida (1961), and the southern volcanic zone the Akitsu-Sensui block also after him.

Andesitic rocks and rhyolitic rocks with great volume of their tuffaceous equivalents in the T-Y-T district have been called by Yoshida (1961) Kisa Andesite and Takada rhyolites respectively. The Takada rhyolites have an either conformable or unconformable relationships to

their underlying Kisa andesite (Yoshida, 1964). Thereafter the Kisa andesite was correlated with the Shunan Group, while the Takada rhyolites with the Hikimi and Abu Groups (Iizumi et al., 1985).

The Kisa andesite had been considered to developed near the southern margin of rhyolitic rocks of the northern volcanic zone as shown in Geological map of Hiroshima Pref. (1963). But, Hayama et al., (1975) suggested that pyroclastic rocks in Osakisimozima Island situated in the southern volcanic zone is possibly correlative with the Kisa andesite. The Takada rhyolites are mainly developed in the northern volcanic zone, consisting mostly of rhyolite and its tuffaceous equivalents, while these in southern volcanic zone consist mainly of dacite and its tuffaceous equivalents (Higashimoto et al., 1985; Yamada et al., 1986).

Yoshida (1964) pointed out that Takada rhyolites are composed mainly of dacitic and rhyolitic pyroclastic formations, frequently intercalated by their equivalent lavas, but the detailed volcano-stratigraphy has not yet been established.

Kawahara and Bammoto (1983) reported an alternation of tuffaceous sandstone and shale intercalated in rhyolitic rocks of the Sandan-kyo block about 8 kilometers north of Kake, showing that it contains *Cunninghamia* cone of Hetonaian. Kawahara (1978) reported the rhyolitic rocks in Mihara belonging to the Akitu-Sensui block are interstratified with subaqueous deposit. Aki Research Group (1983) clarified that the rhyolitic rocks in east of Kure are divided into six formations characterized by dacitic to rhyolitic tuff and interstratified clastic deposit, and suggested that they, as a whole, form a gentle basin structure whose long axis is in E-W trend. The volcanic activities for the formation of the Takada rhyolites appear to have mainly taken place on land (Yoshida, 1964). Concerning to the forming process of these volcanic rocks, Murakami (1974) suggested, on the basis of mode of occurrence, feature of accumulation, mineralogical characteristics and so on, that rhyolitic rocks of the Hikimi Group containing the Sandan-kyo block were accumulated in an E-W trending fissure with volcanic activities.

Granitic rocks in the Chugoku Province, which range from diorite to granite in composition, are widely distributed along the northern coast of Seto Inland Sea, and being traced to the

northern area of Kyushu Province (Fig. 1). They have been so far assumed to occur as stock and/or batholith with various sizes (Murakami, 1981). However their shapes and internal structures have not yet been clearly presented.

In the T–Y–T district, around Hiroshima City, there exists the largest exposure (Hiroshima granite batholith) of the granitic rocks in the San–yo zone, which have been considered to form a large batholith (Fig. 2). They postdate the pre–Cretaceous rocks and Cretaceous volcanic rocks belonging to the Takada rhyolites and Kisa andesites, showing disconcordant relation with their country rocks (Fig. 5).

Although almost all granitic rocks distributed in the T–Y–T district have been considered to be involved in the Hiroshima granite batholith, they have been divided into some masses with reference to lithofacies and intrusion relation. Suzuki, T (1986) classified granitic rocks in east of Kake into three masses based upon their intrusion relation, Kake granite, Mugitani granodiorite and Togouchi granodiorites, each of which was subdivided further into two or three facies based on lithological characteristics. The Togouchi granodiorites is the earliest one among the granitic masses in the area. He regarded the granodiorites as a member of the Central plutonic rocks group after Kojima et al., (1959), Yoshida (1961) and Tomonari (1984). Yoshino and Hayashi (1989) clarified that the Togouchi granodiorites is composed of six different facies which are diorite porphyry, granodiorite porphyry, granite porphyry, quartz diorite, granodiorite and granite. Hara (1955) clarified that the Hiroshima granite batholith in the Hata area on the northeast of Kabe is divided into three units in lithofacies, fine–grained adamellite facies, granodiorite facies and coarse–grained granite facies with pinkish K–feldspar, and that these units form a nearly flat–lying structure. Yoshida et al. (1985) classified the Hiroshima granite batholith in the Takehara area on the basis of lithofacies into three units, fine–grained aplitic granite, medium–grained granite and coarse–grained granite with pinkish K–feldspar. They also show that these units occur as flat–lying layered masses and the fine–grained aplitic granite is situated in the uppermost structural level.

In the Tsuta and Hiroshima areas placed in the northwestern part of the T–Y–T district,

recently Takahashi, Y. et al., (1989) and classified the Hiroshima granite batholith into six masses which are granophyric granite, fine-grained biotite granite, fine- to medium-grained biotite granite, medium- to coarse-grained biotite granite, medium-grained hornblende-biotite granite and quartz diorite, with reference to lithological feature, showing these masses form a flat-lying layered structure and the fine-grained granite is placed in the uppermost structural level. Subsequently in the Hiroshima area on the east of the Tsuta area, Takahashi,Y. (1991) also classified the Hiroshima granite batholith into three masses of fine-grained biotite granite, medium- to coarse-grained biotite granite and medium-grained hornblende biotite granite, showing that these masses form a flat-lying layered structure and that the fine-grained granite is placed in the uppermost structural level.

III DISTRIBUTION AND STRUCTURE OF THE IGNEOUS ROCKS IN THE TOGOUCHI AREA

A. General Geology

Fig. 7 illustrates the distribution of the pre-Cretaceous rocks, Cretaceous volcanic rocks and granitic rocks in the Togouchi area. The pre-Cretaceous rocks are grouped into two formations. The one is pebbly mudstone with various-scaled olistoliths of sandstone and chert, and the other is mudstone accompanied with green rocks. Both of formations are developed in E-W trend, and their boundary is placed near Hosomidani (Yamada et al., 1986). Recently Kusumi et al. (1989) have pointed out that both formations contain radiolarian fossils of Jurassic age, showing that these belong to the accretionary complexes of the Kuga-Tamba-Mino Terrane.

In the Togouchi area Cretaceous igneous rocks are widely distributed, though small bodies of tonalite appear in its southern part. Granitic rocks consist of granodiorite, porphyritic granite, medium-grained granite and fine-grained granite containing aplite (Hayashi, 1989). The porphyritic granite is a dike. Roughly speaking, Cretaceous volcanic rocks of this area belong to the Sandan-kyo block of Takada rhyolites, being widely developed in its western and northwestern part. They are also developed as a roof pendant for the granitic rocks near Mt. Ichima (Figs. 7 and 8).

B. Distribution of rhyolitic and plutonic rocks

1. Rhyolitic rocks

In the Togouchi area, rhyolitic rocks show an extensive distribution as illustrated in Fig. 7. Yoshida(1964) pointed out that the rhyolitic rocks in the northwestern area of the T-Y-T district consist mainly of rhyolitic pyroclastic rocks, and he called them Sandan-kyo formation. The

Sandan-kyo formation is considered to belong to the Hikimi Group (Iizumi et al., 1985; Yamada et al., 1986), which is one of the main constituent of Cretaceous volcanic rocks in Chugoku Province (Fig. 1). Rhyolitic rocks in the Togouchi area occupy the eastern margin of such a large volcanic mass. In the Geological map of Hiroshima Pref. (1963), it is shown that the rhyolitic rocks in this area are intruded by granite porphyry in the vicinity of Uchinashi, and that the granite porphyry is in fault contact with the Hiroshima Granite. Yoshino and Hayashi (1989) pointed out that the rhyolitic rocks are traced over the River Ota at the north of Seizui to the top of Mt.Ichima, and are in contact with the Jurassic accretionary complex with a NW-SE trending boundary surface which dips steeply to the south. The distribution of the rhyolitic rocks extends around the top of Mt.Ichima (Fig. 7).

On the northwestern slope of Mt.Ichima, the rhyolitic rocks are traced as narrowly elongated body of 200 meters in width from north of Seizui to near the top of Mt. Ichima, and at a height of 1000 meters, they are developed in horizontal fashion. On the bed of the River Ota is developed a boundary between the rhyolitic rocks and the Jurassic accretionary complex, having a chilled margin of 2 to 3 meters wide. At height of 800 meters, on the southeastern slope of Mt.Ichima, their distribution is nearly horizontal. The northeastern end of their distribution is marked near Tabuki, and the eastern end is in the west of Tabuki, where the rhyolitic rocks are in contact with granodiorite at low angles and in fault contact with the Jurassic accretionary complex at high angles. The southwestern end of their distribution is near the head of the Sakaidani gorge, showing that they are in contact with chert of the Jurassic accretionary complex at high angles, and are horizontally distributed at a height of 950 meters (Fig. 8).

On the west of Tabuki, a road-cut exposure shows that the rhyolitic rocks are in contact with chert of the Jurassic accretionary complex at high angles, where they become finer in grain size towards the contact suggesting the existing of chilled margin (Plate 1). Recrystallized biotite is found in muddy-beds in the chert, suggesting a contact metamorphic effect. Generally, the rhyolitic rocks near the contact with the Jurassic accretionary complex, which is at high angles, tend to be finer-grained. On the eastern to southeastern slope of Mt.Ichima, many rhyolitic

dikes, which are of 1 to 2 meters in width, appear in the Jurassic accretionary complex (Plate 2). Rhyolitic rocks in the Togouchi area have so far been considered by Yoshida(1964) and Kawahara(1989) to consist of the accumulation of dacitic and rhyolitic pyroclastic rocks. On the basis of the above described geological evidences, however, it would be said at least that some parts of rhyolitic rocks are intrusive.

2. Plutonic rocks

According to Geological map of Hiroshima Pref. (1963) granitic rocks in the Togouchi area consist of biotite granite and hornblende–biotite granodiorite or quartz diorite. Yamada et al. (1986) said that these are divided into 3 types, First type [hornblende–biotite granodiorite (granophyric)], Second type [hornblende–biotite granodiorite and biotite granodiorite to granite], and Third type [biotite granite or hornblende–biotite granite]. The author, based mainly upon their mode of occurrence, has newly classified them into tonalite and the following 4 types of granitic rocks. The granitic rocks are granodiorite, porphyritic granite, medium–grained granite and fine–grained granite or aplite. Tonalite corresponds to the First type by Yamada et al. (1986), a part of the granodiorite to the Second type, and the remaining part of the granodiorite, porphyritic granite, the medium–grained biotite granite and fine–grained to the Third type.

a. Tonalite

Tonalite occurs an elongated body with NE–SW trend in the north of Yoshiwa. It is also found as small bodies which appears to be orientated on a line along the northeastern extension of this body (Fig. 7). They intrude into the Jurassic accretionary complex with high angle boundaries. On the River Ota, is found porphyritic granite intruding into the tonalite with high angle boundaries (Fig. 8).

b. Granodiorite

Granodiorite occurs as an elongated body in NE–SW trend from near Mt.Ichima to near Kajinoki (Fig. 7). Suzuki,T (1986) called this rock "Togouchi granodiorites", and classified it into granodioritic rock facies and granophyric rock facies. The author has clarified that the granodiorite consists of three lithofacies which are intergradationally changed into each other. The first is fine–grained porphyritic, the second medium–grained porphyritic, the third coarse–grained equigranular.

Except for its southeastern part, the granodiorite intrudes into the rhyolitic rocks. In the sub–area from Uchinashi to Shiwagi, it is in contact with rhyolitic rocks with two different fashions. The one is gently dipping contact surface and the other is steeply dipping contact surface. In the sub–area from Shiwagi to Kajinoki, the granodiorite horizontally overlies the rhyolitic rocks. Detailed description of the contact feature will be presented in the section IIIC.

In its southeastern part, the granodiorite is in contact with medium–grained granite and fine–grained granite with low angle contact surfaces. The exact boundary between the granodiorite and the medium–grained granite is not clearly exposed. The granodiorite near the medium–grained granite is characterized by the occurrence of K–feldspar rich veins, which are inferred to have been derived from the latter, suggesting that the latter intrudes into the granodiorite.

The granodiorite has a vertical lithological change. As mentioned before, it consist of three different lithofacies such as fine–grained, medium–grained and coarse–grained granodiorites. These three types granodiorites have also different types dark inclusions in descending order of structural order (Fig. 7), though, strictly speaking, one lithofacies is not distinctly to develop only in one structural level. Below about 400 meters, in the northwestern slope of Mt. Ichima, is developed the coarse–grained granodiorite, and in a level from about 400 meters to about 850 meters occurs the medium–grained granodiorite, which shows a decrease of grain size as the altitude becomes higher. In the level from about 850 meters to about 1000 meters is found the fine–grained granodiorite. It is occasionally in contact with the rhyolitic rocks. But the fine–grained granite or aplite frequently occurs as thin layered body between the fine–grained granodiorite and the rhyolitic rocks (Fig 9).

Under a level below about 400 meters in Nasu–Shiwagi sub–area, is developed the coarse–grained granodiorite. In a level from about 400 meters to about 600 meters occurs the medium–grained granodiorite. Like the case of Mt.Ichima sub–area its grain size decreases as the altitude becomes higher. In a level from about 600 meters to about 670 – 680 meters is developed fine–grained granodiorite as a layer of 20 to 30 meters thick. However, in outcrops cannot always be observed ascertained boundaries between the different lithofacies zones.

In the medium–grained granite appears also occasionally a lithological change such as that of the granodiorite. Near roof contact around Mt.Nabe porphyritic texture is distinctly developed.

c. Medium–grained granite

Medium–grained granite is one of the typical constituents of the Hiroshima Granite. It is distributed mainly from Kajinoki to Togouchi–Hongo, in the northern part of the Togouchi area (Fig.7). In the area from Hagiwara to Sakahara, medium–grained granite is found as small bodies aligned in NE–SW trending intruding into the Jurassic accretionary complex. On the river bed of the River Shiwagi, a small exposure of medium–grained granite is found in fine–grained granite.

The distribution of the medium–grained granite extends with a distance of about 10 kilometers and NE–SW trend from the studied area to Kake Town (Fig. 4). Namely, it can be regarded as an elongated body aligned in NE–SW trend. As mentioned before, It is intruded into the granodiorite, and around Mt.Nabe, into the Jurassic accretionary complex with a nearly horizontal contact at a height of 800 meters, in which a thin layer of fine–grained granite is found on the top of the granite. While, the southern end of the granite in Hagiwara shows a contact to the complex whose plane is steeply dipping to the west (Fig. 8).

d. Porphyritic granite

Porphyritic granite is distributed from Dani to Sakaidani as a narrow body elongated in NE–SW trend. It is intruded into the Jurassic accretionary complex, rhyolitic rocks and tonalite.

The contact plane between the tonalite and the Jurassic accretionary complex is generally at high angles. It is running in two different trends, NE–SW trend and NNW–SSE trend. But, in the head of Sakaidani, the contact plane between this rock and the rhyolitic rocks is changed in orientation to be nearly horizontal. (Figs. 7 and 8)

In porphyritic granite near Dani are found small bodies of rhyolitic rocks sporadically aligned in NE–SW trend. Their mode of occurrence suggests that they are xenolith. Judging from such shape characteristics and its relations to the host rocks, the porphyritic granite seems to be a large–scale dike.

e. Fine–grained granite and aplite

Fine–grained granite is exposed in small bodies scattered along the boundary between the granodiorite and the medium–grained granite (Fig. 7). In Tsubutani, it occurs as a comparatively large body elongated in NE–SW trend. As mentioned before, near the top of Mt.Ichima and the Nasu–Shiwagi sub–area, it occurs as a thin body intercalated between the rhyolitic rocks and the granodiorite. Near the top of Mt.Nabe, the fine–grained granite occurs as a thin body intercalated between the medium–grained granite and the Jurassic accretionary complex. In the south of Shiwagi, fine–grained granite and aplite are found on the river bed of the River Shiwagi (Plate 3). In the granodiorite occurring above the river bed are also found many horizontal dikes of fine–grained granite which are 10cm to 1.5m in thickness (Plate. 4). These fine–grained granites are comparable with the thin bodies developed along the boundaries between the medium–grained granite and the granodiorite, and between the granodiorite and the rhyolitic rocks mentioned above. The fine–grained granite and aplite are considered to be intruded into both of the granodiorite and medium–grained granite (Fig. 8).

f. Granite porphyry

Granite porphyry occurs as a small body in the north of Seizui. It is intruded into both of the Jurassic accretionary complex and the rhyolitic rocks (Fig. 7).

Summing up the above description, the granitic rocks in the studied area are regarded to have been formed as a series of plutonism of five rock types, tonalite, granodiorite, porphyritic granite, medium-grained granite and fine-grained granite in the order of younging.

C. Geological structure

In the Togouchi area, it has been revealed that granodiorite occurs as a layered body with near flat-lying lithological variation, being intruded by underlying the medium-grained granite. The contact plane between the former and the latter is also near horizontal, suggesting that the medium-grained granite as the most dominant constituent of the Hiroshima Granite underlies with great extent throughout the area (Fig. 8).

Detailed geological mapping reveals that mesoscopic contact relationship between the granodiorite and the rhyolitic rocks is characterized by the repetition of roof contact (flat-lying contact) and wall contact (steeply dipping contact). In this paper, such a contact structure is called the "step structure". Though analogous step structure is also for the medium-grained granite and porphyritic granite, it appears most distinctly for granodiorite.

In the Uchinashi-Kajinoki sub-area, the step structure is well developed. From Uchinashi to Nasu, the granodiorite is in a wall contact with the rhyolitic rocks. The wall is in NE-SW trend. From the south of Uchinashi to the top of Mt.Ichima, the trend of the wall contact changes from NE-SW to NNW-SSE. From Nasu to Shiwagi, the granodiorite shows a roof contact with the rhyolitic rocks at a height of 650 to 700 meters. Strictly speaking, the contact plane is not horizontal but dips very gently toward NE. In the northwestern end of the roof contact, it changes into the wall contact, whose plane is developed in NE-SW trend. This wall contact is regarded to be continued to that found at Shiwagi. Near the top of Mt.Ichima there is a roof contact, which continues to the wall contact extending from near Tabuki (Figs. 7 and 8). Therefore, It can be said that the boundary structure of the granodiorite in the studied area is characterized

by the large-scale step structure going down to the northwest as the repetition of pairs of roof contact and wall contact.

Although most of contact planes between the granodiorite and the rhyolitic rocks are irregular in outcrops even for the wall contact, these appear to be commonly sharp zig-zag boundary. Therefore, the contact planes appear to be controlled by planes of fracturing of wall rocks.

Though the porphyritic granite is dominantly in steep wall contact with the Jurassic accretionary complex, which is in NE-SW trend and NW-SE trend, the top of its body at Sakaidani is in a nearly horizontal roof contact with the rhyolitic rocks. The medium-grained granite also shows the steep wall contact and nearly horizontal roof contact with country rocks, suggesting that its emplacement mechanism is essentially the same as that of the granodiorite.

In the sub-area from Shiwagi to Kajinoki, the granodiorite overlies on the rhyolitic rocks (Plate. 5). The grain size of the granodiorite becomes not only finer toward the contact with the rhyolitic rocks, but also toward the upper part of the body (Fig. 8, d-d'profile). The exposure at Kajinoki contains a distinct contact surface between the fine-grained granodiorite and rhyolitic rocks. Judging from these facts, it can be regarded that the granodiorite occurs as a horizontal tabular body intruding the rhyolitic rocks. Because this sub-area is situated in the northern margin of the granodiorite, and also in the northern margin of the Hiroshima Granite, it can be said that the above described modes of occurrence of the granodiorite and others is the clearest evidence available to understand the marginal shape of the Hiroshima Granite, and to clarify the essential features of the intrusion mechanism of the Hiroshima Granite.

IV PETROGRAPHY OF IGNEOUS ROCKS IN THE TOGOUCHI AREA

Petrographical features of main igneous rocks in the Togouchi area are described and discussed in this chapter.

A. Rhyolitic rocks

The rhyolitic rocks in the Togouchi area are almost massive and homogeneous, showing only weak sign for flow and bedded structures. There matrices are gray or dark gray in color. Phenocryst is mainly composed of euhedral or subhedral quartz, plagioclase, K-feldspar, biotite and/or green hornblende whose grain sizes are from 0.5 millimeters to several millimeters. Allanite, zircon and apatite occur in accessory amounts. Rock fragments can rarely be found.

The rocks close to granodiorite show thermal metamorphic feature as follows. Fine-grained recrystallized biotite frequently occurs not only in a matrix but also replacing phenocryst of biotite and hornblende. Phenocrystic hornblende is completely or partially replaced by aggregate of fine-grained biotite and actinolite. Recrystallized quartz and feldspars whose grain size is about 0.02 millimeters are found in phenocrysts of feldspars. In such thermally metamorphosed rocks the matrix is changed to holocrystalline texture in which quartzo-feldspathic minerals of about 0.02 millimeters partly appear showing a granoblastic texture. In some cases, matrix-forming minerals become coarse-grained up to 0.1 millimeters in diameter. Moreover andalusite is sometimes crystallized. It has been found in specimens obtained from near the top of Mt.Ichima and a river bed of the River Ota near the west of Uchinashi. On the western slope of Mt.Ichima, garnet has also been found as one of thermally metamorphic minerals (Suzuki,M., Hayashi and Yoshimura, 1992).

Many rhyolitic dikes are observed in the Jurassic accretionary complex on the eastern slope of Mt.Ichima, and their phenocrysts and matrix-forming minerals are rather fine-grained in size.

B. Plutonic rocks

1. Tonalite

The size of the constituent minerals of the tonalite body is rather small, and its lithofacies varies in wide range. The rock is massive and dark greenish gray in color, and shows more or less porphyritic texture. Foliation and linear structure cannot be observed in outcrops (Plate 6). In the marginal zone of the body, close to the Jurassic accretionary complex, there is finer-grained facies whose grain size are finer than 0.5 millimeters. In the central part of the body, there is medium-grained facies whose grain size is from 1 millimeters to 3 millimeters in diameter and additionally, gabbroic pegmatite pools, whose grain sizes reach to 3 centimeters in length, are sometimes found. Average content ratio of colored minerals is about 35 percent throughout the body (Fig. 10). The tonalite is mainly composed of plagioclase, green hornblende, biotite, clino-pyroxene and orthopyroxene, regardless of lithofacies. Quartz rarely occurs in small amount, and apatite, zircon and Fe-Ti oxide occur in accessory amounts.

Orthopyroxene and clinopyroxene are frequently enclosed in hornblende, and are partially converted into uralite. Hornblende is replaced by the aggregate consisted chiefly of actinolite, chlorite and epidote. Furthermore, biotite is partially replaced further by chlorite. Plagioclase occurs in two different forms. One occurs as subhedral or anhedral crystal with polysynthetic twin. It has rather weak zonal structure. Another is comparatively large crystal which occurs in the form of euhedral or subhedral phenocryst showing distinct zonal structure. Its grain size ranges from 2 millimeters to 3 millimeters. Quartz appears as a interstitial crystal (Plate 7). The conversion phenomena found mainly in hornblende and pyroxenes are regarded to be caused by the intrusion of the porphyritic granite mentioned later.

Kojima(1964) pointed out that mafic plutonic rocks accompanied with the Hiroshima Granite are closely related with the felsic activity. According to his opinion, the present body is regarded as such the case. The tonalite may be cognate with dark inclusion in the granodiorite as will be shown later.

2. Granodiorite and its associated dark inclusion

a. Granodiorite

Yoshino and Hayashi (1989) classified the granodiorite into six types based upon the petrographical characteristics. It seems for the author to be more available to classify the rock into three lithofacies types as follows.

The granodiorite is generally massive and glomeroporphyritic. Its mafic minerals are commonly found as mineral clusters whose grain sizes are from about 3 millimeters to 6 millimeters. The granodiorite contains a lot of dark inclusions, but any other rock fragment except for dark inclusions is not found.

Constituent minerals are mainly plagioclase, quartz, K-feldspar, hornblende and biotite. Allanite, zircon, apatite, sphene and Fe-Ti oxide occur in accessory amounts. Secondary minerals are actinolite, chlorite, epidote and some biotite. Modal Q+Kf - MM - Pl and modal Q - Kf - Pl are shown in Fig. 11 and Fig. 12 respectively. Modal analysis has been done by a common method using thin sections as well as by the image processing method using rock slabs, which has been proposed by Hayashi and Suzuki (1990). Color index are commonly about 10, but in some specimens the index reaches to about 20. Many specimens are dotted in "granodiorite" and "quartz-adamellite" region, and some other specimens in "granite" and "monzonite" regions.

Plagioclase occurs in two forms. One occurs all over the rock as subhedral or anhedral crystal with polysynthetic twin. It has rather weak zonal structure. Another is fairly large crystal which occurs in the form of euhedral or subhedral phenocryst, whose grain size ranges from 1 millimeters to 5 millimeters. It has distinct zonal structure in which the composition varies from andesine in the core to oligoclase in the rim. Their detailed chemical data will be presented in the Chapter V.

Myrmekite is commonly found in quite small amount. In general, K-feldspar is almost anhedral perthite, and it appears often as an intergrowth with quartz forming micrographic texture. Small anhedral K-feldspar grains are also sometimes found along cleavage of large plagioclase grains. Quartz generally occurs as anhedral crystal. But coarse-grained anhedral quartz

occurs often forming intergrowth with K-feldspar. Hornblende is almost green in color. In some specimens, the rim is replaced by biotite. Cummingtonite is rarely found replacing orthopyroxene.

As mentioned in Chapter III, the granodiorite shows remarkable lithological variation. Generally speaking, the lithofacies varies from fairly coarser-grained equigranular to finer-grained porphyritic texture. Therefore six rock types classified by Yoshino and Hayashi (1989) are grouped into the following three lithofacies types, based mainly upon the grain size and texture as well as the mineral composition. These types of lithofacies are developed in the granodiorite body, forming "stratigraphical" horizons each of which is namely flat-lying, and so named the lower, middle and upper lithofacies respectively. The lithofacies changes from the coarse-grained equigranular one in the lower horizon, through medium-grained porphyritic one in the middle horizon, to the fine-grained porphyritic one in the upper horizon. It is noticeable that these three lithofacies occupy the different levels in the body. Mineral compositions of the lower, middle and upper lithofacies are similar to each other.

The lower lithofacies:

Texture of the lower lithofacies of the granodiorite is closely similar to the general type granite, though it is more or less porphyritic (Plate 8) and coarse-grained micrographic texture is frequently developed in this type (Plate 9). Average grain size is 2 to 4 millimeters. As mentioned above, it is notable that small anhedral K-feldspar is sometimes scattered as a pockmark crystal along cleavages in large plagioclase grains (Plate 10). Occasionally it is developed cutting across the grain boundary of plagioclase. It seems likely that such the K-feldspar was produced by permeation of potassium along the cleavage of plagioclase which was opened by deformation. Near the bottom part of the lower lithofacies which is placed closely to the medium-grained granite, the granodiorite is intruded by a lot of flaky veins of pink K-feldspar. These veins are ascribed to micro-fracturing of the lower lithofacies.

The middle lithofacies:

The middle lithofacies rocks are characterized by the porphyritic texture (Plate 11). Grain size of phenocryst minerals is 1 to 5 millimeters in diameter, and of matrix-forming minerals is 0.02 millimeters to 0.2 millimeters. The former appears to show occasionally rounded shape. The matrix ranges from 40% to 60% in volume. Fine-grained micrographic texture is frequently found in matrix (Plate 12). The middle lithofacies is the main constituent in the granodiorite body.

The upper lithofacies:

The upper lithofacies rocks have a distinct porphyritic texture (Plate 13). Phenocrysts of 2 to 4 millimeters are found in their matrix consisting of mineral grains of 0.05 to 2 millimeters. These phenocrysts occur generally in rounded shape. The grain size of matrix-forming minerals is finer than that in the middle lithofacies. Fine-grained micrographic texture frequently appears in the matrix. A few amount of K-feldspar is rarely found in interstitial fashion, as seen in the rock of chilled margin (Plate 14). In this lithofacies, such rocks as diorite porphyry are also sometimes found especially close to the dark inclusion.

b. Dark inclusion

Dark inclusion is commonly accompanied with the granodiorite, and sometimes with the porphyritic granite and medium-grained granite. It is commonly irregular in shape, varying in size (length of long axis) from few millimeters to several meters. Small-sized fragments of dark inclusion are often scattered around large ones. Dark inclusion tends to occur with concentration in flat-lying zones in the central and marginal parts of the granodiorite body. For instance, it is found as a wide zone in the level of higher than 600 meters on the northwestern slope of Mt.Ichima, and as a narrow zone lying horizontally at a height of 550 meters in near Shiwagi. In the body near Togouchi, however, dark inclusion is scarcely found.

Constituent minerals of dark inclusions are mainly plagioclase, green hornblende and bio-

tite. Sphene, apatite, allanite, zircon and Fe–Ti oxide are in an accessory amounts. Quartz and K–feldspar are occasionally accompanied. Actinolite, chlorite and biotite are found as secondary minerals. Both plagioclase and hornblende are classified into two populations with reference to grain size: One is fine–grained ranging from 0.2 to 0.5 millimeters in length, and the other is coarse–grained with about 1 millimeters in length. Generally, plagioclase of both types appears as tabular crystal, showing zonal structure of which cores consist of andesine, and rims of oligoclase. In the dark inclusion, occasionally appears plagioclase ranging from 1 millimeters to 4 millimeters in a length. Such the plagioclase has also distinct zonal structure, and is very similar to that of the host granodiorite in grain size and compositional range. Biotite with length larger than 3 centimeters is sometimes found in needle–like shape.

The lithofacies of dark inclusion appears to change in response to surrounding to the three lithofacies of the granodiorite body. Namely, it is roughly classified into three types of lithofacies, lower type, middle type and upper type. The upper lithofacies, the middle lithofacies and the lower lithofacies of granodiorite shows a tendency to be accompanied with the upper type, the middle type and the lower type of dark inclusion. These three types of dark inclusion are described in detail in the following section. Roughly speaking, from the lower to upper types via the middle type, the rock changes from angular to rounded in shape, and from coarser–grained heterogeneous to finer–grained homogeneous in texture.

Lower type:

The boundary between the dark inclusion and the host granodiorite is not distinct but rather intergradational. Rocks, which seem to be comparable with granodiorite but are highly richer in mafic minerals than it, are found with obscure outlines (Plate 15). Such rocks are also referred to the one type of dark inclusion.

The lower type is constituted by two components, which are distinguished from each other with reference to grain size: One consists of minerals of finer than 0.5 millimeters, and another of coarse–grained minerals which range from 0.5 millimeters to 1 millimeters. The latter compo–

nent frequently sporadically occurs in the former. Phenocryst-like plagioclase often appears. Quartz and K-feldspars are often found in interstitial fashion forming intergrowth with each other (Plate 16). Dioritic to granodioritic veins and pools frequently appear with various scales in this type of dark inclusion. The constituent minerals of such the rocks are comparable in size with these of the host granodiorite. Pools are often linked with each other by veins. The formation of the veins and pools is ascribed to fracturing of dark inclusion.

Middle type:

The middle type is the dominant one of dark inclusion and occurs in the middle lithofacies of granodiorite body. It is compact and massive with a few patches consisted of coarse-grained minerals. The type dark inclusion is more melanoclatic than the lower type one. It tends to be rounded in shape. The boundaries between the middle type rocks and the host granodiorite are distinct, as observed along them, the mineral grains of the latter are incorporated with former (Plate 17). As seen in the lower type, the pools and veins cutting across dark inclusion are developed, but their petrographical characteristics seem to be more dioritic than that of the lower type dark inclusion. Furthermore these pools and veins tend to be smaller in size than those in the lower type and also the constituent minerals of the former finer than in size than those of the latter (Plate 18).

In the middle type there are occasionally leucocratic spheres whose size ranges from 5 millimeters to 3 centimeter in diameter (Plate 19). They are composed mainly of quartz, K-feldspar and hornblende (Plate 20), accompanied with plagioclase, biotite, epidote and sphene in accessory amounts. Their grain size ranges from 1 millimeter to 4 millimeters in length. Constituent minerals in the spheres do not enclave any mineral from host dark inclusion.

Upper type:

The upper type dark inclusion in square-like or angular shapes (Plate 21). The boundaries between the dark inclusion and the host granodiorite are fairly distinct and sharp. Occasionally,

quartzo-feldspathic veins are intruded into the dark inclusion. The upper type dark inclusion is finer and more melanoclatic than the middle type (Plate 22). It is compact and homogeneous. It is unique in containing clinopyroxene as main constituents. Clinopyroxene rims are replaced by green hornblende. Such dark inclusion can be sometimes found on the northwestern slope of Mt.Ichima.

It can be said that the dark inclusion is originally fine-grained dioritic rock. In order to compare the above-described types of dark inclusion with the host granodiorite, Q - Kf - Pl modal composition diagram for them is shown in Fig. 12. Color index ranges from 10 to 35. Almost all specimens are plotted around the quadripartitive intersection point among the "tonalite", "granodiorite", "quartz-monzonite" and "quartz-diorite" regions.

Modal volumes of quartz and K-feldspar in dark inclusion vary, though they are generally poor, showing their regular decreasing from the lower to the upper type. The inclusions seem to preserve more their original feature and shape. As a result, it is supposed that granitic materials are supplied to the dark inclusion from the granodiorite. The amount of materials seems to decrease from the lower to upper types via the middle type.

The lithological change of dark inclusion is characterized by the formation of phenocryst-like plagioclase in the lower type, the disappearance of clinopyroxene in the lower-middle type and the decreasing of modal volume of quartz and K-feldspar from the lower type to upper type accompanying coarsening of constituent minerals. It would be regarded as the granitization process of dark inclusion the result of contamination with the host granodiorite body. The degree of contamination increased toward the lower level of the host body. As mentioned before, because the granodiorite is affected by the underlying medium-grained granite, the contamination effects for the dark inclusion may be partly ascribed to the medium-grained granite. The shapes of dark inclusion and associated quartzo-feldspathic veins and pools indicate that the granitization process occurred together with fracturing of dark inclusion rocks. Such a phenomenon suggest that the emplacement of the granodiorite has occurred accompanied with fracturing of its host rocks.

3. Porphyritic granite

The granite body in Dani area has generally been described as a member of the Hiroshima Granite in the Geological map of Hiroshima Pref.(1963). Detailed field and petrographical studies by the author reveal that this body is composed mainly of porphyritic granite, being associated by small amount of medium-grained granite, granodiorite and rhyolitic rocks.

Porphyritic granite is mainly composed of quartz, plagioclase, K-feldspar, biotite and hornblende. Allanite, zircon and Fe-Ti oxide occur in accessory amount. As phenocrystic minerals, quartz and plagioclase are predominant.

Plagioclase of phenocryst is euhedral or subhedral and has zonal structure. K-feldspar is almost anhedral and has perthite structure, rarely showing microcline grill. K-feldspar sometimes occurs in intergrowth with quartz. Quartz shows two modes of occurrence: One is subhedral grain as phenocryst, and another is anhedral grain in matrix, sometimes showing interstitial texture.

Porphyritic granite shows lithofacies variation based on the degree of development of porphyritic texture. It is classified broadly into the following two types: In the one (P-type) distinct porphyritic texture is observed by naked eyes (Plate 23), and in the other (E-type) it is observed only under microscope, though it seems equigranular by naked eyes (Plate 24). In porphyritic granite body is prevailed the E-type. Both types occasionally occur together in an outcrop. In the P-type, grain size of matrix forming minerals less than 0.01 millimeters, and that of phenocryst is from 0.5 millimeters to 4 millimeters. The P-type granite is found in some place of the upper part of Sakaidani gorge and in contact with the rhyolitic rocks. The boundary between them is difficult to determine exactly its position in outcrops as the matrix of the granite is as fine as the rhyolitic rocks.

In the E-type grain size of matrix-forming minerals is from 0.1 to 2 millimeters, and that of phenocryst is from 1 to 4 millimeters. Modal Q+Kf - MM - Pl and modal Q - Kf - Pl components are shown in Fig. 13 and Fig. 14 respectively. Almost all specimens are plotted in the "granodiorite" region.

Medium-grained granite are mainly found as small blocks-like bodies in the core part of the porphyritic granite body. The boundaries between the medium-grained granite and the host porphyritic granite are not always observed clearly and may be intergradational. It is not clear whether the medium-grained granite predated or postdated the porphyritic granite. Granodiorite is also found as small block-like bodies enclosed by the porphyritic granite, especially in its marginal part.

The porphyritic granite locally contains a small amount of dark inclusion, for instance, at the river bed of the River Ota in Dani. The mode of occurrence of dark inclusion is similar to that in the granodiorite mentioned above. The porphyritic granite contains no rock fragment except for the dark inclusion. The above-described occurrences and lithological features of the porphyritic granite may be ascribed to rapid cooling of magma.

4. Medium-grained granite

The medium-grained granite is characterized by bearing pink K-feldspar. This type has been considered to belong to main constituent of the "Hiroshima Granite batholith". Component minerals are mainly quartz, plagioclase, K-feldspar and biotite. Modal Q+Kf - MM - Pl and modal Q - Kf - Pl components are shown in Figs. 13 and 14 respectively. All examined specimens are plotted in the "adamellite" region. Hornblende occurs in accessory amount. Most of these minerals are generally anhedral.

The Medium-grained granite is almost massive and poor in lithological change. But, in the zone of roof contact in Mt.Ichima area, its lithofacies changes from medium-grained equigranular type to fine-grained type with phenocrysts. It contains dark inclusion in a small amount. The dark inclusion is scarcely granitized.

In the north of Tsubutani there is medium-grained granitic rock rich in mafic minerals. The rock can be regarded as a member of the granodiorite mentioned above. But it has not porphyritic texture, and is rich in pink K-feldspar.

5. Fine-grained granite and aplite

The fine-grained granite has equigranular texture. Its average grain size is from 0.02 to 2 millimeters and its mineral component is almost similar to that of the medium-grained granite mentioned above. Occasionally, it contains large quartzo-feldspathic phenocrysts whose size ranges from 2 millimeters to 5 millimeters. This type rock frequently changes to aplite which is rich in pink K-feldspar and contains little amount of mafic minerals. The aplite is often associated with pegmatite pools.

V MINERALOGY OF IGNEOUS ROCKS IN THE TOGOUCHI AREA

A. Chemical characteristics of main constituent minerals

Granitic rocks and rhyolitic rocks in the studied area are composed of minerals such as quartz, K-feldspar, plagioclase, biotite and Fe-Ti oxides with or without amphiboles and pyroxenes (orthopyroxene and clinopyroxene) . In this chapter, the chemical characteristics of these mineral will be described, in order to clarify genetical relationship among the granitic rocks as well as to discuss crystallization conditions of some of them.

Their chemical analysis has been performed by means of JEOL electron microprobe analyzer (JCMA-II) in the department of Earth and Planetary System Science, Faculty of Science, Hiroshima University. The specimen numbers and analyzed mineral are listed in Table 1. In this chapter, the medium-grained granite is called "granite".

1. Pyroxenes

Pyroxenes are present in the tonalite and dark inclusion in the granodiorite. The tonalite contains both orthopyroxene and clinopyroxene. Commonly, they are partially or almost perfectly altered into the aggregate of actinolite or mica minerals. Othopyroxene is sometimes altered into cummintonite. In dark inclusion there is only clinopyroxene in very minor amount.

a. Orthopyroxene

The chemical compositions of orthopyroxene are listed in Table 2 and plotted in En-Fs-Wo diagram (Fig. 15). They contain about 4% of Wo content and En content ranging from 55% to 74%. All of them are regarded as hypersthene. Al_2O_3 content ranges from 0.6 to 2.4 Wt%. Generally speaking, orthopyroxenes show a chemical zoning in which En and Al_2O_3 contents decrease from the core to the rim.

b. Clinopyroxene

The chemical compositions of clinopyroxenes are listed in Table 3 and plotted also in En–Fs–Wo diagram (Fig. 15). They contain Fs content ranging from 55% to 74% and Wo content ranging from 32% to 45%. They are commonly augite and sometimes ferro–augite. Their chemical characteristics show no systematic change: e.g., in one grain, En content tends to increase from the core to the rim, but in the other grain, En content changes in reciprocal manner.

2. Amphiboles

Amphiboles analyzed here can be grouped into such two types as calcium–poor amphiboles (iron–magnesium–manganese amphiboles) and calcic amphiboles after the criteria by Leake (1978). The former type has rarely been found only in the granodiorite and its dark inclusion, but the latter type has been commonly found in all rock types except for aplite. Amphiboles of these two types are often partially replaced by actinolite.

a. Calcium poor amphiboles

The chemical compositions of the calcium–poor amphiboles are listed in Table 4. This type amphiboles are "cummingtonite" after the criteria by Leake (op. cit.), whose Mg^{+2} content ranges from 0.3 to 0.4. They are plotted in Mg–poor part of cummingtonite region. Each cummingtonite grains appear as relic minerals enclosed by actinolite aggregate. They may be regarded as secondary minerals, probably derived from orthopyroxenes.

b. Calcic amphiboles

Analytical results of calcic amphiboles are listed in Table 5. The amphiboles show wide chemical variation in each rock type. The amphiboles in tonalite tend to be richer in Mg than those in the other rock types. As shown in Fig. 16, the proportion of Mg/(Mg+Fe), called "mg value" hereafter, of them ranges from 0.40 to 0.62. In dark inclusion, the amphiboles also tend to

be relatively rich in Mg, and mg values range from 0.35 to 0.54. In the granodiorite, all amphiboles except for only one data are somewhat poor in Mg with mg value ranging from 0.32 to 0.49. The granite and porphyritic granite contain amphiboles with rather lower mg value ranging from 0.27 to 0.31. As seen in Fig. 17, both Ti and Si contents of amphiboles are not appreciably variable in each rock type. However, they show wider range in the granodiorite than in the other rock types, showing that Ti and Si values range from 0.03 to 0.25 and from 6.26 to 7.55 respectively. Amphiboles in every rock types commonly show such a crystallization trend that Ti content increases and Si content decreases with decrease of Mg content. Almost all of analyzed amphibole grains show distinct chemical zoning (Figs. 16 and 17). All grains in the granite and one grain of the tonalite show wide variation in both Ti content and Si content. One amphibole grain in dark inclusion shows also wide variation in Ti content. The growth history for some amphibole grains is opposite from the crystallization trend mentioned above.

As mentioned in the Chapters III and IV, the granodiorite shows three lithofacies with different types of dark inclusion, but the chemical composition of amphiboles is not severely different among the three types lithofacies of the granodiorite and dark inclusion.

All calcic amphiboles analyzed here are plotted in Leake's diagram (Fig. 18). Among them, magnesio-hornblende is most predominant and ferro-hornblende is subdominant throughout the whole rock types. Others are actinolitic hornblende, ferro-actinolitic hornblende, ferro-edenitic hornblende, magnesian hastingsitic hornblende, tschermakitic hornblende and tschermakite.

3. Biotites

Biotites are commonly present in all rock types in the studied area. Their chemical compositions are listed in Table 6. The chemical characteristics of biotite are different among rock types. In the tonalite, biotites are rich in Mg with mg value ranging from 0.40 to 0.49 (Figs. 19 and 20). In dark inclusion, biotites are also fairly rich in Mg with mg value widely ranging from

0.31 to 0.47, the value being involved in the mg value range of the granodiorite and the tonalite. In the granodiorite, biotite is rather poor in Mg, and its mg value is in a narrower range of 0.32 to 0.39. In the granite, biotite is poorer in Mg with mg value ranging from 0.25 to 0.32.

Si content of biotite is not significantly different among all types of granitic rocks (Figs. 19 and 20), but Ti content of biotite seems to be different among them (Fig. 21). The latter is richer ranging from 0.43 to 0.58 than in the tonalite and dark inclusion than in the other rock types. For many biotite flakes of all types of granitic rocks, Ti content increases with increase of mg value, but for some biotite flakes it shows a reciprocal manner. Al^{VI} content in biotite decreases commonly with increase of Ti content (Fig. 22). Except for two biotite flakes of dark inclusion and the granite, Al^{VI} content of biotite tends to decrease with increase of Al^{IV} content (Fig. 23).

The chemical zonation of biotite is generally weak, but some biotite flakes in the porphyritic granite and the rhyolite show distinct chemical zoning in Ti content.

In the granodiorite and associated dark inclusion, biotite flakes from three lithofacies have not appreciably different chemical characteristics from each other (Figs. 19, 21, 22 and 23). Biotite flakes are microscopically grouped into two populations, coarse-grained type and fine-grained type. The latter was produced by recrystallization of the former, but the chemical composition is not different from each other.

4. Iron-titanium oxides

Fe-Ti oxides are present in almost all type of granitic rocks. Their chemical compositions are listed in Table 7 and plotted in $FeO-Fe_2O_3-TiO_2$ diagram (Figs. 24 and 25). They are classified into ilmenite and magnetite. The former is found in all rock types, but the latter has been found only in the granodiorite and its associated dark inclusion. Fe_2O_3 content in ilmenite is commonly less than 5 mol% but it sometimes reaches to 10 mol% in the tonalite. Magnetite commonly has ulvospinel content of less than 6 mol%. In the granodiorite, however, this content continuously varies from 4 mol% to 15 mol%. In the $FeTiO_3-MnTiO_3-Fe_2O_3$ system (Fig. 26),

ilmenite in the tonalite contains $FeTiO_3$ of more than 95%. In ilmenite in the other rock types, $FeTiO_3$ content ranges from 83% to 94%. Ilmenite in the granitic rocks of the studied area commonly contains a little amount of Fe_2O_3. In the granodiorite and its associated dark inclusion there are Fe–Ti oxides rich in Fe_2O_3. Ilmenite in all types of granitic rocks of the studied area is plotted in the compositional range for that in igneous rocks of the San–yo zone which has been clarified by Imaoka (1985).

5. Garnet

Garnet has not yet been found in the Takada rhyolitic rocks. In this study, garnet has been newly found in rhyolitic rocks in the Sakane sub–area of the Togouchi area. On the other hand, garnet is also found in the rhyolitic rocks distributed in the Hinokidani area (Fig 27). The chemical compositions of garnets from the Sakane sub–area are listed in Table 8, and the chemical compositions of garnets from the Sakane sub–area and Hinokidani area are plotted in Figs. 28 and 29. They are almandinous with the range of Xalm from 0.750 to 0.790. The mole fractions of pyrope and grossular are in the range of 0.042–0.053 and 0.059–0.072 respectively. Xspes ranges from 0.095 to 0.145. The core part tends to be more abundant in Mg and Ca, and poorer in Mn than the rims. Garnets from Sakane sub–area are regarded to formed by contact metamorphism of the granodiorite, while those from Hinokidani area are phenocrysts crystallized directly from felsic magma (Suzuki,M., Hayashi and Yoshimura, 1992).

6. Plagioclase

The chemical composition of plagioclase was analyzed on positions such as core, mantle and rim. The chemical data are listed in Table 9.

As mentioned in the Chapter IV, plagioclase in the tonalite, granodiorite, dark inclusion and porphyritic granite can be grouped into two populations with reference to grain size: The

one is fine-grained forming ground mass, and the other is coarse-grained forming phenocrysts.

All grains of plagioclase show more or less chemical zoning. The characteristics of the chemical zoning for plagioclase in all types of granitic rocks will be described in detail.

The chemical composition of plagioclase cores is especially different among the rock types. Coarse-grained plagioclase in the tonalite is richest in Ca with An content ranging from 37% to 91% in cores, ranging from 50% to 92% in mantles and ranging from 31% to 77% in rims (Fig. 30). An content for rims except for one data is less than 60%. That for cores is frequently more than 76%. Plagioclase in the tonalite shows that Or content increases continuously to 10% with decreasing of An content. With regard to chemical composition, fine-grained plagioclase is not appreciably different from coarse-grained one.

In the dark inclusion, plagioclase varies widely in chemical composition (Fig. 31). An content for cores ranges from 28% to 78%, showing bimodal concentration of 34% to 40% and higher than 50%. An content for rims ranges from 15% to 76% with a marked maximum between 15% and 25%. An content for mantles is plotted within the compositional range for the cores. Though plagioclase is not significantly different in chemical feature among three types lithofacies (Figs. 32 and 33), if forced to say, core composition is rather An-rich in the upper and middle lithofacies than in the lower lithofacies. Rims of the coarse-grained plagioclase are richer in An content than those of fine-grained plagioclase.

In the granodiorite, An content of plagioclase widely ranges from 12% to 88%, and contains Or content of less than 5% (Fig. 34). An content for cores ranges mainly from 25% to 61%. Range of An content for mantles is similar to that for the cores. Rims are poor in An content, ranging from 12% to 28%. Though plagioclase is not significantly different in chemical feature among three types lithofacies (Figs. 35 and 36), if forced to say, core composition of plagioclase from the middle lithofacies widely varies. The fine-grained plagioclase is not appreciably different in chemical feature from the coarse-grained plagioclase.

In the porphyritic granite, plagioclase is poor in An content, ranging from 17% to 48% (Fig. 37). It contains Or content of less than 5%. An content for rims ranges from 17% to

22%, and that for cores ranges from 23% to 48%. The range for mantles is similar to that for the cores. The fine-grained plagioclase is not appreciably different in chemical feature from the coarse-grained plagioclase.

Plagioclase in the granite is also poor in An content (Fig. 38). The chemical feature of plagioclase is similar to that in the porphyritic granite mentioned above. Plagioclase in the aplite is extremely poor in An content, narrowly ranging from 2% to 14% (Fig. 39). In the rhyolite, it is also poor in An content (Fig. 40).

Plagioclase in all types of granitic rocks shows distinct chemical zoning whose features are grouped into two types: The one is of ordinary type characterized by decreasing of An content from cores to rims. The other is of extraordinary type in which An content increases from cores to mantles, and decreases from the mantles to rims. Such a chemical zoning is called here abnormal type.

In the tonalite, though An content for plagioclase cores varies from 38% to 74%, it for mantles shows high values ranging from 72% to 80%, and it for rims ranges from 52% to 60% (Fig. 41). The zoning feature of plagioclase in the dark inclusion is more complicated showing two types: In the first type, An content increases from cores to mantles, and decreases from the mantles to rims. In the second type, it increases only slightly by about 2% from cores to mantles and shows further increase from the mantles to rims. The former type appears in plagioclase from the middle and lower lithofacies which were highly granitized (Fig. 42).

In the granodiorite, An content of plagioclase cores varies from 21% to 41%. That for rims shows a wide range from 12% to 46%, while that for mantles ranges only from 34% to 43% (Fig. 43). The zoning feature of plagioclase in the granodiorite, except for that of one grain, is commonly similar to the first type zoning of plagioclase in the dark inclusion, but that for the exceptional grain is comparable with the second type zoning. In the other rock types such as medium-grained granite, porphyritic granite, aplite and rhyolitic rocks is generally found the abnormal zoning of plagioclase which is comparable to the first type zoning for plagioclase of the dark inclusion (Fig. 44). In all types of granitic rocks, coarse-grained plagioclase distinct-

ly shows the abnormal zoning rather than fine-grained one.

7. K-feldspar

K-feldspar occurs in almost all types of granitic rocks, but its chemical analysis has not been performed for that in the tonalite and rhyolitic rocks due to the scarcity and intense alteration respectively . K-feldspar contains mostly Or content of larger than 80% and An content of all K-feldspar is less than 3%. The chemical data for K-feldspar are listed in Table 10.

K-feldspar in the dark inclusion, which occurs in small spheres mentioned in the chapter IV, has Or content ranging from 87% to 93% (Fig. 45). In the granodiorite, many K-feldspar grains have Or content ranging from 85% to 96%, but Or content of some other grains shows a range lower than 82% (Fig. 46). In the porphyritic granite, Or content of many K-feldspar grains ranges from 88% to 97%, except for two grains with Or content of 71% and 82% (Fig. 47). K-feldspar in the granite has generally Or content ranging from 79% to 94% (Fig. 48). In aplite, it shows a range of Or content from 76% to 90% (Fig. 49).

B. Geothermobarometry

Several kinds of geothermometers and geobarometers may be available to estimate the P-T conditions during the crystallization and cooling processes of the granitic rocks in the Togouchi area.

1. Two pyroxene geothermometer

Wells (1977) proposed a method to obtain the temperature under which orthopyroxene and clinopyroxene are crystallized with an equilibrium relation. Using the method, the temperatures for the crystallization of two pyroxenes in the tonalite were estimated for three specimens. The

detailed procedure for the calculation is not described here. The results obtained are listed in Table 11, showing some variation. The estimated temperatures vary depending upon data source such as cores and rims. The temperature based on the core data appears to be commonly higher than that based on the rim. Pyroxenes in the tonalite are considered to have crystallized under the temperature higher than 800°C.

2. Hornblende geobarometer

Quite recently, Vyhnal et al. (1991) proposed an empirical geobarometer which gives a pressure during the crystallization of hornblende based on the assumption that the activity of Al in calc–alkaline magmas clearly varies with pressure. The proposed formula is as follows;

$$P(\pm 0.5\text{kbar}) = -3.46 + 4.23Al^{total}$$

They further have shown the empirical relation fact that there is such a strong correlation between pressure and temperature for the crystallization of hornblende from calc–alkaline magma as shown by the following formula;

$$T(°C) = 25.3P + 654.9$$

After their methods, the pressure and temperature for the crystallization of hornblende in the granitic rocks of the studied area are estimated. The obtained data are plotted in Fig. 50. Except for the data (pressure over 7kb and temperature above 830°C), for a specimen of from the granodiorite, the estimated pressure and temperature are less than about 4.5kb and 770°C respec–tively. The pressure and temperature are different between rock types but even between analyzed points in one hornblende grain. Although estimated pressures for the tonalite and granodiorite widely vary from 0.2 to 3.3 kbar, many of them for the granodiorite vary only in a short range from 2.2 to 3.3 kbar.

Amphiboles in the tonalite show a distinct tendency for Al content to decrease from cores to rims. Such the growth history would be ascribed to the cooling of magma in which amphiboles crystallized. Fig. 51 illustrates the spatial variation of Al content in amphibole, showing that it

seems to decrease toward the south and so the crystallization temperature of amphiboles decreases toward the south.

3. Two feldspars geothermometer

Whitney & Stormer (1977) proposed a geothermometer based upon the partitioning of $NaAlSi_3O_8$ between microcline and plagioclase solid-solutions. In order to determine the crystallization temperature of the granitic rocks in the studied area using their method, 28 pairs of coexisting plagioclase and K-feldspar were selected from the granodiorite and its associated dark inclusion, granite, porphyritic granite and aplite. Fig. 52 is Whitney & Stormer's diagram for these 28 pairs. The equilibrium temperatures of many pairs range from 400°C to 500°C with an average value of 450°C, though some values are around and over 600°C.

C. Discussion

Crystallization environment of the granitic rocks in the studied area will be discussed on the basis of such chemical characteristics of minerals as mentioned above.

In general, the higher the crystallization temperature of calcic amphiboles are, the richer they are in Al, Ti, Na and K (Leake, 1971 and so on). Kanisawa (1976), Tainosho et al. (1979) and Murakami (1981) indicated that, in amphiboles from plutonic rocks, the higher their mg value is, the richer their Si content is, and pointed that during the crystallization of amphiboles, the lower the oxygen partial pressure is, the poorer their Si content is. Some amphiboles from the tonalite, dark inclusion, granodiorite and porphyritic granite show a tendency for mg value and Si content to decrease from cores to rims. If the decrease of mg value is in accordance with decrease of the oxygen partial pressure, the fact that the mg value decreases toward rims with increasing of Si content may be related to the descent of the oxygen partial pressure during cooling of magma. On the other hand, Sakiyama (1986) pointed out that the chemical composi-

tion in amphiboles changes depending on mineral species crystallized in earlier magmatic stage. It seems to be difficult to estimate the genetical condition for the granitic rocks in question on the basis of the above-described amphibole data.

It is well known that biotites show a tendency to become poorer in Ti and richer in Si and Al^{VI} through the progress of crystallization. Analogous tendency is also equally obvious for those in the granitic rocks in question. Czamanske and Wones (1973), Guidotti et al., (1975) and Anderson (1980) pointed out that it depends on the falling down of magma temperature and compositional change of its residual liquid. Following their opinions, almost all of biotites in the granitic rocks of the studied area are regarded to have normally crystallized through magma cooling.

The abnormal zoning of plagioclase has been found in all types of granitic rocks, especially for coarse-grained plagioclase in the tonalite, dark inclusion, granodiorite and porphyritic granite. Such a zoning of plagioclase would be probably ascribed to the rising of vapor pressure during the progress of crystallization.

It is noteworthy that in the tonalite the cores of plagioclases with the abnormal zoning is commonly poorer in An content than those of plagioclases with ordinary zoning. Therefore, it would be said that the rising of vapor pressure occurred after some plagioclase had started to crystallize. Plagioclases in the granodiorite and its associated dark inclusion show essentially the same property of the chemical zoning as that in the tonalite mentioned above.

The rising of vapor pressure during the progress of crystallization is in harmonic with the change of physical environment suggested by the chemistry of mafic minerals mentioned before. Chemical reduction environment is yielded in magma by rising of hydrothermal vapor pressure. In such a magma, Fe may be consumed to form rather Fe-Ti oxides, especially ilmenite, than mafic minerals.

Then, the origin of the dark inclusion is discussed in terms of the composition of plagioclase in relation to the formation of the tonalite. In the dark inclusion, the cores of plagioclase widely vary in An content. Plagioclase cores with high An content, which are mainly found in

coarse-grained plagioclase of the upper lithofacies, are chemically similar to those of the tonalite. Such plagioclase cores can be regarded to be relict plagioclase survived from granitization which occurred when the dark inclusion rocks were coupled with the granodiorite magma. The cores of plagioclases from the middle lithofacies widely vary in An content, showing that some grains have similar composition to those of the dark inclusion. Such the grains in the granodiorite are possibly interpreted to be fragmental grains derived from the dark inclusion.

The chemical characteristics of amphiboles and biotite in the dark inclusion appear to be intermediate between those of the tonalite and those of the granodiorite. Furthermore, cummingtonite derived from orthopyroxene has been found, and clinopyroxene is rarely found as a relic mantled by amphiboles. It may then well be said that the chemical characteristics of the dark inclusion, except for its granitized part, is similar to those of tonalite, especially of the fine-grained tonalite as its marginal part.

Ayrton (1988) presented a hypothesis that the origin of mafic enclaves in zoned plutons is attributed to fragmentation of ring dike as an earlier phase product of their related magmatism. Following his opinion, it may be said that the tonalite and dark inclusion in the studied area were of the same generation in age and that the former shows the original characteristics and the latter is the part dismembered through the tectonics related to the emplacement of the granodiorite.

Orthopyroxene and clinopyroxene in the tonalite crystallized in the temperature of higher than 800°C. Amphiboles in the tonalite and dark inclusion appear to have crystallized under the condition of about 2kbar and 700°C, and those in granodiorite and granite around 3kbar and 730°C. These data do not immediately indicate the depth of emplacement but indicate the crystallization condition. Namely the crystallization of amphiboles appears to have begun at greater depth than the emplacement depth of the tonalite. While feldspars in all types of granitic rocks indicate that the later stage crystallization of their related magmas occurred under the temperature of ca. 450°C.

VI HIGH-LOW INVERSION OF QUARTZ FROM GRANITIC ROCKS IN THE TOGOUCHI-YUU-TAKEHARA DISTRICT

A. Characteristics of high-low inversion of quartz

It is well known that quartz have high-low inversion point near 573°C under an atmosphere condition. Keith and Tuttle (1952) clarified that quartz crystallized under the low temperature condition indicates high-low inversion with higher temperature than and that crystallized under the high temperature condition. They are based upon the comparative study of inversion point of quartz between rhyolitic rocks and granitic rocks. Iiyama (1954) gave analogous interrelation for quartz in metamorphic rocks.

High-low inversion point for quartz from various types igneous rocks, chert and gneisses in the studied area and surrounding region has been determined using DTA method. A preliminary report for this study has been given by Hayashi (1981).

In the method, specimens powdered to about 200 mesh are heated to 650°C at a rate of 5°C per minute, and continuously they are cooled at the same rate. The inversion point on heating and that on cooling of each sample are obtained by extrapolating endothermic and exothermic curve recorded on a recording paper. The results are shown in Fig. 53, in which each inversion point is represented by the point of intersection of the temperature on heating on abscissa and that on cooling on ordinate. However, the inversion point of each sample does not indicate its own absolute inversion point because each datum is obtained in comparison with that for a synthesized quartz as a standard sample for oscillator. All of inversion points of quartz from the medium- to coarse-grained granitic rocks fall in a narrow area (Fig. 53) regardless of its mode of occurrence. Quartz in medium to coarse grained granitic rocks are regarded to have spent for a long time under sufficient heat supply.

B. High–low inversion of quartz from the porphyritic granite

The porphyritic granite is considered to have been produced under different condition from the medium– to coarse–grained granite. The inversion data of quartz from the porphyritic granite are illustrated in Fig. 54. These show a wider range than the data from the medium– to coarse–grained granite (Fig. 53.). It would be ascribed to the variation of genetic condition of the porphyritic granite consisting of two lithofacies.

VII MAGNETIC SUSCEPTIBILITY OF GRANITIC ROCKS IN THE TOGOUCHI AREA

Ishihara (1977) proposed that granitic rocks are classified into magnetite-series and ilmenite-series separated by $50x10^{-6}$emu/g of magnetic susceptibility: granitic rocks with magnetic susceptibility of lower than the value belongs to ilmenite-series, and those with magnetic susceptibility of higher than the value to be magnetite-series. Granitic rocks in the Togouchi area are generally situated in the San-yo zone. Ishihara (1979) said that granitic rocks in the San-yo zone are commonly of ilmenite-series and those in San-in zone are of magnetite series. Strictly speaking, the studied area is situated in a transitional zone between the San-yo zone and the San-in zone. Therefore, the detailed study of magnetic susceptibility of granitic rocks in the area may give an information on tectonic condition of the boundary between the San-yo and the San-in zones.

Magnetic susceptibility for the granodiorite, porphyritic granite, medium-grained granite and fine-grained granite bodies was measured by the instrument of BISON-3101A type. The results are shown in Fig. 55

Most of specimens from the granitic rocks, except for the fine-grained granite gave magnetic susceptibility of lower than $50X10^{-6}$emu/g, showing that almost all of granitic rocks belong to the ilmenite-series. Suzuki,M (1987) pointed out that granodiorite has the high magnetic susceptibility referred to the magnetite-series. The discrepancy between both studies may be ascribed to the difference between the measurement method. Although many specimens from rhyolitic rocks show magnetic susceptibility of lower than $50X10^{-6}$emu/g, that of some others is much higher. The specimens with higher values have been collected from near Nasu where the rocks are in wall contact with the granodiorite. Near the contact, the fine-grained granite occurs as thin layered body.

Specimens from the lower lithofacies of the granodiorite, especially those from its bottom part, tend to show the magnetic susceptibility which is as high as that for the magnetite-series.

Most of specimens from the fine-grained granite, even those from small dikes or veins observed in outcrops of the granitic rocks, tend to show the magnetic susceptibility of higher than $50X10^{-6}$emu/g. Generally, magnetic susceptibility tends to increase with increase of mafic minerals. But, as shown in Fig. 56, its data from the granodiorite are not positively related to the amounts of mafic minerals. The magnetic susceptibility of the dark inclusion is rather lower than that of the host granodiorite. It may be supposed that original magnetite in the granodiorite changed to ilmenite during their cooling process affected by successive magmatism. Similar interpretation was given for the Takiyama-kyo granite in the Takiyama-kyo area to the north of Kake (Hayashi et al., 1992; Suzuki,M. et al., 1993). It is an important but unsolved problem why the fine-grained granite shows the higher value of magnetic susceptibility so that it is comparative with the magnetite series, while that of its host granitic rocks are as low as that for the ilmenite series.

VIII MICROFABRIC OF QUARTZ IN GRANITIC ROCKS IN THE TOGOUCHI AREA

A. Microfracture of quartz in the granodiorite and medium-grained granite

In quartz of the granodiorite and medium-grained granite are commonly found sealed microfractures defined by preferred orientation of fluid inclusions cutting across its grain boundaries. Such microfractures are rarely also developed in feldspars. Hereafter, the sealed microfracture will be called "FIPS". Orientation of FIPS in quartz has measured using universal stage, in order to clarify the tectonic environment during the cooling of granodiorite and granite. FIPS would be probably referred to the "rift" or the "grain" after Dale (1923).

Wise(1964) described the characteristics of such microfracture system of the Precambrian basement of Montana and Wyoming including rift and grain, and discussed the relationship between the microfracture system and the tectonic environment. Plumb et al.(1984) discussed correlation between near surface *in situ* stress and microcrack fabric in the New Hampshire granites which had be studied by Dale (1923). No data for such a microfracture system has yet been reported from any granite in Japan.

In the Togouchi area, thirty five localities were selected to clarify the orientation of the healed microfracture throughout the granodiorite body (locality No. 1 to 34 in Fig. 57) and the medium-grained granite body (locality No. 35). Three thin sections perpendicular to each other were prepared from an oriented specimen collected from each locality. The measurement has been done for all microfractures observed within a domain of about 1.5cm X 2.0cm on every thin section. The observation numbers of FIPS in individual specimen should have a significance for discussing the timing and spatial environments of fracturing of quartz.

Two types of FIPS have been discriminated as shown in Plate 25. The one is shown an as aggregate of short microfractures parallel to each other in quartz. Every FIPS of this type contains tiny inclusions. The other is long microfractures with straight or greatly curved shapes,

sometimes extending into and throughout feldspar grains. Although two types of microfractures may have been produced under different age or stress fields, they appear to be commonly oriented parallel to each other. Therefore, the orientation data for the two types microfractures have been plotted indiscriminately on each diagram shown below.

The data of FIPS from each section are illustrated in Figs. 58-1 to 58-35. The data from three sections measured at each locality have been synthesized into a synoptic diagram. As is obvious in the figures, nearly vertical FIPS is predominant all over the localities, showing preferred orientation in selected directions. FIPS as flat or gently dipping planes is generally poor. In most of the localities, FIPS oriented nearly in NE-SW trend appears to be a prominent set and nearly NW-SE trending FIPS appears to be a subordinate set. Other concentration directions are nearly E-W and N-S, as shown in localities 9, 16, 18, 22, 28 and 35. FIPS from the locality No.16 and the locality No.27 shows a girdle-like pattern suggesting squeezing-type deformation. Many synoptic diagrams indicate that microfractures tend to develop with two or three prominent and subordinate sets in each locality (Fig. 59). They are called here the first set, the second and/or the third set depending on the order of point densities. The directions of these sets of FIPS at each locality are listed in Table 12 and the first set at each locality is also plotted on Fig. 60.

The orientation pattern of the first set of FIPS indicates that the granodiorite body is divided into three domains, N-domain, Central domain and S-domain (Fig. 60). The first set of FIPS is running in near NE-SW trend which is oblique at small angles to the elongation direction (NNE-SSW) of the granodiorite body, while in the central domains its orientation is complicated and it appears to be running in NW-SE to NNE-SSE trend. The trend of these domains is ENE-WSW, and appears to be slightly oblique to the orientation direction of the first set in the N-domain and S-domain. The first set of the Central domain is oriented oblique at high to moderate angles to the trend of the domains.

Lespinasse and Cathelineau (1990) proposed a method for relating fluid flow evolution to the bulk brittle network (microfracture system) which involves the use of fluid inclusions as a

tool for the establishment of the physco-chemical conditions under which fluids were entrapped. In the St Sylvestre batholith, central France, they classified three different types of quartz based on its formation stage and showed the ice melting and homogenization temperatures of each type of quartz. Furthermore, they showed that these temperatures of fluid inclusions trapped in healed microcracks of those three types of quartz, whose orientation is N-S, E-W and NW-SE respectively, are different from each other.

Then, the homogenization temperatures for fluid inclusions in quartz of the granodiorite of the Togouchi area have been measured. The results are shown in Fig. 61. Although the homogenization temperature widely varies ranging mainly from 200°C to 380°C in all localities, it appears to change depending on the orientation of FIPS. FIPS trending in near NE-SW tends to show relatively higher temperature, many of which are higher than 350°C in all localities. FIPS trending in near NW-SE shows around 340°C and those of trending in near E-W mainly show lower temperature than 300°C (Figs. 61 and 62).

Thus, it would be said that the healed microfracture in quartz was produced in near NE-SW trend under higher temperature than in near NW-SE trend and that those were produced in near E-W trend under lowest temperature among the three trends. Therefore, it is inferred that FIPS was initially produced in NE-SW to NNE-SSW trend, followed by near NW-SE trend and terminated by near E-W trend through cooling of the magma.

Vollbrecht et al. (1991) presented a hypothesis that the vertical FIPS of quartz is caused mainly by the internal thermal stress at the earlier stage during uplift of granitic magma and subhorizontal one mainly by external (unloading) stress at later stage. However, it is not clear whether or not the vertical FIPS of NE-SW to NNE-SSE trend and NW-SE to NNW-SSE trend in the Togouchi area is the Vollbrecht et al.'s case.

It may be said that FIPS trending nearly NE-SW dominated both in the N-domain and S-domain was reflected the fracturing formed by the compression with the axis of near NE-SW trend. While the Central domain may be a strain concentration zone, which was produced by sinistral movement trending near E-W in the later stage.

Based on studies of Late Mesozoic dike swarms in the Inner Zone of Southwest Japan, Yokoyama(1984) clarified that the direction of the largest horizontally compressive stress had initially been E–W, followed by N–S, and then changed again to E–W in the period. Although at least some of these compressions may be related with formation of FIPS in the Togouchi area, a definite conclusion must be reserved.

Yoshimura and Hayashi(1989) reported on the orientation of joint system in the northern part of the granodiorite body. According to them, vertical joints trending in NE–SW are predominant, and vertical joints trending in NW–SE and N–S and flat–lying sheeting joint are rather subordinate. The formation of NE–SW trending joints would be related to the activity of the major faults trending in NE–SW in Chugoku Province which postdated the Cretaceous volcano–plutonism.

B. Grain contact ratio for constituent minerals in the granodiorite and medium–grained granite

Sakurai and Hara (1979) and Hara et al.(1980) indicated that, in general, the more intensely the granitic rocks are deformed, the higher the value of grain contact ratio of quartz versus quartz becomes. Arita (1988) reported that the Hiroshima Granite has higher value of contact ratio of K–feldspar versus K–feldspar than the Ryoke granites in Kojima Peninsula and Shiwaku Island, Okayama Pref..

In order to clarify the deformation style of the granitic rocks in the Togouchi area during their emplacement, the grain contact ratios of the constituent minerals have been measured with the method proposed by Rogers and Bogy (1957). The obtained results are listed in Table 13. It would be said that the contact ratios of quartz versus quartz are low, and those of quartz versus K–feldspar are high. The contact ratios of quartz versus quartz for the granodiorite ranges from 0.18 to 0.46, and those for the medium–grained granite is 0.38 (Fig. 63). These for the granodiorite in the Togouchi area are extremely low and comparable with those for the Ishizuchi granite

(Sakurai and Hara, 1979), which was emplaced in a cauldron subsidence. Therefore, it would be said that the granodiorite was scarcely deformed in ductile fashion during cooling. High contact ratio of quartz versus K–feldspar in the granodiorite is well correlated with the development of micrographic texture for these minerals.

IX STRUCTURE OF THE HIROSHIMA GRANITE

A. Geological and structural features of the Hiroshima Granite in the areas other than the Togouchi area

The Hiroshima Granite distributed in the six areas, Ozegawa area, Saeki area, Hiroshima–Kake area, Yachiyo area, Kumano area and Takehara area, in the T–Y–T district has been further investigated and reviewed in detail in this paper, focusing mainly upon its lithological features and geological structures. From the obtained data it can be concluded that such lithological features and geological structures of granitic rocks as mentioned in the Togouchi area are commonly found throughout the T–Y–T district. The data will be described and discussed in the following paragraphs.

1. Ozegawa area

The Ozegawa area is situated to the west of Otake (Fig. 2). The Hiroshima Granite of this area forms a large mass developed continuously to near Kake (Fig. 4). The mass has been so far regarded as a batholithic mass. Namely, the granitic rocks of the Togouchi area occupy the northwestern margin of the mass and those of the Ozegawa area is situated in the southwestern margin (Fig. 4). The geological and petrographical studies on the granitic rocks of the Ozegawa area have been done by Yoshino and Hayashi (1979).

The granitic rocks in the Ozegawa area, which are composed mainly of medium–grained granite, are distributed eastwesterly, intruding into pre–Cretaceous Kuga Group composed mainly of pebbly mudstone, sandstone and chert (Fig. 64).

The boundary between the granitic rocks and the Kuga Group shows a step structure consisting of roof contact and wall contact (Fig. 65). All walls of the area steeply dip to the south with E–W trend, and all roofs gently dip to the west. The step structure is characterized by

stepping down from north to south. Therefore, the overall picture of the contact can be regarded as a plane gently dipping toward the south. In the roof contact, granitic rocks show a tendency to be fine-grained.

In the Kuga Group near the contact there are many dikes of fine-grained granite. These are placed in flat-lying and gently southward dipping attitude (Plate. 26). These dikes are derived from the granitic rocks. From these structural data, it is said that the granitic rocks was emplaced along the flat-lying fracture zone in the Kuga Group.

All rock types of the Kuga Group are thermally metamorphosed widely throughout the area by the granitic rocks, forming tiny cordierite spots of less than 3mm in diameter. Higashimoto et al. (1986) point out that the Hiroshima Granite occurs widely beneath the Kuga Group with nearly flat-lying contact plane.

2. Saeki area

The Saeki area is situated to the northeast of the Ozegawa area and to the south of the Togouchi area occupying western part of the Hiroshima Granite mass (Fig. 2). The granitic rocks of this area occur in contact with the pre-Cretaceous formations composed of the Nishiki and Kuga Groups (Takahashi, Y. et al.,1989; Takahashi, Y., 1991,1993). The granitic rocks which occur as flat-lying layered bodies are subdivided into three types of lithofacies based on grain size. They are medium-grained hornblende biotite granite, medium- to coarse-grained biotite granite and fine-grained granite. The first type is relatively mafic-rich facies. The thin layer of the fine-grained granite (here termed fine-grained facies) is situated in the uppermost part of the granite mass and is in contact with pre-Cretaceous formations. The medium- to coarse-grained biotite granite (here termed biotite granite facies) tends to occur in lower part of the mass. The relatively mafic-rich facies is widely distributed in the area and appears to be placed in the middle horizon of the granite mass. (Fig. 66).

3. Hiroshima–Kake area

The Hiroshima–Kake area is situated to the east of the Saeki area and occupies the central part of the Hiroshima Granite mass (Fig. 2). The granitic rocks in this area occur in contact with the Kuga Group which is distributed especially along the River Ota (Yamada et al., 1986), and consist of three types of lithofacies which are comparable with those in the Saeki area mentioned above. The mafic–rich facies, which extends from the Saeki area, occupies the upper part of the granite mass of this area. The biotite granite facies widely occurs in the lower part of the mass. Fine–grained facies is also found in the contact zone between the mafic–rich facies and the biotite granite facies. The mass is considered to be a layered body consisting of flat–lying layers of various lithofacies with various width. Such a layered structure is well observed at Numata, Hiroshima City. In the northern part of the area, the granite seems to have homogeneous lithology, in which the biotite granite facies is predominant (Fig. 67).

Yamada et al. (1986) has shown that the contact plane between the Hiroshima Granite and the Kuga Group sometimes dips to the southwest especially in the sub–areas along the River Ota. Many dikes of fine–grained granite parallel to the contact plane are found in the Kuga Group near the contact (Plate 27). Near Kake the biotite granite facies is intruded cutting across the boundary between the Kuga Group and its overlying rhyolitic rocks, which gently dips to the southwest (Fig. 67, A–A' profile).

Also in the Shiraki area to the northeast of Kabe, the contact plane between the Hiroshima Granite and the Nishiki Group dips to the south (Hayashi, 1978).

From these facts it may be said that the granitic rocks was emplaced along the fracture zone dipping gently to the southwest in the Kuga Group, Nishiki Group and their overlying rhyolitic rocks.

4. Yachiyo area

The Yachiyo area is situated to the north of the Hiroshima–Kake area (Fig. 2). The Hiroshima Granite mass in the area occurs in contact with both rhyolitic rocks and the Kuga Group (Yamada et al., 1986). As shown in Fig. 68, it consists of three types of lithofacies, each of which occurs as flat–lying layer (Hara, 1955). They are medium– to coarse–grained biotite granite, medium–grained hornblende–biotite granodiorite and fine–grained granite in ascending order, which are comparable with the biotite granite facies, mafic–rich facies and fine–grained granite facies in the Hiroshima–Kake area respectively. Fine–grained granite which occurs in the uppermost part of the granite mass is in horizontal contact with the Kuga Group and overlying rhyolitic rocks (Hara, 1955; Yamada et. al., 1986).

5. Kumano area

The Kumano area is situated to the east of Hiroshima City (Fig. 2). The Hiroshima Granite of the area is composed of fine–grained granite facies and biotite granite facies, and intruded into the pre–Cretaceous formation and the rhyolitic rocks as country rock (Fig. 69). The contact between the granite and their country rocks forms a step structure in which the steep wall contact is running in NW–SE trend and the roof contact in the central part of the area, being near horizontal but gently dipping to the south, cuts across the boundary between the pre–Cretaceous formation and its overlying rhyolitic rocks. The fine–grained granite facies occurs as a layered body in the uppermost part of the mass, especially in the roof contact. The biotite granite facies occurs widely in the lower part of the mass.

6. Takehara area

The Takehara area extends over the northern part of Takehara City (Fig. 2) and is situated in the eastern marginal area of the T–Y–T district. The Kuga Group and Cretaceous volcanic rocks which consist of dacitic to rhyolitic rocks (Yamada et al., 1986) are developed especially in the southern part of the area. The Hiroshima Granite is widely distributed throughout the area, intruding into the Kuga Group and the Cretaceous volcanic rocks.

Yoshida et al.(1985) has subdivided the Hiroshima Granite into three types based on grain size, each of which occurs as a flat–lying layer. They are fine–, medium– and coarse–grained granites (Fig. 70). In the medium–grained granite is rarely found hornblende. Therefore it can be said that these three facies are roughly comparable with those in other areas mentioned above.

The fine–grained granite occupies the uppermost part of the granite mass, like the cases of other areas mentioned above. The medium–grained granite occupies the middle part of the mass, and the coarse–grained granite the bottom part.

Analogous relationship between the lithofacies and the structure of the Hiroshima Granite is also equally obvious in the Takiyama–kyo area to the north of Kake (Hayashi et al., 1992) and Nomizima area, the Seto Inland Sea (Hayashi, in prep.).

On the basis of the above–described data, it can be concluded that the Hiroshima Granite in the T–Y–T district shows, as a whole, a flat–lying layered structure consisting mainly of three types of lithofacies, which are fine–grained granite (fine–grained granite facies), medium–grained hornblende–biotite granodiorite (mafic–rich facies) and medium– to coarse–grained biotite granite (biotite granite facies). The fine–grained granite facies tends to commonly occupy the upper part of the mass, sometimes scattered among its constituent layers. The mafic–rich facies is mainly placed in the middle horizon of the mass, and the biotite granite facies tends to occupy mainly the lower horizon.

B. Shape and structure of the Hiroshima Granite

Fine-grained granite is well developed in the uppermost part of the large mass developed throughout the T-Y-T district, and in almost all of cases, it is in direct contact with pre-Cretaceous formations or Cretaceous volcanic rocks. In other words, this type rock lies between the wall rocks and the other type granitic rocks. Furthermore, this type rock frequently occurs as small layered bodies between layers of other type granitic rocks. Boundary surfaces between the fine-grained granite and the other type granitic rocks are commonly sharp.

In the western-central part of the district, especially in and around the Saeki and Hiroshima-Kake areas, there is hornblende-biotite granite occupying the upper part of the mass. Additionally, other types of rocks rich in mafic minerals are frequently found in the marginal part i.e. marginal part of the mass: These are the granodiorite and tonalite in the Togouchi area, the granodiorite near Kure and the granodiorite on the south of Iwakuni etc.. But boundaries between such mafic-rich facies and the biotite granite facies are frequently obscure, and both appear as rather intergradational relation. The biotite granite facies is widely distributed all over the district, occupying lower part of the mass. The granite is also sometimes in direct contact with the wall rocks. As shown especially in the Togouchi area, the mafic-rich facies is an earlier stage intrusive than the biotite granite facies. The mafic-rich facies or granitic rocks remaining more or less mafic-rich facies are also found in the uppermost part of the biotite granite facies.

Cretaceous volcanic rocks are predominantly distributed with NE-SW trend in the northern area of the district, being accumulated on pre-Cretaceous formations as a basement. As mentioned before, the volcanic rocks belong to the northern volcanic zone. In general, the northern limit of the distribution of the Hiroshima Granite appears to correspond to the southern limit of the northern volcanic zone. Along the northern coast of the Seto Inland Sea, especially in near Kure, there is an other zone of Cretaceous volcanic rocks, which has been called "Akitu-Sensui block" by Yoshida (1964). The volcanic rocks are composed mainly of dacite and its tuffaceous equivalents (Aki Research Group, 1983, Higashimoto et. al., 1985). It has been already said that

those belong to the southern volcanic zone. The southern volcanic zone, as well as the northern one, is running in NE–SW trend. They are traced toward Okayama Pref.. These two volcanic zones are considered to have been two great fracture zones. The granodiorite is in direct contact with the rocks in the southern volcanic zone and underlain by the biotite granite facies (Figs. 4 and 5).

Hara et al. (1991) has presented the detailed geological map of the Oshima–Yanai–Kuga area, which is situated in the Ryoke zone and contains the southernmost of the T–Y–T district, and said that older Ryoke granites of this area occurs as layered bodies, being tectonically piled up each other. They also indicated that the younger Ryoke granites of this area appear in balloon–shaped bodies intruded into the older Ryoke granite and metamorphics.

The Hiroshima Granite in the south of Iwakuni is in direct contact with the older Ryoke granites. Although the boundary between them has not yet been exactly determined in the field, their boundary surface appears to dip gently to the south or southwest judging from their distribution features. Radiometric age data for granitic rocks of the Iwakuni–Yanai district indicate that the younger Ryoke granites are younger in radiometric age than the older Ryoke granites and the Hiroshima Granite and that the latter two are of the same radiometric ages (cf. Hara et al., 1991). Therefore, the latter two would be probably of the same generation in age. The Ryoke metamorphic rocks placed near the southernmost margin of the Hiroshima Granite appear to have been produced at 2–3kb depth (cf. Okudaira et al., 1993).

The western margin of the Hiroshima Granite of the T–Y–T district is in contact with Cretaceous volcanic rocks as shallow depth intrusives and/or terrestrial sediments in the northernmost part, with the only weakly metamorphosed Kuga Group sediments in the central part and with the Ryoke metamorphic and older Ryoke granitic rocks in the southernmost, showing that the contact plane dips gently toward the south from near the ground surface in the northernmost part to 2–3kb depth in the southernmost part. The internal layered structure of the Hiroshima Granite mentioned in the preceding pages is generally oriented parallel to such a southward dipping contact.

The northern volcanic zone is placed in and around the northern margin of the Hiroshima Granite. The eastern part of the Hiroshima Granite is in contact with the northern volcanic zone and also with the southern volcanic zone along the northern coast of Seto Inland Sea, The granite in contact with the southern volcanic zone can be regarded to be a small derivative intrusive from the major mass of the Hiroshima Granite.

On the basis of the above-described evidence and consideration, it is supposed that the Hiroshima granite occurs, as a whole, as a large sheet-like mass gently inclined toward the south or southwest (Hayashi et al., 1992) (Fig. 71). Fig. 72 schematically summarizes the above-mentioned geological setting as well as the tectonic framework of the Hiroshima Granite. The symbols E and W in this figure indicate east and west as the present geographic directions respectively.

X INTRUSION TECTONICS OF THE HIROSHIMA GRANITE

A. Recent history of studies on the intrusion mechanism of granitic rocks

The most momentous problem on the intrusion mechanism of granite is so called the "space problem". It has been emphasized on how to produce space for accommodation of granite magma forming apparently so large rock mass, as well as on how granite magma ascend from the deeper crust. It would be important to discuss such problems not only based upon local geological evidences, but also taking account of global tectonic environments.

Several models for explaining the intrusion mechanism have been so far proposed, based mainly on the geological and rock structures of granitic rocks. The famous and classical models are "diapirism", "cauldron subsidence" and, needless to say, mechanisms comprising these two in various degrees. Some studies concerning to these models are summarized in the following.

The diapirism model has well been developed, frequently being applied to explain intrusion mechanisms of various granites. Theoretical hypotheses and experimental studies for the diapirism within the crust have been performed by Biot and Ode (1965), Hamilton et al.(1967), Ramberg (1967, 1970), Berner et al.(1972), Hara and Shimamoto (1979) and others, clarifying the relationship between the shapes of diapirs and the physical properties of related rocks such as density and viscosity and the deformation style of host rocks related to the diapirism.

Sweeny (1975) pointed out that, judging from gravity data, both of Mt.Waldo and Lucerne granite batholiths in south-central Maine are relatively thin and tabular in shape and their emplacements would be explained in terms of buoyant diapirs that reach shallow depth within the crust, though their emplacements were possibly aided by pre-existing faults or fracture system in the host rocks.

Sylvester et al.(1978) also reported that the Mesozoic Papoose Flat pluton as a satellite of Sierra Nevada batholiths is a typical epizonal pluton forcibly emplaced into the present structural level as a viscous, almost completely crystalline mass. Their opinion base is the structural rela-

tionship between the pluton and its envelope, and deformation fabrics of both. As to creating "room" for the pluton in the country rocks, they placed great emphasis not only on its forcible-emplacement mechanism but also on the contrasting response of anhydrous and hydrous parts of the host strata to the elevation of temperature and to the radial pressure related to the invading pluton.

Bateman (1984) pointed out that the mode of magma ascending changes depending upon the ratios between melt and crystals: Many magmas begin their ascent through the crust as mushes with at least 50% melt, and when a magma becomes too crystalline (melt<25%) to continue its ascent, it is immobilized and then forms a pluton growing as a ballooning diapir by accretion of magmas. He also pointed out that, emphasizing the distinction between processes that operate during ascent and those that determine the mode of final emplacement, diapiric deformation is not directly a function of depth of emplacement, but of ductility contrast between intrusive magma and envelope. Moreover, he suggests that magmas, which are able to ascend to shallow depths largely by virtue of lower water content and higher initial temperature, tend to be finally accommodated by such brittle processes as stoping and cauldron subsidence, and that shallow level intrusions tend to become tabular, being fed through dikes or conduit. Further Bateman (1985) considered the evolution of Cannibal Creek Granite in northeastern Australia with reference to close connection between structural development and petrological development, concluding that a change from slow fractional crystallization to much more rapid equilibrium and cotectonic crystallization can be directly related to a change from ascent to final emplacement.

Woodcock and Underhill (1987) reported the other complexities of ballooning at shallow levels in a heterogeneous crust than the deep-level, emphasizing heterogeneous stretching and uplift strongly controlled by a nonuniform stratigraphy and by reactivation of older faults. In addition to vertical diapirism above mentioned, Courrioux (1987) presented a hypothesis of oblique diapirism for the emplacement of Criffel granodiorite/granite zoned pluton in SW Scotland, clarifying uneven distribution pattern of strain within the pluton.

The mode of "cauldron subsidence" has also been frequently applied to explain emplacement of granite batholiths with reference to connection between the formation of the batholiths and their contemporaneously associated or closely related volcanism. Cobbing and Pitcher (1972) mapped the Coastal Batholith in Peru and clarified the variety of intrusives composing batholith and structural interrelationships among them, suggesting that cauldron subsidence and associated stoping played an important role on the emplacement of the batholith, i.e. fracturing and stoping might have been the dominant process in the rigid plate of overlying volcanics. Myers (1975) also showed that the Coastal Batholith is constituted by piles of thin tabular shaped plutons with flat roofs and steep walls which pass downward into ring dikes and upward into ring dikes and calderas, and that it was formed through the process of repeated cauldron subsidence. He also showed how those intrusives rose through their last few kilometers by a process of magmatic stoping. In his opinion, each subsidence was preceded by the formation of small shear zone. Pitcher and Bussell (1977) regarded for magmas of the Coastal Batholith to have been emplaced along major fault lines in ancient crystalline basements and for the emplacement of individual plutons to have been closely controlled by transcurrent faults and smaller scale joint patterns. Pitcher (1978) showed schematically that the Coastal Batholith was intruded and emplaced along the vertical shear zones which possibly reach the asthenosphere. Furthermore, Pitcher (1979) stated that only in Andinotype batholiths there is a clear space/time relationship between plutonism and volcanism and that, in emplacement of Andinotype batholiths, cauldron subsidence is a dominant process accompanied by stoping of brittle basements of calderas or volcanic ejecta, while, in that of Hercynotype batholith, diapir ascending and *in situ* ballooning in the ductile crust is dominant. He emphasized that the batholith emplacements may be controlled by major deep shear zone in the crust.

In Chugoku Province, Imaoka (1986) reported several examples for the igneous complex bodies consisting of volcanic rocks and contemporaneous plutonic rocks in the San-in zone, which appear to have formed through such a process of cauldron subsidence. In Kyushu Province, Takahashi, M. (1985) reported that the Okueyama zoned pluton was emplaced through

stoping like the case of the Coastal Batholith shown by Myers (1975).

Although such two models may be relevant to the interpretation of the intrusion mechanism of the Hiroshima Granite, some authors have recently presented a new interpretation for the intrusion mechanism of Cretaceous granite in the Inner Zone of Southwest Japan to which belongs the Hiroshima Granite (for example, Kanaori, 1990; Kanaori et al., 1990). They said that the space for the granites were produced by the movement of the major strike-slip faults such as the Median Tectonic Line, Atera Fault, Yanagase Fault and many others. Their interpretation is based only on such evidence that these strike-slip faults occurred during Cretaceous age. They do not take any account for the internal structure of granitic rocks and the structural relationship between the granitic rocks and the host rocks.

Ramsey (1981) and Holder(1981) calculated the increasing of pluton diameter during the emplacement process. Brun and Pons (1981) presented simple simulation for the orientation pattern of the foliation produced by interference between the ballooning of magma and the regional deformation events.

Hutton (1982) proposed a tectonic model for the emplacement of the Main Donegal Granite in NW Ireland. The model is that the shear zone locally created high strain rate and instability which caused the zone to bend, split lengthwise and progressively create an internal low pressure zone into which the magma for the Main Granite was emplaced.

Meneilly (1982) also discussed the relationship between the formation of the regional structure and the granite intrusion in the Dalradian of the Gweebara Bay area, southwesterly adjacent to the Main Donegal Granite. Davis (1982) reported plutons are associated with the Njad fault system characterized by wrench fault, shear zone of which had a role of conduit for their magmas.

Castro (1985, 1986) presented a hypothesis for the intrusion mechanism of the Central Extremadura "Batholith" in Hercynian belt, Spain: Several plutons, which are considered to be a batholith in genetic viewpoint, were emplaced and deformed in an E-W, dextral, deep, intracontinental shear zone characterized by extensional fracture after the first Hercynian deformation

phase.

Bruno et al., (1987) proposed that the Variscan Mortagne granite in France was emplaced in a pull-apart void formed by the early movement of the South Armorican Shear Zone characterized by a sinistral shear.

Hutton (1988) proposed that the Caledonian Storontian granite in Scotland was emplaced essentially passively in the extensional termination of a dextral transcurrent shear zone, which is a splay controlled by a slight releasing bend in the major Great Glen fault and by a large, pre-existing, asymmetrical synform in Proterozoic metasedimentary country rocks.

B. Intrusion mechanism of the Hiroshima Granite (discussion and conclusion)

The intrusion mechanism of the Hiroshima Granite will be discussed in the light of above-mentioned previous works.

The late Cretaceous to Palaeogene igneous rocks in the Inner Zone of Southwest Japan, which contains the Hiroshima Granite, have been thought to be a series of volcano-plutonisms. Judging from their distribution features, the volcanic rocks appear to be arranged in at least two different volcanic rows with vigorous acidic volcanic rocks on the pre-Cretaceous formations as the basement. As shown before, the one of the rows is referred to the northern volcanic zone, and the other to the southern volcanic zone. In the beginning of the volcanism, in general, it is characterized by relatively mafic ones as Kisa andesite and dacite of lower Takada rhyolites (Iizumi et al., 1985). The northern volcanic zone is the main zone of volcanism and is associated with the development of andesite and early Cretaceous sedimentary rocks (Kanmon Group) (Fig. 4). The southern volcanic zone is only the subordinate one.

Murakami (1974) has proposed that the NE-SW trending in central-western Chugoku Province was probably active fissures since the Mesozoic period and the Cretaceous volcanic activities took place along the fissures. It is said that the intrusion of the Hiroshima Granite followed the volcanism. However, the Hiroshima Granite is mainly developed just on the south

of the northern volcanic zone, showing that the boundary between its main body and host rocks is gently inclined toward the south, intruding the volcanic rocks in the northern margin and the Ryoke metamorphic rocks of 2–3kb depth in the southern margin.

The geological structures related to cauldron subsidence such as collapse topography for caldera, ring dikes and circularly distributed plutons as well as evidences for stoping, have not yet been found in any area of the Hiroshima Granite, even in near the rhyolitic rocks. On the other hand, the layered structure of the Hiroshima Granite and the step structure of the granite contact characterized by combination of roof contact and wall contact described in the preceding pages may interpreted in terms of the vertical subsidence of the crustal rocks during the em-placement which is a fundamental factor of cauldron subsidence, like the case of the Coastal batholith (Myers, 1975).

As many authors pointed out, generally, diapirism, as well as ballooning, is not character-ized only by the ductile deformation of country rocks, but also by that of the pluton itself. The ductile deformation of the Hiroshima Granite and country rocks is scarcely found. The apparent diameter of the Hiroshima Granite mass of the T–Y–T district is greater than 50km. The diapiric intrusive and/or ballooning of such great mass must induce the great deformation of the host rocks throughout great extent. However, such a great deformation of the host rocks is not found in any fashion but commonly shown only by the formation of granite veins (and dikes) in narrow zone adjacent to the granite. Therefore, it can be said that the emplacement of the Hiroshima Granite was accompanied by fracturing of the host rocks just near its contact. The development of the step structure in the Hiroshima Granite may be closely related to the fracturing. The Hiroshima Granite had not brought also the stoping of the country rocks in great extent.

It may be notable that a diapiric granite intruded into shallow crust can be thin and tabular (Sweeny, 1975). Besides, batholith formed by cauldron subsidence can be constructed by layered granite masses with different lithofacies (Myers, 1975; Pitcher & Bussell, 1977; Pitcher, 1978). These also indicate that the "tabular mass" is a common specific phenomenon of granites intrud-ed into higher level in the crust. The Hiroshima Granite seems to be also tubular mass with

layered structure consisting of different types of lithofacies. However, it is notable that the layered tabular mass was not of flat-lying type but gently inclined toward the south or southwest.

It is important that so large mass of the Hiroshima Granite had not printed significant deformation effects on the country rocks and within the mass itself through its intrusion process. Judging from such field evidences, the granite seems to have come in contact with the country rocks in rather static condition. The granite undoubtedly formed through "passive intrusion".

On the basis of the above-described evidence and consideration, it may be said that the shape of the Hiroshima Granites is a fossil of a path of magma ascend which was placed along great fracture zone. The layering within the granite mass, which consist of different type lithofacies, may indicate continuous but episodic intrusion by magma pulse, which was controlled by episodic activity of shear zone. The shear zone was oriented with southward inclination (Fig. 72). The northern volcanic zone must have been placed at the top of the shear zone. As mentioned before, the granodiorite in the Togouchi area is an earlier stage constituent of the Hiroshima Granite, which postdated the original rocks for the dark inclusion. The Kisa andesite and dacite may be volcanic equivalent of these rocks. The southern volcanic zone may be a branch from the shear zone for the main body of Hiroshima Granite. The Hiroshima Granite appears to be different from both the Hercynotype batholith and the Andinotype batholith (Pitcher, 1979). Anyway these two types of batholith are essentially characterized by process of vertical magma movement. While the Hiroshima Granite appears to be related to "lateral magma movement" along gently dipping shear zone. Consequently, the author wishes to propose flat-dike type mass for the emplacement mechanism of a large granite mass. Fig. 73 illustrates the general model for the granite intrusions of flat-dike type in magma arc.

REFERENCES

Aki Research Group (1983): Late Cretaceous igneous rocks in Akitsu area, Hiroshima Prefecture. *MAGMA*, **67**, 13–19. (J)

Anderson,A.T.(1980): Mineral equilibria and crystallization conditions in the late Precambrian Wolf River rapakivi massif, Wisconsin. *Amer. Jour. Sci.*, **280**, 289–332.

Arita,M.(1988): Petrographical studies on granitic rocks in the Kojima Peninsula and Shiwaku Islands, the central parts of Seto Inland Sea, Southwest Japan: proterogenetic and magmatogenetic origin of granitic rocks. *Jour. Geol. Soc. Japan*, **94**, 279–293. (J+E)

Ayrton,S.(1988): The zonation of granitic plutons:the "failed ring-dike" hypothesis. *Schweiz. Mineral. Petrogr. Mitt.*, **68**, 1–19.

Bateman,R.(1984): On the role of diapirism in the segregation, ascent and final emplacement of granitoid magmas. *Tectonophys.*, **110**, 211–231.

Bateman,R.(1985): Progressive crystallization of a granitoid diapir and its relationship to stages of emplacement, *Jour. Geol.*, **93**, 645–662.

Berner,H., Ramberg,H and Stephansson,O.(1972): Diapirism theory and experiment. *Tectonophys.*, **15**, 197–218.

Biot,M.A. and Odé,H.(1965): Theory of gravity instability with variable overburden and compaction. *Geophys.*, **30**, 213–227.

Brun,J.P. and Pons,J.(1981): Strain patterns of pluton emplacement in a crust undergoing noncoaxial deformation, Sierra Morena, Southern Spain. *Jour. Struct. Geol.*, **3**, 219–229.

Bruno,G., Bouchez,J.L. and Vigneresse,J.L.(1987): The Mortagne granite pluton (France) emplaced by pull-apart along a shear zone: Structural and gravimetric arguments and regional implication. *Geol. Soc. Amer. Bull.*, **99**, 763–770.

Castro,A.(1985): The Central Extremadura batholith: Geotectonic implications (European Hercynian belt) – An outline. *Tectonophys.*, **120**, 57–68.

Castro,A.(1986): Structural pattern and ascent model in the Central Extremadura batholith,

Hercynian belt, Spain. *Jour. Struct. Geol.*, **8**, 633–645.

Cobbing,E.D. and Pitcher,W.S.(1972): The Coastal Batholith of central Peru. *Jour. Geol. Soc. Lond.*, **128**, 421–460.

Courrioux,G.(1987): Oblique diapirism: the Criffel granodiorite/granite zoned pluton (southwest Scotland). *Jour. Struct. Geol.*, **9**, 313–330.

Czamanske,G.K. and Wones,D.R.(1973): Oxidation during magmatic differentiation, Finnmarka complex, Oslo area, Norway: Part 2, the mafic silicates. *Jour. Petrol.*, **14**, 349–380.

Dale,T.N.(1923): The commercial granites of New England. *U. S. Geol. Survey Bull.*, **738**.

Davis,F.B. (1982): Pan–African granite intrusion in response to tectonic volume change in a ductile shear zone from northern Saudi Arabia. *Jour. Geol.*, **90**, 467–483.

Geological Survey of Japan(1982): *Geological Atlas of Japan*, 119. (J)

Guidotti,C.V., Cheney,J.T. and Connature,P.D.(1975): Interrelationship between Mg/Fe ratio and octahedral Al content in biotite. *Amer. Mineral.*, **36**, 884–901.

Hamilton,W. and Mayers,W.B.(1967): The nature of batholith, *U.S. Geol. Survey Prof. Paper*, 554C.

Hara,I.(1955): Granitic rocks and associated quartz deposits in Hata area, Chiyoda Town, Yamagata District, Hiroshima Prefecture. *Graduation Th., Hiroshima Univ.*

Hara,I., Higashimoto,S., Mikami,T., Nishimura,Y., Okimura, Y., Sawada,T., Takeda,K., Yokoyama,S. and Yokoyama,T.(1979): Palaeozoic–Mesozoic Group of the Yasaka gorge district. *Landscape and Environment*. Joint scientific committee for research into the Yasaka gorge scenic reserve. 283–324. (J+E)

Hara,I. Sakurai,Y., Arita,M. and Paulitsch,P.(1980): Distribution pattern of quartz– evidence of their high temperature deformation during cooling. *N. Jb. Miner. Mh.* **H. 1**, 20–30.

Hara,I., Sakurai,Y., Okudaira,T., Hayasaka,Y., Ohtomo,Y. and Sakakibara,N.(1991): Tectonics of the Ryoke belt. *In: Excursion guidebook. the 98th annual meeting of the Geological Society of Japan*. 1–20. (J)

Hara,I. and Shimamoto,T.(1979): Fold and folding. *In: Uemura,T. and Mizutani,S. (eds.), Chik–*

yu-kagaku, No.9, Iwanami Shoten, Tokyo, 187–238. (J)

Hara,I., Shiota,T., Hide,K., Kanai,K., Goto,M., Seki,S., Kairiki,K., Takeda,K., Hayasaka,Y., Miyamoto,T., Sakurai,Y. and Ohtomo,Y.(1992): Tectonic evolution of the Sambagawa schists and its implications in convergent process. *Jour. Sci. Hiroshima Univ. Ser.C*, **9**, 495–595.

Hayama,Y., Yamada,N., Yamada,T., Kutsukake,T., Nakai,Y., Akahane,H., Ikeda,K. and Tanabe,M.(1975): The metamorphosed Paleozoic sediments and the Cretaceous igneous rocks of the Osaki-shimojima Island in Seto-naikai (Inland Sea), Western Japan. *Earth Sci.*, **29**, 1–17. (J+E)

Hayashi,T.(1978): A metagabbroic rock mass at Mt.Kannokura, Hiroshima City. *Bull. Fac. Sch. Educ. Hiroshima Univ.*, II, **1**, 181–185. (J+E)

Hayashi,T.(1981): Studies on the high-low inversion of quartz. *Bull. Fac. Sch. Educ. Hiroshima Univ.*, II, **4**, 89–92. (J+E)

Hayashi,T.(1989): Classification and geological structure of granitic rocks of Aki-Seibu Mountains, northwestern part of Hiroshima Prefecture. Proceed. *Nishinihon Bran. Geol. Soc. Japan*, **92**, 7. (J)

Hayashi,T., Madokoro,K., Ishikura,H. and Suzuki,M.(1992): "Undivided Granite" near Kake Town, northwestern part of Hiroshima Prefecture (I) – field occurrence and geological structure –. *Nishinihon Bran. Geol. Soc. Japan*, **101**, 3–4. (J)

Hayashi,T. and Suzuki,M.(1990): Modal analysis of granitic rocks by image processing on a personal computer. *J. Min. Petr. Econ. Geol.*, **85**, 60–95. (J+E)

Hayashi,T., Suzuki,M. and Hara,I.(1992): Structure and intrusion mechanism of Hiroshima granites in the Yuu-Kake district, Southwest Japan. *Abst. 99th Ann. Meet. Geol. Soc. Japan*, 435. (J)

Higashimoto,S., Matsuura,H., Mizuno,K. and Kawada,K.(1985): *Geology of the Kure district.* Quadrangle Series, scale 1:50,000, Geol. Surv. Japan, 93. (J+E)

Higashimoto,S., Nureki,T., Hara,I., Tsukuda,E. and Nakajima,T. (1983): *Geology of the Iwakuni*

district. Quadrangle Series, scale 1:50,000, Geol. Surv. Japan, 79. (J+E)

Higashimoto,S., Takahashi,Y., Makimoto,H., Wakita,K. and Tsukuda,E.(1986): *Geology of the Otake district*. With Geological Sheet Map at 1:50,000, Geol. Surv. Japan, 70. (J+E)

Hiroshima Prefecture (1963): *The geological map of Hiroshima Prefecture*. (J)

Holder,M.T.(1981): Some aspects of intrusion by ballooning (abstract). *In: Coward, M.P. Diapirism and Gravity Tectonics: report of a Tectonic Studies Group conference at Leeds Univ., 25–26 March 1980. Jour. Struct. Geol.*, **3**, 93.

Hutton,D.H.W.(1982): A tectonic model for the emplacement of the Main Donegal Granite, NW Ireland. *Jour. Geol. Sci. Lond.*, **139**, 615–631.

Hutton,D.H.W.(1988): Igneous emplacement in a shear zone termination: The biotite granite at Strontian, Scotland. *Geol. Soc. Amer. Bull.*, **100**, 1392–1399.

Ichikawa,K.(1990): Pre–Cretaceous Terrane of Japan. *In: Ichikawa,K. et al. (eds.), Pre–Cretaceous Terrane of Japan*, 1–11.

Iiyama, T.(1954): High–low inversion point of quartz in metamorphic rocks. *Jour. Fac. Sci. Tokyo Univ., Ser. 2,* **65**, 193– 200.

Iizumi,S., Sawada,Y., Sakiyama,T. and Imaoka,T.(1985): Cretaceous to Paleogene magmatism in the Chugoku and Shikoku District, *Earth Sci.*, **39**, 372–384. (J+E)

Imaoka,T.(1986): Paleogene igneous activity in the West San–in district. *Geol. Rep. Hiroshima Univ.*, No. 26, 1–109. (J+E)

Ishihara,S.(1977): The magnetite–series and ilmenite–series granitic rocks. *Mining Geol.*, **27**, 293–305.

Ishihara,S.(1979): Lateral variation of magnetic susceptibility of the Japanese granitoid.*Jour. Geol. Soc. Japan*, **85**, 509–523.

Kanaori,Y.(1990): Late Mesozoic – Cenozoic strike–slip and block rotation in the inner belt of Southwest Japan. *Tectonophys.*, **177**, 381–399.

Kanaori,Y., Endo,Y., Yairi,K. and Kawakami,S.(1990): A nested fault system with block rotation caused by left–lateral faulting: the Neodani and Atera faults, centaral Japan. *Tectono–*

phys., **177**, 401–418.

Kanisawa, S.(1976): Chemical compositions of hornblendes and biotites in granitic rocks. *Special paper,* No.1, Japan. Assoc. Miner. Petrol. Econ. Geol., 243–249. (J+E)

Kawahara,F.(1978): "Takada rhyolitic rocks" in the eastern part of Mihara City, Hiroshima Prefecture, Southwest Japan. *Jour. Geol. Soc. Japan*, **84**, 425–432. (J+E)

Kawahara,F.(1989): The Takada rhyolitic complex in the Mt. Jippou district, northwest Hiroshima Pref., Southwest Japan. *Land and Life of the Tateiwa area*, 59–91. (J+E)

Kawahara,F. and Bammoto,M.(1983): On *Cunninghamia* cone from the Takada rhyolitic rocks. *Jour. Geol. Soc. Japan*, **89**, 469–470. (J+E)

Keith,M.L. and Tuttle,O.F.(1952): Significance of variation in the high–low inversion of quartz. *Amer. Jour. Sci.*, **Bowen vol.**, 203–280.

Kojima,G.(1953): Contributions to the knowledge of mutual relations between three metamorphic zones of Chugoku and Shikoku, southwest Japan, with special reference to the metamorphic and structural features of each metamorphic zone. *Jour. Sci. Hiroshima Univ., Ser. C,* **1**, 17–46.

Kojima,G.(1964): Plutonic rocks. *The explanatory text of the geological map of Hiroshima Pref.*, 87–101. (J)

Kojima,G., Yoshida,H. and Nureki,T.(1959): On acidic igneous rocks of the Sandankyo district, Hiroshima Prefecture, with special reference to late Mesozoic igneous activity in Chugoku. *Scientific research of the Sandankyo gorge and Yawata highland.* The board of education of Hiroshima Prefecture, 45–63. (J+E)

Kusumi,H., Katayama,S., Okumura,Y., Irise,O., Miyake,S., Fujii,M., Banmoto,M. and Fujikawa,Y.(1989): Geomorphology and geology of drainage basin of the Tateiwa reservoir, northwest Hiroshima Prefecture. *Land and life of the Tateiwa area*, 33–57. (J+E)

Leeke,B.E.(1971): On aluminous and edenitic hornblende. *Miner. Mag.*, **38**, 389–407.

Leeke,B.E.(1978): Nomenclature of amphiboles. *Miner. Mag.*, **42**, 533–63.

Lespinasse,M. and Cathelineau,M.(1990): Fluid percolation in a fault zone: a study of fluid

inclusion planes in the St Sylvestre granite, northern Massif Central, France. *Tectonophys.*, **184**, 173–187.

Meneilly,A.W.(1982): Regional structure and syntectonic granite intrusion in the Dalradian of the Gweebarra Bay area, Donegal. *Jour. Geol. Soc. Lond.*, **139**, 633–646.

Murakami,N.(1974): Some problems concerning late Mesozoic to early Tertiary igneous activity on the innerside of Southwest Japan. *Pacific Geol.*, **8**, 139–151.

Murakami,N.(1981) Compositional variation of Mesozoic igneous rocks and their constituent minerals of the area between Masuda and Matsuyama, Southwest Japan, with reference to the plutonic rocks from Masuda–Yanai area. *Jour. Fac. Lib. Art. Yamaguchi Univ.*, **15**, 33–74. (J+E)

Murakami,N. and Imaoka,T. (eds.) (1986): Acid to intermediate igneous activity in West Chugoku and its adjacent areas, Southwest Japan. *Jour. Fac. Lib. Art. Yamaguchi Univ.*, **Prof. Murakami, N. Memo. vol.**, 1–419. (J+E)

Myers,J.S.(1975): Cauldron subsidence and fluidization: Mechanisms of intrusion of the Coastal batholith of Peru into its own volcanic ejecta. *Geol. Soc. Amer. Bull.*, **86**, 1209–1220.

Nishimura,Y.(1990): "Sangun Metamorphic Rocks": Terrane Problem. *In: Ichikawa,K., et al. (eds.), Pre-Cretaceous Terranes of Japan*, 63–79.

Okudaira,T., Hara,I., Sakurai,Y. and Hayasaka,Y.(1993):Tectonometamorphic processes of the Ryoke belt in the Iwakuni–Yanai district, Southwest Japan. *Mem. Geol. Soc. Japan*, No. 42 (in press)

Pitcher,W.S.(1978): The anatomy of a batholith. *Jour. Geol. Soc. Lond.*, **135**, 157–182.

Pitcher,W.S.(1979): The nature, ascent and emplacement of granitic magmas. *Jour. Geol. Soc. Lond.*, **136**, 627–662.

Pitcher,W.S. and Bussell,M.A.(1977): Structural control of batholithic emplacement. *Jour. Geol. Soc. Lond.*, **133**, 249–256.

Plumb,R., Engelder,T. and Yale,D.(1984): Near–surface in site stress 3. Correlation with micro–crack fabric within the New Hampshire Granite. *Jour. Geophy. Research*, **89**, B11,

9350–9364.

Ramberg,H.(1967): *Gravity, deformation and the Earth's Crust.* Academic Press, London, 1–214.

Ramberg,H.(1970): Model studies in relation to intrusion of plutonic bodies; *In: Mechanism of Igneous Intrusion*. Liverpool, Gallery Press, 261–286.

Ramsey,M.T. (1981): Emplacement mechanics of the Chindamora Batholith, Zimbabwe (abst.). *In: Coward,M.P.(ed), Diapirism and Gravity Tectonics: report of a Tectonic Studies Group conference at Leeds Univ., 25–26 March 1980. Jour. Struct. Geol.*, **3**, 93.

Rogers,J.J.W. and Bogy,B.(1957): A study of grain contacts in granitic rocks. *Science*, 127, 470–294.

Sakiyama,T.(1986): Geological and petrological studies on the late Cretaceous to Paleogene plutonic rocks in the eastern San–in district, Southwest Japan. *Geol. Rep. Hiroshima Univ.*, No.26, 111–194. (J+E)

Sakurai,Y. and Hara,I.(1979): Studies on microfabrics of granites, with special reference to quartz fabric. *Memo. Geol. Soc. Japan*, No.17, 287–294. (J+E)

Suzuki,M.(1987): Plutonic rocks belonging to the San–yo zone in the central Chugoku Province. *In Igi, S., Murakami, N. and Okubo, M.(eds), Regional Geology of Japan part 7 Chugoku*, Kyoritsu Shuppan, Tokyo, 82–84. (J)

Suzuki,M., Hayashi,T., Ishikura,H. and Madokoro,K.(1993): Magnetic susceptibility of granitic rocks in the Takiyama–kyo area, Southwest Japan. *Bull. Fac. Sch. Educ. Hiroshima Univ.*, II, **15**, 87–92. (J+E)

Suzuki,M., Hayashi,T. and Yoshimura,N.(1992): Findings of almandinous garnets from the Mesozoic Takada rhyolitic rocks, Southwest Japan. *Jour. Geol. Soc. Japan*, **98**, 271–274.

Suzuki,T.(1986): Kake – Sandan–kyo area. *In Murakami,N. and Imaoka,T. (eds.), Acid to intermediate igneous activity in West Chugoku and its adjacent areas, Southwest Japan. Jour. Fac. Lib. Art. Yamaguchi Univ.*, **Prof. Murakami, N. Memo. vol.,** 162–173. (J)

Sweeney,J.F.(1975): Diapiric granite batholiths in south–central Maine. *Amer. Jour. Sci.*, **275**,

1183–1191.

Sylvester,A.G., Oertel,G., Nelson,C.A. and Christie,J.M. (1978): Rapoose Flat pluton: A granitic blister in the Inyo Mountains, California. *Geol. Sci. Amer. Bull.*, **89**, 1205–1219.

Tainosho,Y., Honma,H. and Tazaki,K.(1979): Mineral chemistry in granitic rocks of East Chugoku, Southwest Japan. *Memo. Geol. Soc. Japan*, No.17, 99–112. (J+E)

Takahashi,M.(1985): Okueyama zoned pluton: solidified gravitationally zoned voluminous felsic magma chamber beneath volcanic edifices. *MAGMA*, **73**, 123–133. (J)

Takahashi,Y.(1991): *Geology of the Hiroshima district.* With Geological Sheet Map at 1:50,000, Geol. Surv. Japan, 41. (J+E)

Takahashi,Y.(1993): Hiroshima Granite – Enormous vertically zoned pluton. *J. Min. Petr. Econ. Geol.*, **88**, 20–27. (J+E)

Takahashi,Y., Makimoto,H, Wakita,K. and Sakai,A.(1989): *Geology of the Tsuta district.* With Geological Sheet Map at 1:50,000, Geol. Surv. Japan, 56. (J+E)

Tomonari,S.(1984): Petrographic features and interrelations of granitic and rhyolitic complexes in the Middle Belt of the Palaeozoic Terrain in Hiroshima Prefecture. *Geol. Rep. Hiroshima Univ.*, **24**, 65–97. (J+E)

Vollbrecht.A., Rust,S. and Weber,K.(1991): Development of microcracks in granites during cooling and uplift: examples from the Variscan basement in NE Bavaria, Germany. *Jour. Struct. Geol.*, **13**, 787–799.

Vyhnal,C.R., McSween,H.Y.Jr. and Speer, J.A.(1991): Hornblende chemistry in southern Appalachian granitoid: Implications for aluminum hornblende thermobarometry and magmatic epidote stability. *Amer. Mineral.*, **76**, 176–188.

Yamada,N., Higashimoto,S., Mizuno,K., Hiroshima,T. and Suda,Y.(1986): *1:200,000 Geological Map, Hiroshima*, Geol. Surv. Japan. (J)

Yokoyama,S.(1984):Geological and Petrological studies of late Mesozoic dike swarms in the Inner zone of Southwest Japan. *Geol. Rep. Hiroshima Univ.*, No.24, 1–63.

Yoshida,H.(1961): The late Mesozoic igneous activities in the Middle Chugoku Province. *Geol.*

Rep. Hiroshima Univ., No.8, 1–39. (J+E)

Yoshida,H.,(1964): Cretaceous volcanic rocks. *The explanatory text of the geological map of Hiroshima Pref.*, 73–86. (J)

Yoshida,H., Soeda,A., Hara,I., Okimura,Y., Takeno,S., Watanbe,M., Suzuki,M., Miyamoto,T., Kitagawa,R. and Yano,T.(1985): *Surface geological map TAKEHARA*. With explanatory text, 31–46, (J)

Yoshimura,N. and Hayashi,T.(1989): Erosion surface and fracture systems in the Ohta River valley. *Land and life of the Tateiwa area*, 15–32. (J+E)

Yoshino,G. and Hayashi,T.(1979): Granitic rocks of the Yasaka gorge district. *Landscape and Environment*. Joint scientific committee for research into the Yasaka gorge scenic reserve. 337–354. (J+E)

Yoshino,G. and Hayashi,T.(1989): Granitic rocks of Tateiwa district, Hiroshima Prefecture. *Land and life of the Tateiwa area*, 107–145. (J+E)

Wells,P.R.A(1977): Pyroxene thermometry in simple and complex system. *Contrib. Miner. Petrol.* **62**, 129–139.

Whitney,J.A. and Stormer,J.R(1977): The distribution of $NaAlSi_3O_8$ between coexisting microcline and plagioclase and its effect on geothermometric calculations. *Amer. Mineral.*, **62**, 687–691.

Wise,D.U.(1964): Microjointing in Basement, Middle Rocky Mountains of Montana and Wyoming. *Geol. Soc. Amer. Bull.*, **78**, 287–306.

Woodcock,N.H. and Underhill,J.R.(1987): Emplacement–related fault pattern around the Northern Granite, Arran, Scotland. *Geol. Soc. Amer. Bull.*, **98**, 515–527.

J: in Japanese, J+E: in Japanese with English abstract

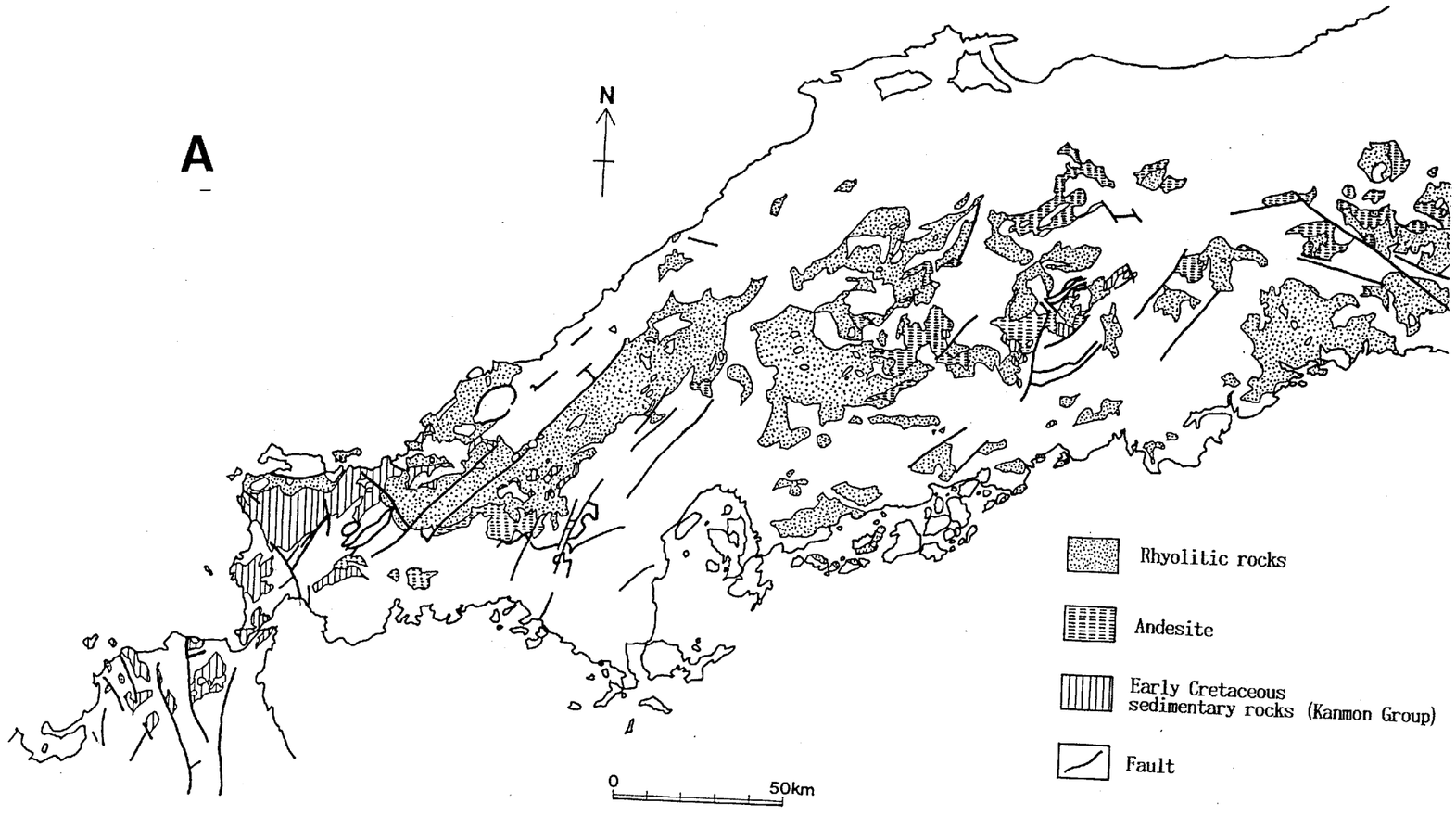

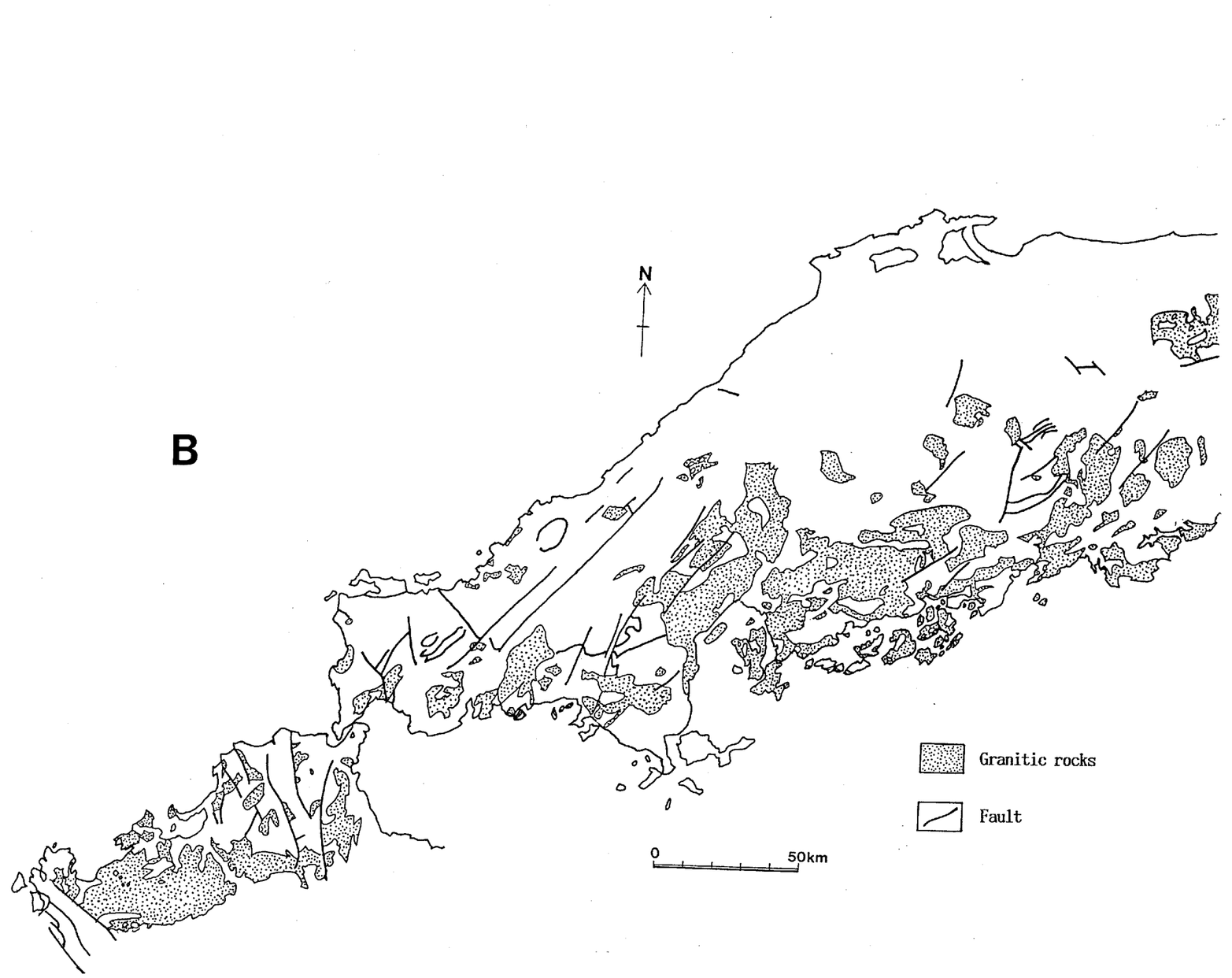

Fig. 1. Distribution of late Cretaceous to early Palaeogene igneous rocks and sedimentary rocks in Chugoku – Kyushu Province (compiled from Geological Survey of Japan, 1982 and Hayashi, 1989).
A:volcanic and sedimentary rocks, B:granitic rocks in the San–yo zone.

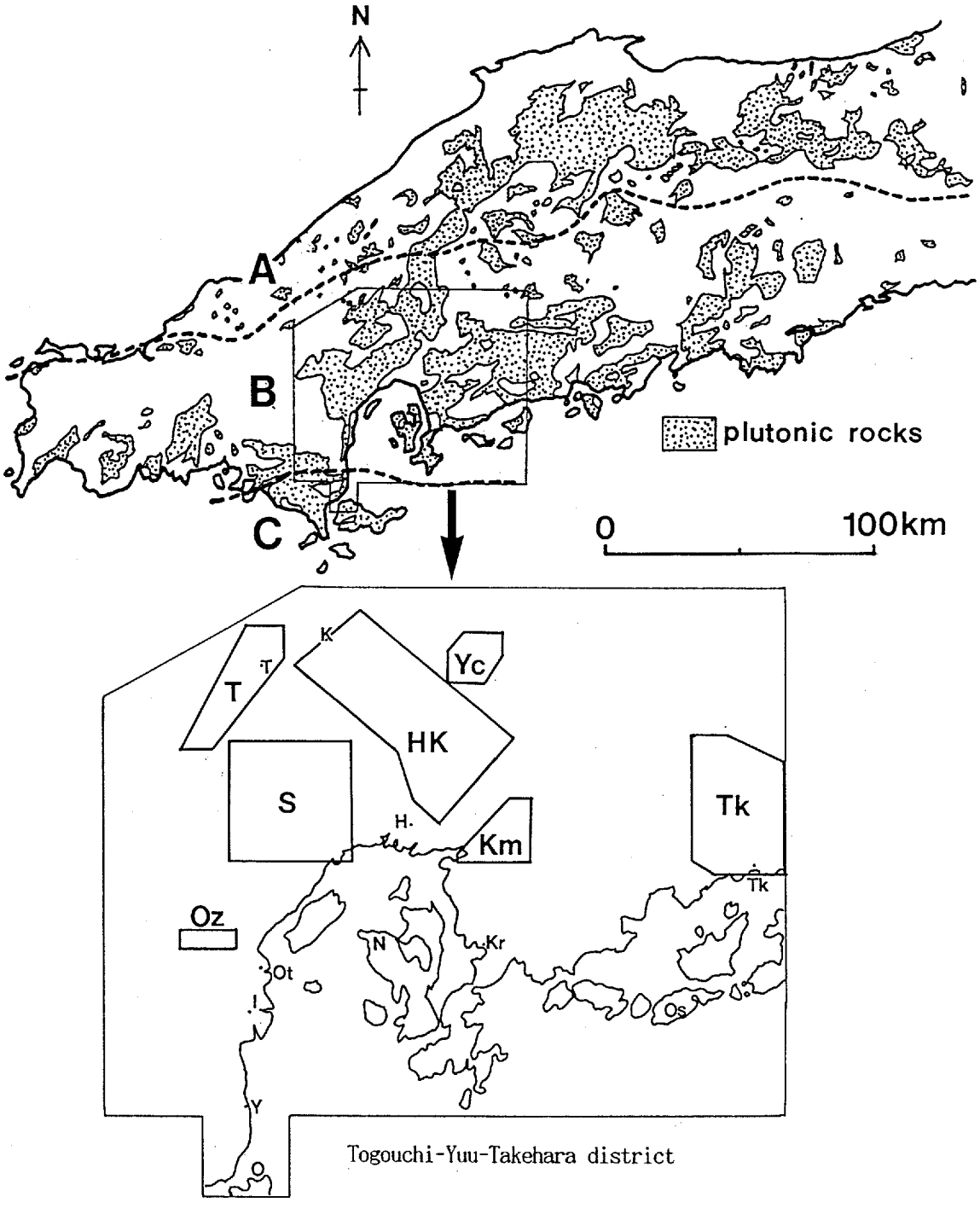

Fig. 2. Diagram showing the distribution of granitic rocks in Chugoku Province and the location of the studied area.
A: San-in zone, B: San-yo zone, C: Ryoke zone
HK:Hiroshima-Kake area, Km:Kumano area, O:Ozegawa area, S:Saeki area, T:Togouchi area, Tk:Takehara area, Y:Yachiyo area.
H:Hiroshima, I:Iwakuni, K:Kake, Kr:Kure, N:Nomizima, O:Oshima, Os:Osakishimozima, Ot:Otake, T:Togouchi, Tk:Takehara, Y:Yuu.

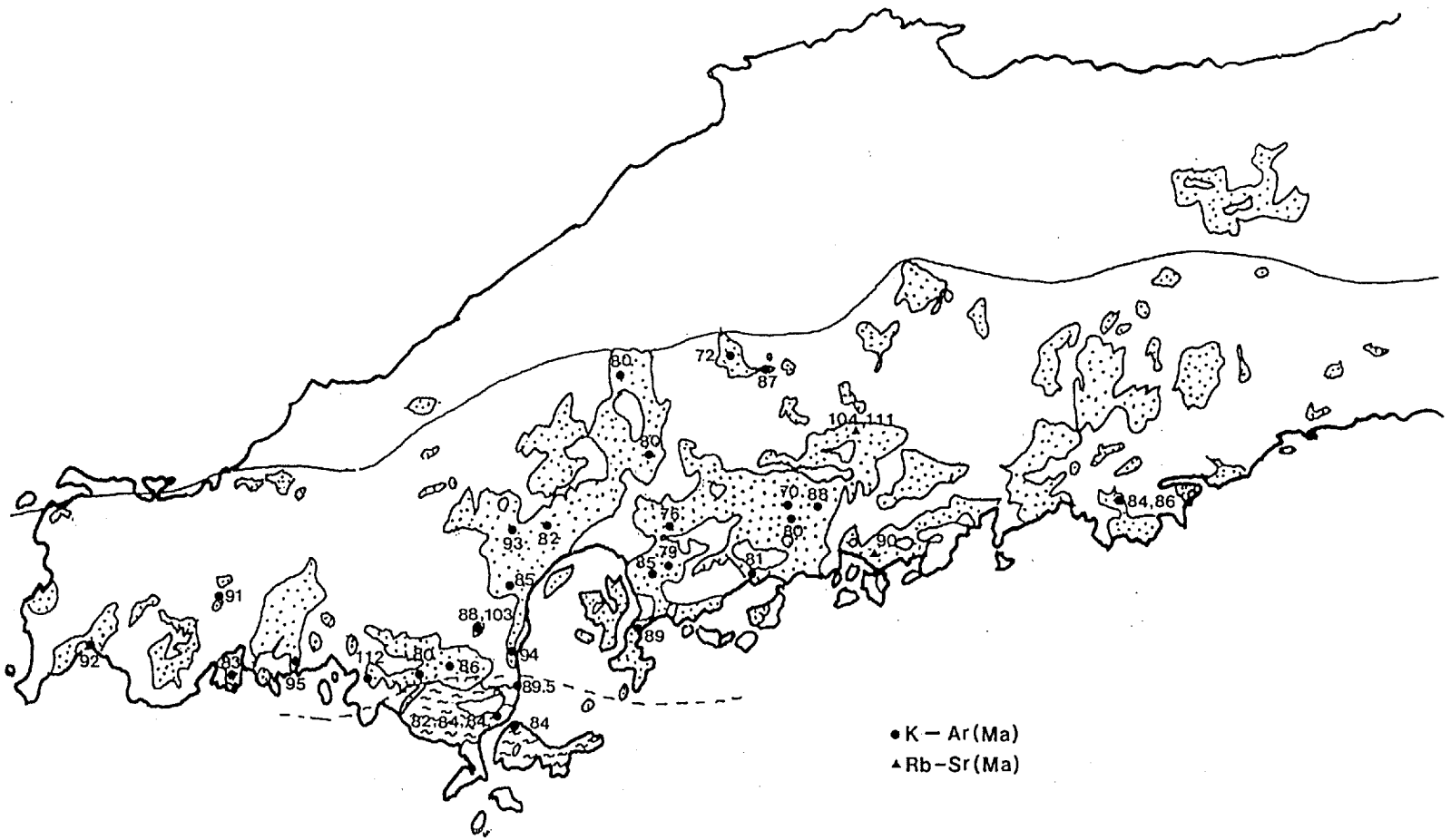

Fig. 3. Spatial variation of the radiometric ages of granitic rocks in the San–yo and Ryoke zones (compiled from Geological Survey of Japan,1982; Higashimoto et al., 1983,1985,1986).

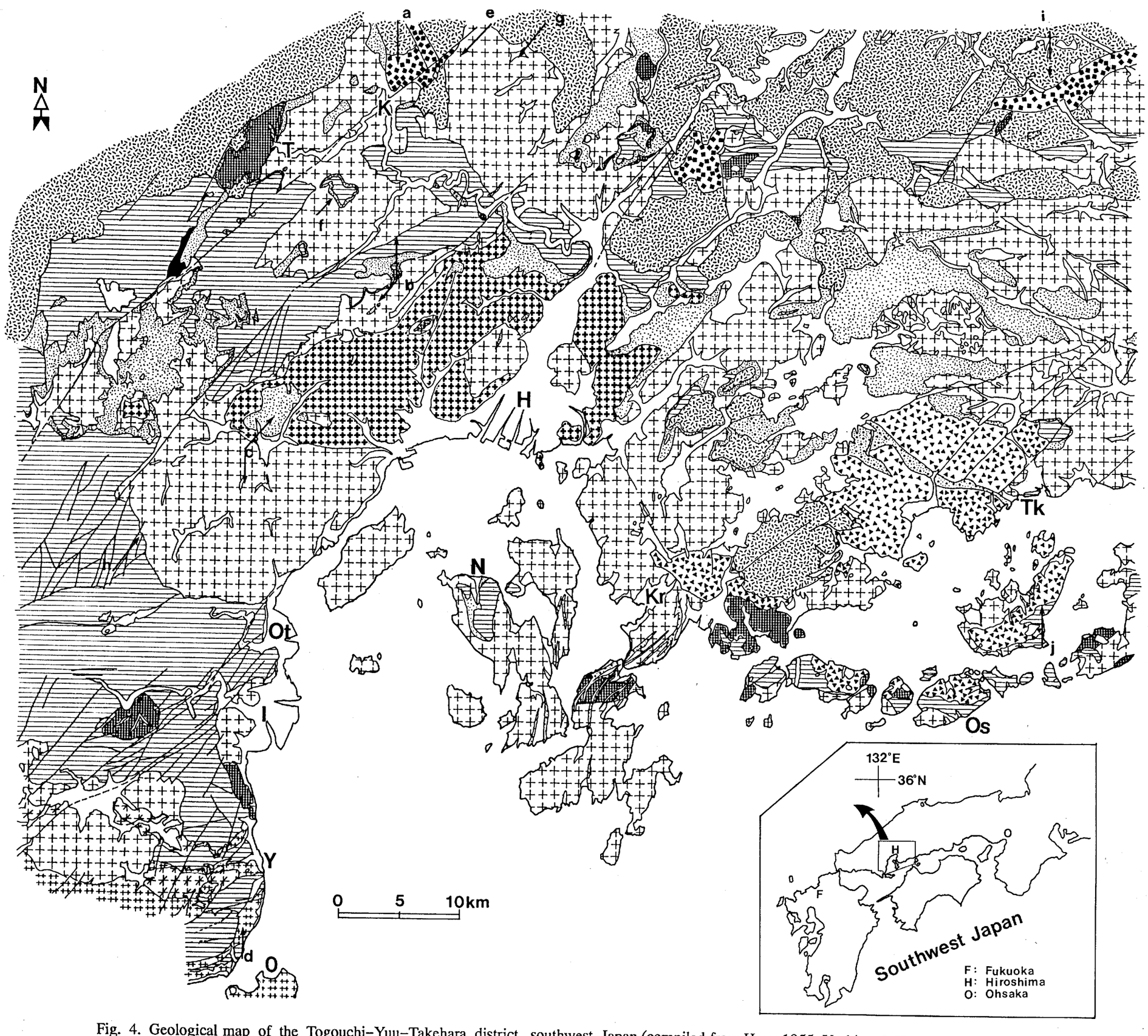

Cenozoic Group
Granite porphyry
Fine-grained granite
Medium-to coarse-grained biotite granite
Medium-to coarse-grained hornblende-biotite granite
Medium-to coarse-grained granodiorite
Fine-grained granodiorite
Tonalite
Rhyolitic rocks
Dacitic-rhyolitic rocks
Andesite
Younger Ryoke granitic rocks
Older Ryoke granitic rocks
Pre-Cretaceous formations
Fault

H Hiroshima
I Iwakuni
K Kake
Kr Kure
N Nomizima(Isd.)
O Oshima(Isd.)
Os Osakisimozima(Isd.)
Ot Otake
T Togouchi
Tk Takehara
Y Yuu

Fig. 4. Geological map of the Togouchi-Yuu-Takehara district, southwest Japan (compiled from Hara, 1955; Yoshino & Hayashi, 1979; Yoshida et al., 1985; Suzuki,T., 1986; Yamada et al., 1986; Takahashi,Y. et al., 1989; Yoshino & Hayashi, 1989; Hayashi, 1989; Takahashi,Y 1991; Hara et al., 1991 and the present author's data).

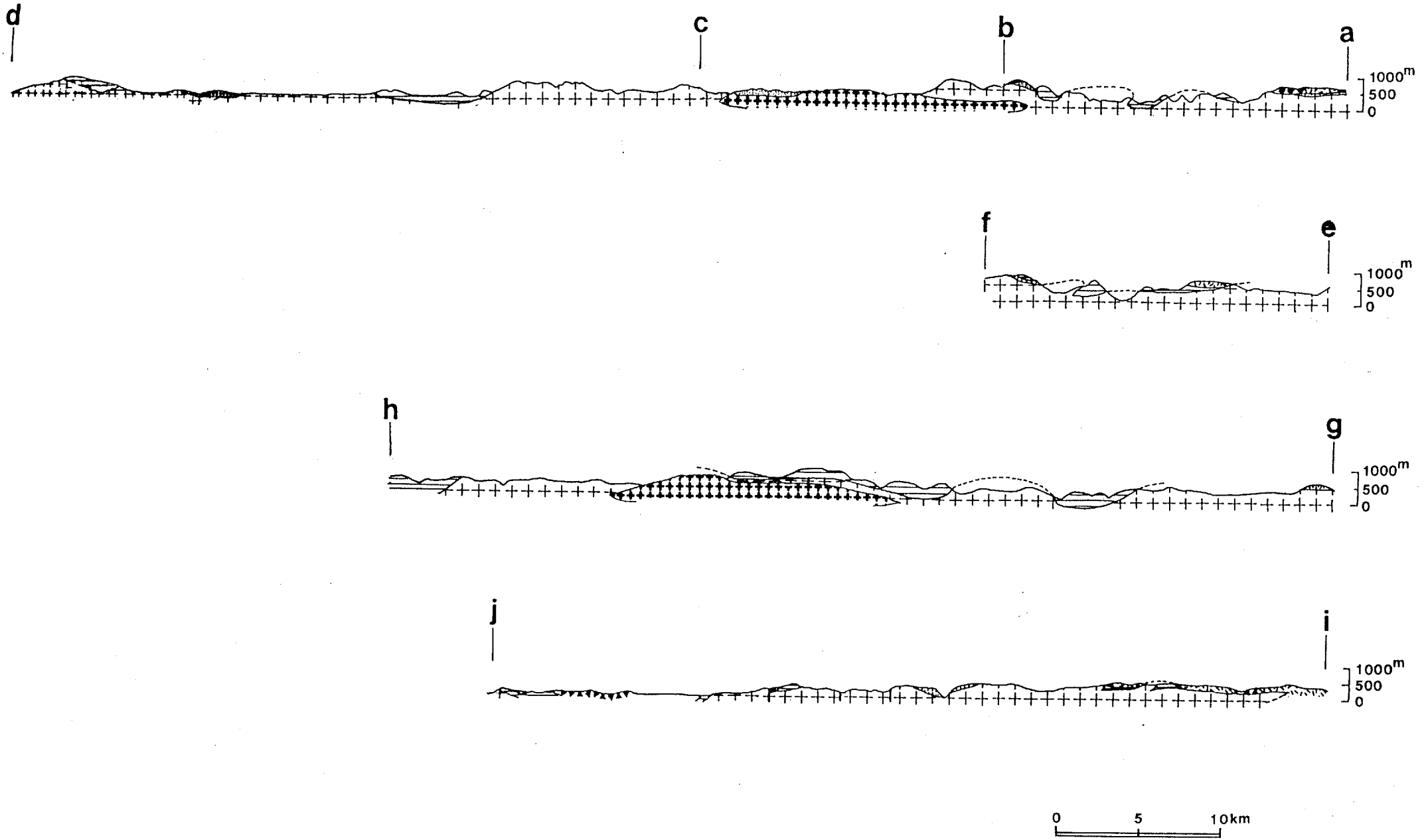

Fig 5. Geological profiles of the Togouchi–Yuu–Takehara district. See Fig. 4 for legend and location of the profiles lines.

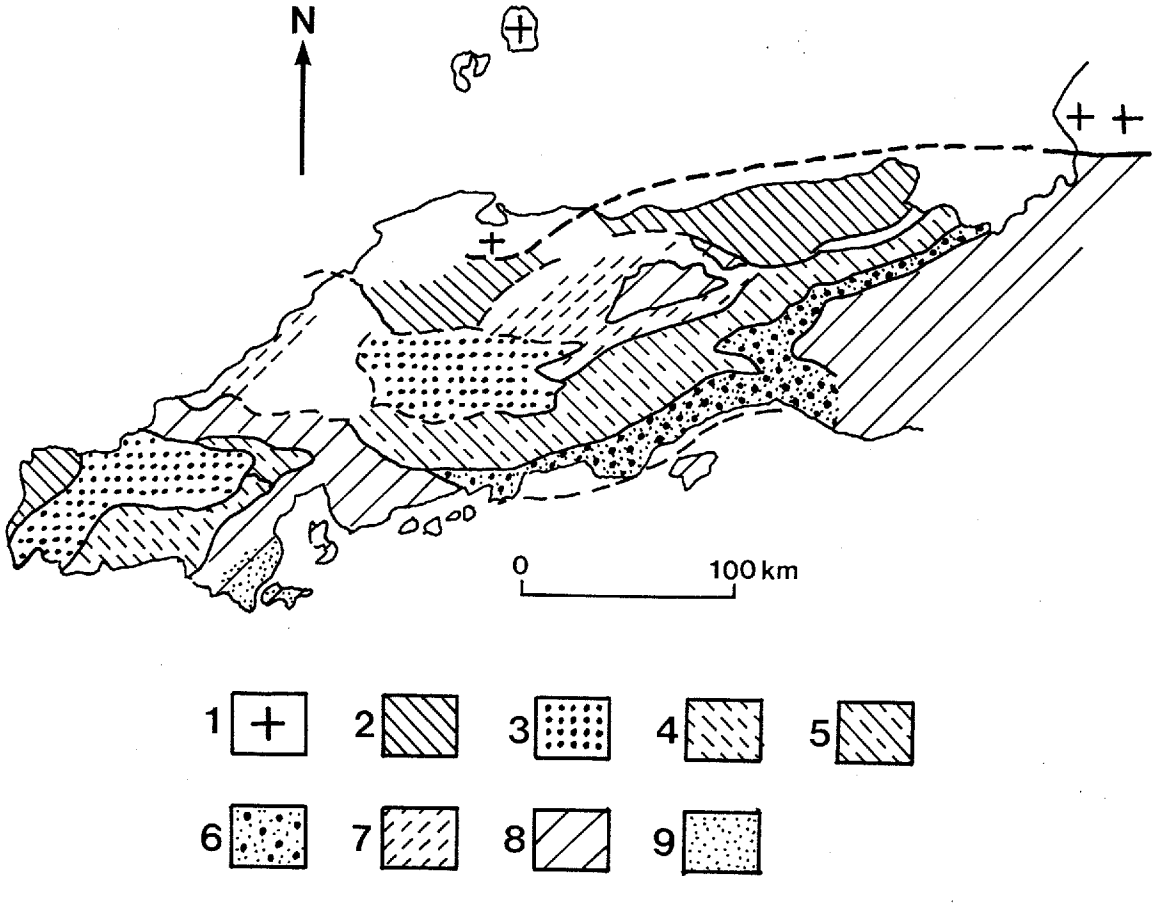

Fig. 6. Distribution of pre-Cretaceous terranes in Chugoku Province.
1:Hida Terrane, 2:Sangun-Renge belt (Hida "Gaien" belt), 3:Akiyoshi Terrane, 4:Suo Tarrane, 5:Maizuru Terrane, 6:Ultra-Tamba Terrane, 7:Chizu Terrane, 8:Kuga-Tamba-Mino-Ashio Terrane, 9:Ryoke metamorphic belt (compiled from Ichikawa, 1990 and Hara et al., 1992).

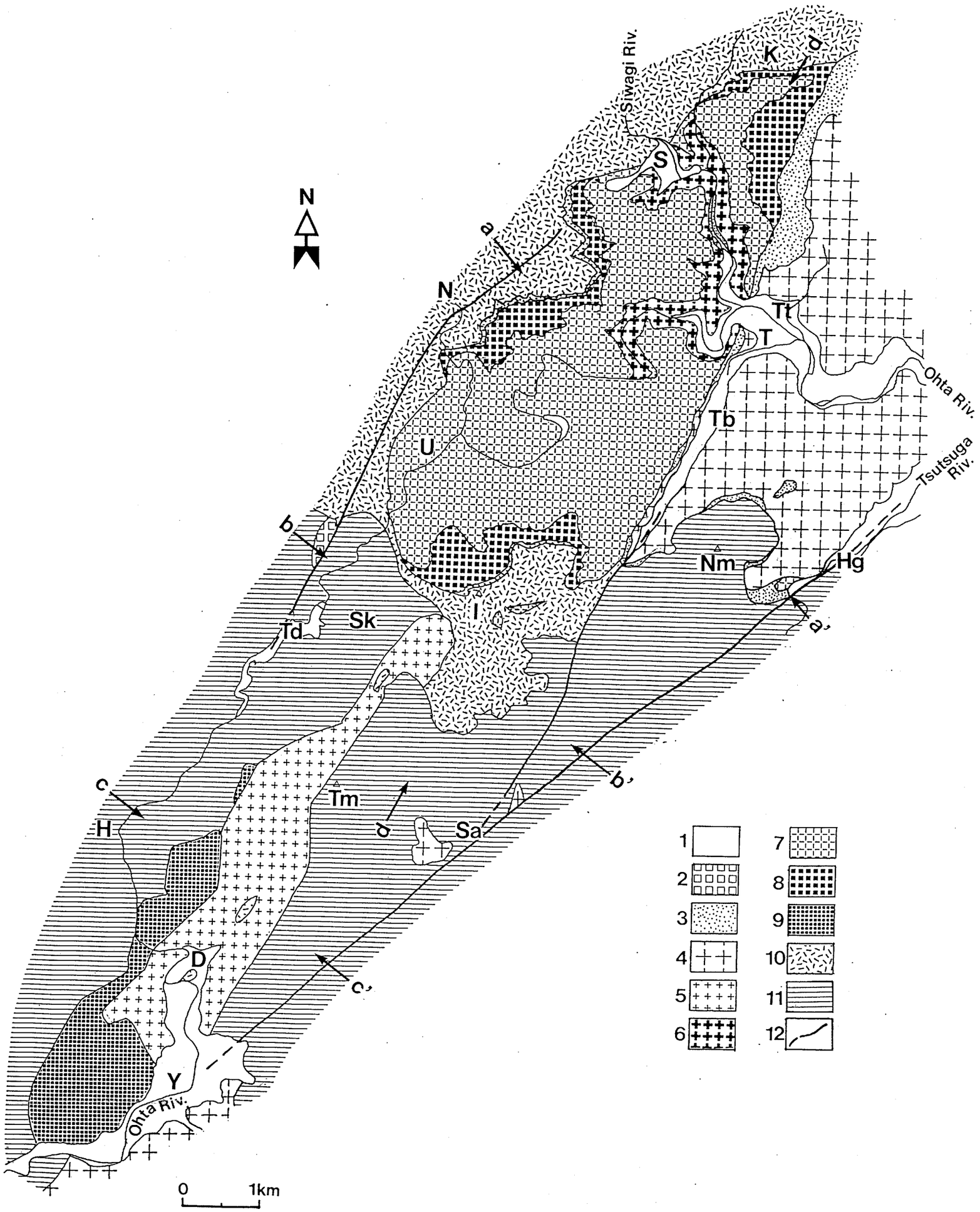

Fig. 7. Geological map of the Togouchi area placed in the northwestern marginal part of the Togouchi–Yuu–Takehara district, southwest Japan.
1:Quaternary, 2:granite porphyry, 3–9:Hiroshima granites, 3;fine–grained granite and aplitic rocks, 4;medium–grained granite, 5;porphyritic granite, 6–8;granodiorite (6,7 and 8;lower, middle and upper lithologic facies respectively, See text in detail), 9;tonalite, 10:Takada rhyolitic rocks, 11:pre–Cretaceous Yoshiwa formation, 12:fault.
D:Dani, H:Hosomidani, Hg:Hagiwara, I:Mt.Ichima, K:Kajinoki, N:Nasu, Nm:Mt.Nabe, S:Shiwagi, Sa:Sakahara, Sk:Sakaidani T:Togouchi, Tb:Tabuki, Td:Tateiwa dam, Tm:Mt.Tateiwa, Tt:Tsubutani, U:Uchinashi, Y:Yoshiwa.

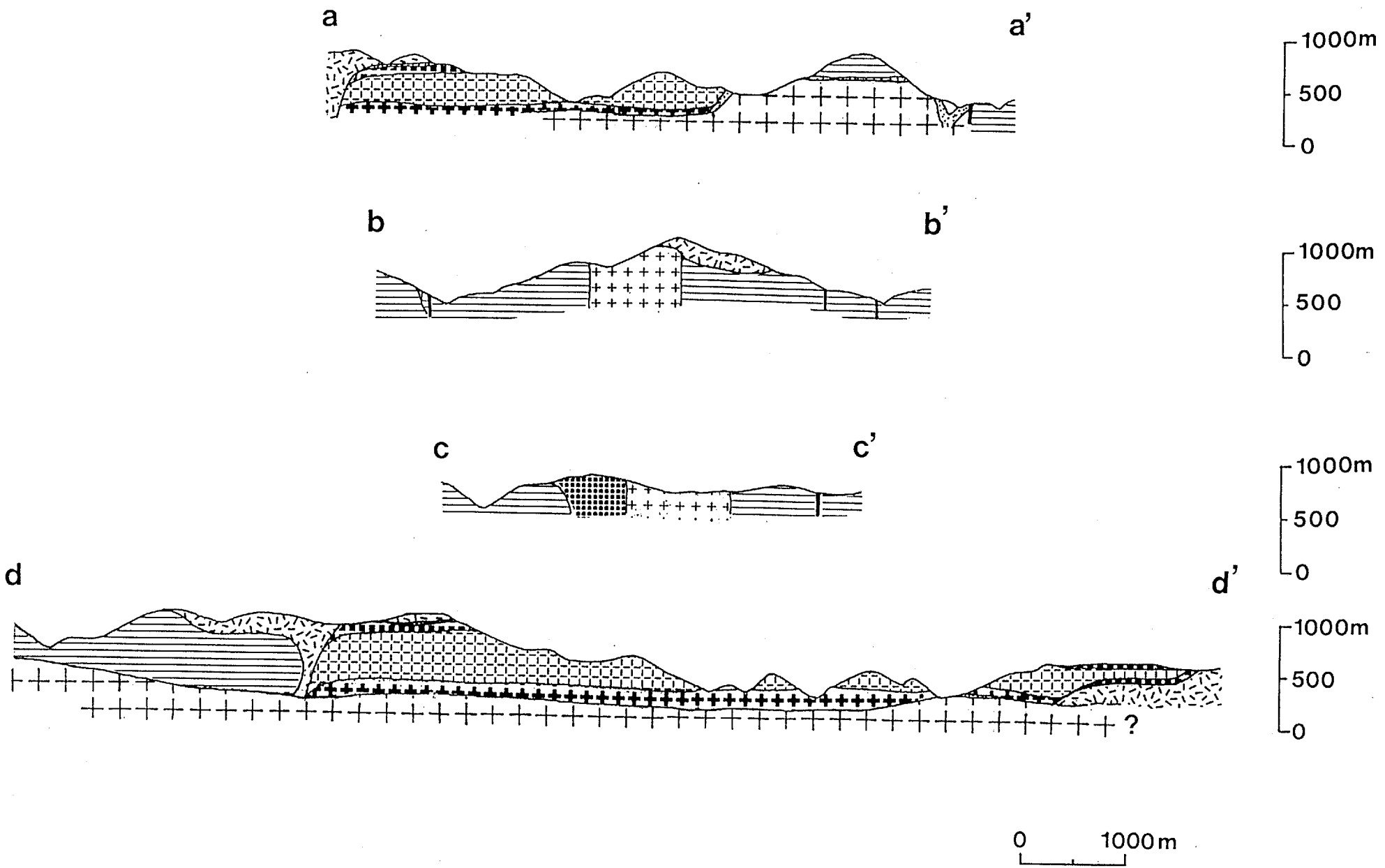

Fig. 8. Geological profiles of the Togouchi area. See Fig. 7 for legend and location of the profile lines.

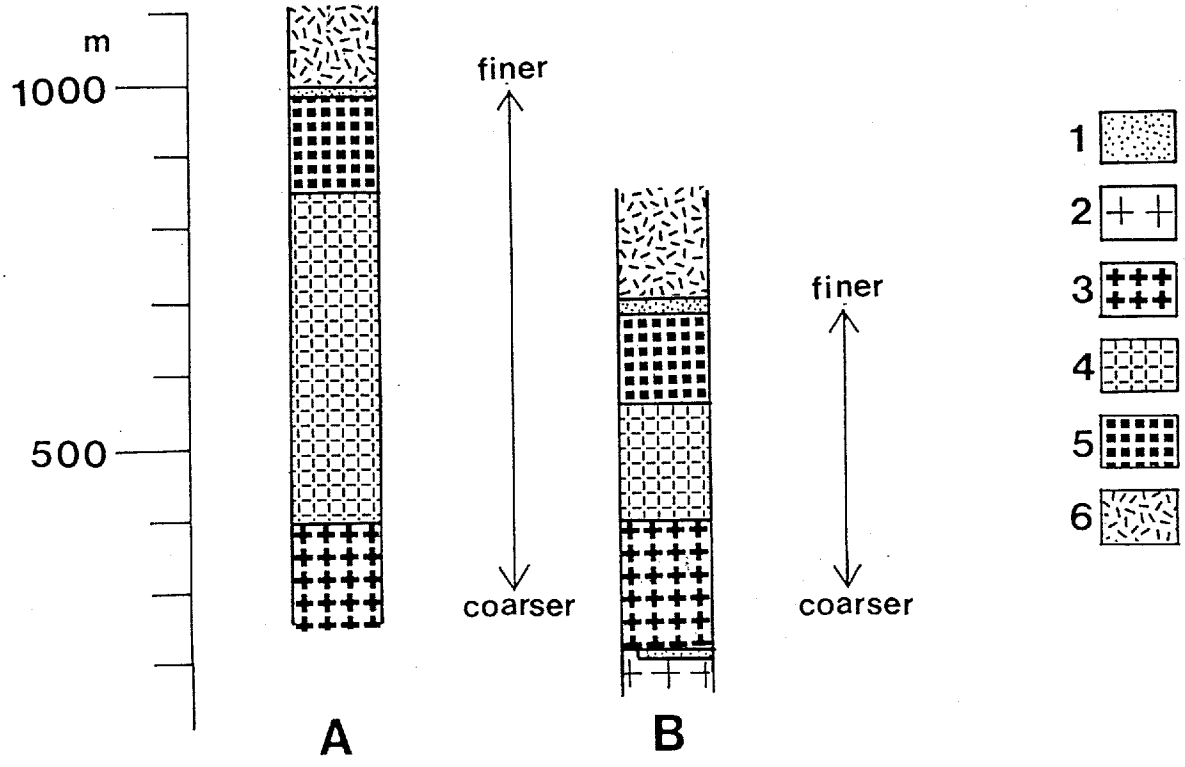

Fig. 9. Schematic diagram illustrating the vertical variation of lithofacies in the granodiorite.
A: Mt. Ichima sub-area, B: Shiwagi-Nasu sub-area.
1:fine-grained granite or aplitic rocks, 2: medium- to coarse-grained granite,
3-5:granodiorite (3;lower lithologic facies, fine-grained porphyritic facies,
4;middle lithologic facies, medium-grained porphyritic or equigranular facies,
5;upper lithologic facies, coarse-grained equigranular facies), 6: rhyolitic rocks
Numbers (meters) show altitude above sea level.

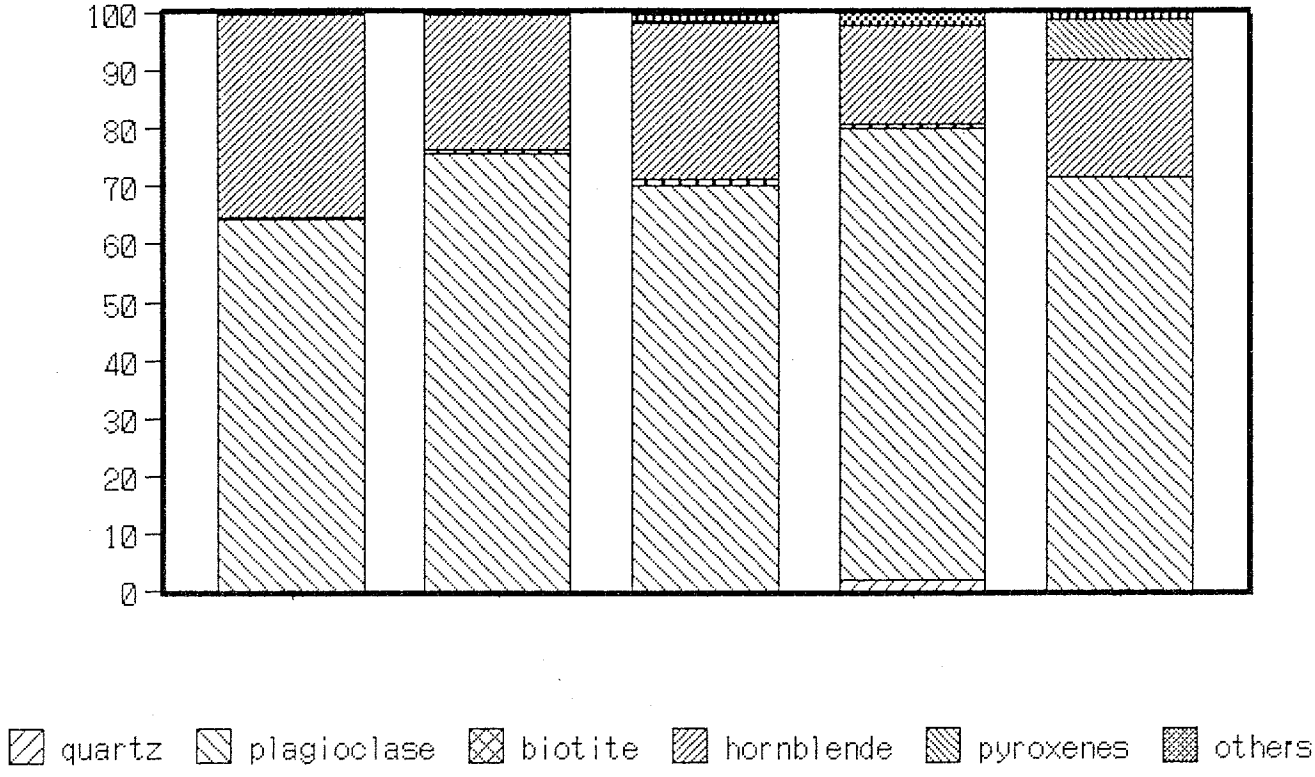

Fig. 10. Modal variation of constituent minerals in the tonalite.

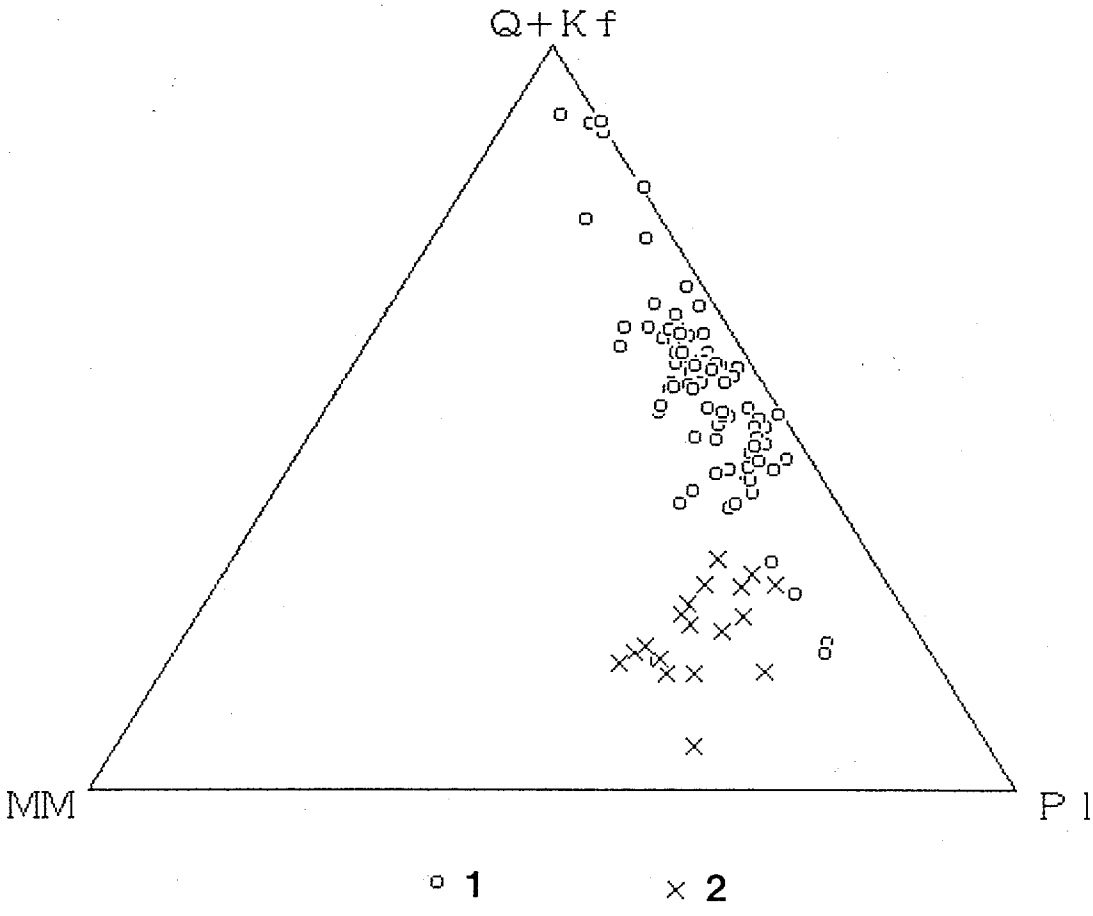

Fig. 11. Modal Q+Kf – MM – Pl diagram for the granodiorite and its associated dark inclusion.
Q:quartz, Kf:K–feldspar, Pl:plagioclase, MM:mafic minerals.
1: granodiorite, 2: dark inclusion.

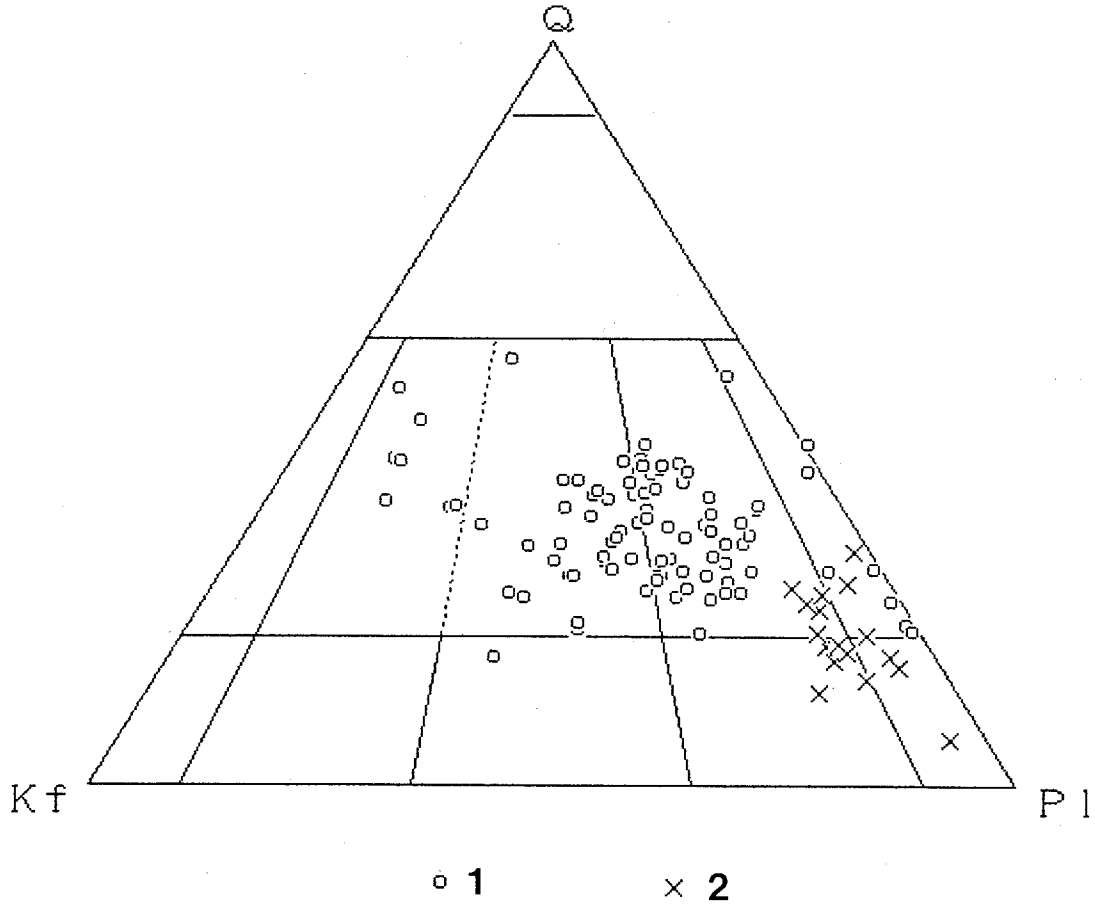

Fig. 12. Modal Q – Kf – Pl diagram for the granodiorite and its associated dark inclusion.

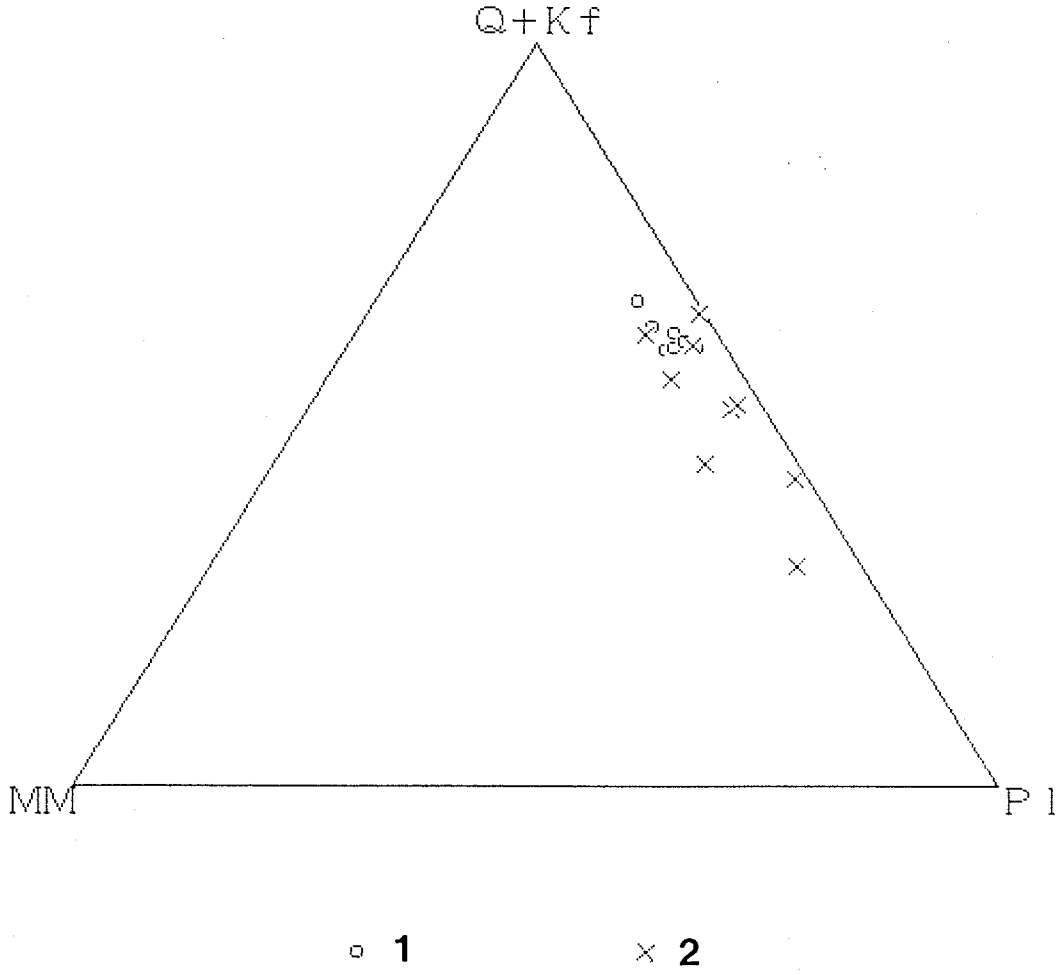

Fig. 13. Modal Q+Kf – MM – Pl diagram for the medium–grained granite and porphyritic granite.
1: medium–grained granite, 2: porphyritic granite.

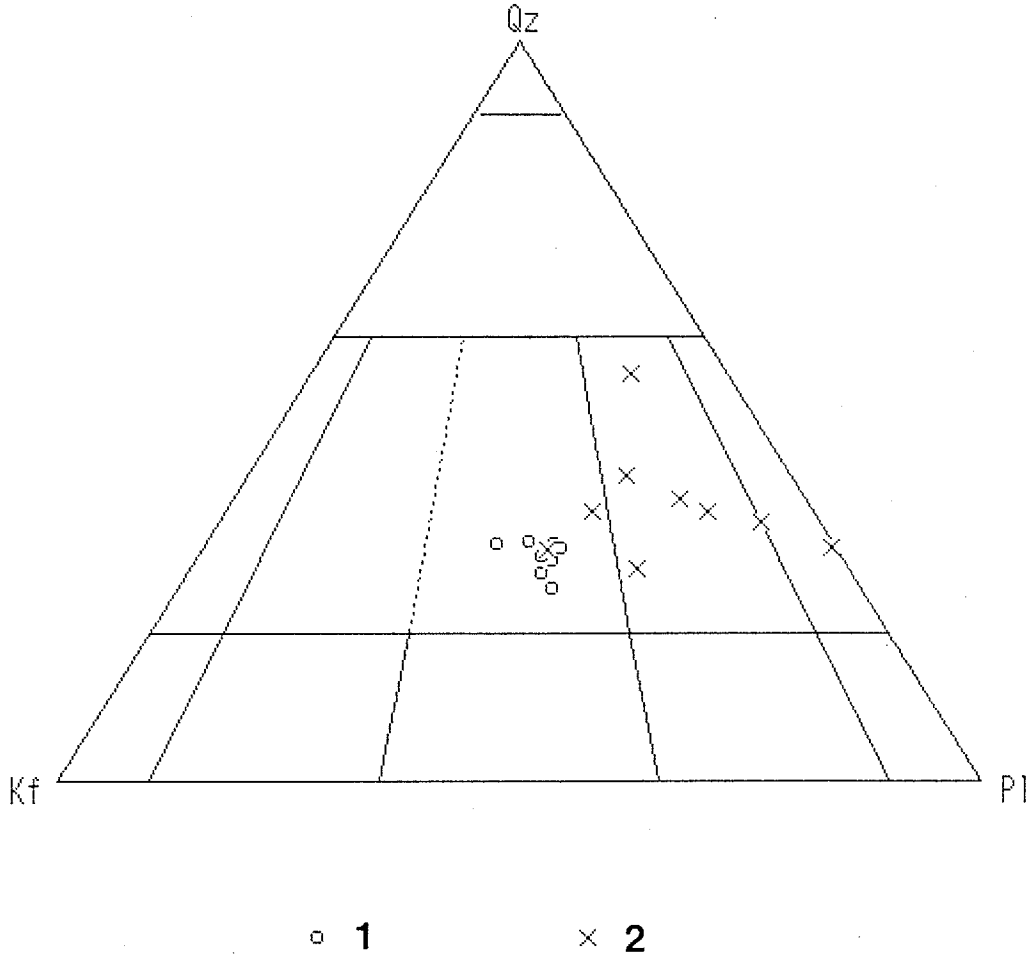

Fig. 14. Modal Q – Kf – Pl diagram for the medium–grained granite and porpyritic granite.

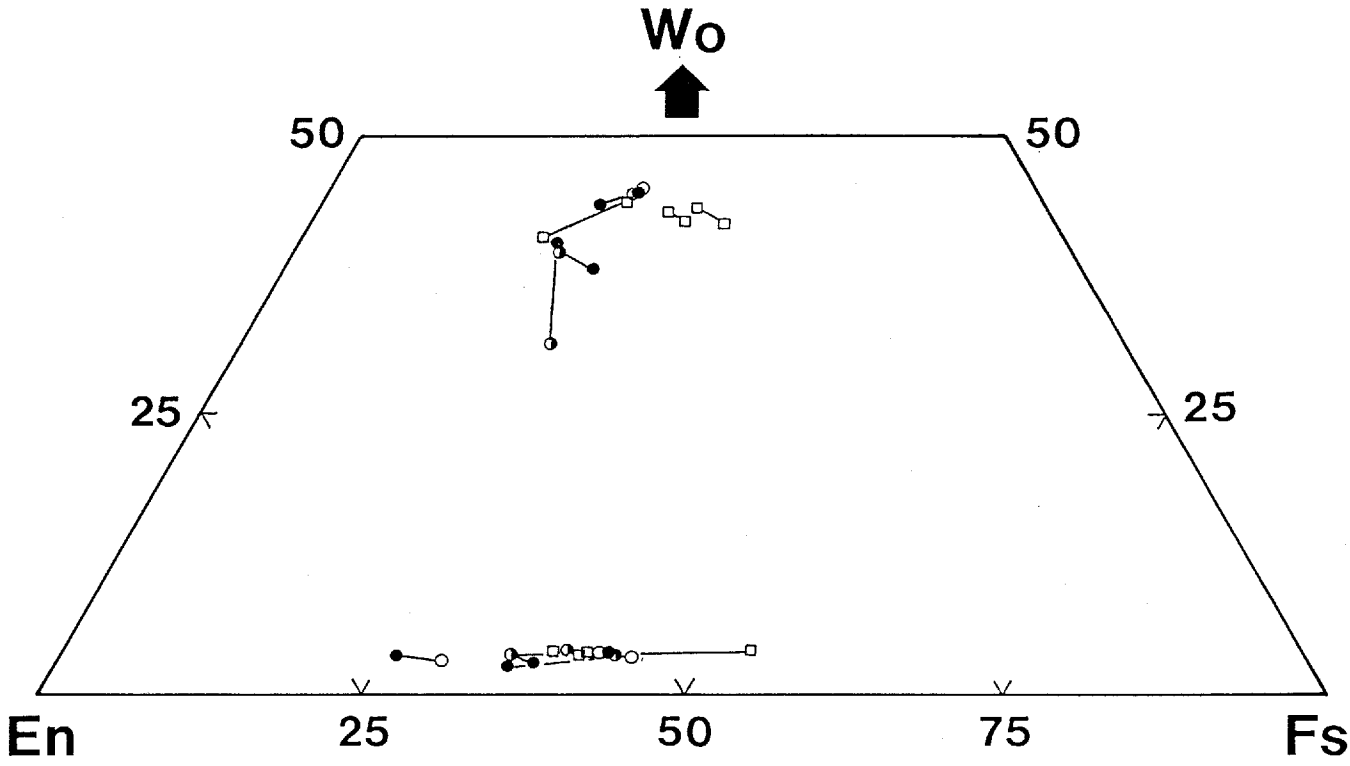

Fig. 15. En – Fs – Wo diagram for pyroxenes from the tonalite.
open circle:data for rim, solid circle:data for core, half solid circle:data for mantle, square:data for non–zoned grain.

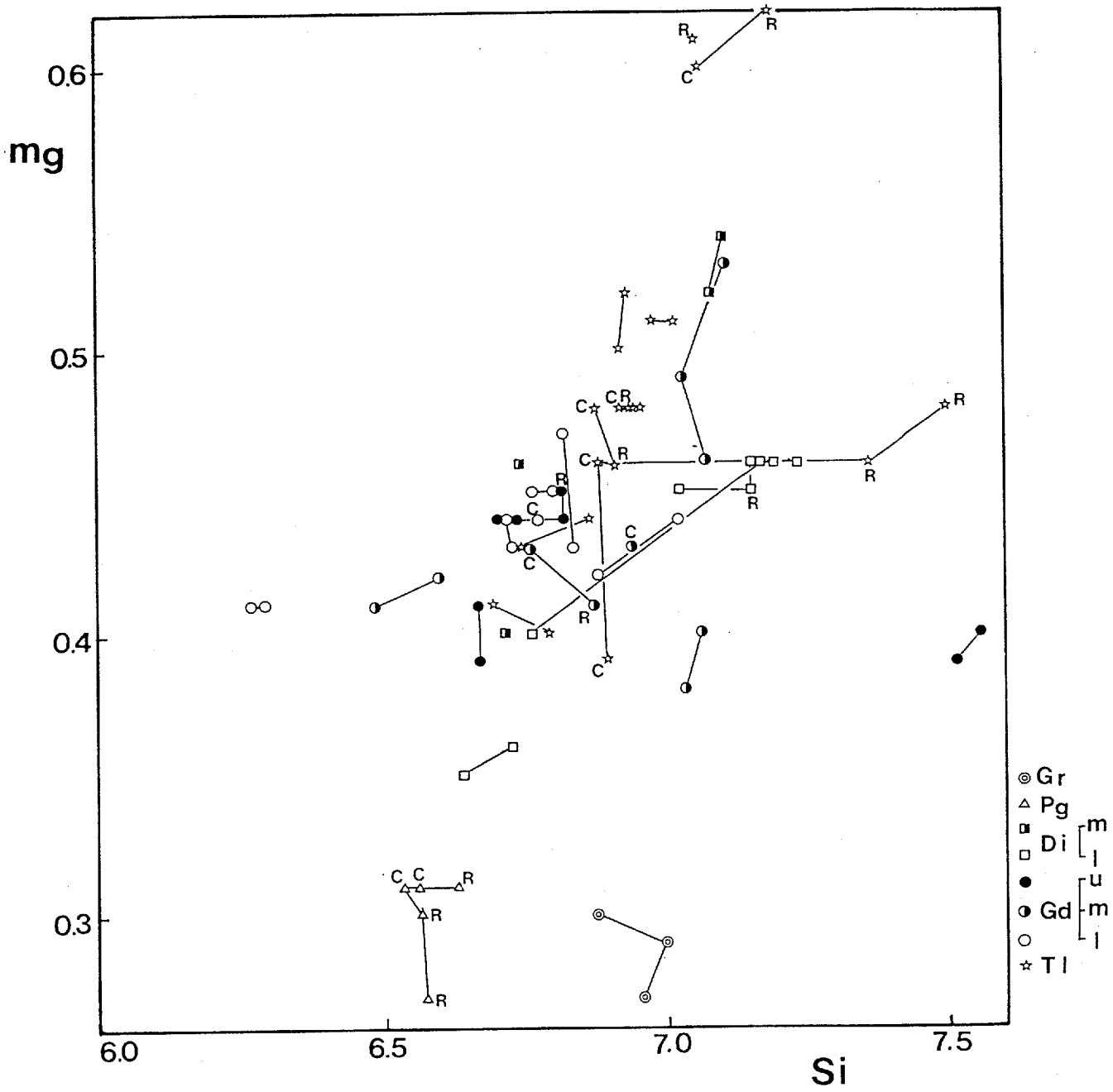

Fig. 16. mg–Si diagram for calcic amphiboles.
Gr: granite, Pg: porphyritic granite, Di: dark inclusion,
Gd: granodiorite, Tl: tonalite.
"u", "m" and "l" in the Gd and the Di show the upper, middle and lower litholofacies of the granodiorite respectively (See text).
C: core, R:rim.

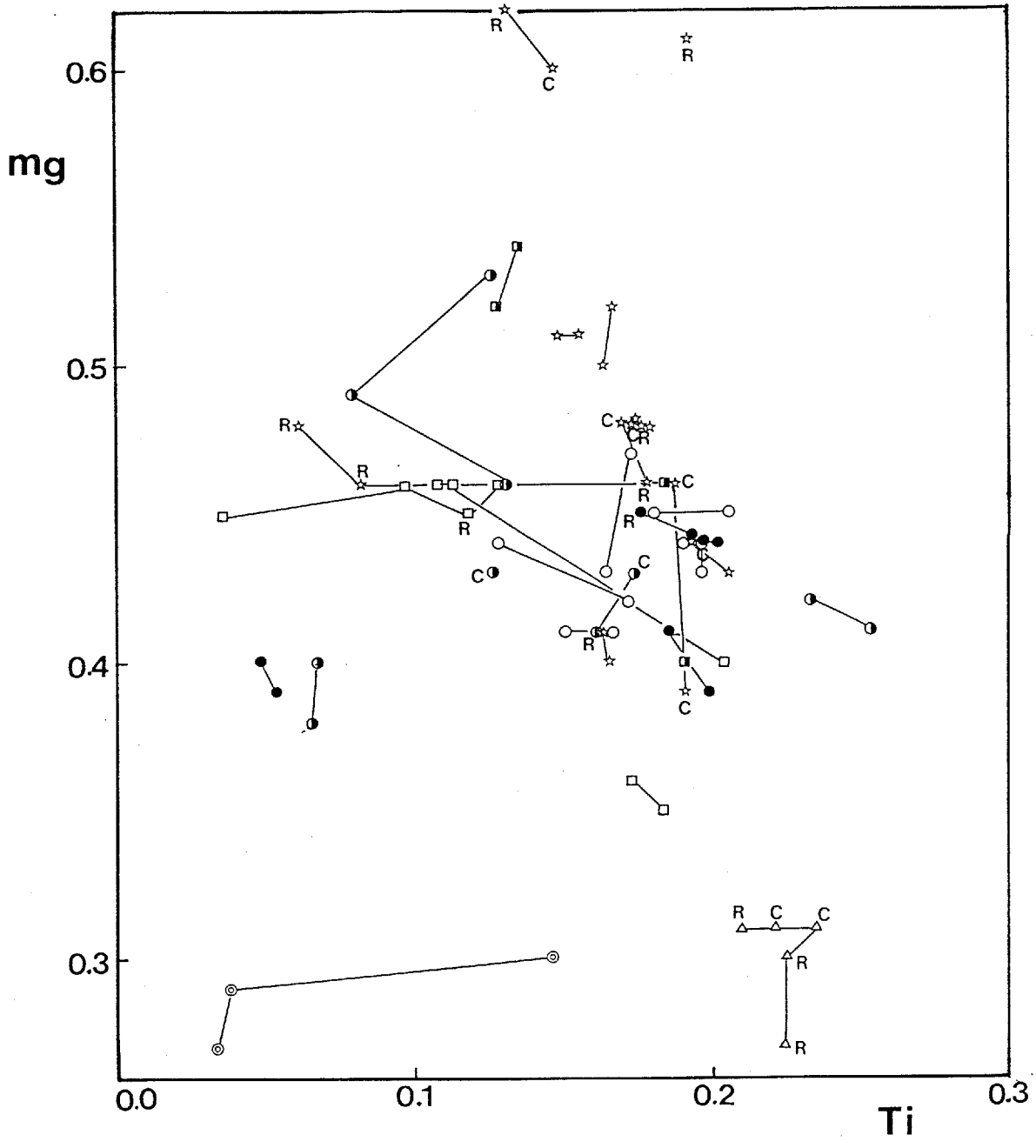

Fig. 17. mg–Ti diagram for calcic amphiboles.
For symbols and abbreviations see Fig. 16.

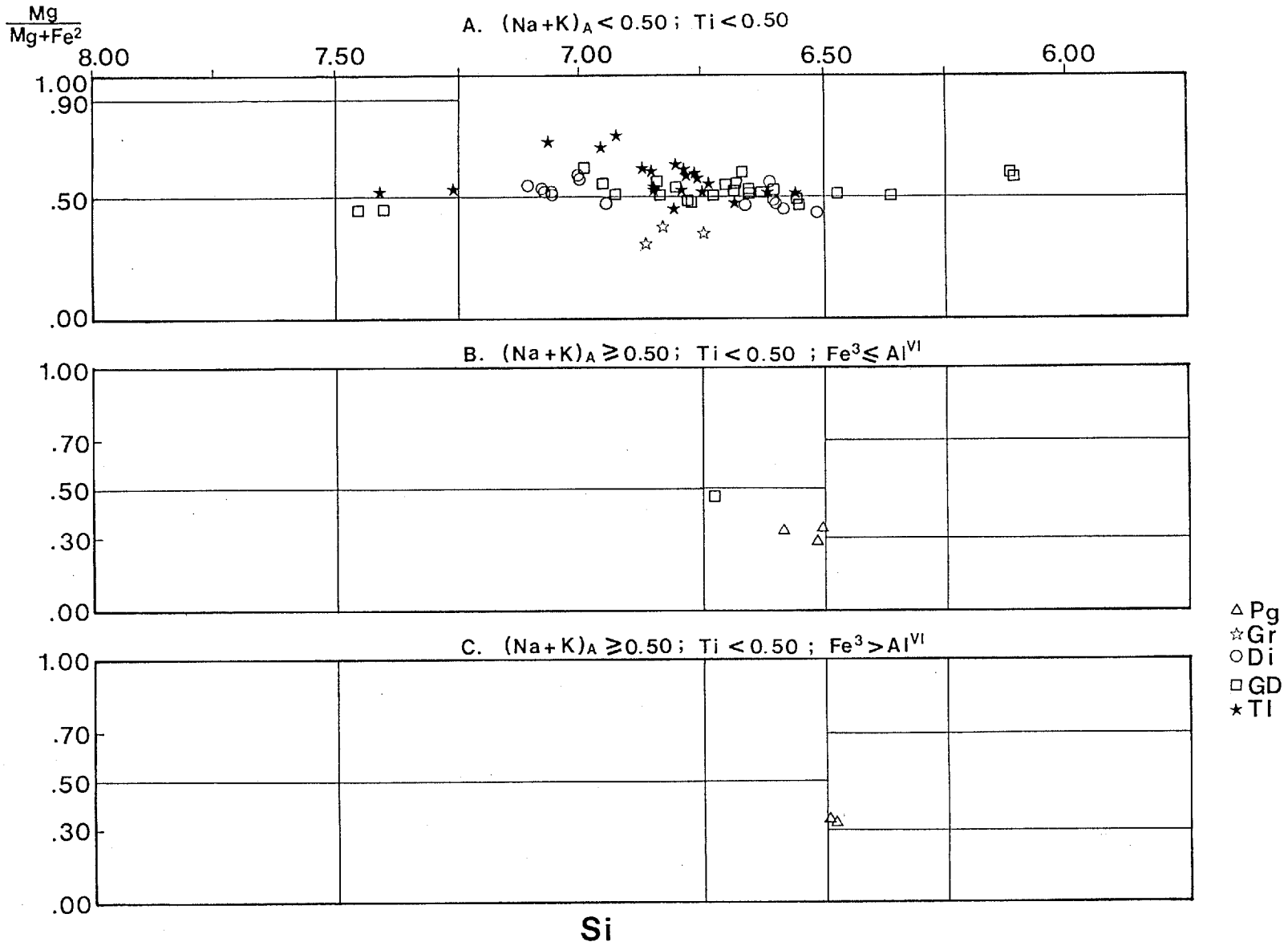

Fig. 18. Plots of calcic amphiboles on Leake's(1978) diagram.
For abbreviations see Fig. 16.

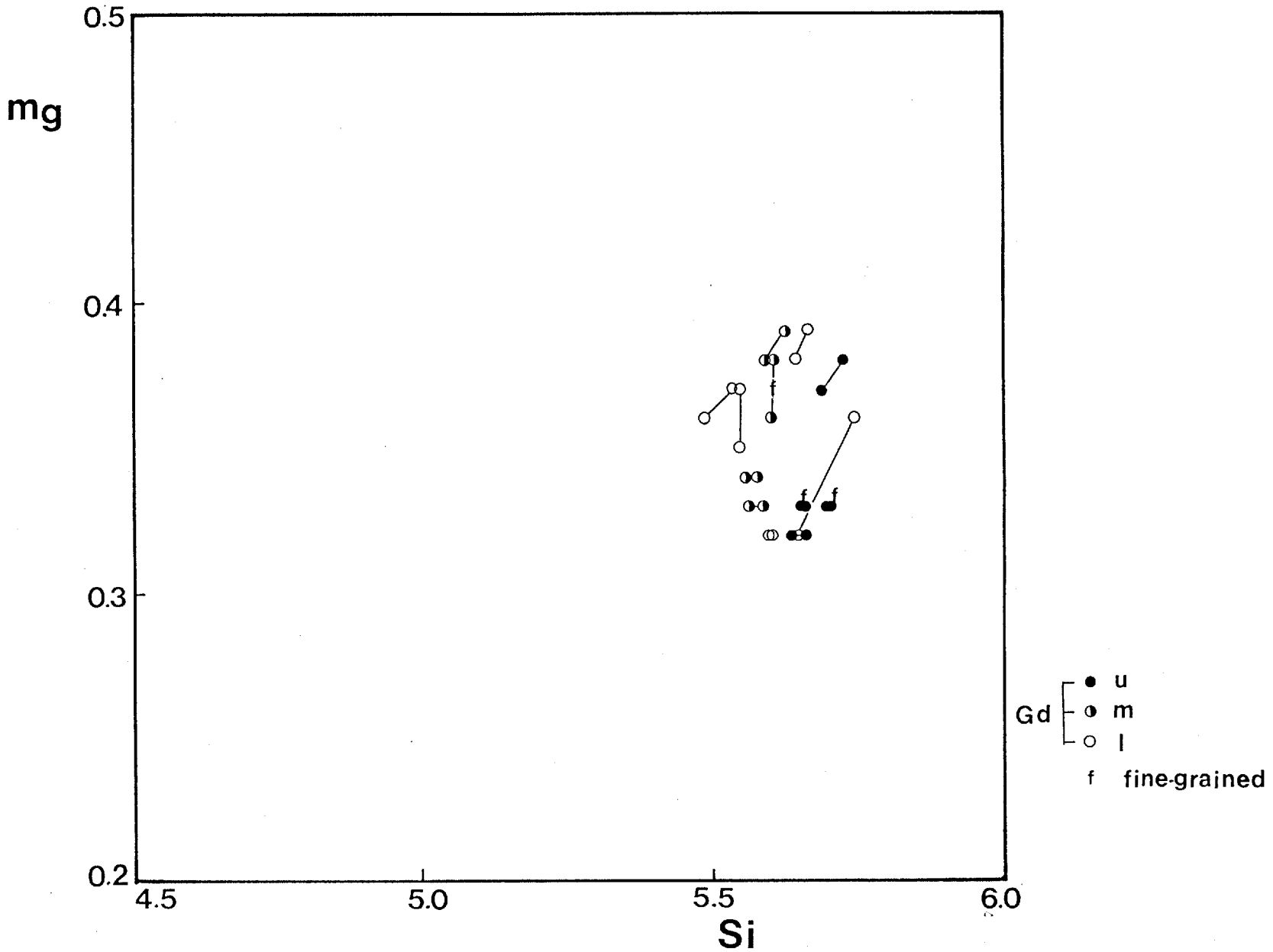

Fig. 19. mg–Si diagram for biotite from the granodiorite.
For abbreviations see Fig. 16.

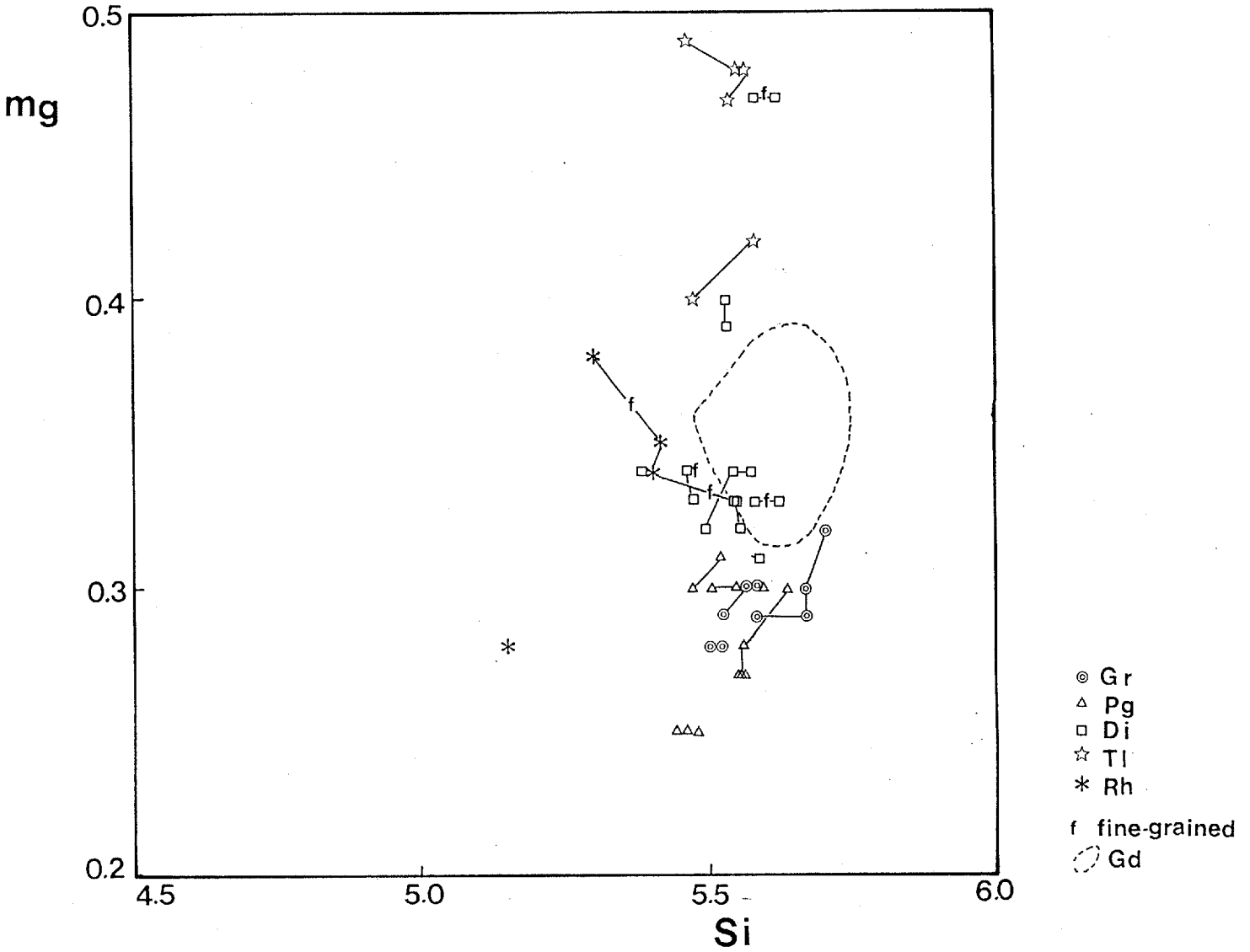

Fig. 20. mg–Si diagram for biotite from the other types of rocks than the granodiorite.
For abbreviations see Fig. 16.
Broken line shows the mg–Si compositional range of biotite in the granodiorite.

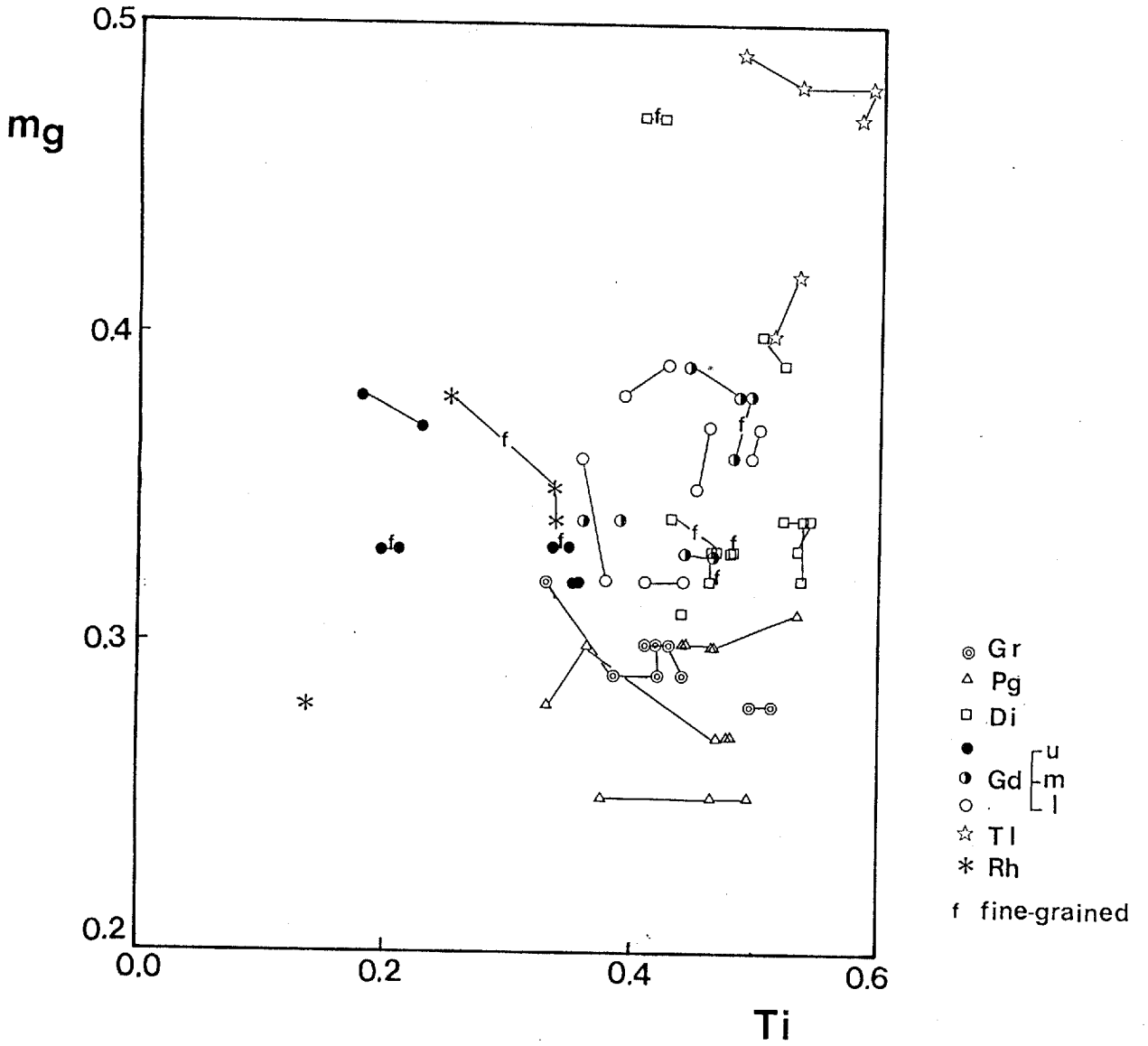

Fig. 21. mg–Ti diagram for biotite.
For abbreviations see Fig. 16.
Rh:rhyolitic rocks.

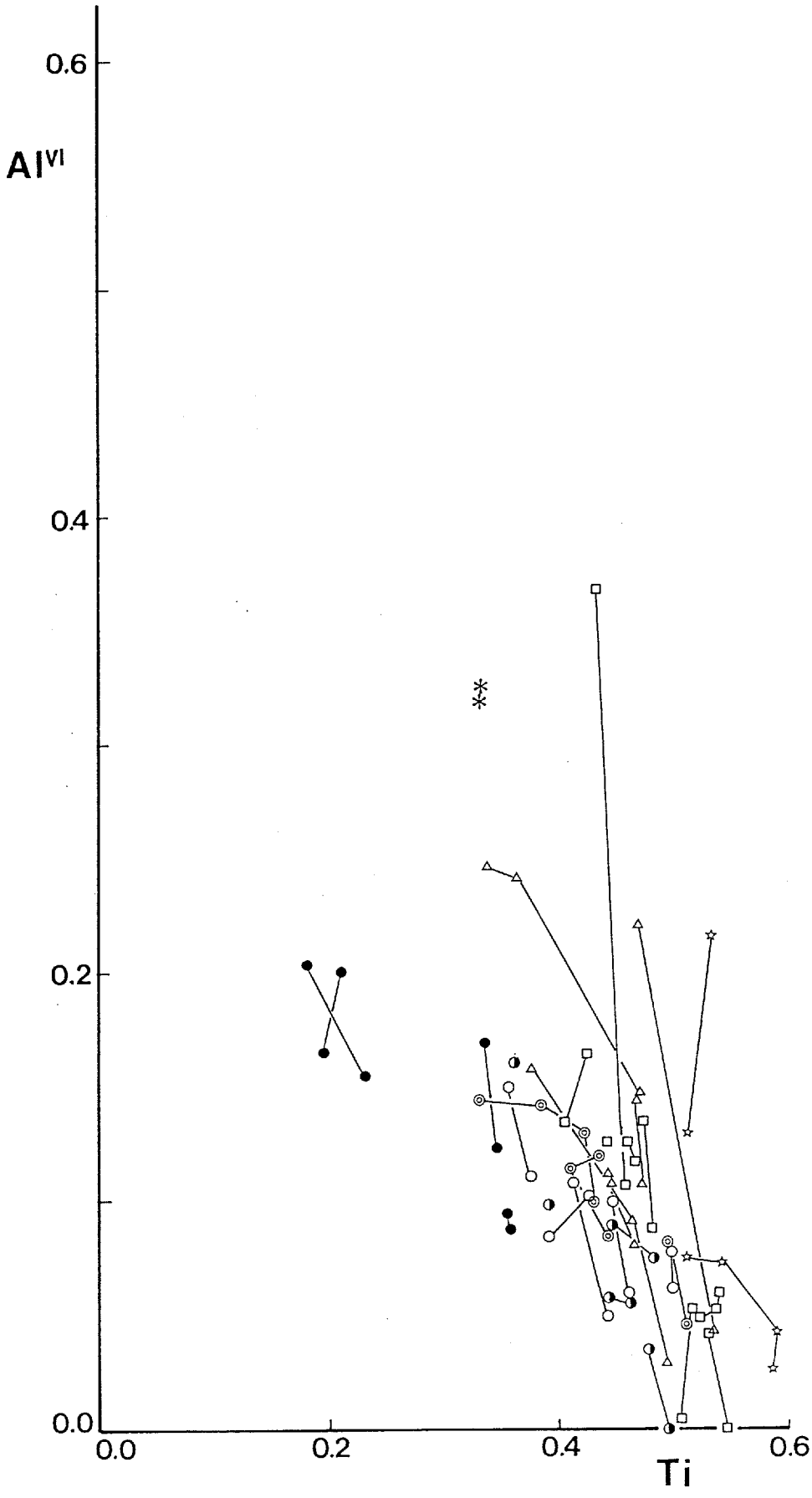

Fig. 22. Al^{VI}–Ti diagram for biotite.
For symbols see Figs. 20 and 21.

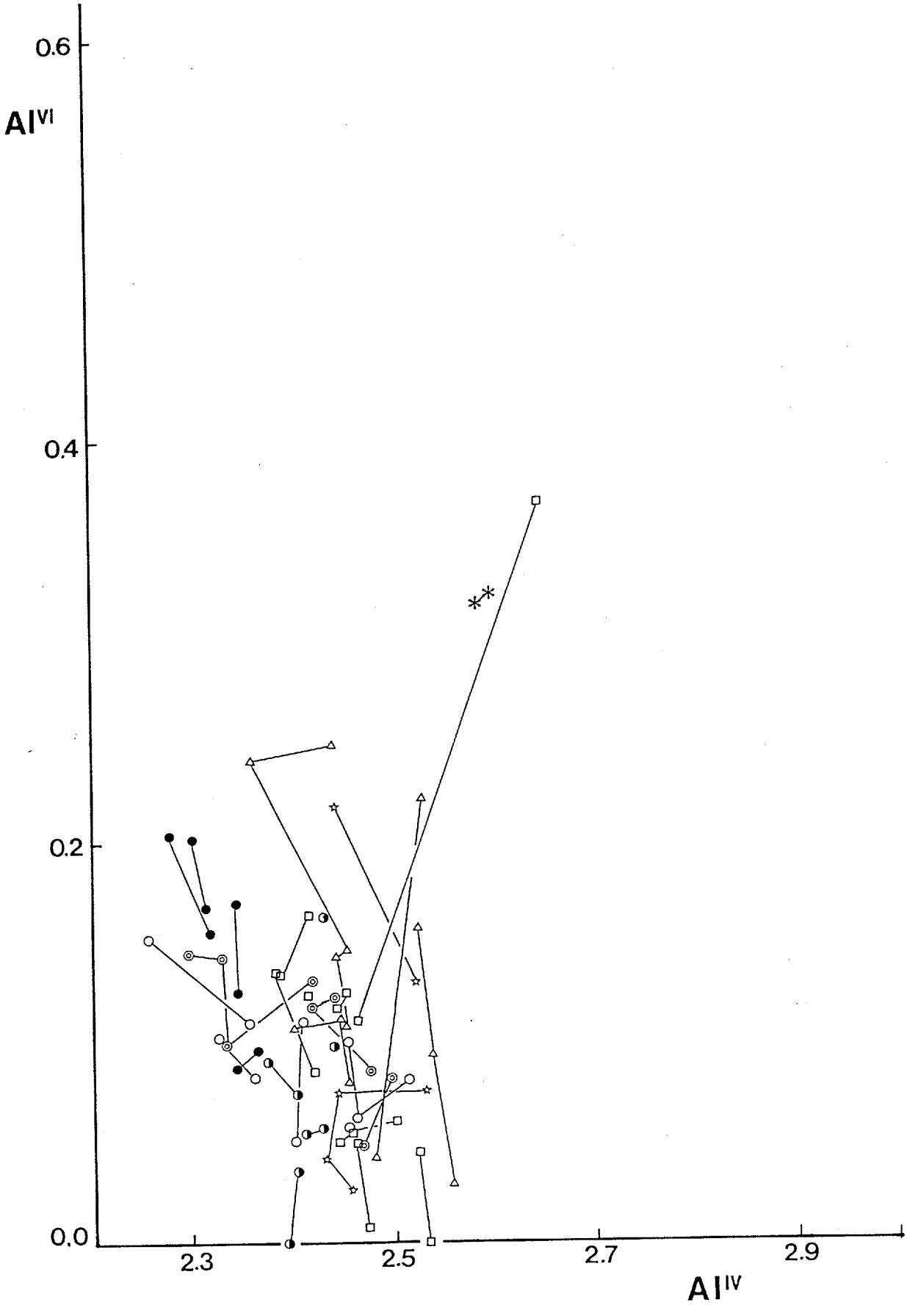

Fig. 23. Al^{VI}–Al^{IV} diagram for biotite.
For symbols see Figs. 20 and 21.

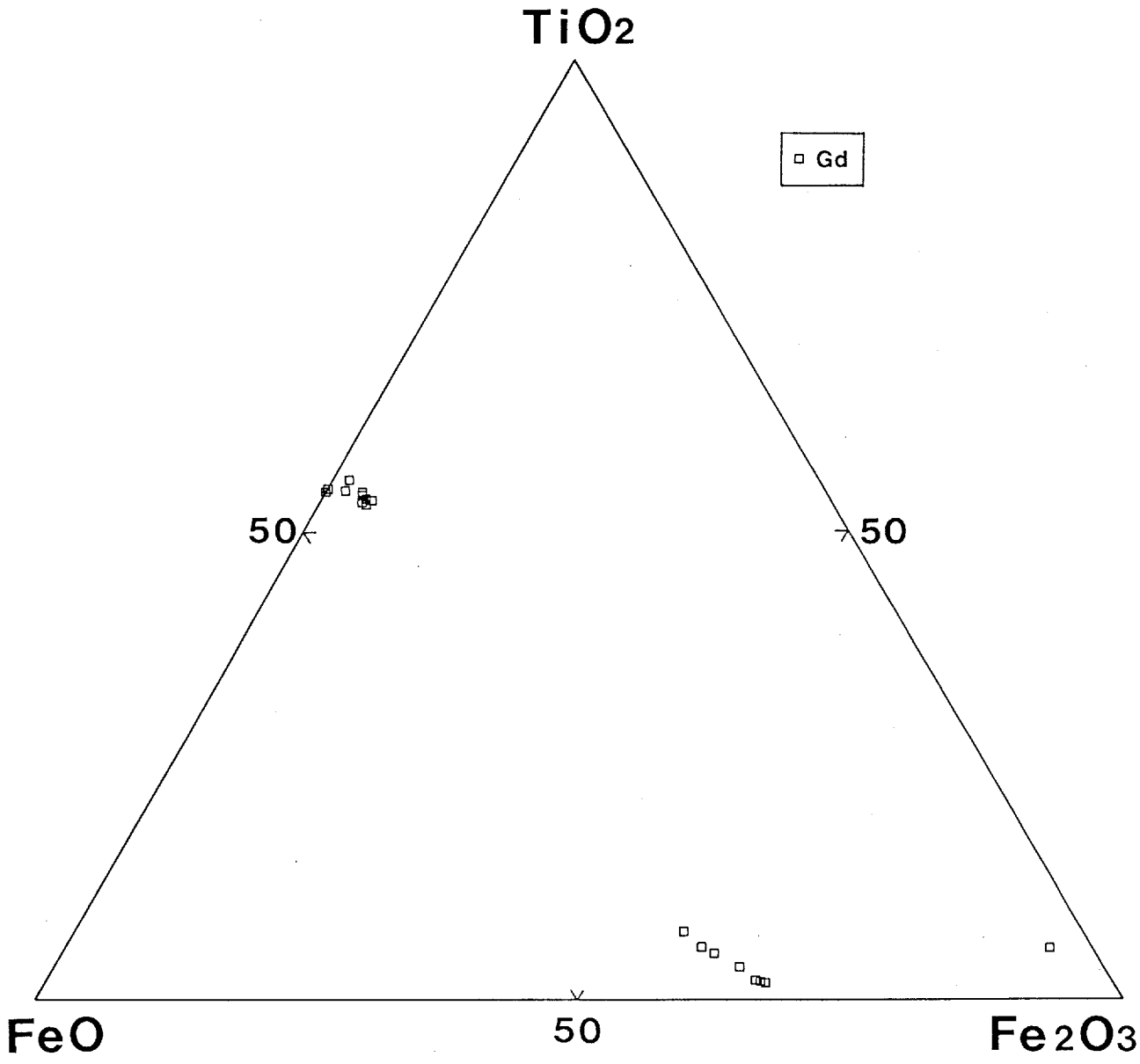

Fig. 24. $FeO–Fe_2O_3–TiO_2$ diagram for iron–titan oxides from the granodiorite. For abbreviations see Fig. 16.

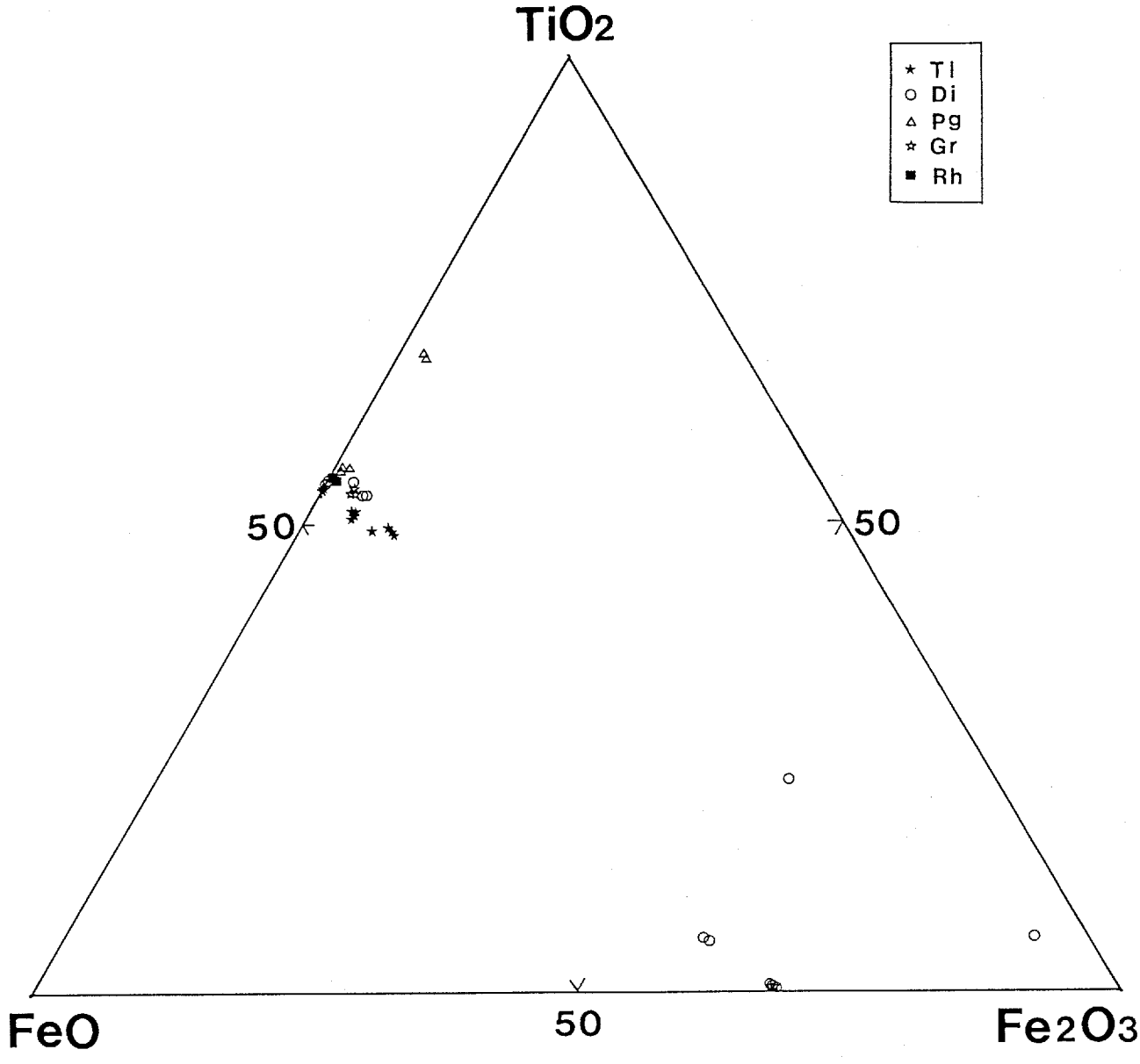

Fig. 25. FeO–Fe_2O_3–TiO_2 diagram for iron–titan oxides from the other types of rocks than the granodiorite.
For abbreviations see Fig. 20.

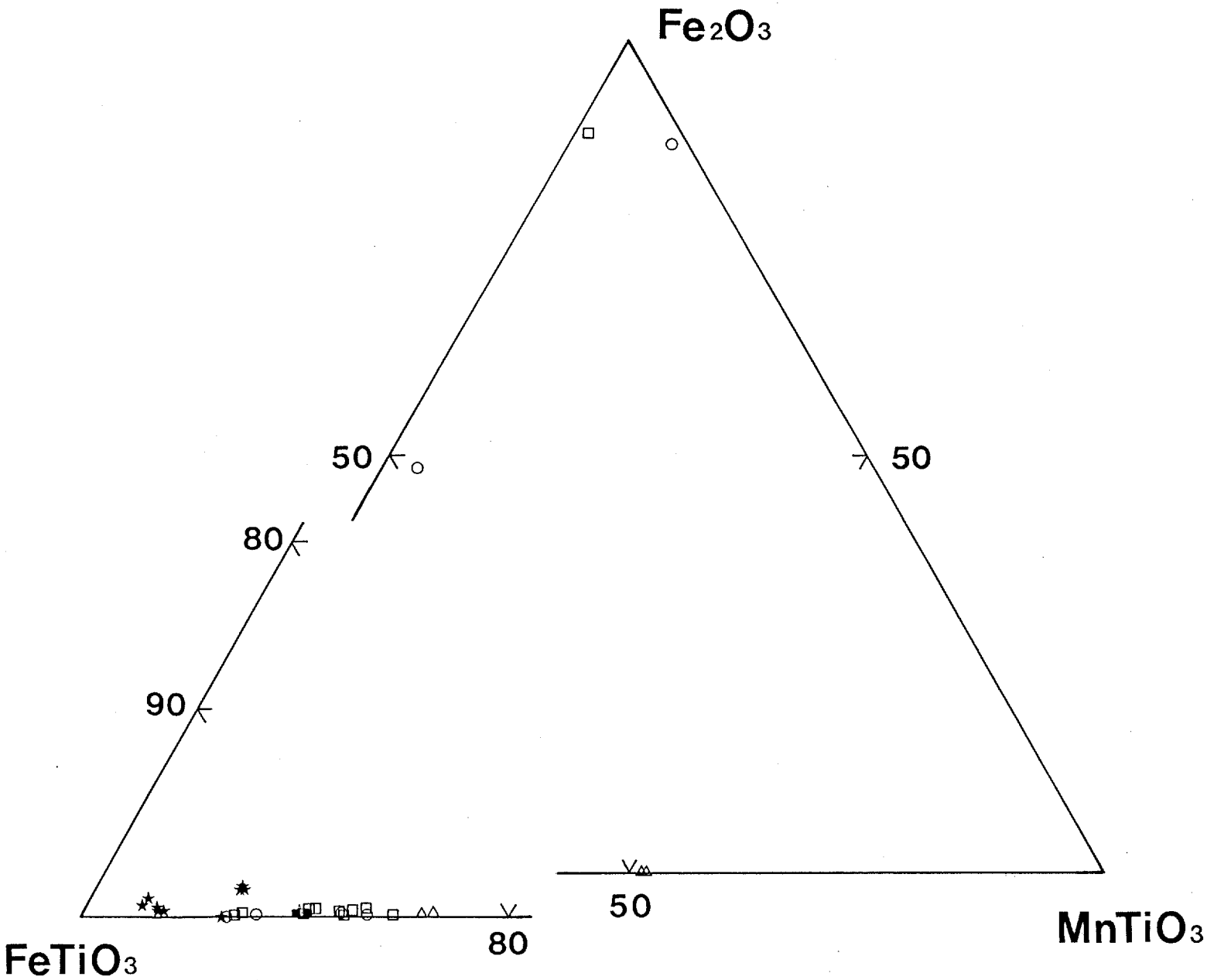

Fig. 26. $FeTiO_3$–$MnTiO_3$–Fe_2O_3 diagram for ilmenite.
For symbols see Figs. 24 and 25.

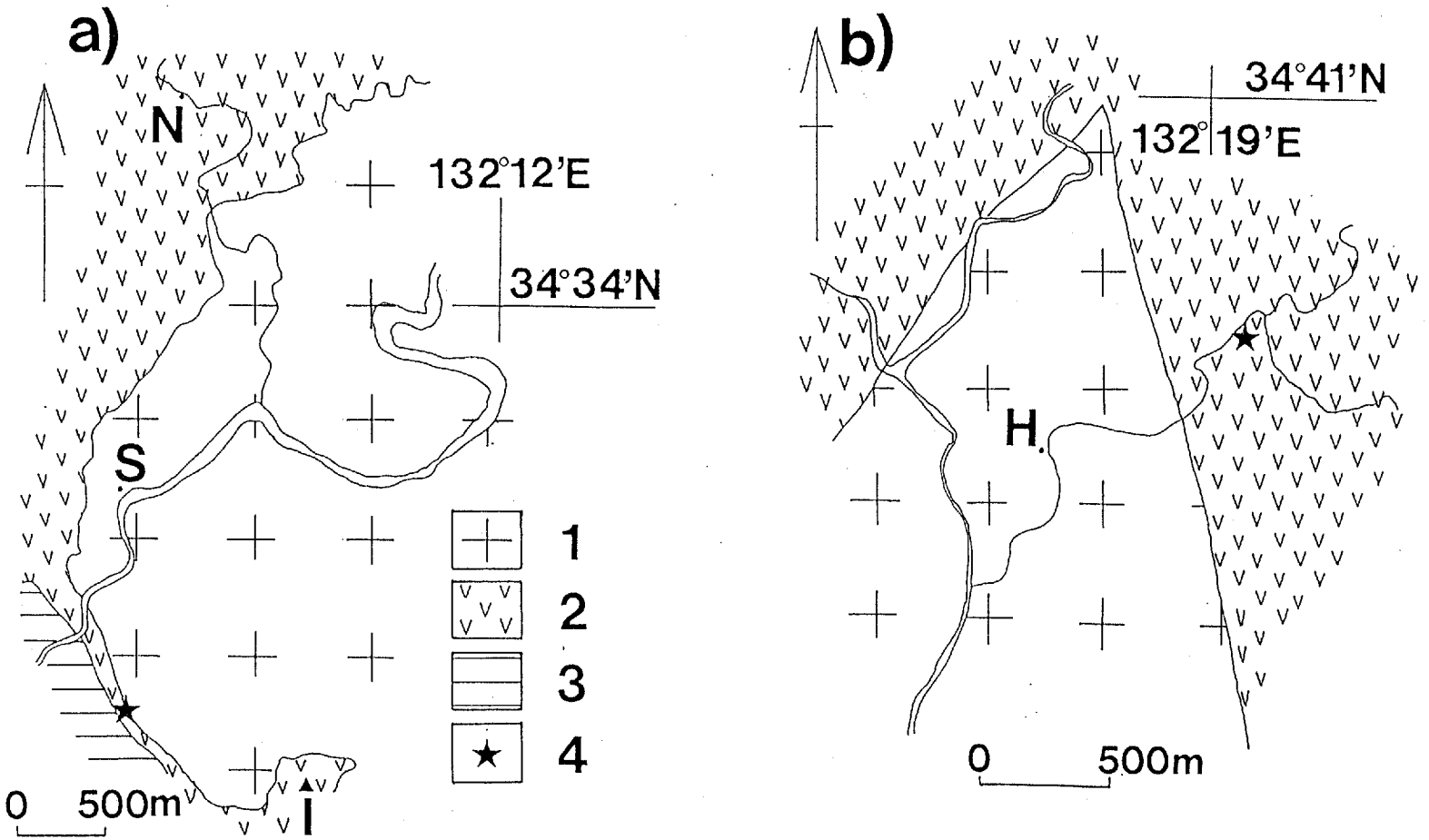

Fig. 27. Geological maps of the Sakane sub-area in the Togouchi area (a) and the Hinokidani area (b) and garnet localities.
1:granitic rocks, 2:rhyolitic rocks, 3:pre-Cretaceous formations, 4:garnet locality, H: Hinokidani, I:Mt.Ichima, N:Nasu, S:Sakane.

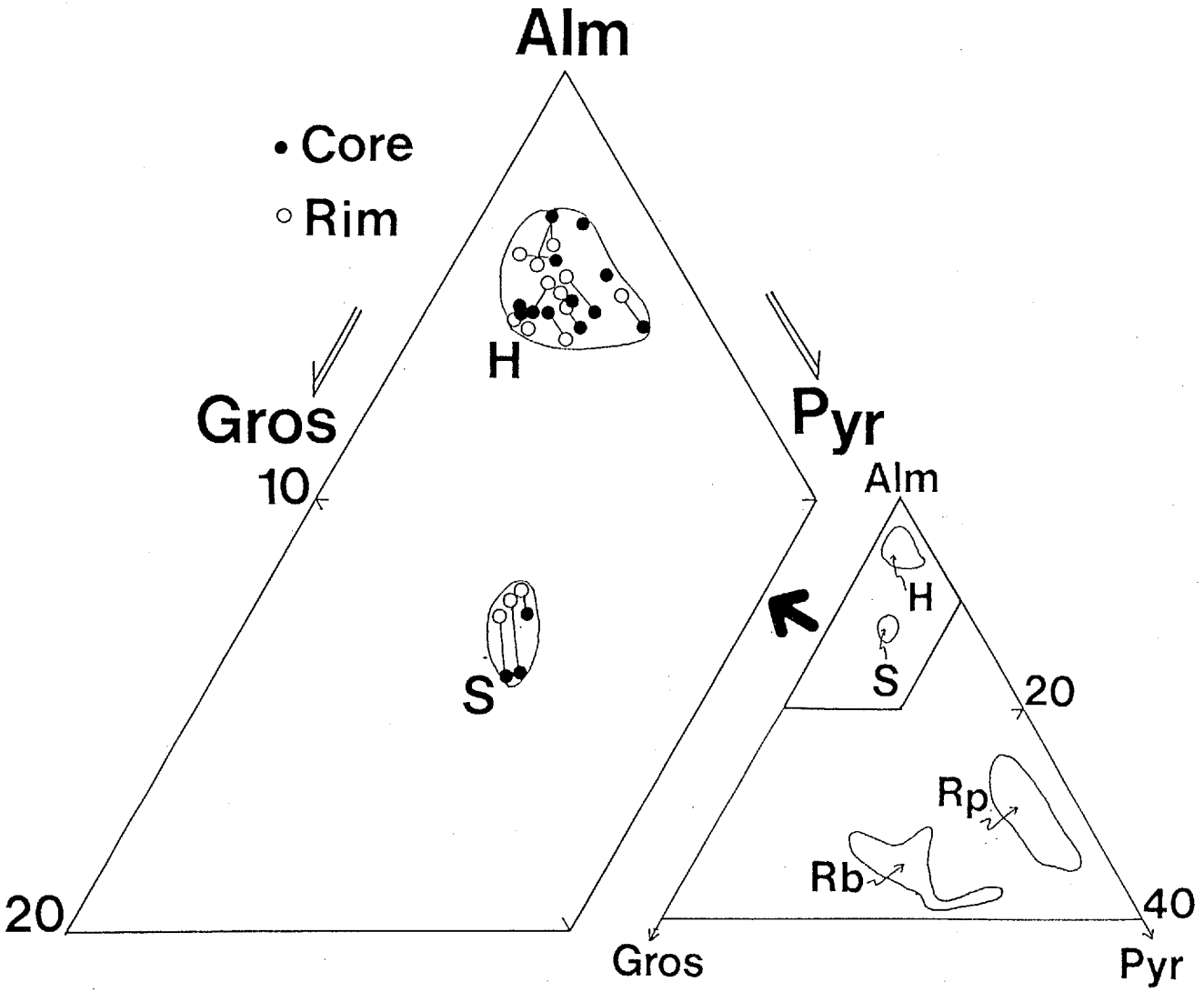

Fig. 28. Garnet from the Takada rhyolitic rocks and Pre–Ryoke or Paleo–Ryoke metamorphites (after Hayama, 1987,1991).
Alm:almandine, Gros:grossular, Pyr:pyrope: Hinokidani area, S: Sakane sub–area
RP: metapelites from pre–Ryoke or Paleo–Ryoke land fragments, RB:metabasites from pre–Ryoke or Paleo–Ryoke land fragments.
open circle:rim, solid circle:core.

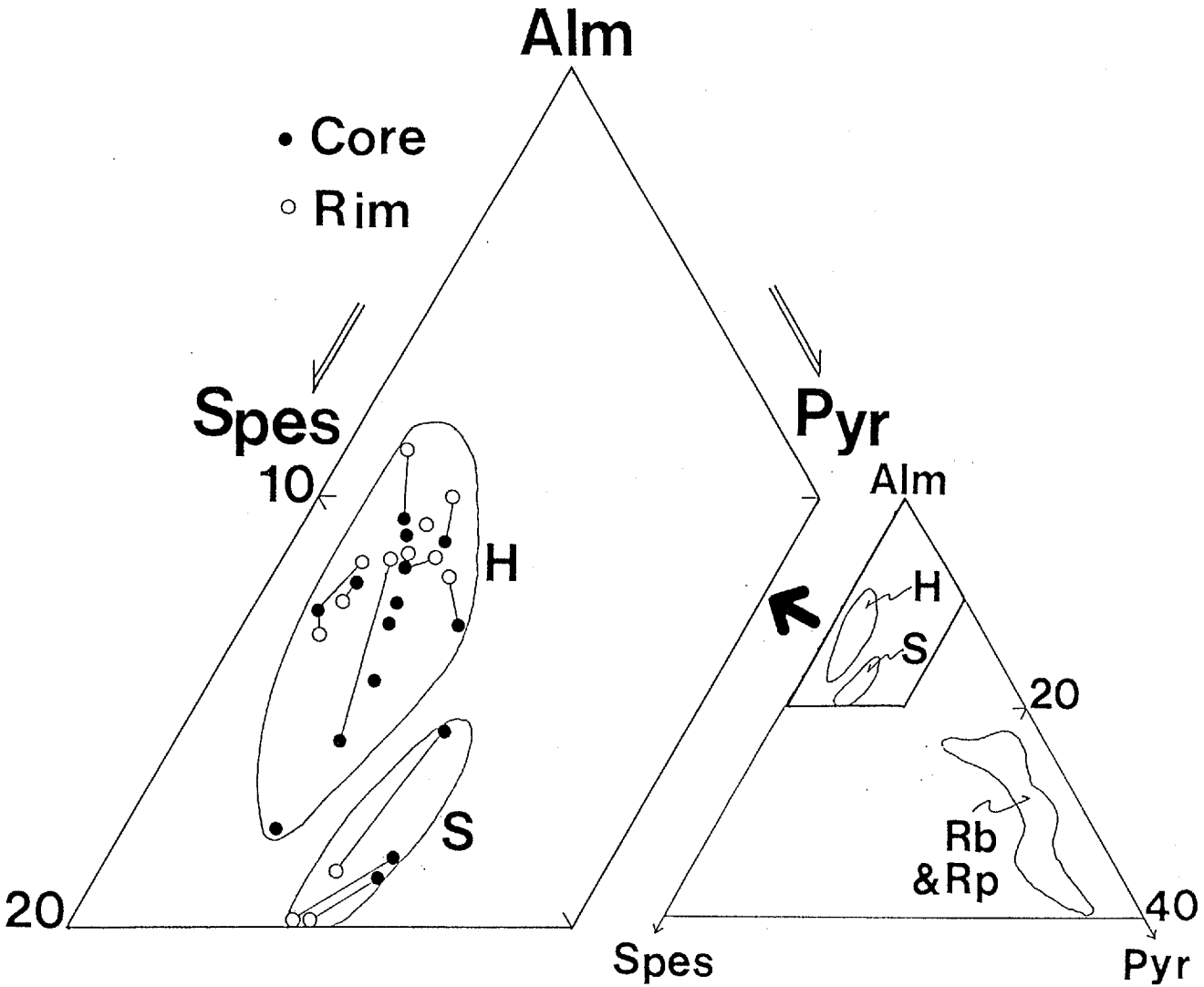

Fig. 29. Garnet from the Takada rhyolitic rocks an Pre–Ryoke or Paleo–Ryoke metamorphites(after Hayama, 1987,1991). Spes:spessartine. For other abbreviations see Fig. 28.

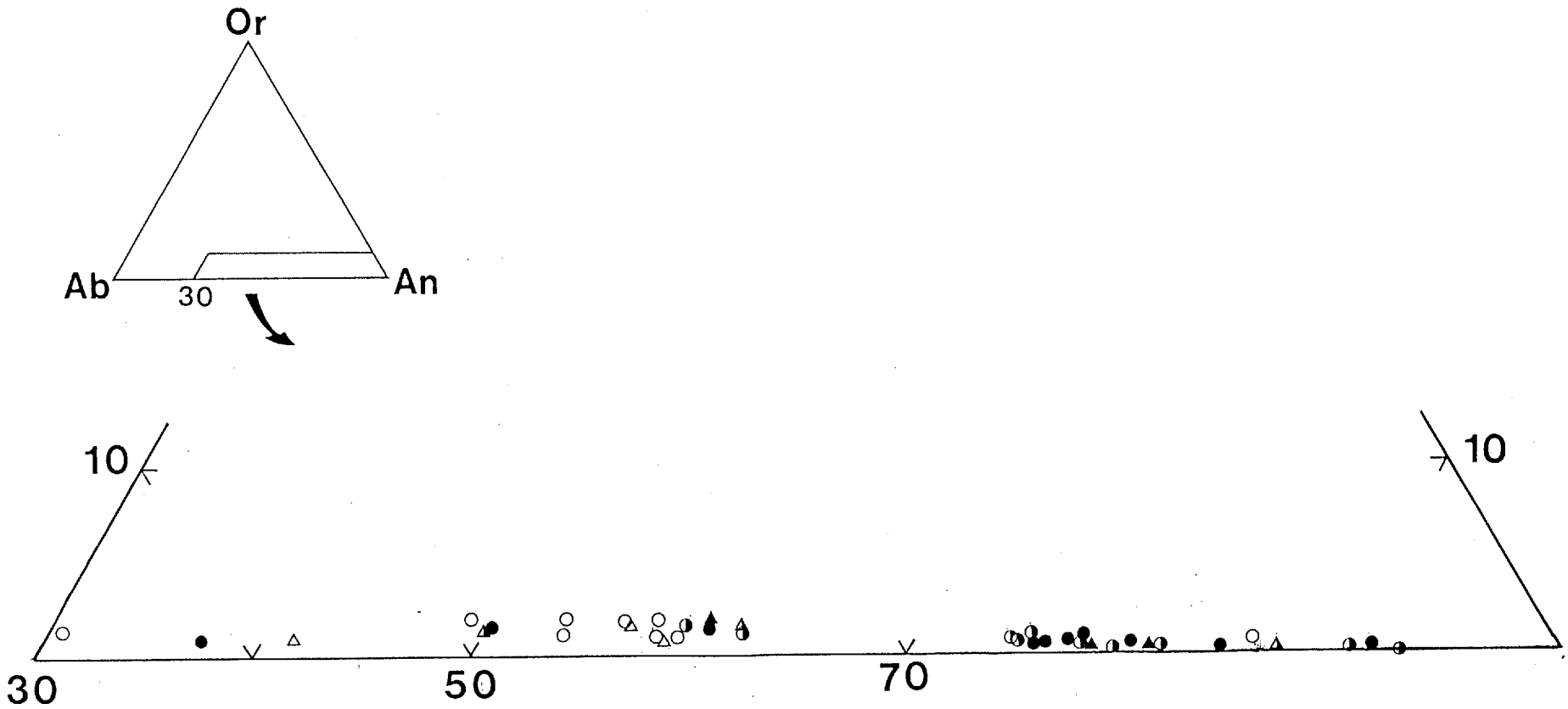

Fig. 30. Ab–An–Or diagram for plagioclase from the tonalite.
circle: coarse–grained, triangle: fine–grained.
solid:core, half solid: mantle, open: rim.

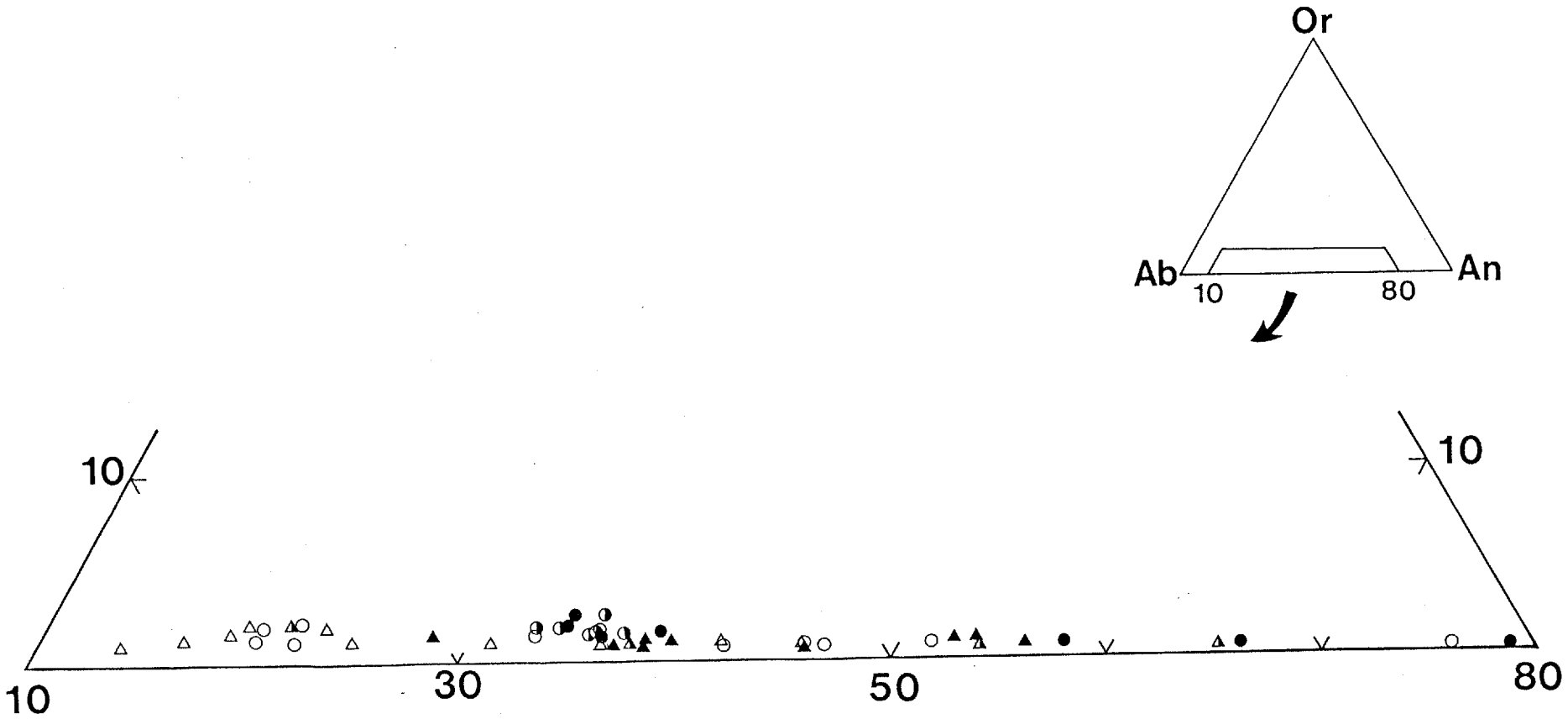

Fig. 31. Ab–An–Or diagram for plagioclase from the dark inclusion.
For symbols and abbreviations see Fig. 30.

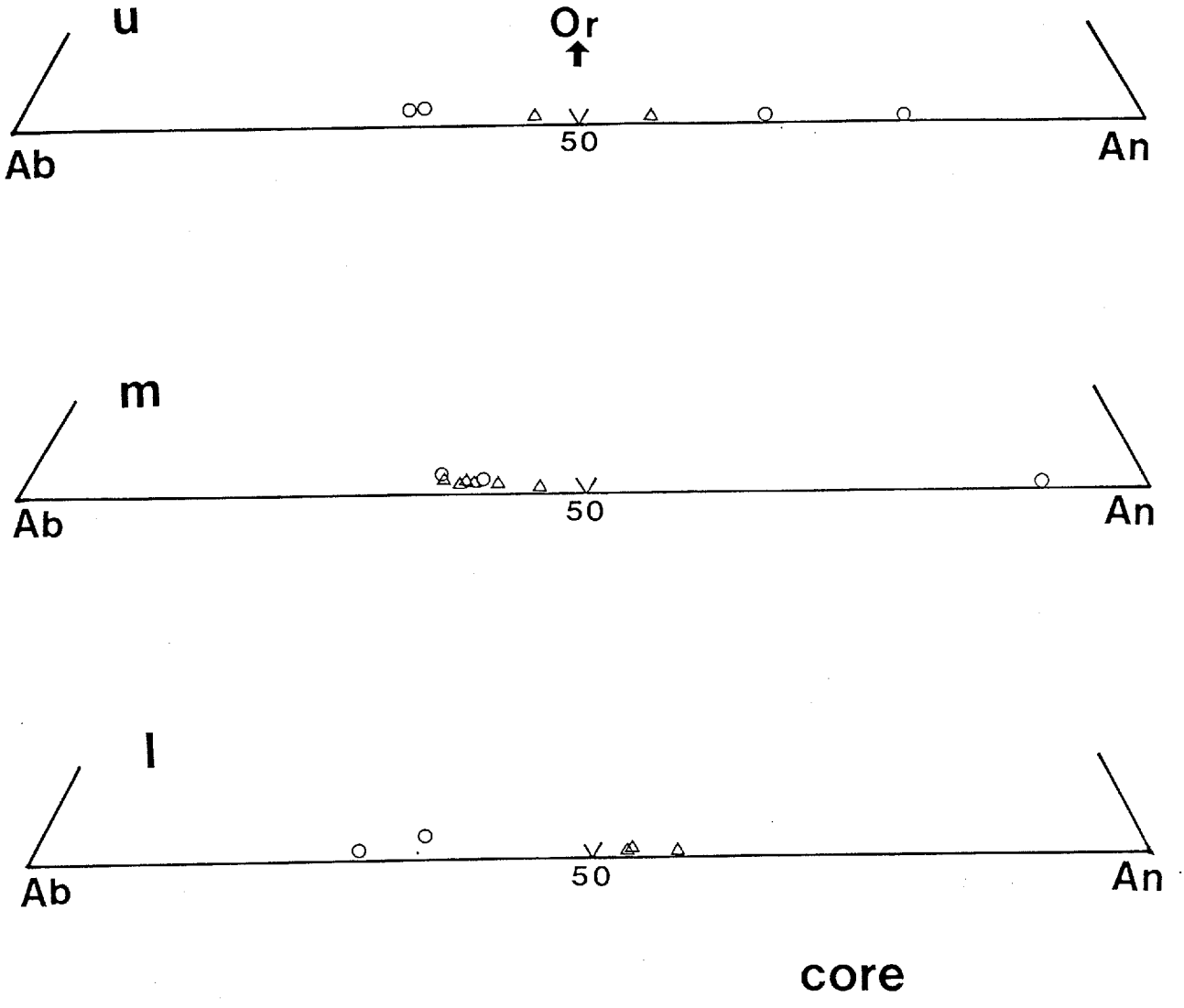

Fig. 32. Ab – An – Or diagram for cores of plagioclase in the dark inclusion from various lithofacies. "u", "m" and "l" show the upper, middle and lower lithofacies of the granodiorite in which the dark inclusion are included.
circle:coarse-grained, triangle:fine-grained.

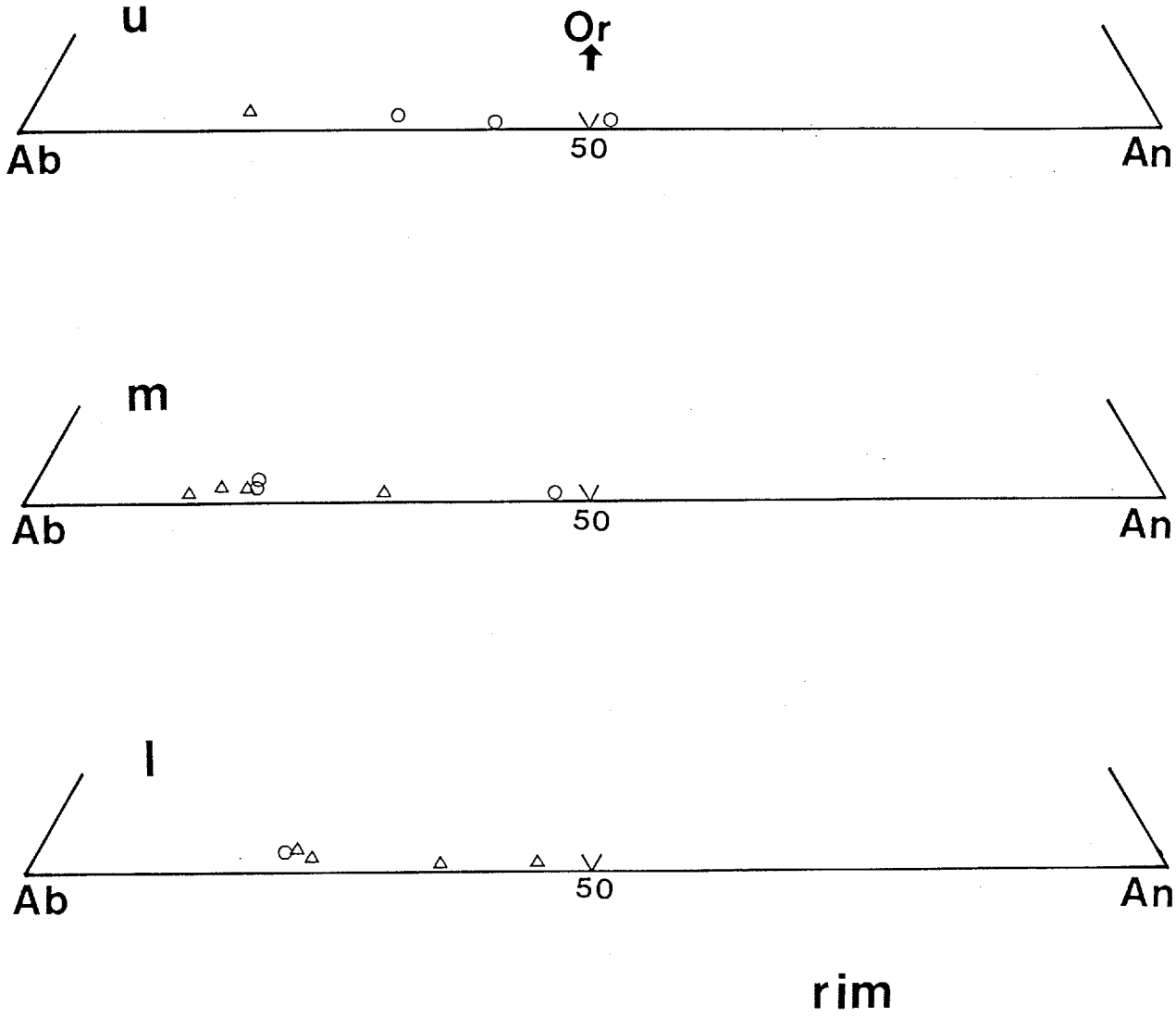

Fig. 33. Ab – An – Or diagram for rims of plagioclase in the dark inclusion from various lithofacies. For symbols and abbreviations see Fig. 32.

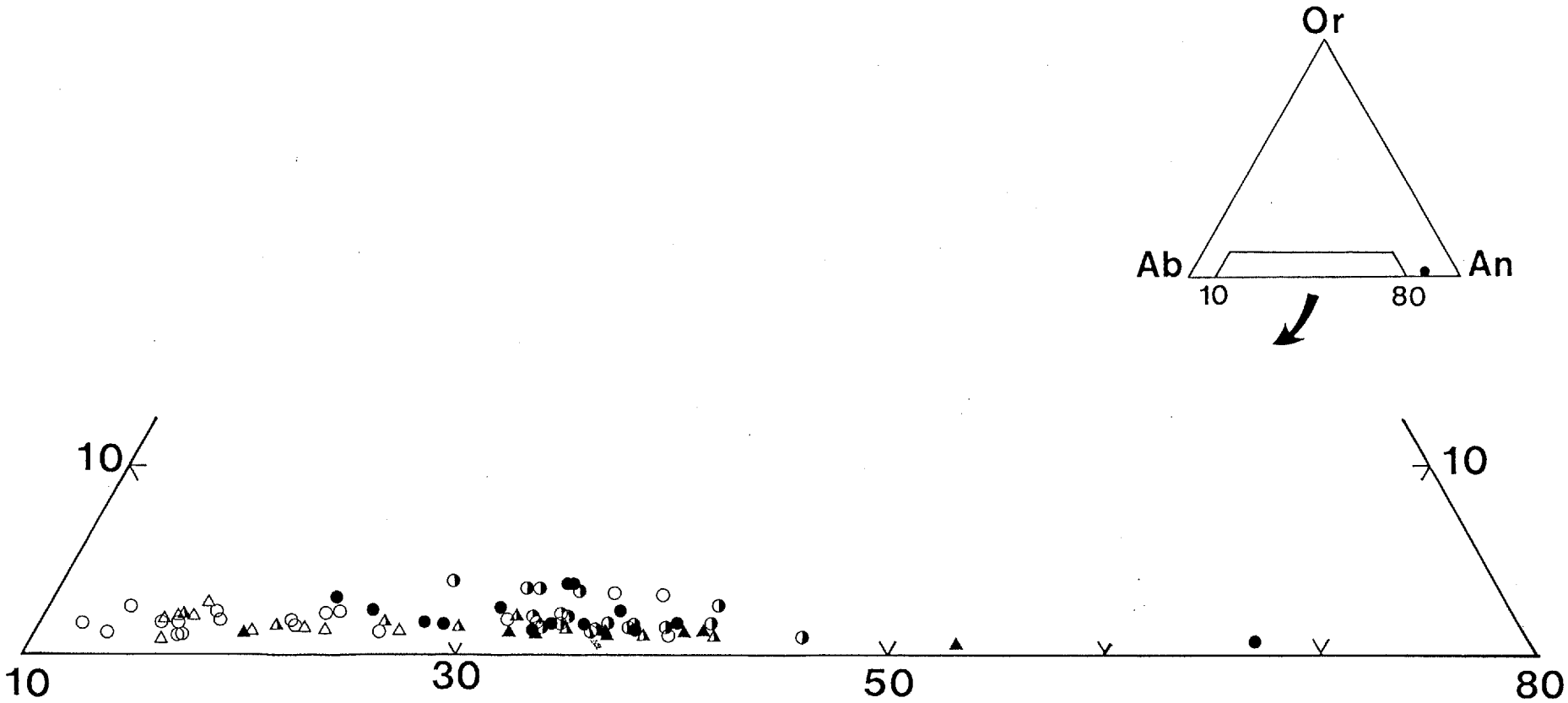

Fig. 34. Ab – An – Or diagram for plagioclase from the granodiorite.
For symbols see Fig. 30.

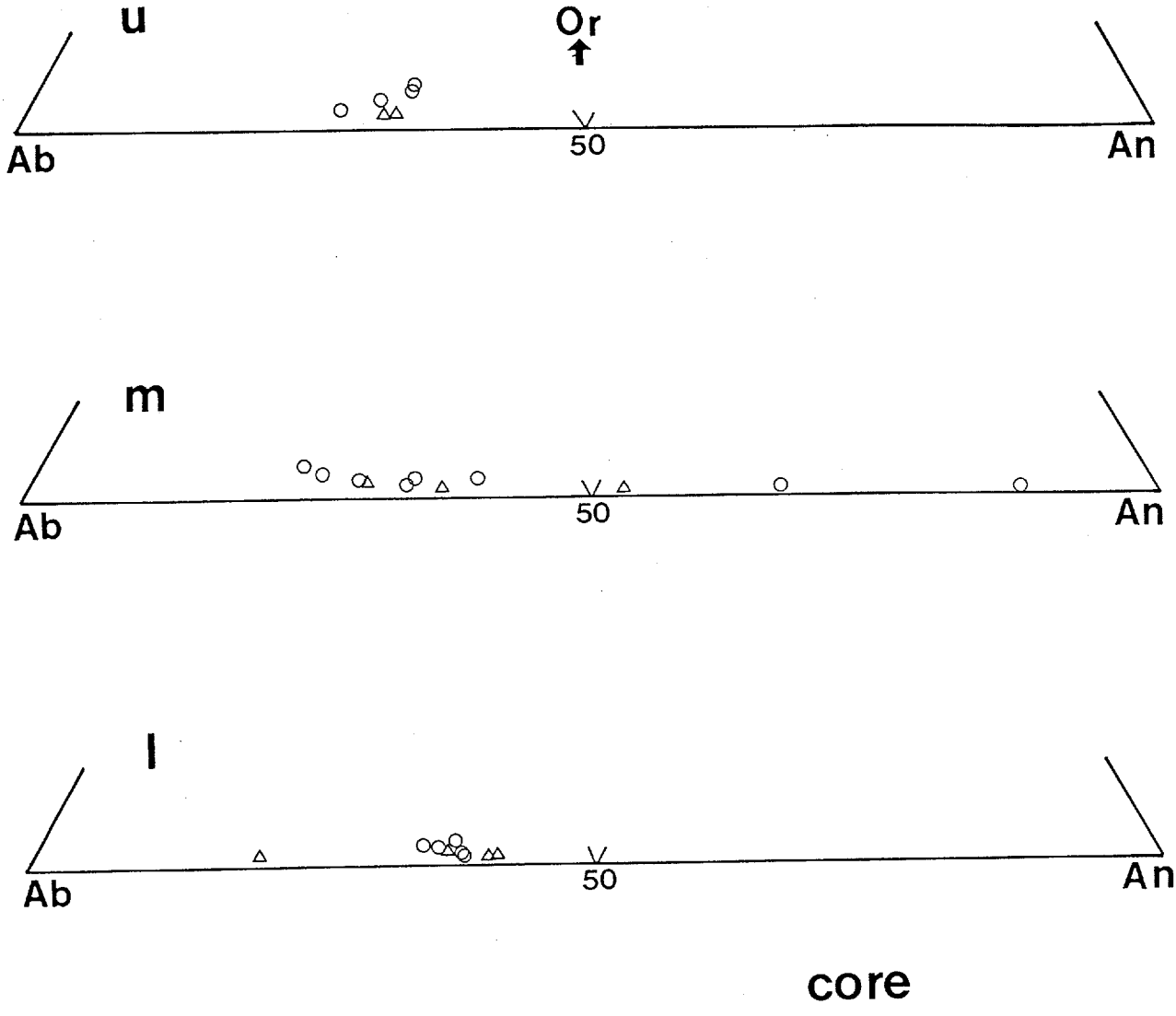

Fig. 35. Ab – An – Or diagram for cores of plagioclase from various lithofacies in the granodiorite. "u", "m" and "l" show the upper, middle and lower lithofacies of the granodiorite respectively. circle:coarse–grained, triangle:fine–grained.

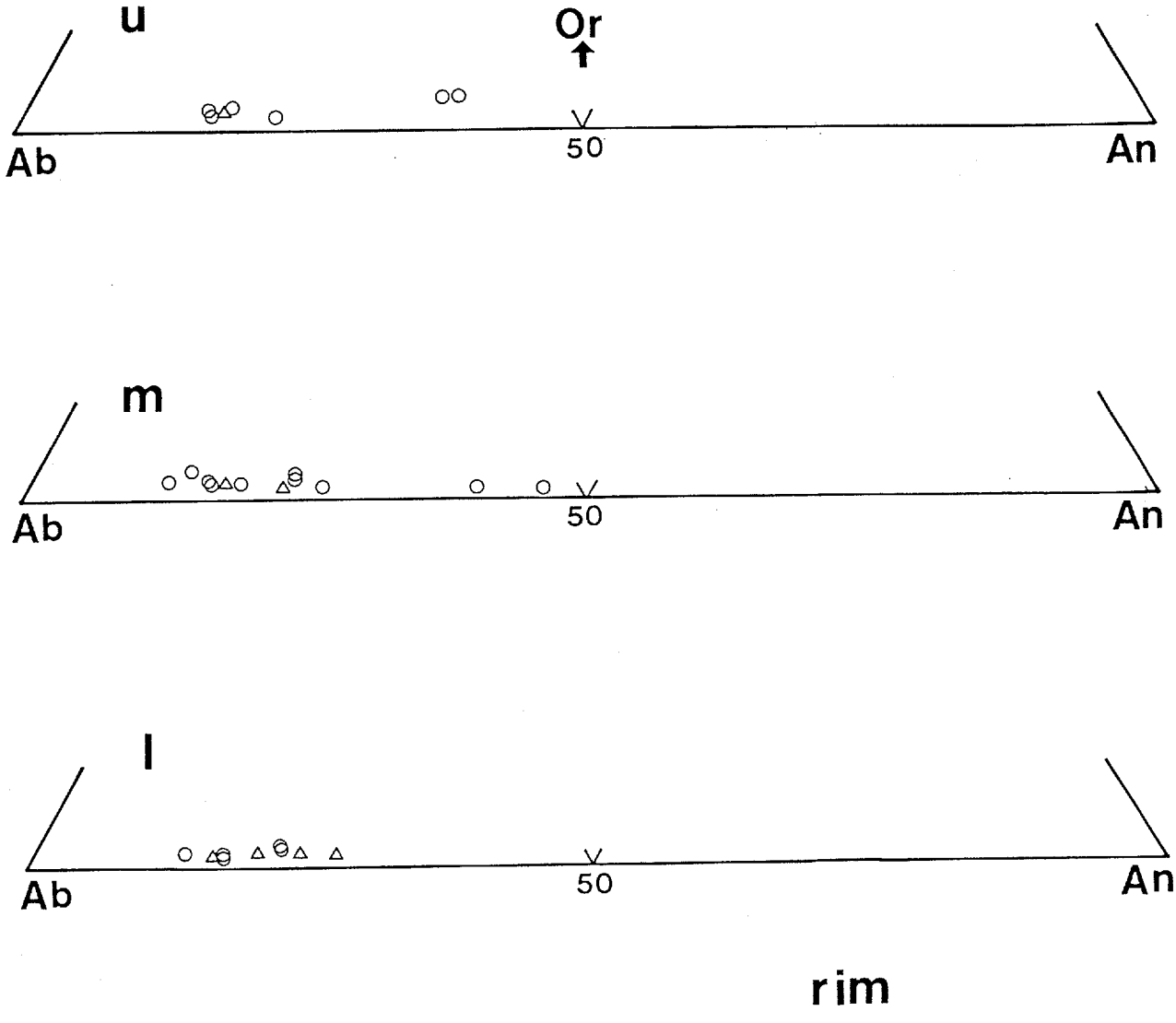

Fig. 36. Ab – An – Or diagram for rims of plagioclase from various lithofacies in the granodiorite. For symbols and abbreviations see Fig. 35.

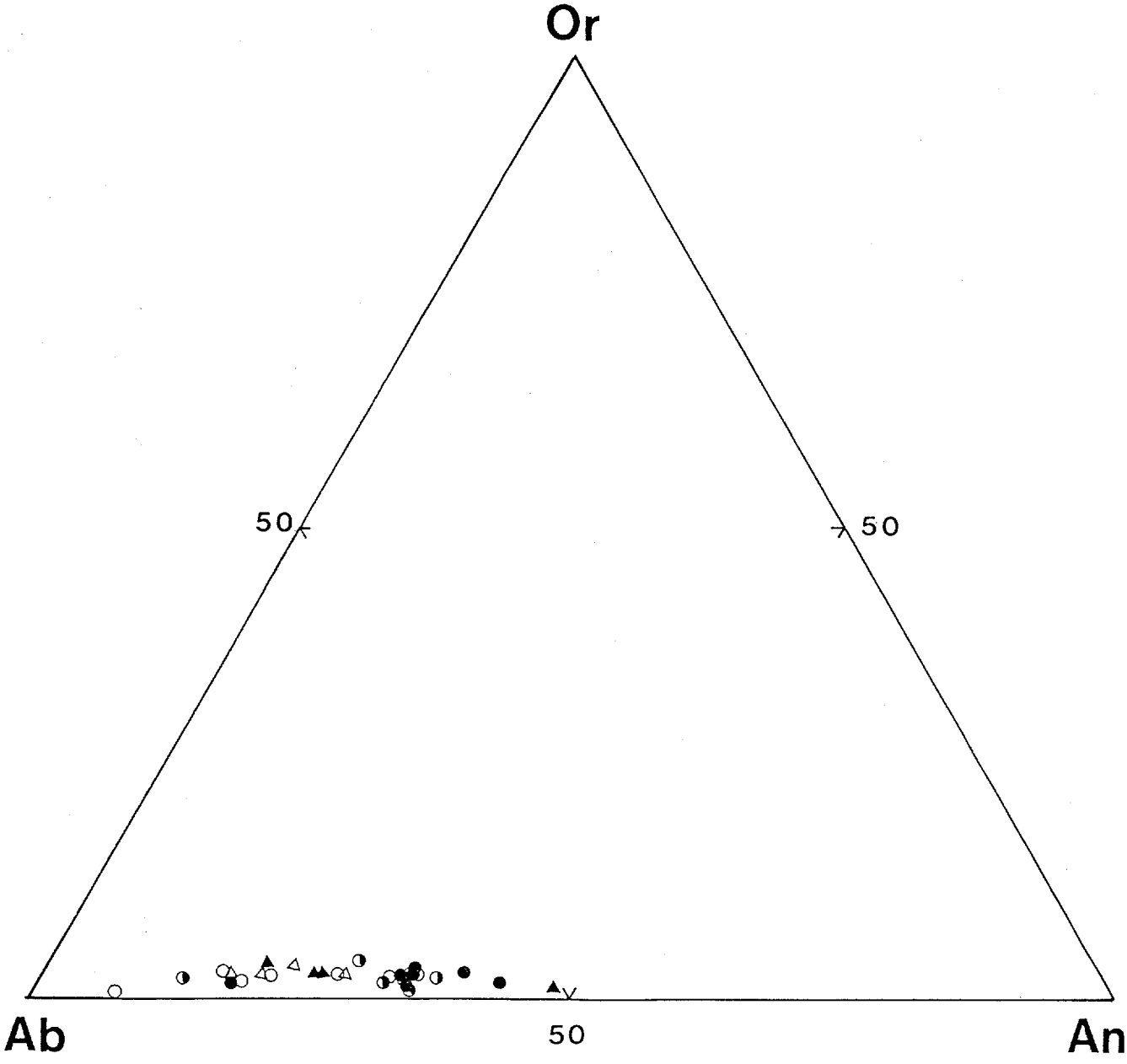

Fig. 37. Ab – An – Or diagram for plagioclase from the porphyritic granite. For symbols see Fig. 30.

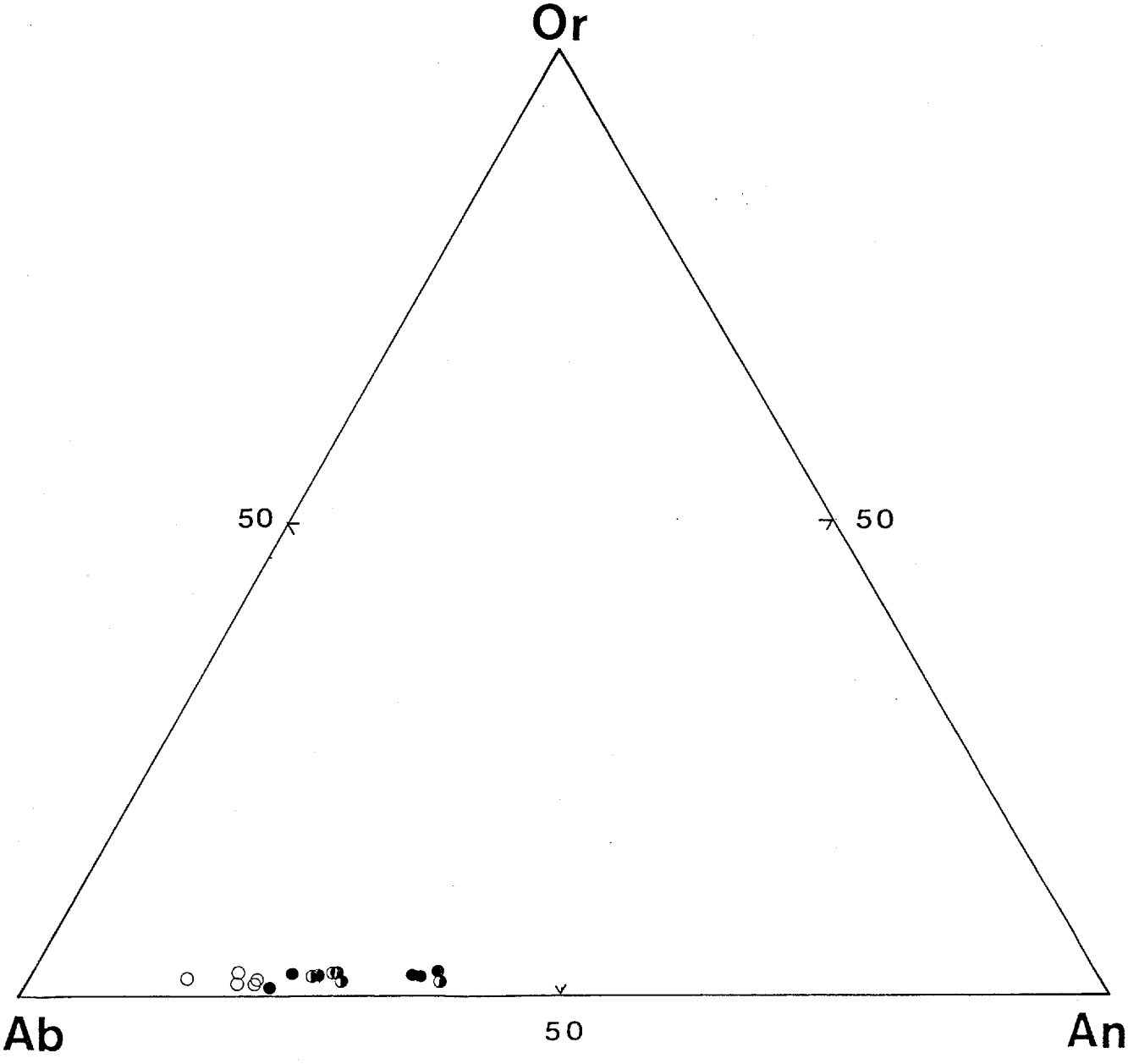

Fig. 38. Ab – An – Or diagram for plagioclase from the granite.
solid:core, half solid:mantle, open:rim.

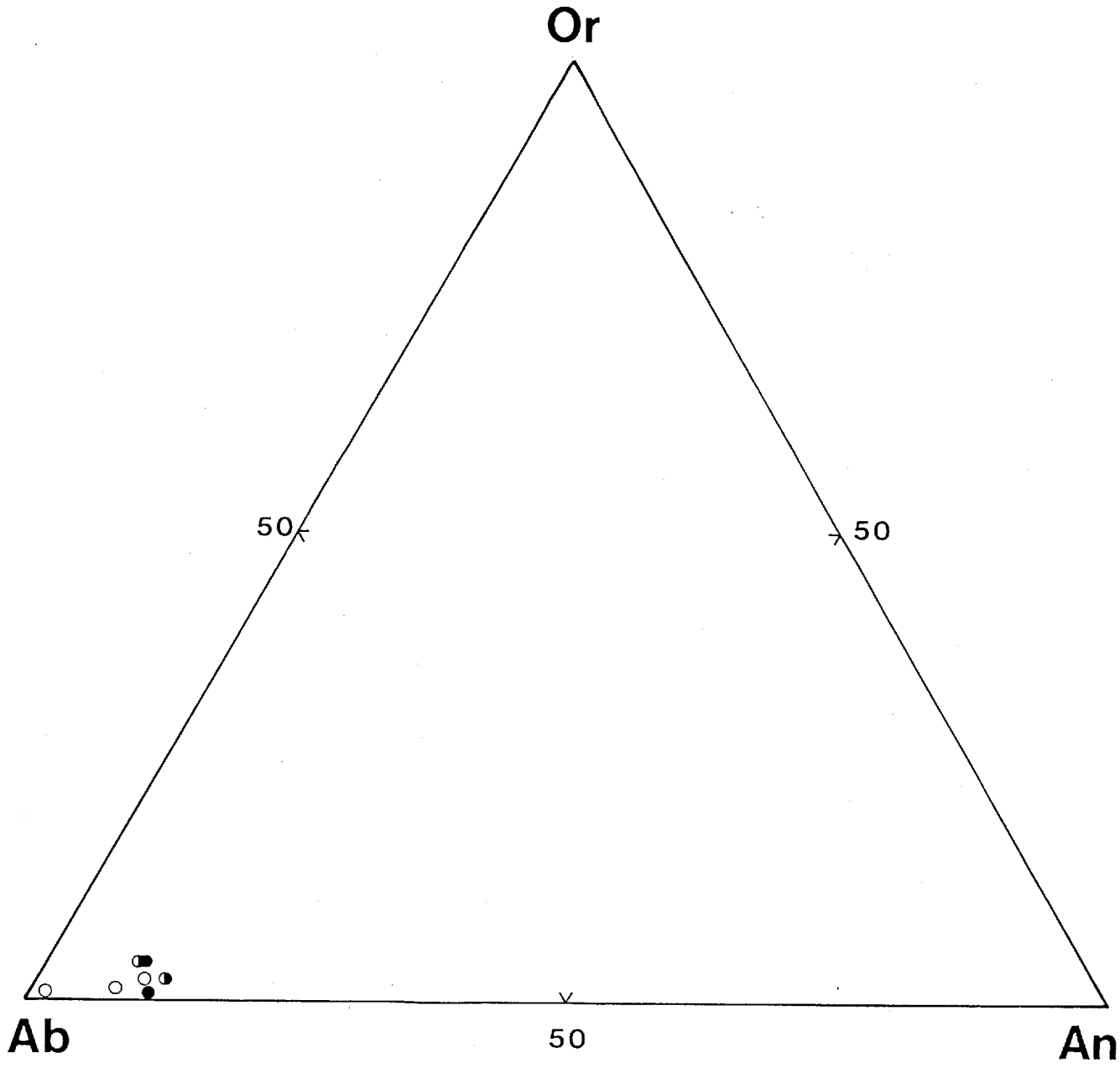

Fig. 39. Ab – An – Or diagram for plagioclase from the aplite.
For symbols see Fig. 38.

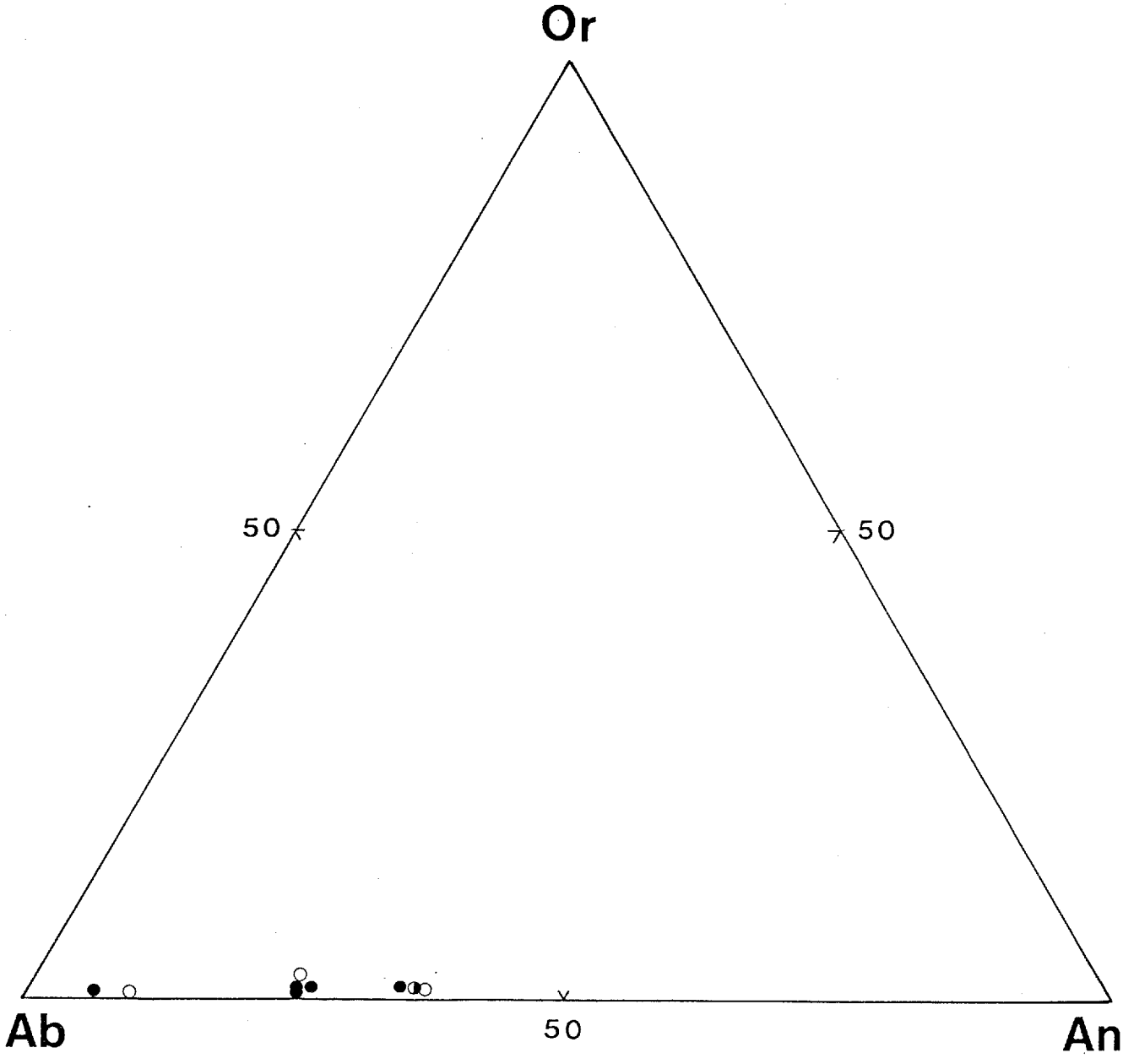

Fig. 40. Ab – An – Or diagram for plagioclase from the rhyolitic rocks. For symbols see Fig. 38.

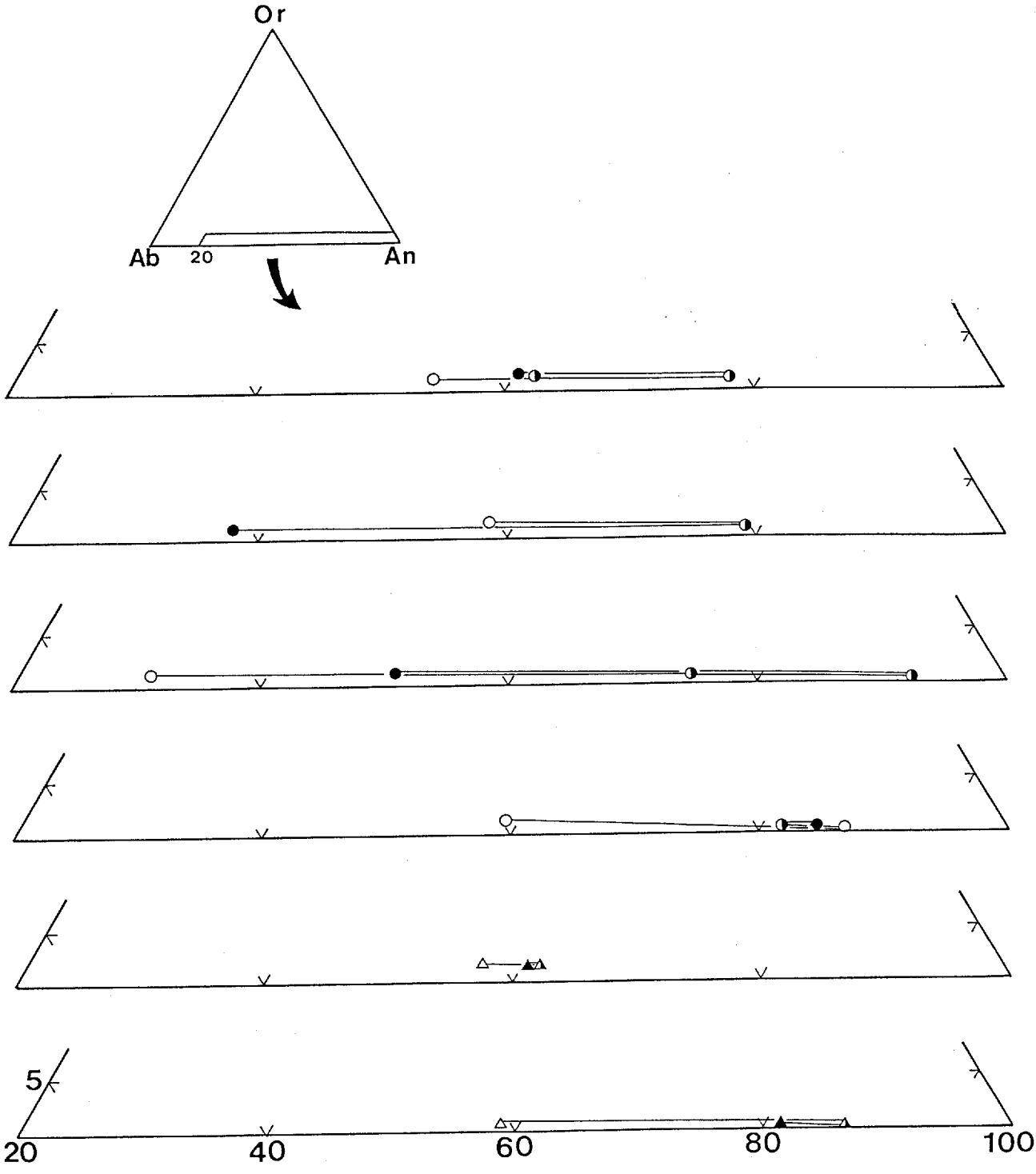

Fig. 41. Ab – An – Or diagram for abnormal–zoning plagioclase from the tonalite. For symbols see Fig. 30.

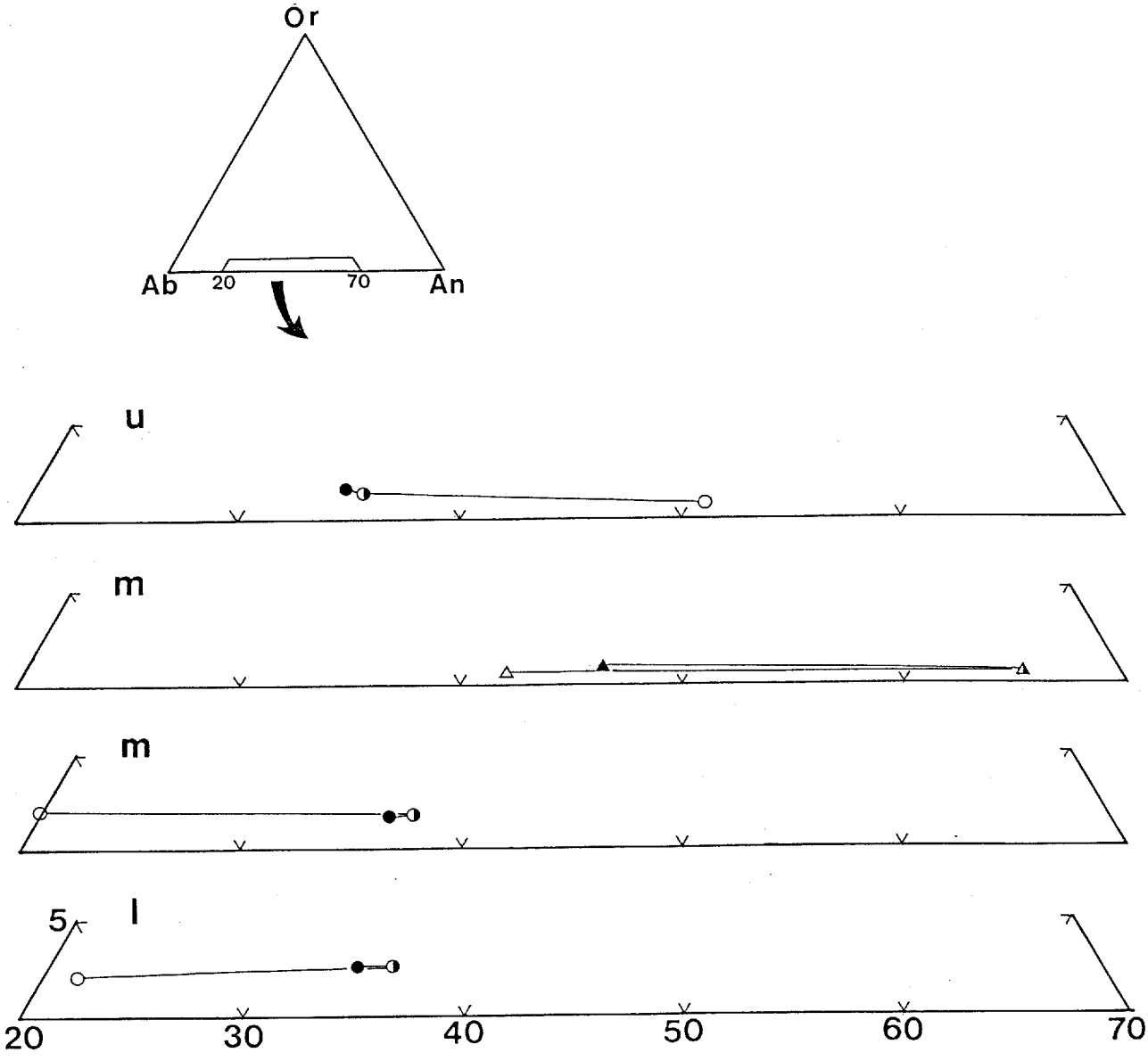

Fig. 42. Ab – An – Or diagram for abnormally zoned plagioclase from the dark inclusion. For abbreviations see Fig. 32. circle: coarse-grained, triangle: fine-grained, solid:core, half solid:mantle, open: rim.

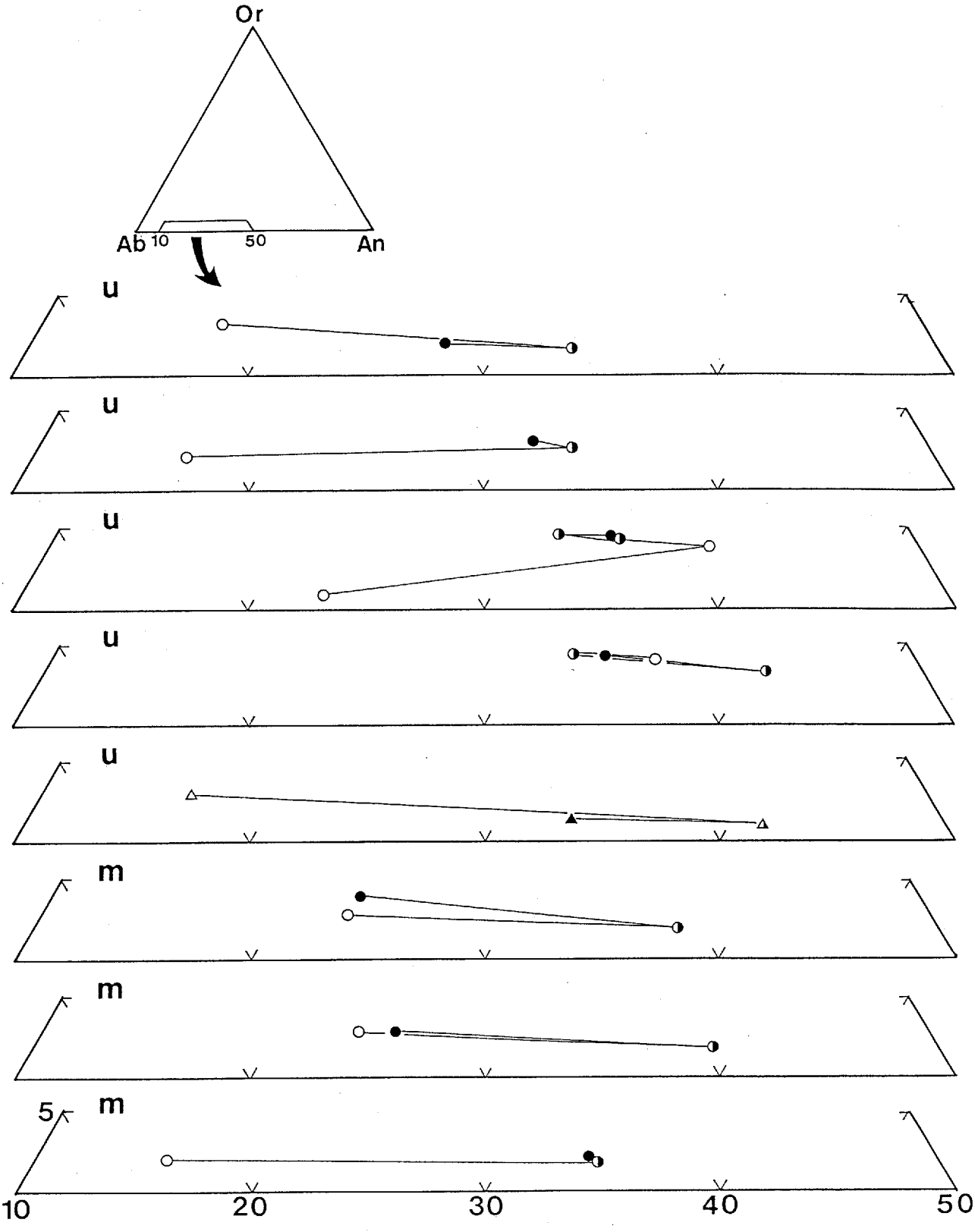

Fig. 43. Ab – An – Or diagram for abnormally zoned plagioclase from the granodiorite. For abbreviations see Fig. 35. circle: coarse–grained, triangle: fine–grained, solid:core, half solid:mantle, open: rim.

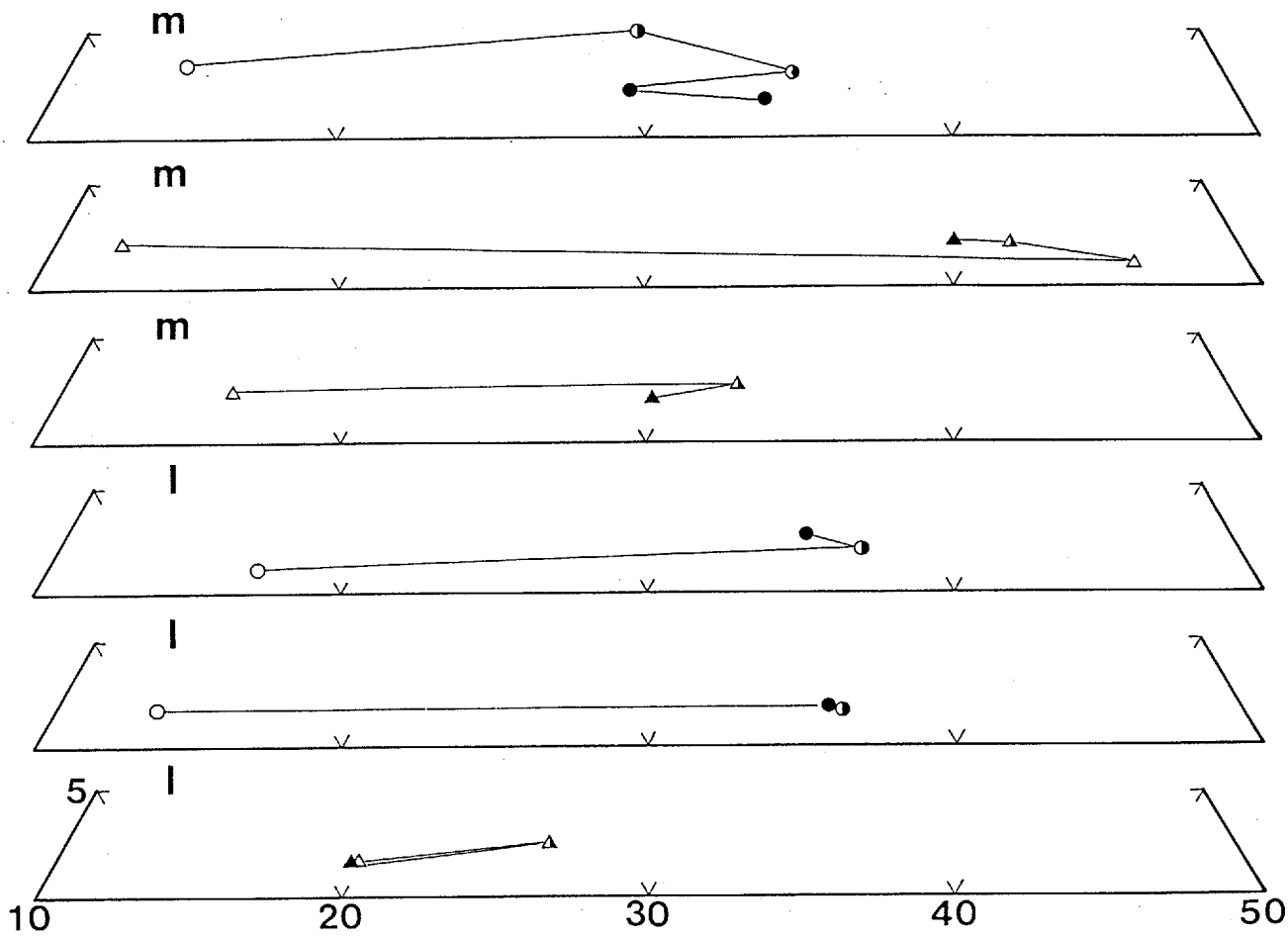

(Fig. 43 continued)

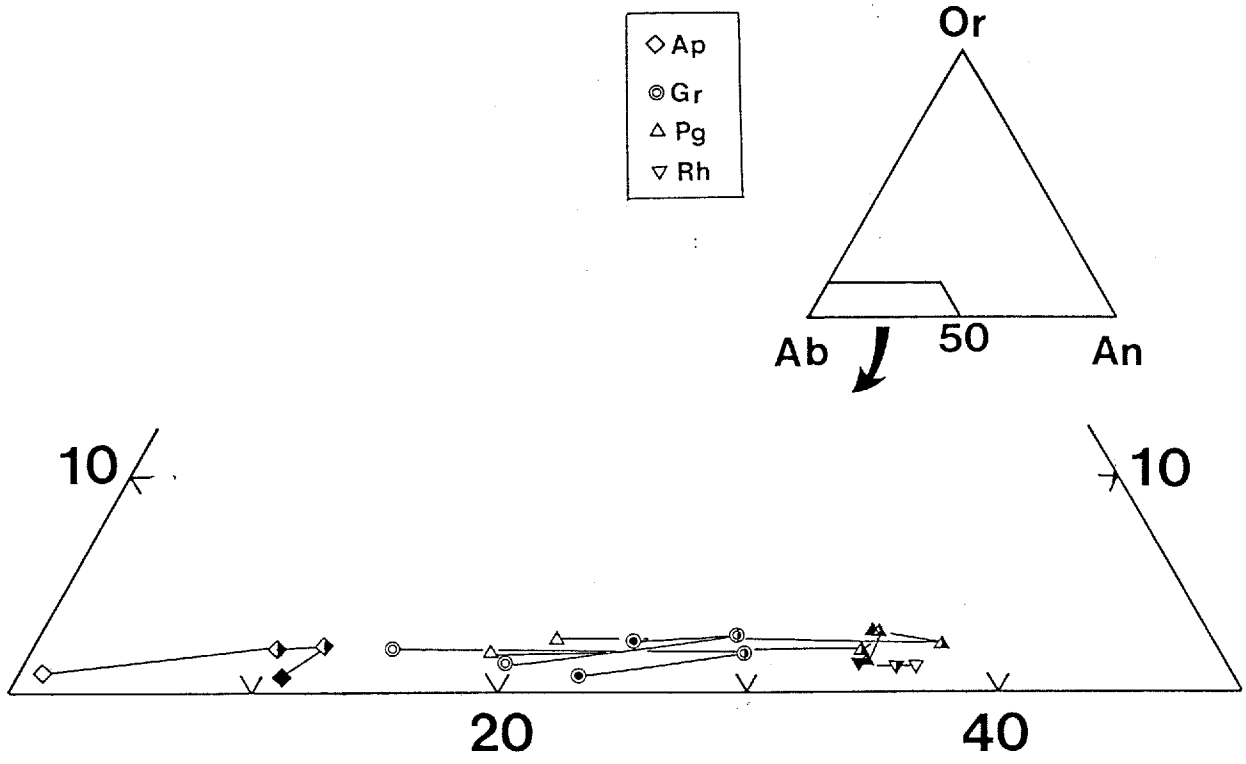

Fig. 44. Ab – An – Or diagram for abnormally zoned plagioclase from the aplite (Ap), granite (Gr), porphyritic granite (Pg) and rhyolitic rocks (Rh).
solid:core, half solid:mantle, open: rim.

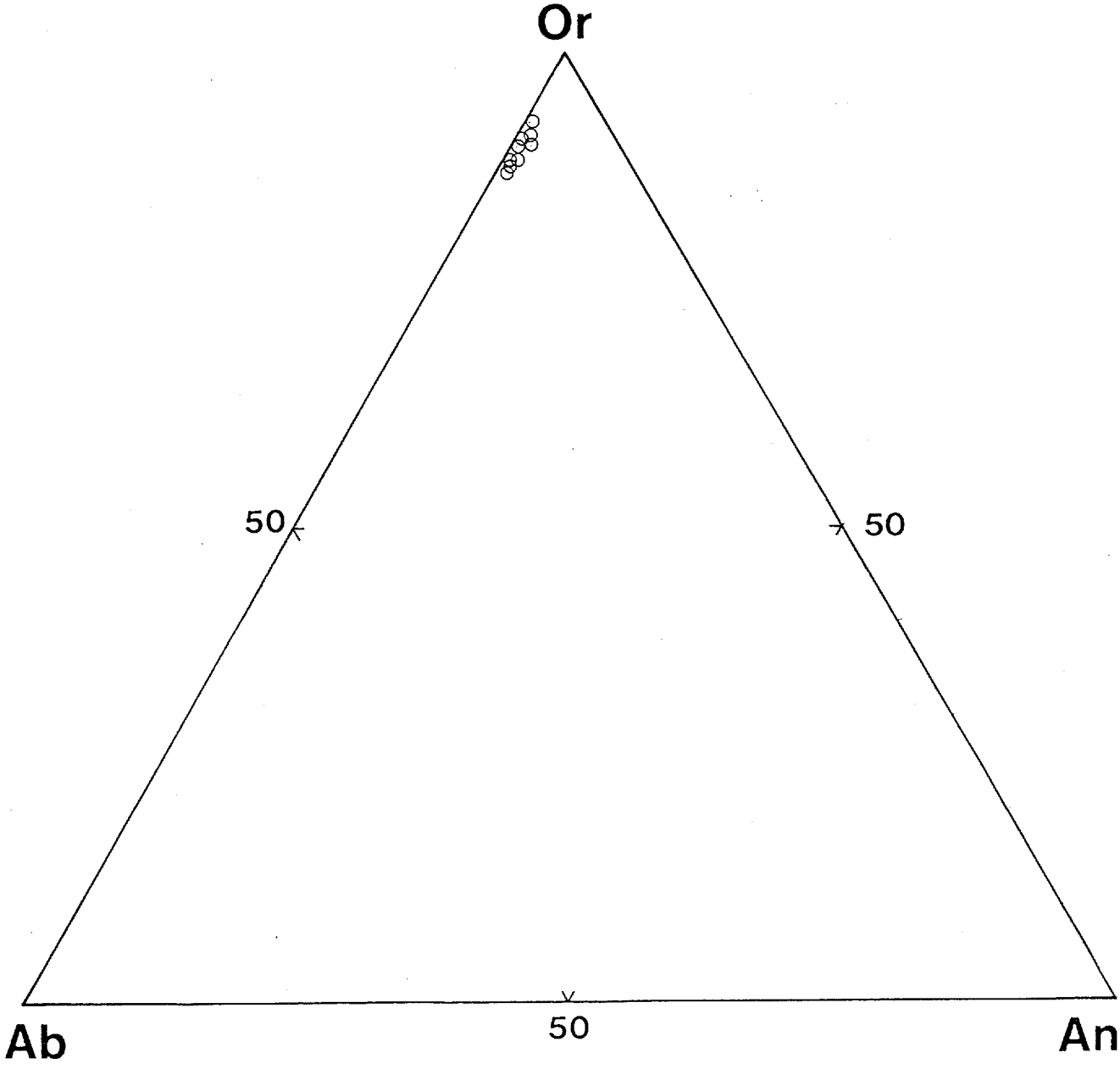

Fig. 45. Ab – An – Or diagram for K–feldspar from spheres in the dark inclusion.

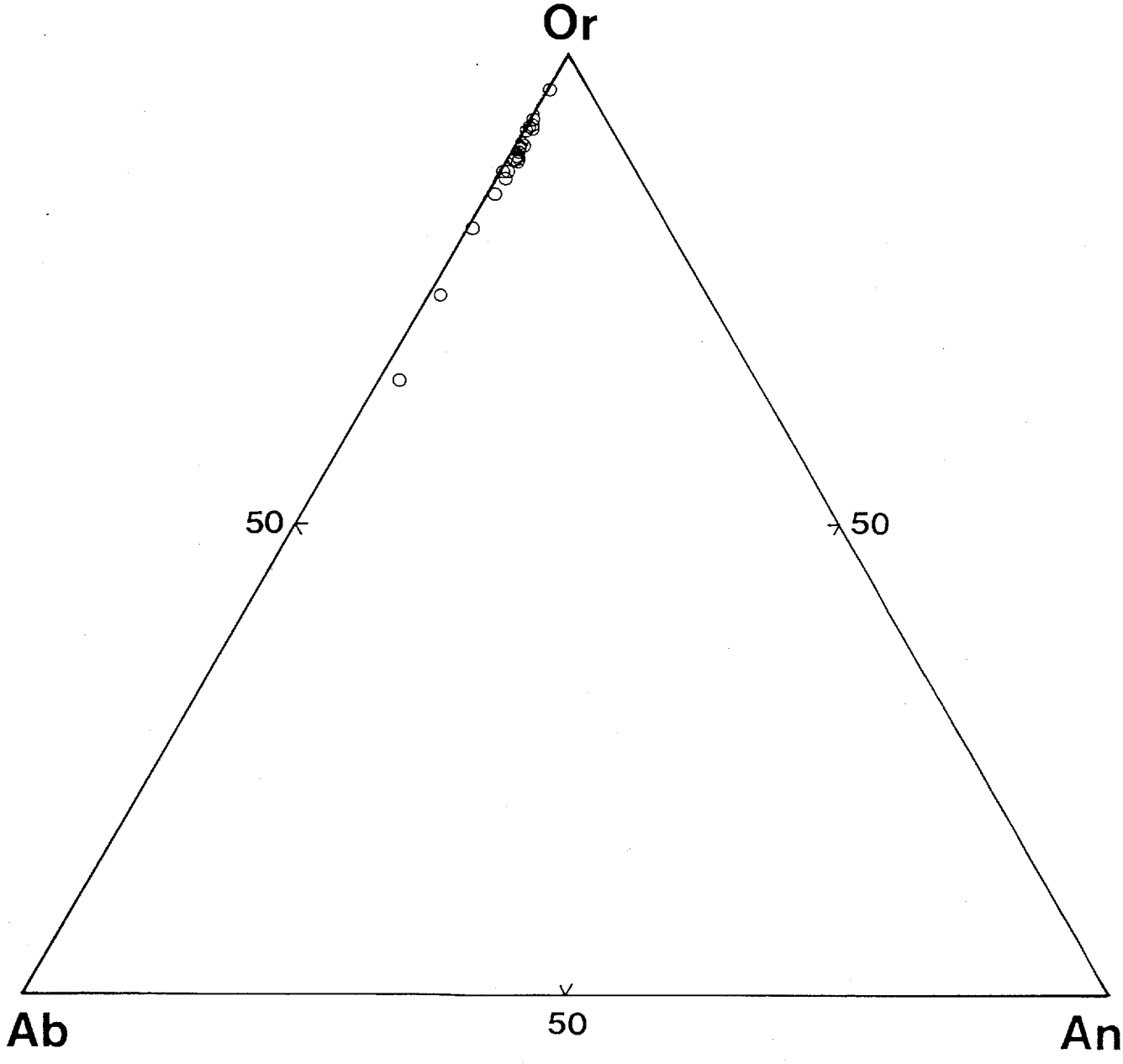

Fig. 46. Ab – An – Or diagram for K–feldspar from the granodiorite.

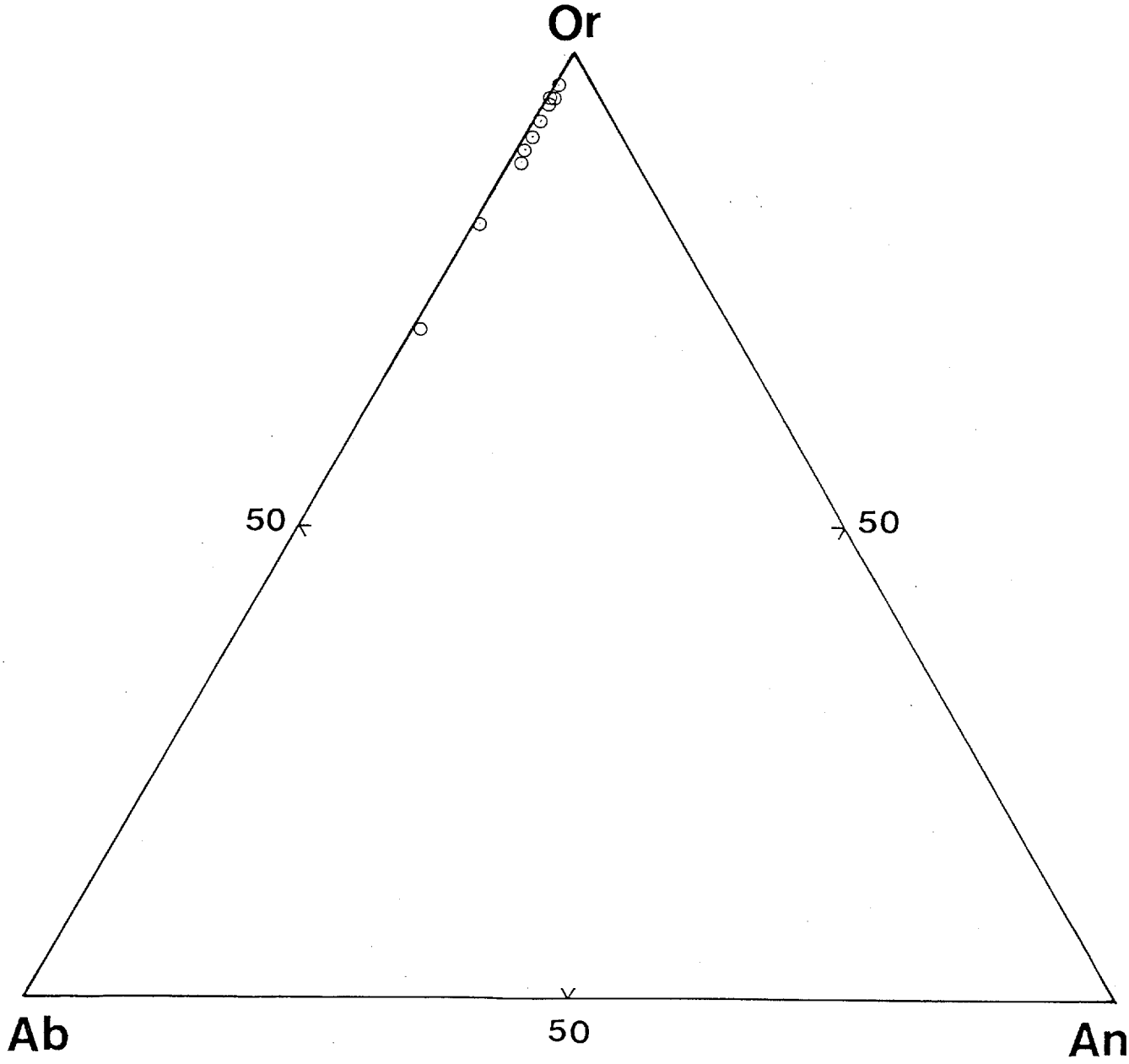

Fig. 47. Ab–An–Or diagram of K–feldspar from the porphyritic granite.

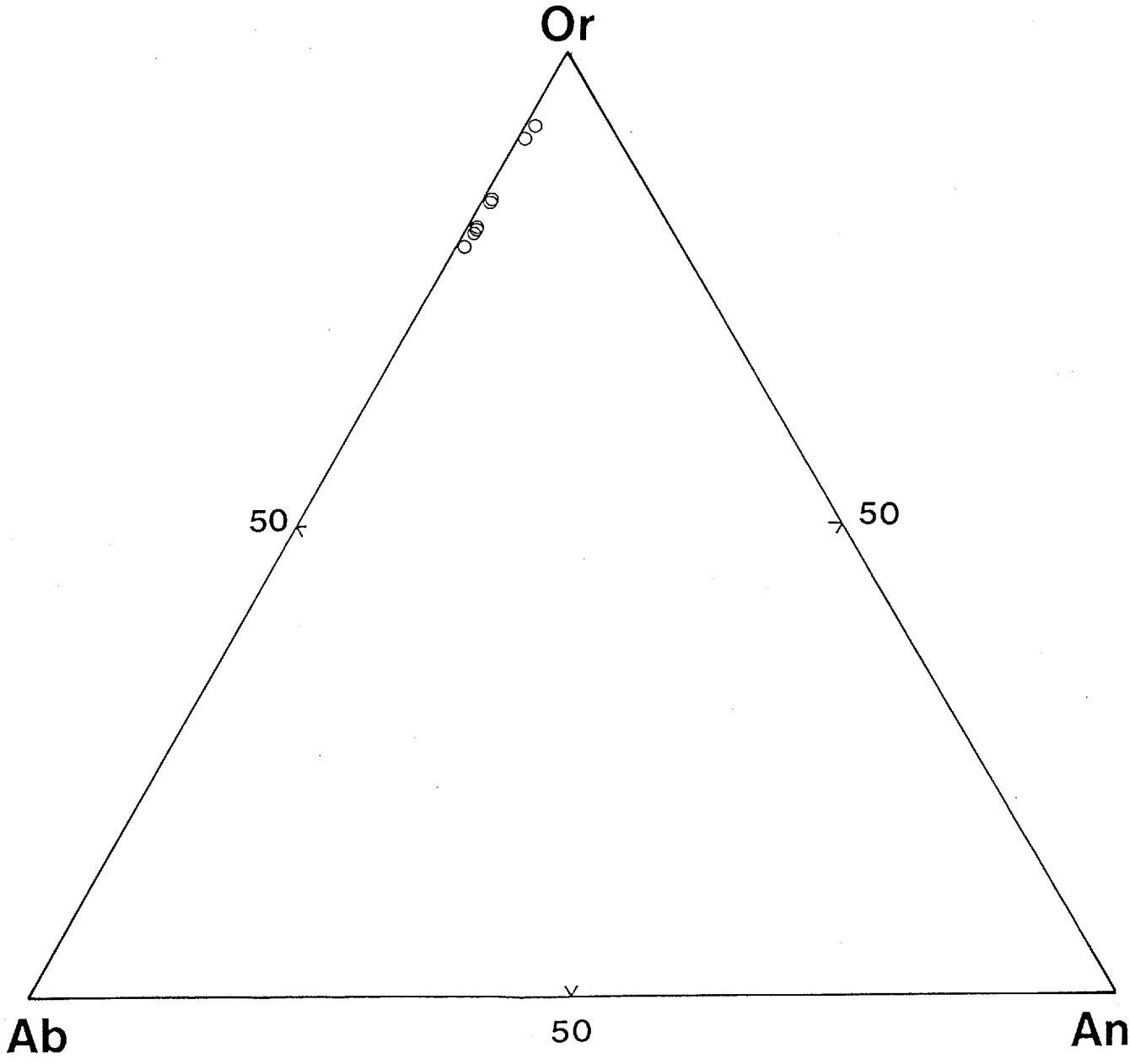

Fig. 48. Ab – An – Or diagram for K–feldspar from the granite.

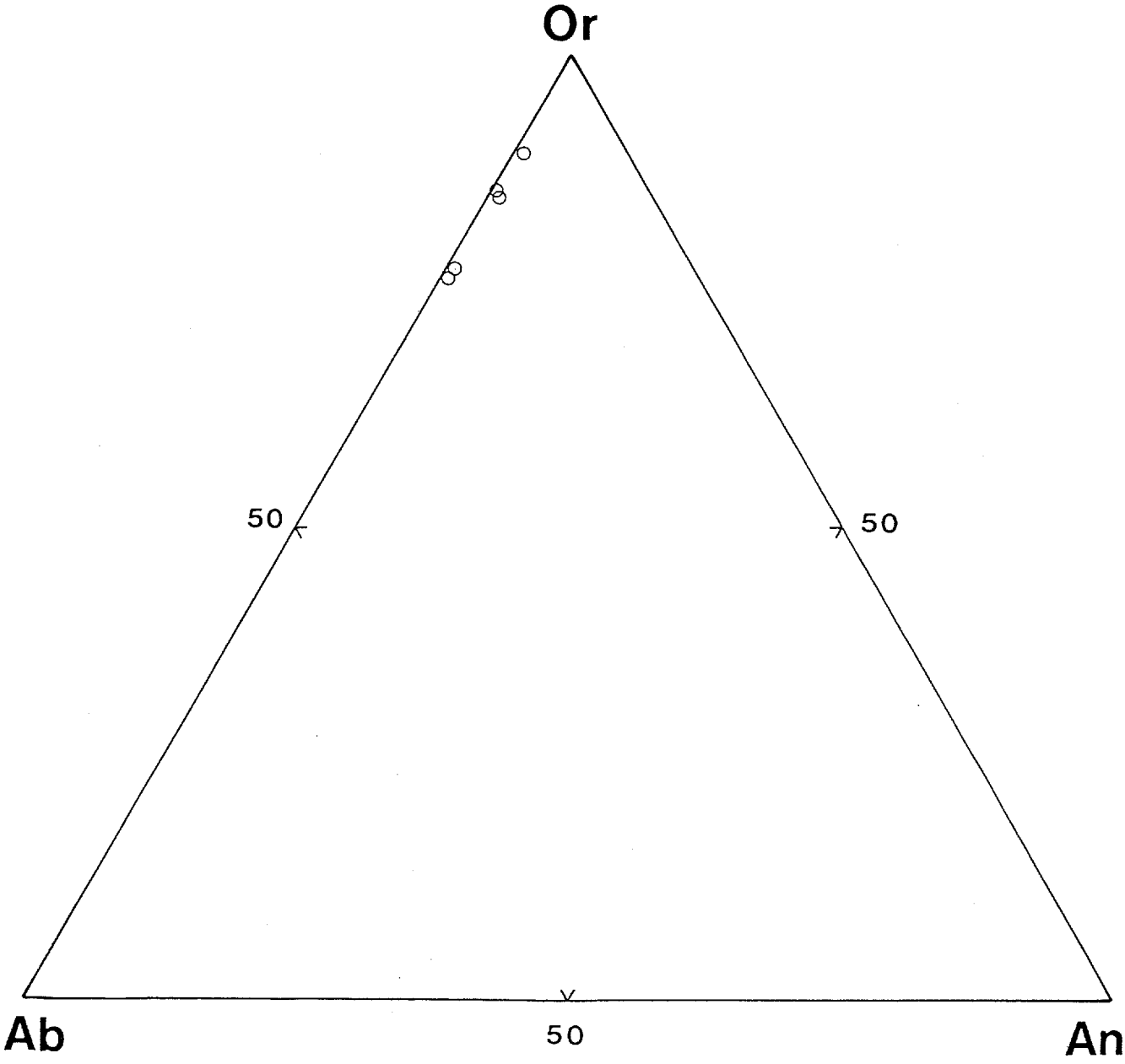

Fig. 49. Ab – An – Or diagram for K–feldspar from the aplite.

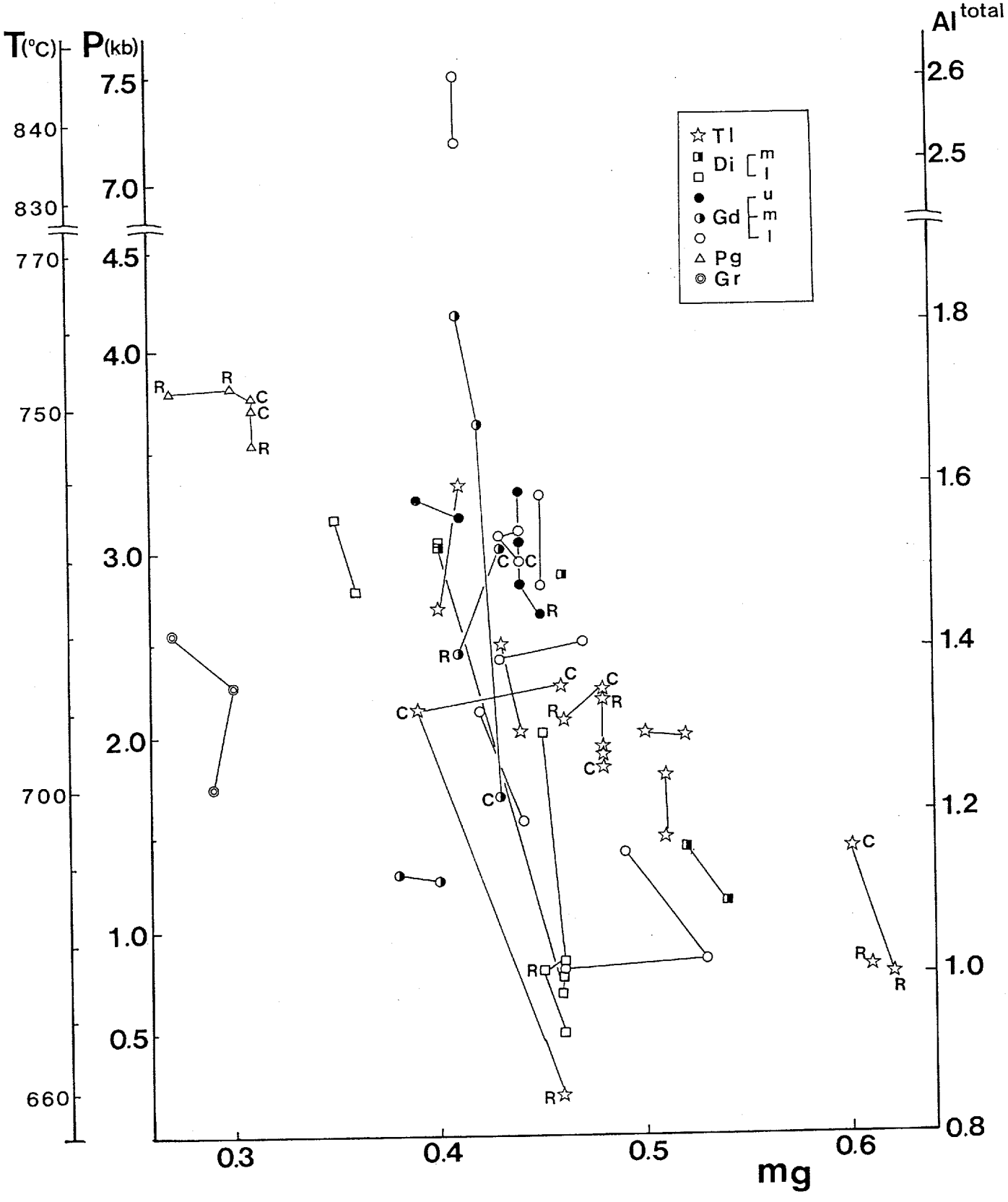

Fig. 50. Relationship between mg value and crystallization pressure and temperature for calcic amphiboles from the Togouchi area.
T:temperature, P:pressure, Al^{total}:total aluminum cation(O=23).
For symbols and abbreviations see Fig. 16 and for explanation see text.

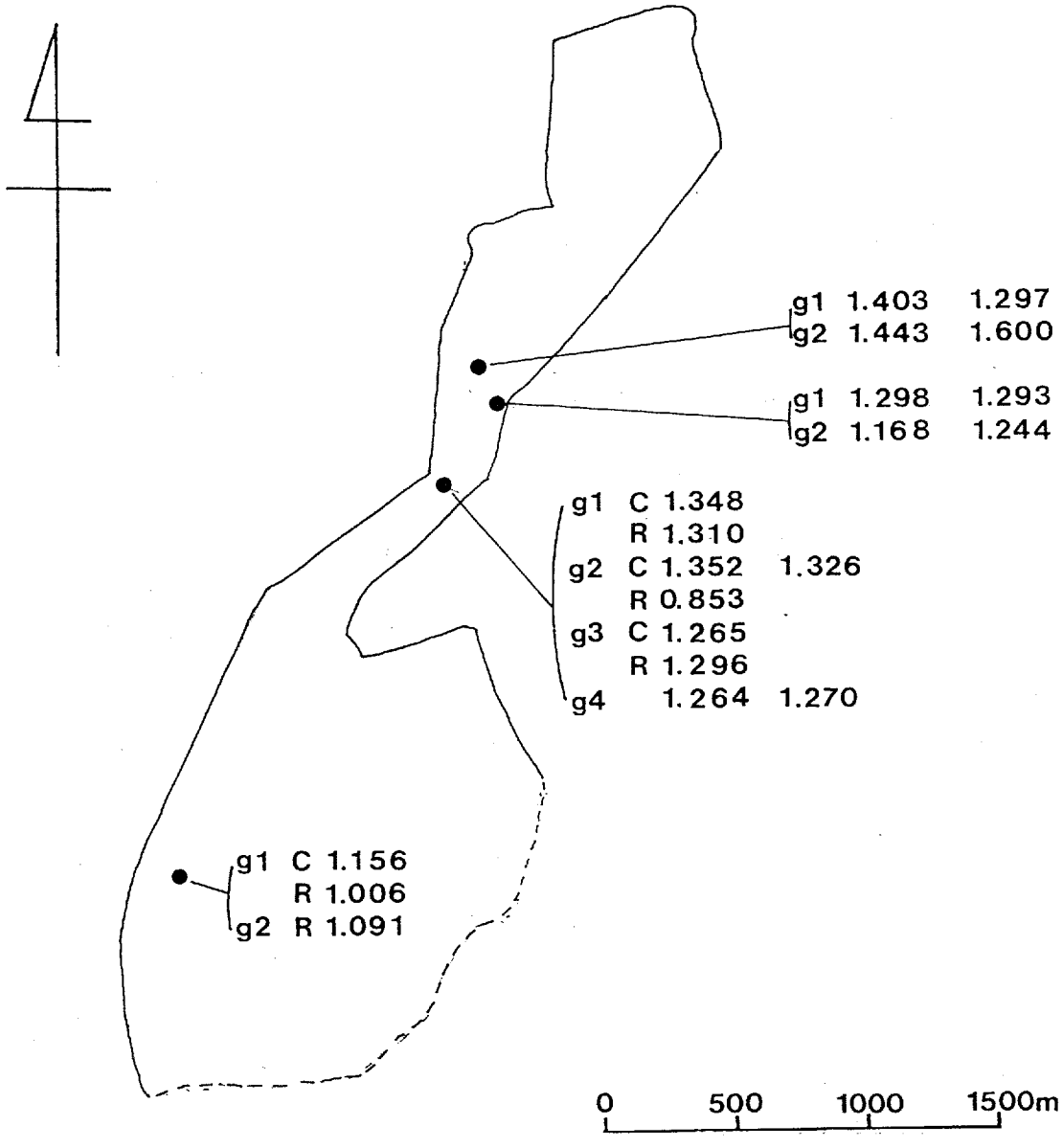

Fig. 51. Spatial variation of total Al(O=23) of calcic amphiboles in the tonalite.
g1 to g4:analyzed grain number, C:core, R:rim.

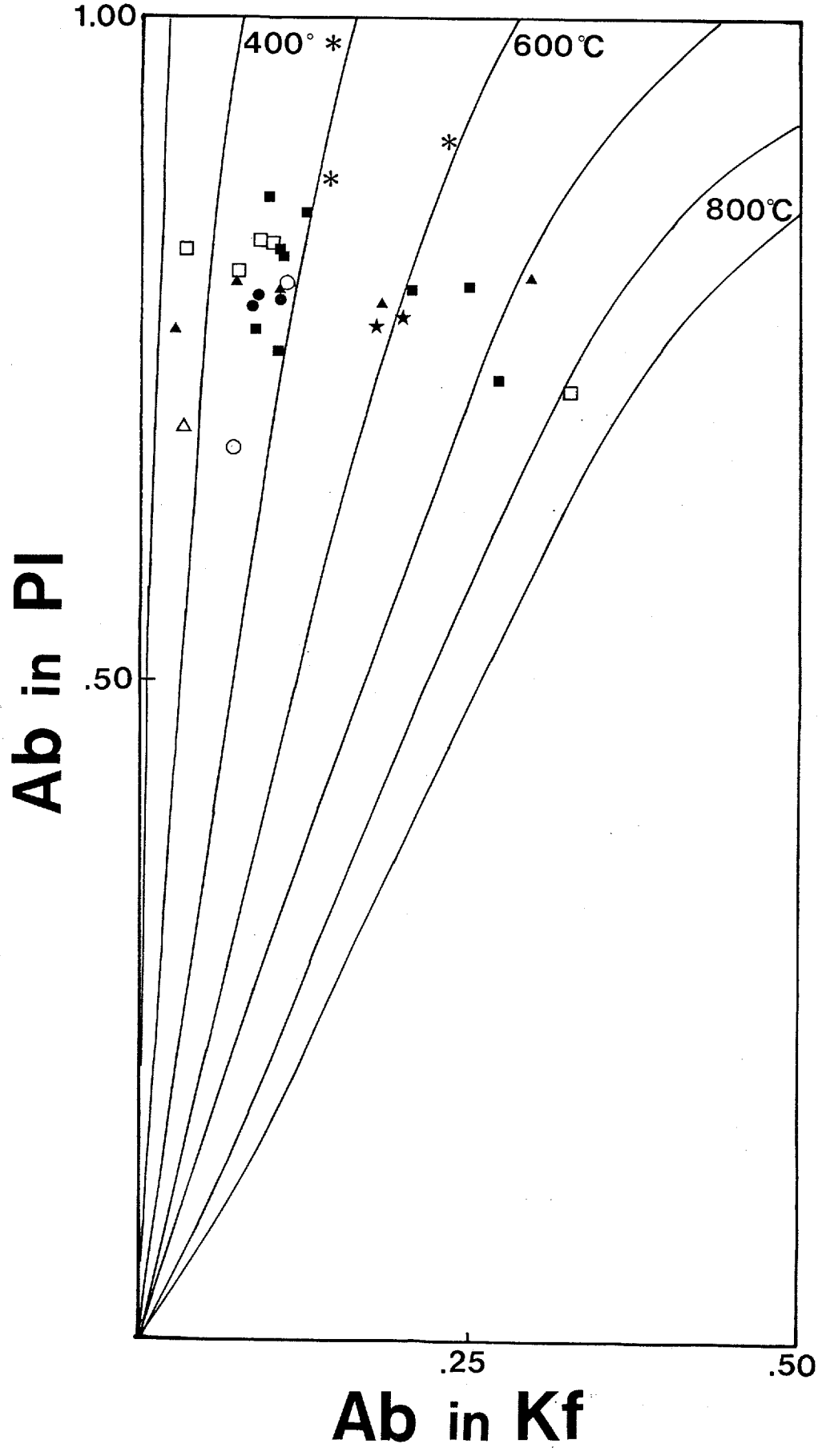

Fig. 52. Crystallization temperature deduced from two feldspars geothermometer by Whitney & Stormer(1977).
circle:dark inclusion, square:granodiorite, triangle:porphyritic granite, star:granite, asterisk:aplite.
solid:coarse-grained plagioclase, open:fine-grained plagioclase.

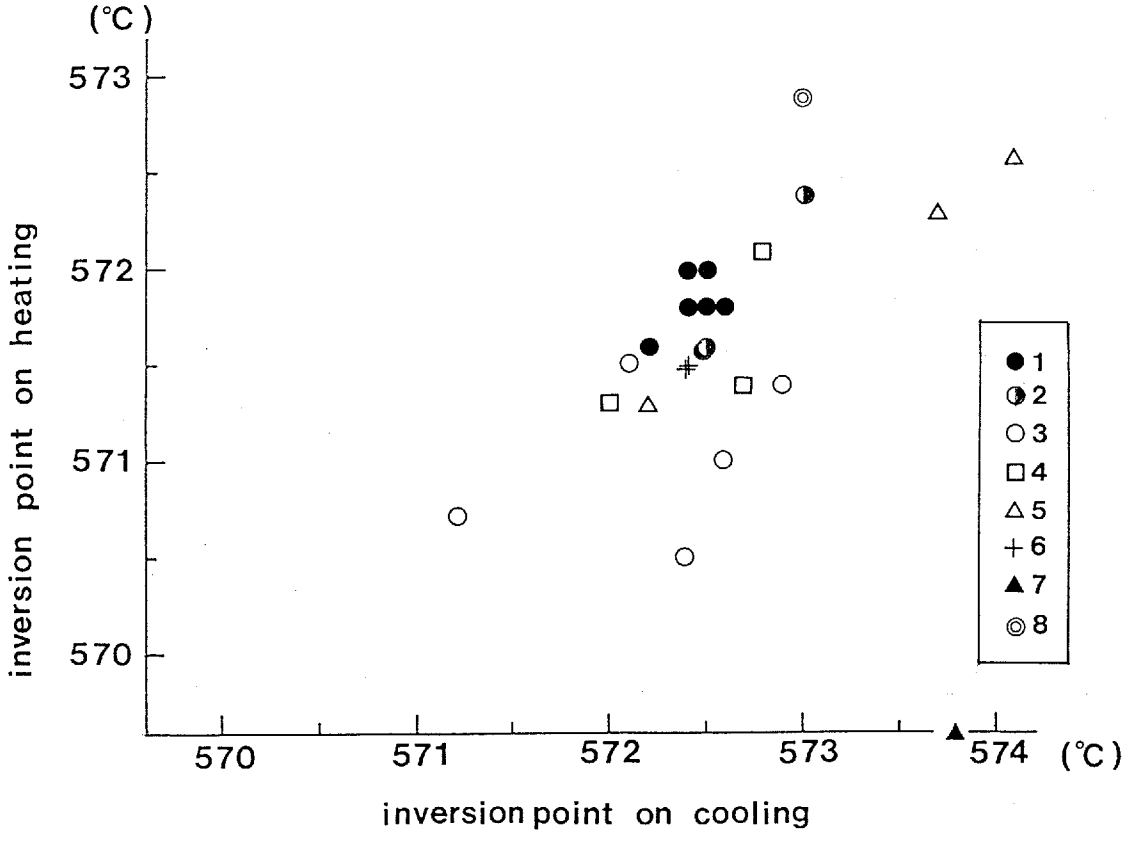

Fig. 53. High–low inversion data of quartz from various rocks in the Togouchi–Yuu–Takehara district and other areas.
1:medium– to coarse–grained granite, 2:quartz vein, 3:fine–grained granite, mylonite and pegmatite, 4:rhyolitic rocks, 5:chert, 6:gneiss, 7:segregated quartz vein, 8:synthesized quartz. For explanation see text.

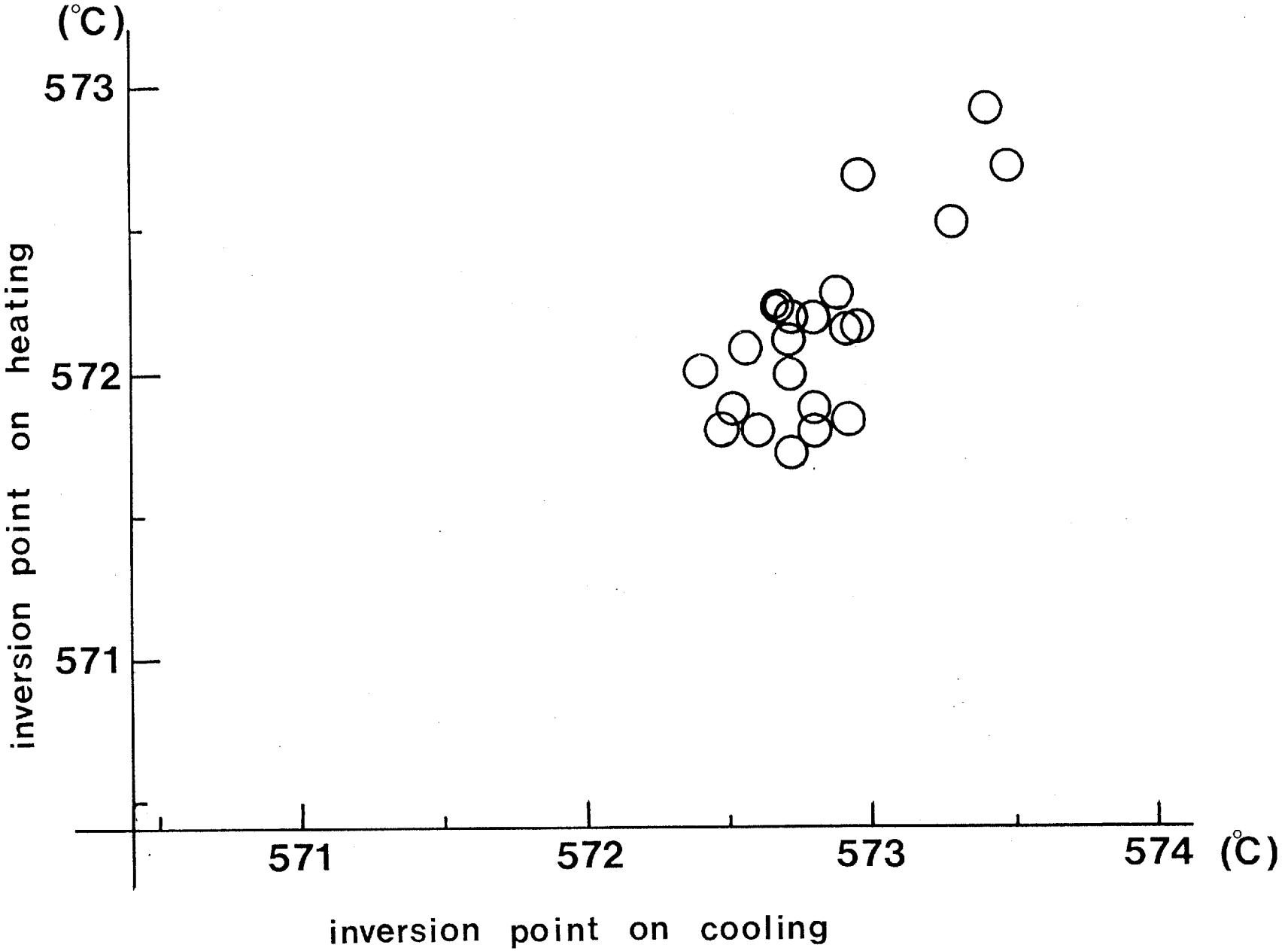

Fig. 54. High–low inversion data of quartz from the porphyritic granite.

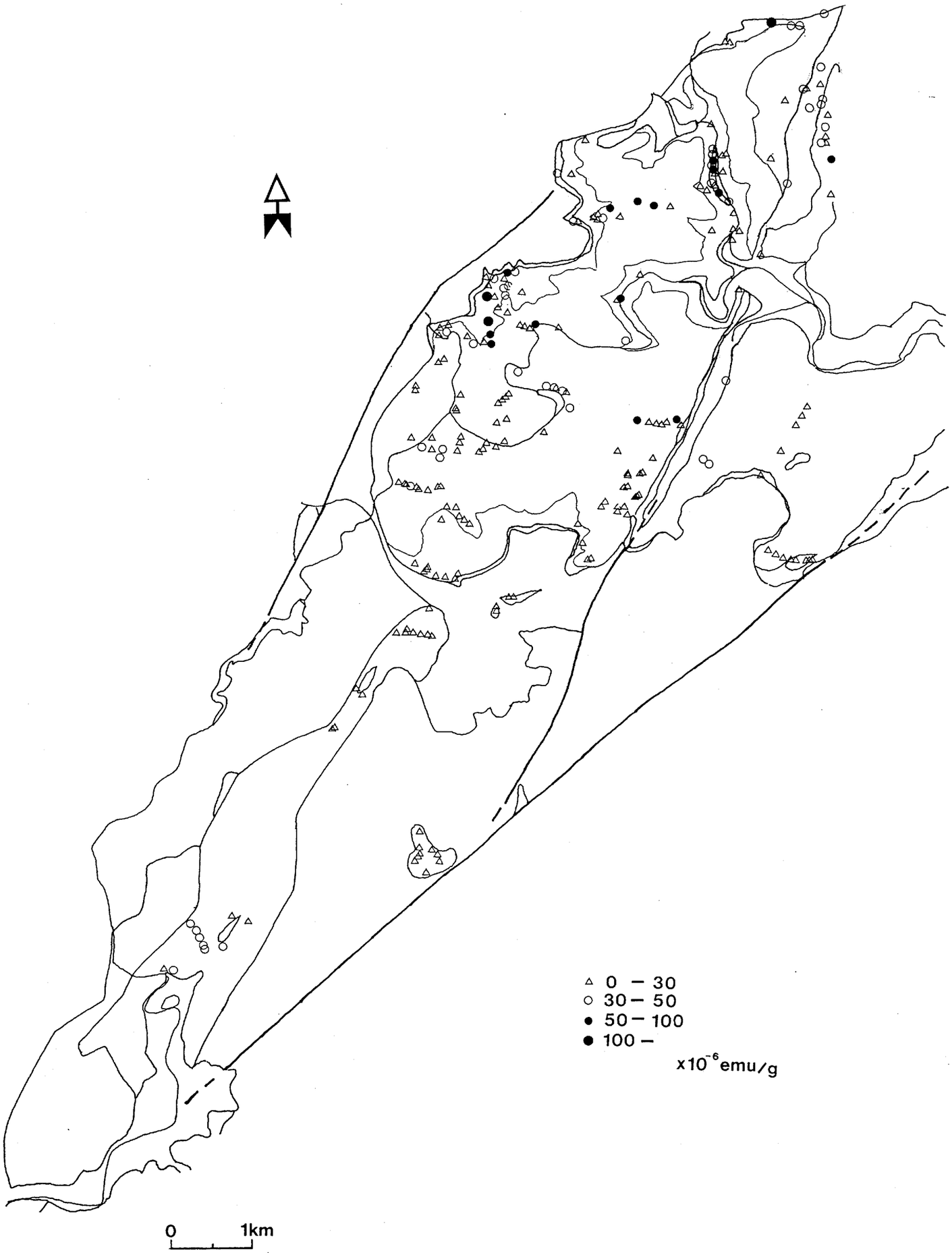

Fig. 55. Spatial variation of magnetic susceptibility of the granitic rocks in the Togouchi area.

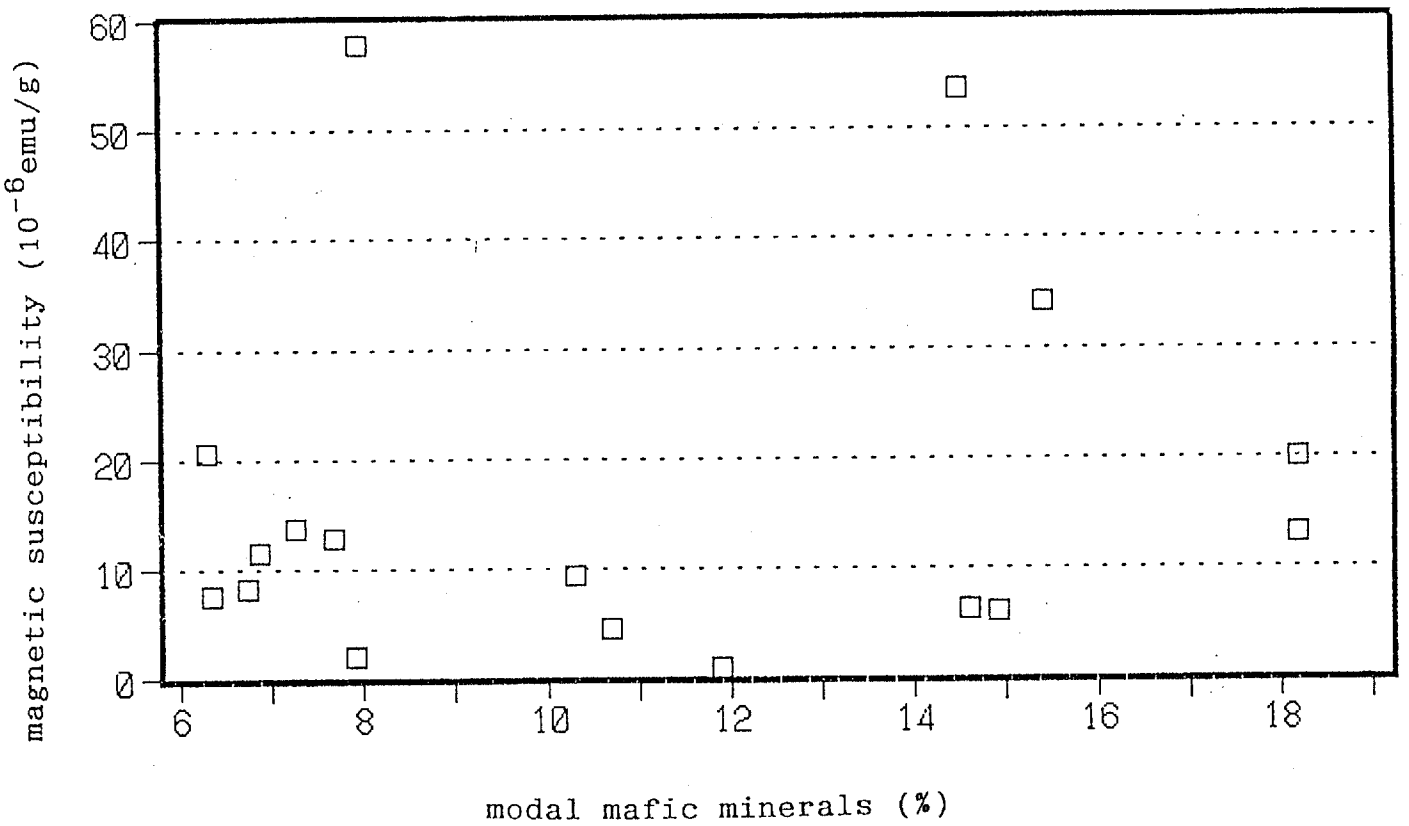

Fig. 56. Relationship between magnetic susceptibility and amounts of mafic minerals in the granodiorite.

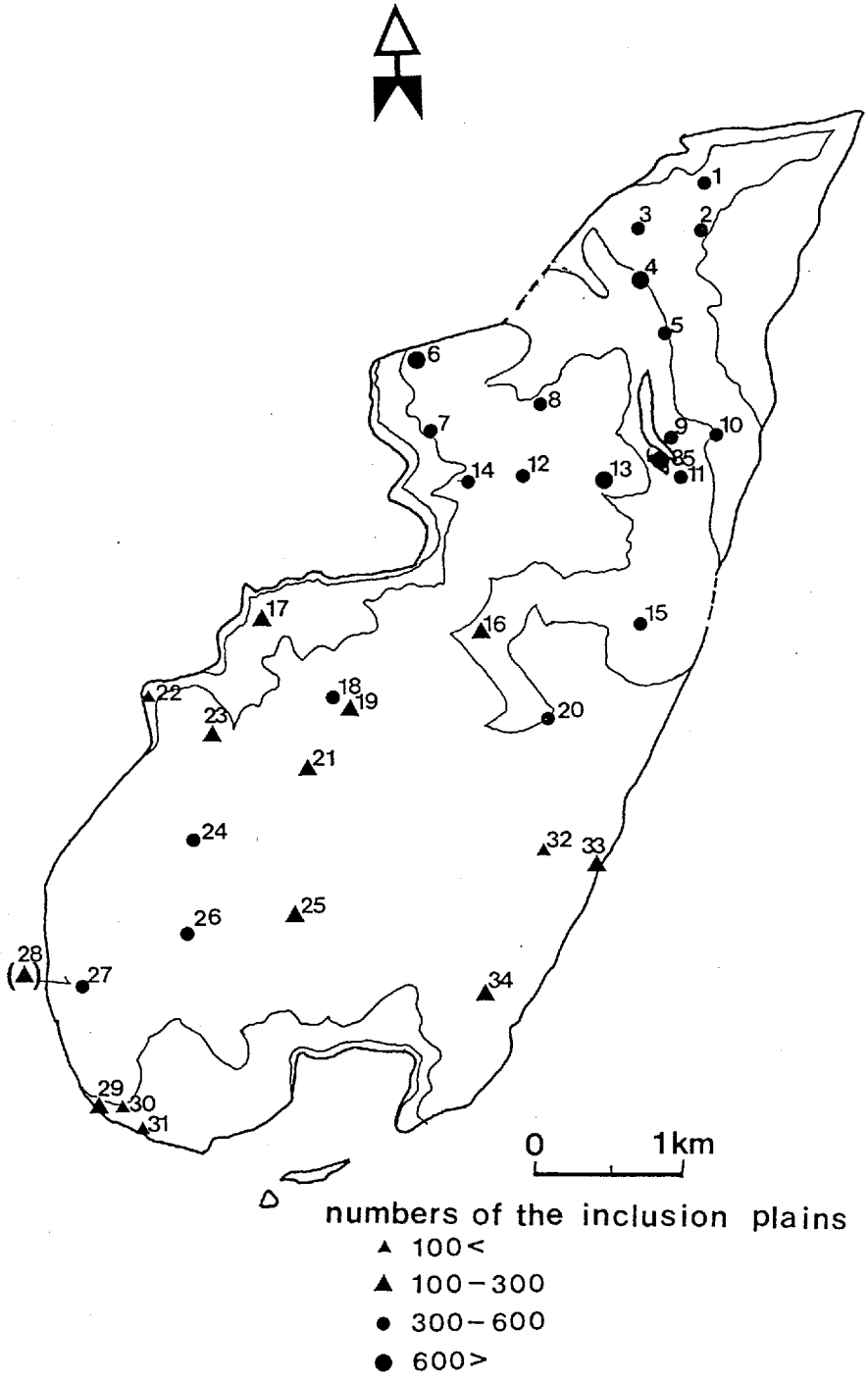

Fig. 57. Spatial variation of numbers of fluid inclusion planes found in quartz grains of the granodiorite.
1 to 35: locality numbers.

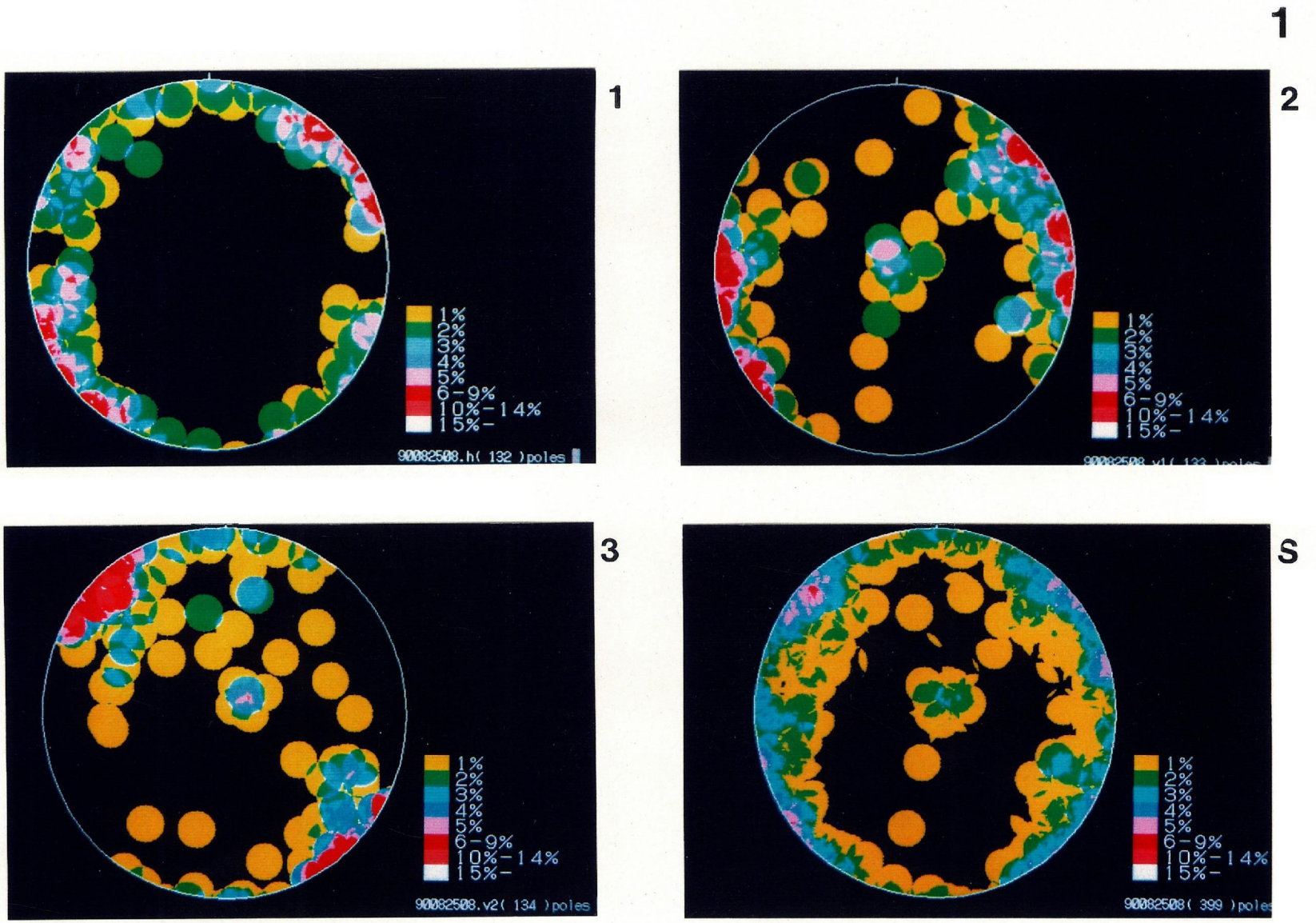

Fig. 58-1. Contour diagram of microscopic fluid inclusion planes of quartz at locality No. 1.
1 to 3:examined result on each thin section, S:synoptic (1, 2 and 3)

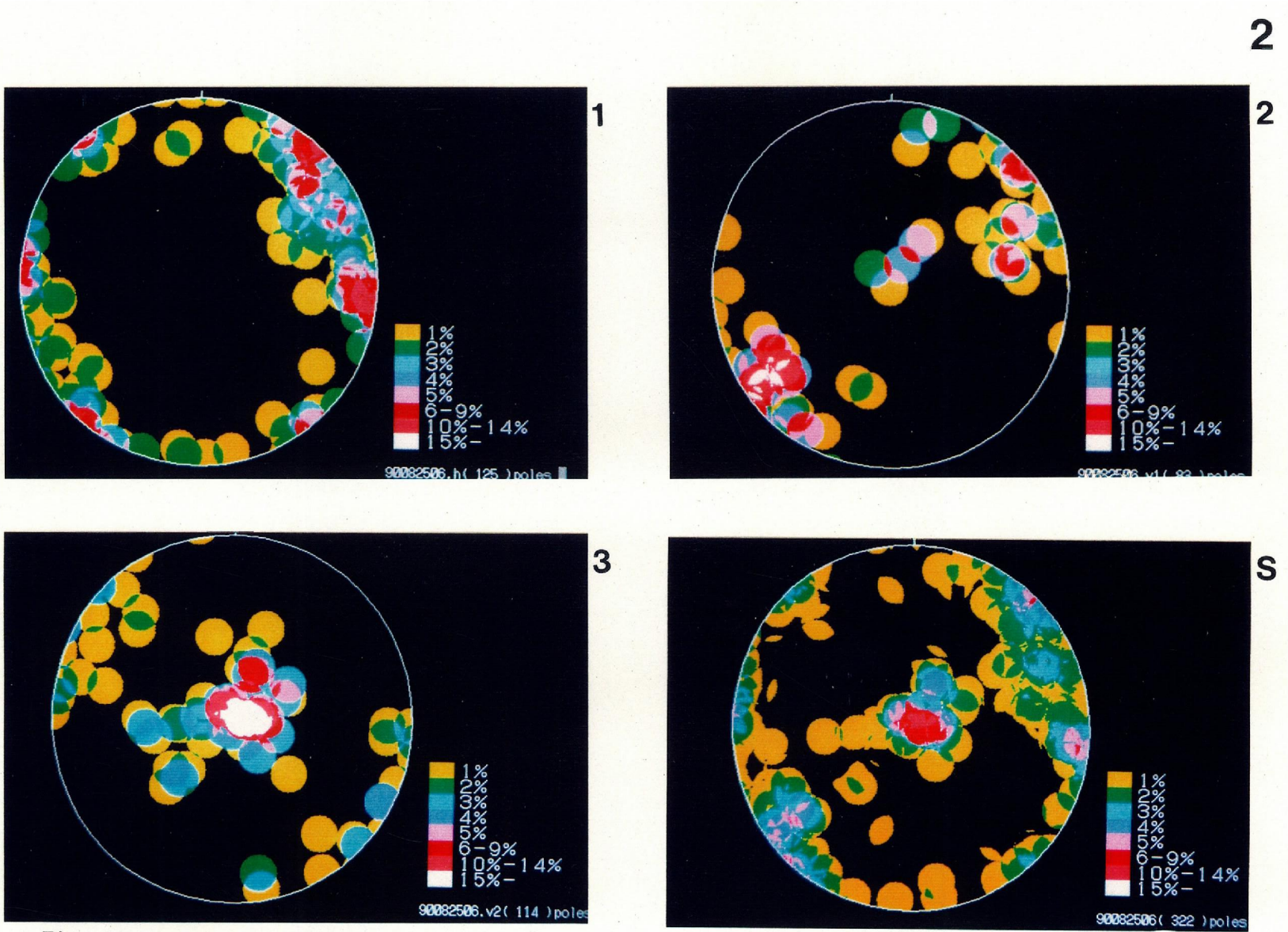

Fig. 58-2. Contour diagram of microscopic fluid inclusion planes of quartz at locality No. 2.
1 to 3:examined result on each thin section, S:synoptic (1, 2 and 3)

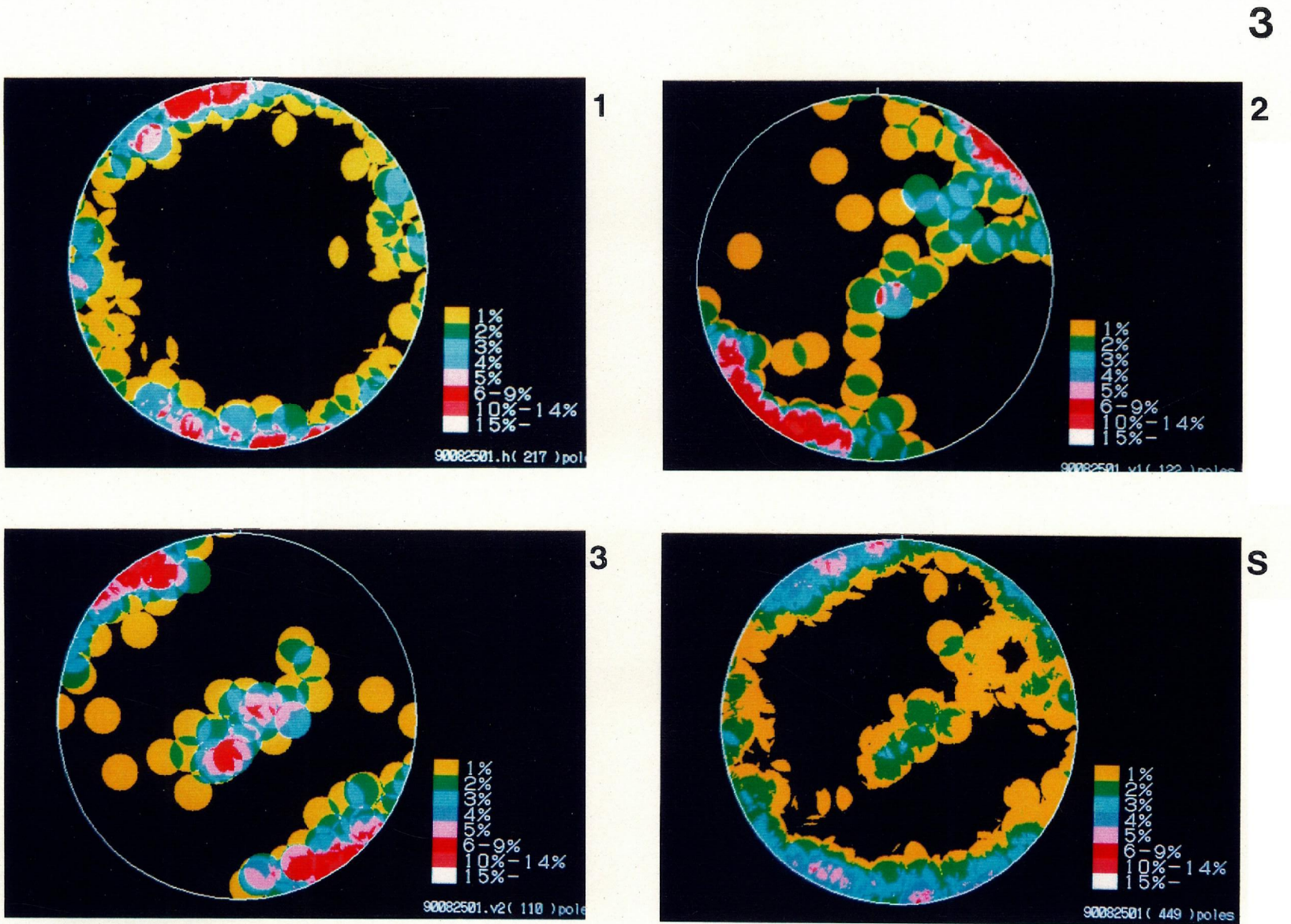

Fig. 58-3. Contour diagram of microscopic fluid inclusion planes of quartz at locality No. 3.
1 to 3:examined result on each thin section, S:synoptic (1, 2 and 3)

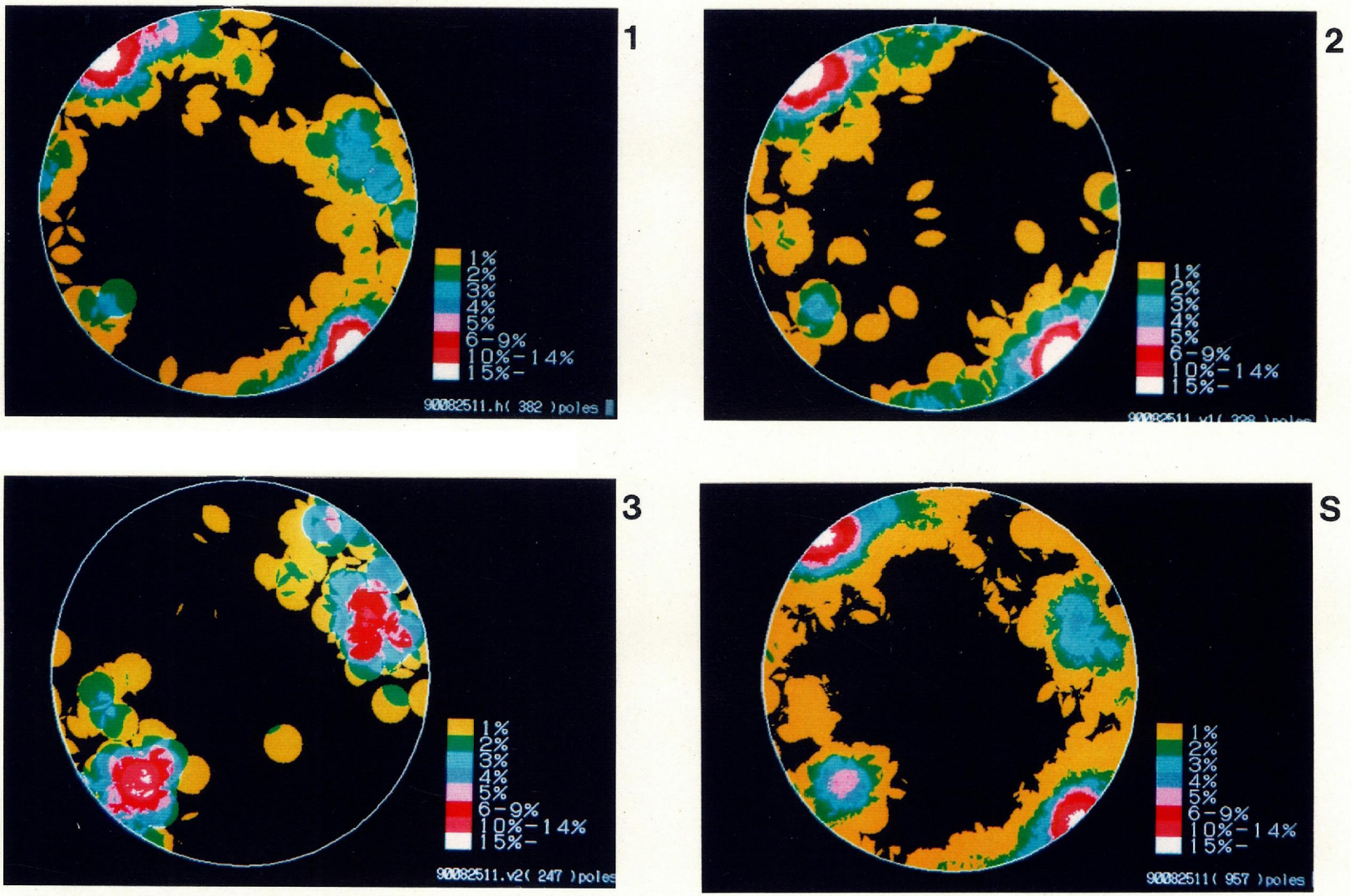

Fig. 58-4. Contour diagram of microscopic fluid inclusion planes of quartz at locality No. 4.
1 to 3:examined result on each thin section, S:synoptic (1, 2 and 3)

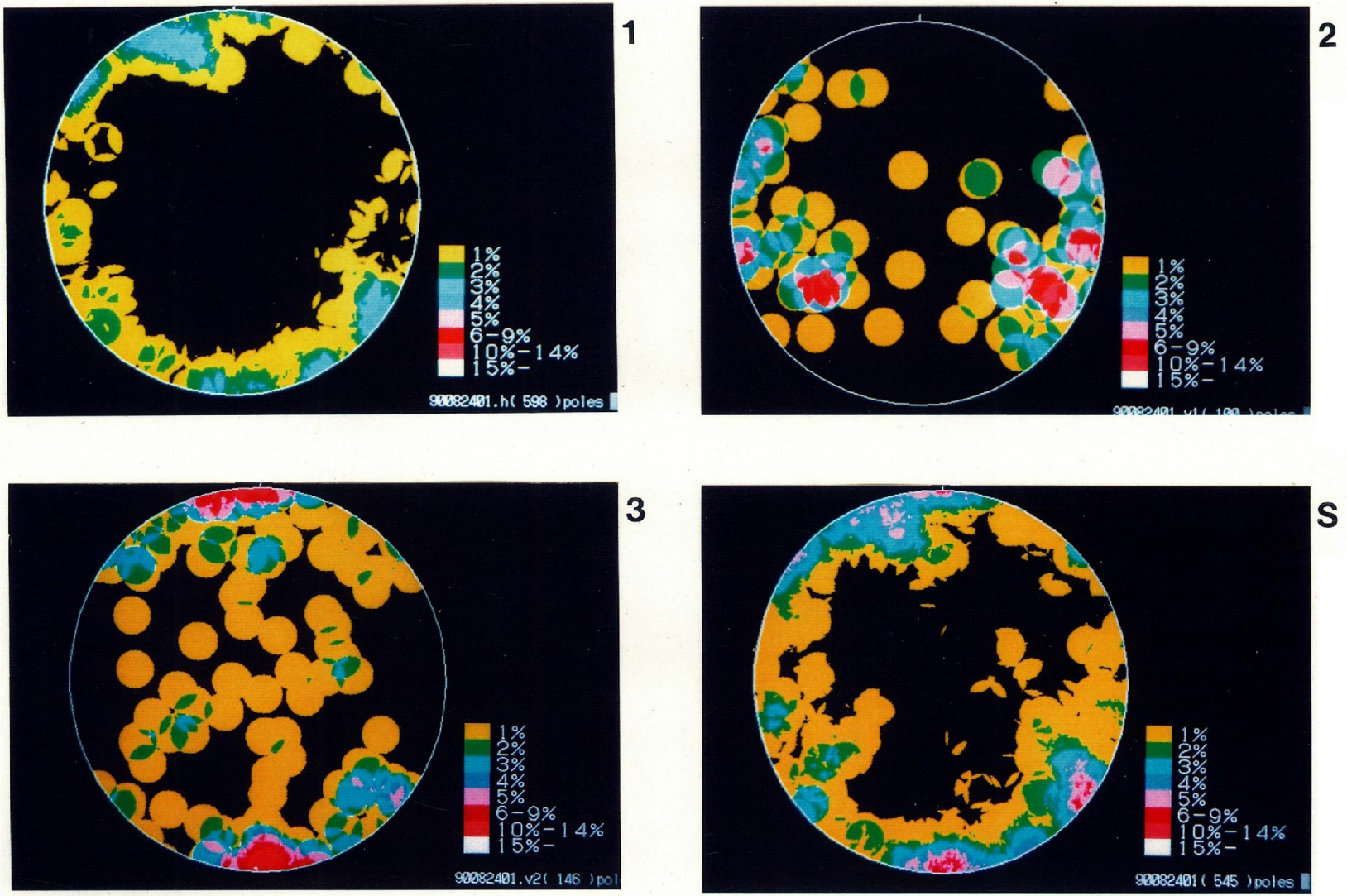

Fig. 58-5. Contour diagram of microscopic fluid inclusion planes of quartz at locality No. 5.
1 to 3:examined result on each thin section, S:synoptic (1, 2 and 3)

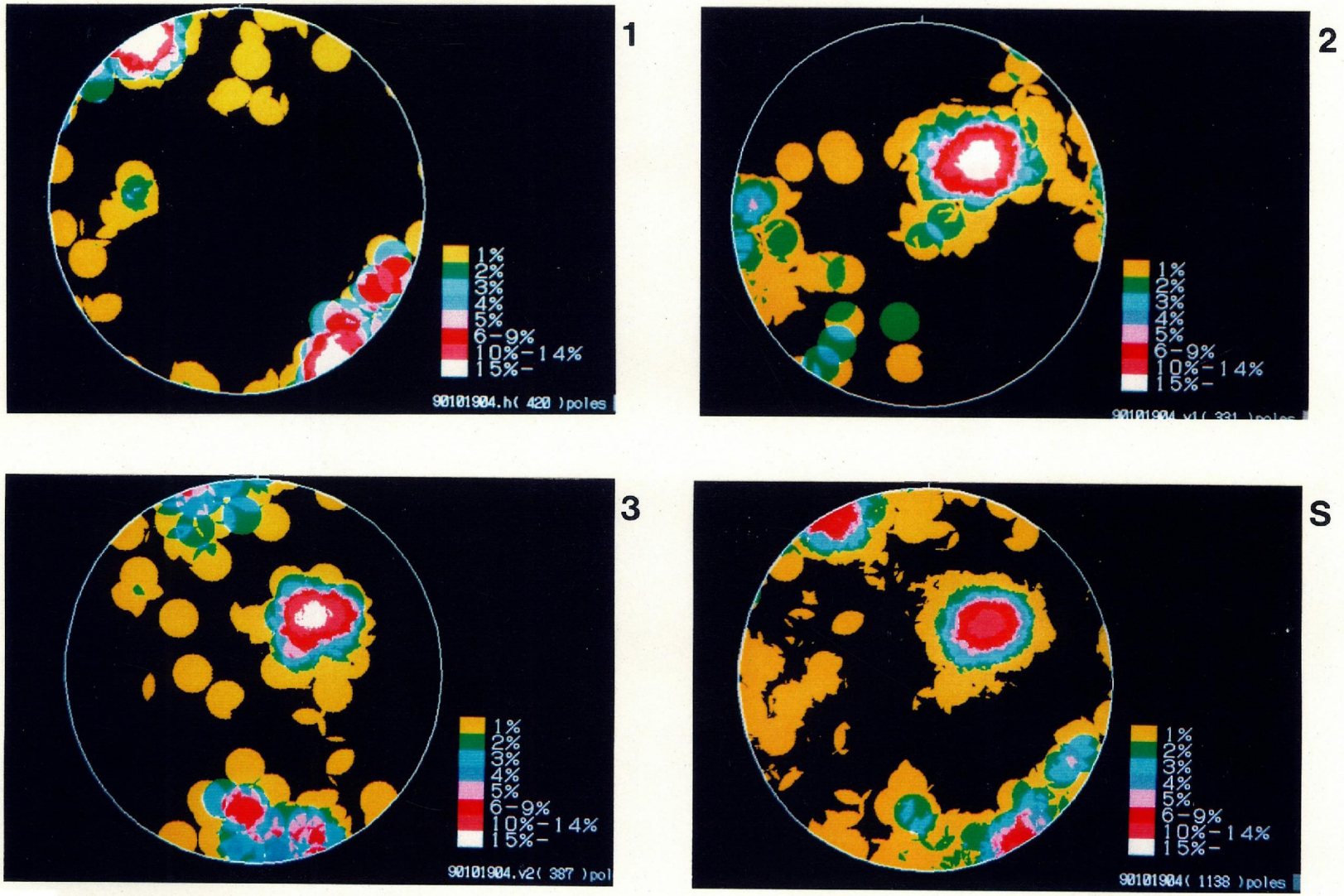

Fig. 58-6. Contour diagram of microscopic fluid inclusion planes of quartz at locality No. 6.
1 to 3:examined result on each thin section, S:synoptic (1, 2 and 3)

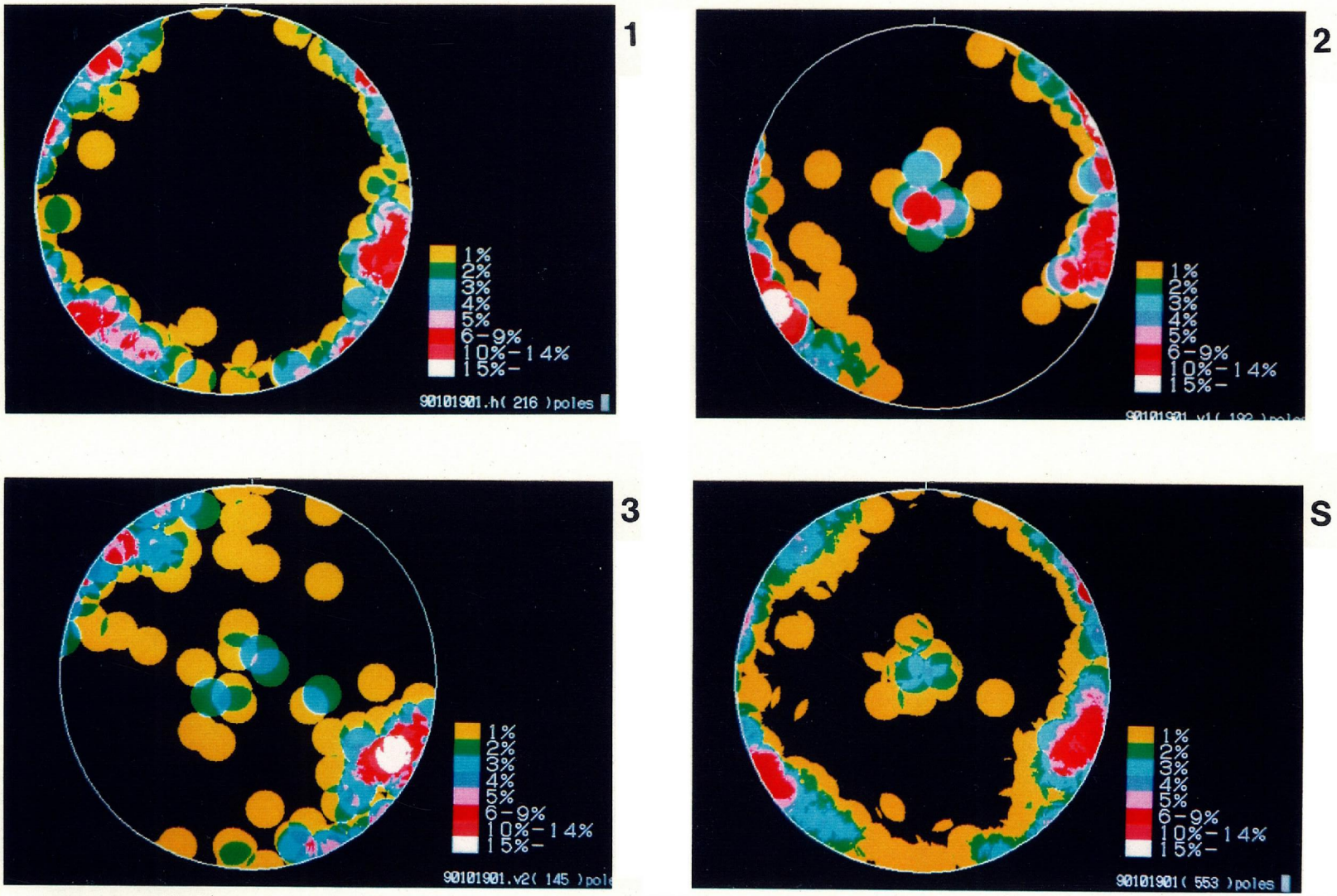

Fig. 58-7. Contour diagram of microscopic fluid inclusion planes of quartz at locality No. 7.
1 to 3:examined result on each thin section, S:synoptic (1, 2 and 3)

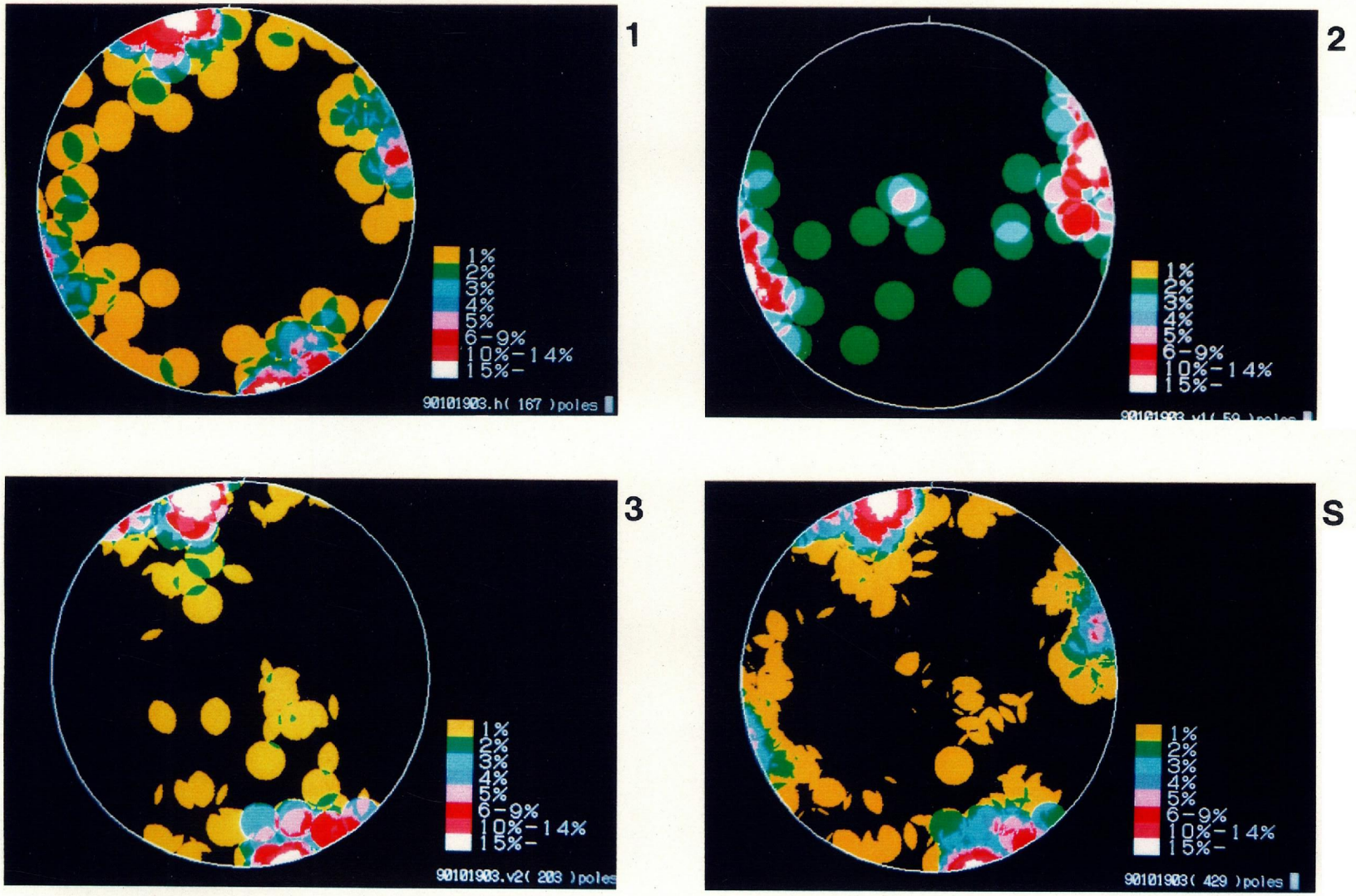

Fig. 58-8. Contour diagram of microscopic fluid inclusion planes of quartz at locality No. 8.
1 to 3:examined result on each thin section, S:synoptic (1, 2 and 3)

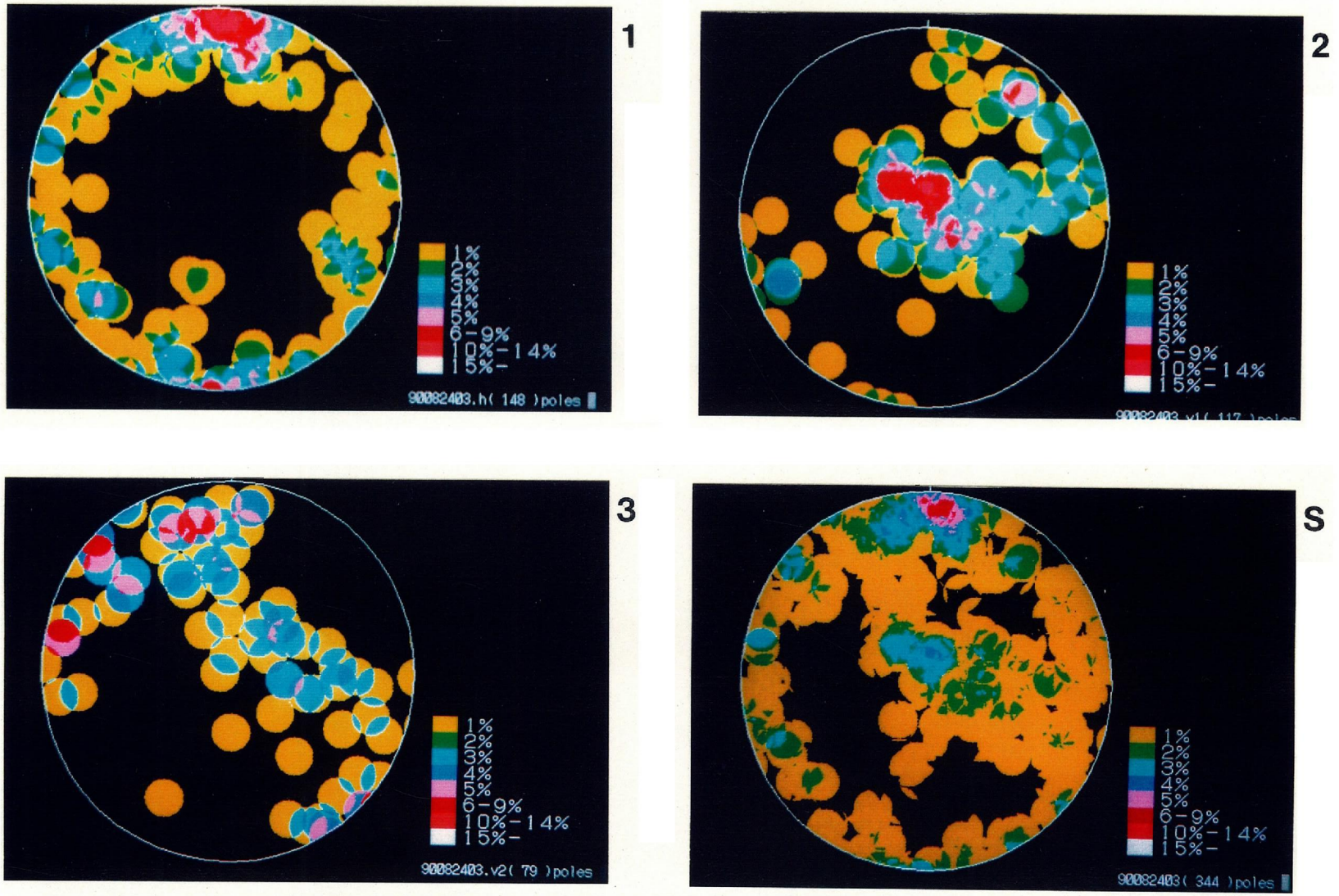

Fig. 58-9. Contour diagram of microscopic fluid inclusion planes of quartz at locality No. 9.
1 to 3:examined result on each thin section, S:synoptic (1, 2 and 3)

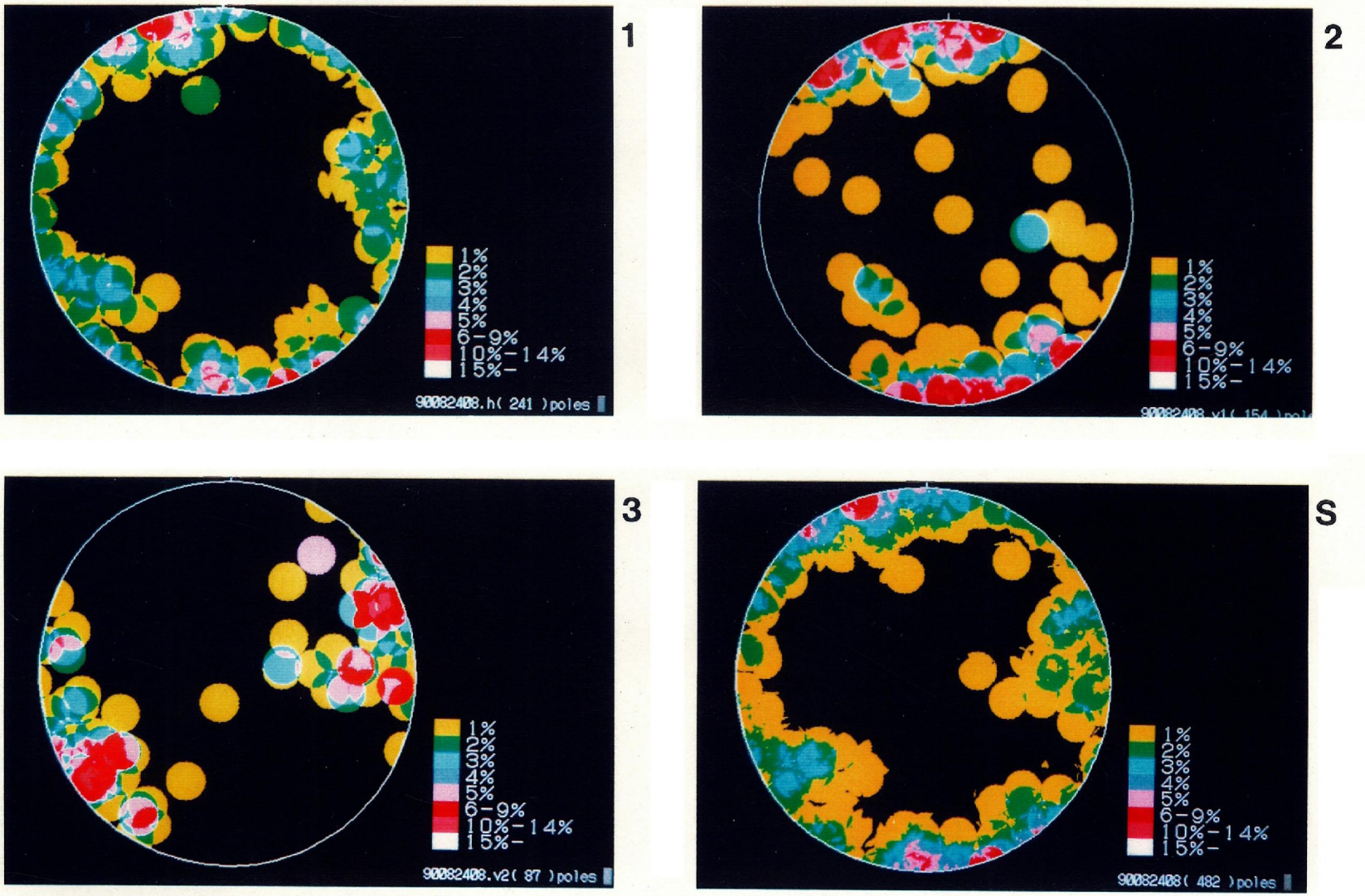

Fig. 58-10. Contour diagram of microscopic fluid inclusion planes of quartz at locality No. 10.
1 to 3:examined result on each thin section, S:synoptic (1, 2 and 3)

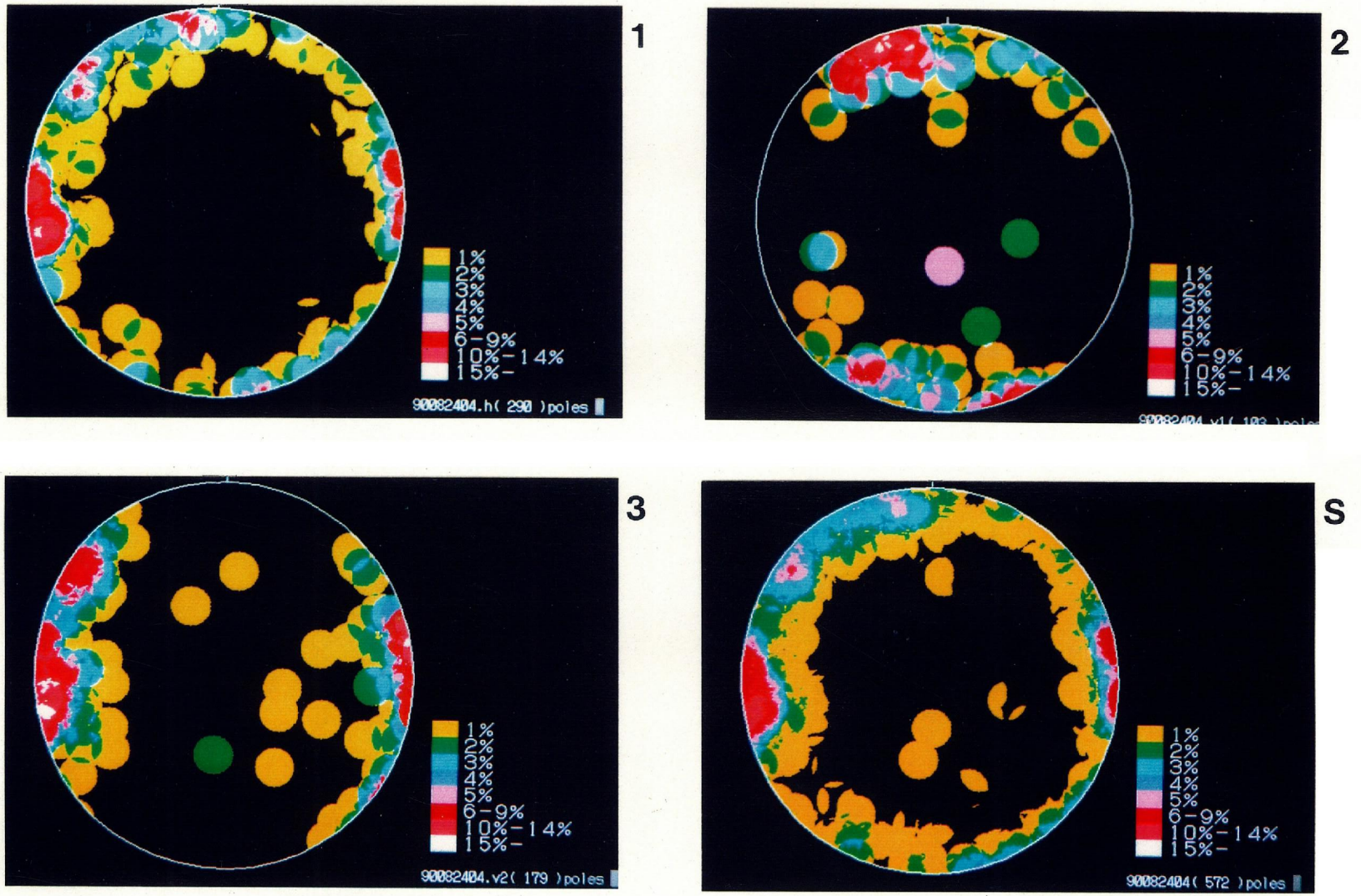

Fig. 58-11. Contour diagram of microscopic fluid inclusion planes of quartz at locality No. 11.
1 to 3:examined result on each thin section, S:synoptic (1, 2 and 3)

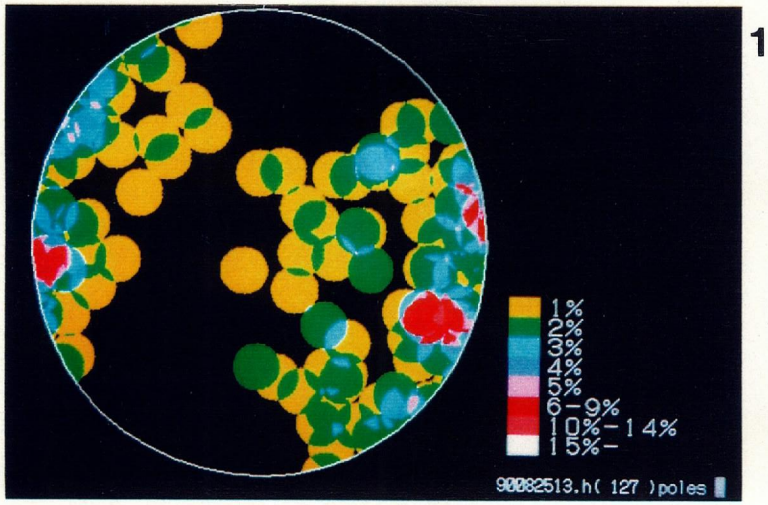

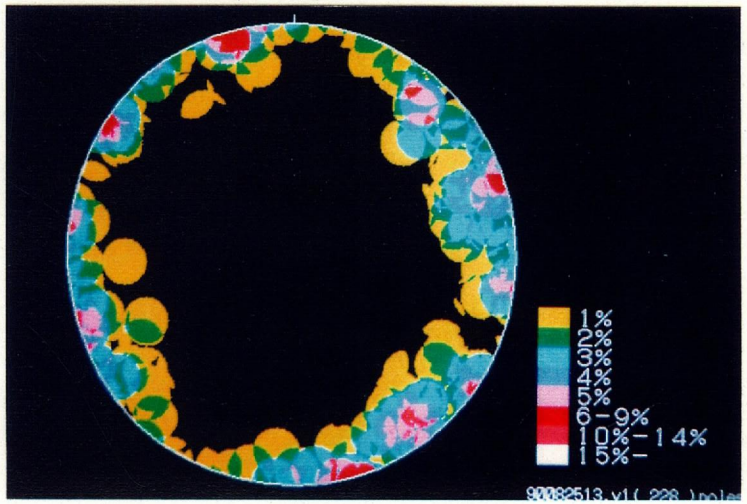

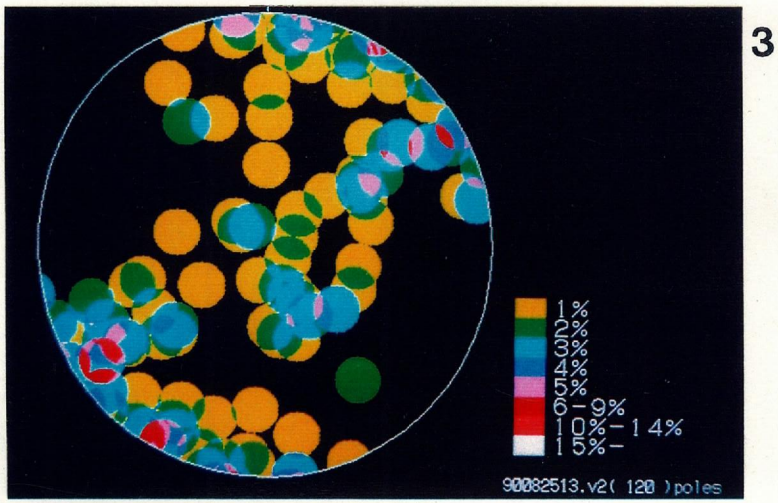

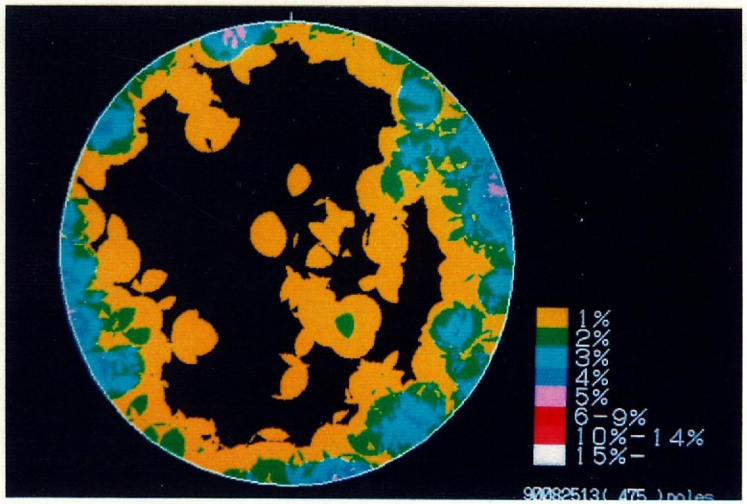

Fig. 58-12. Contour diagram of microscopic fluid inclusion planes of quartz at locality No. 12.
1 to 3:examined result on each thin section, S:synoptic (1, 2 and 3)

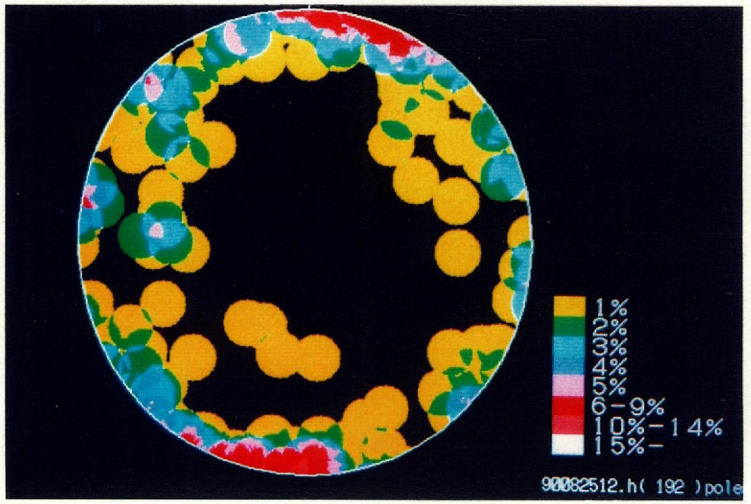

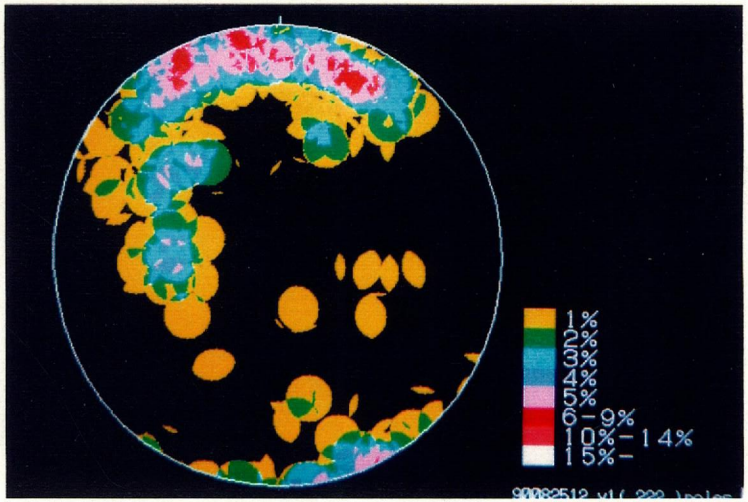

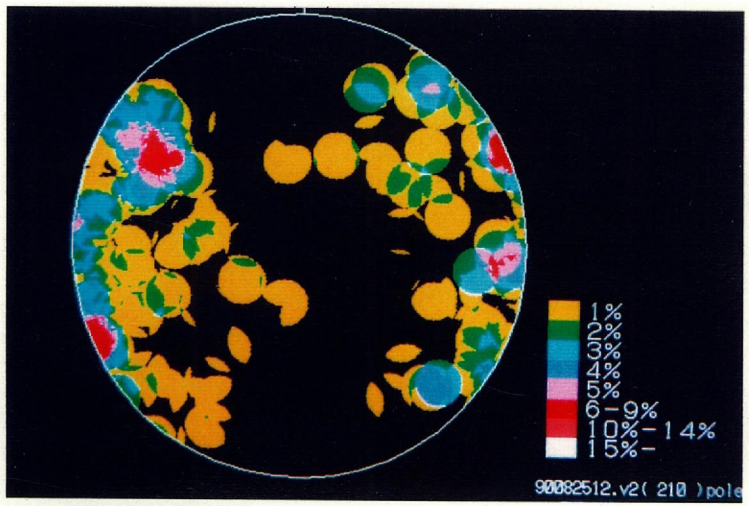

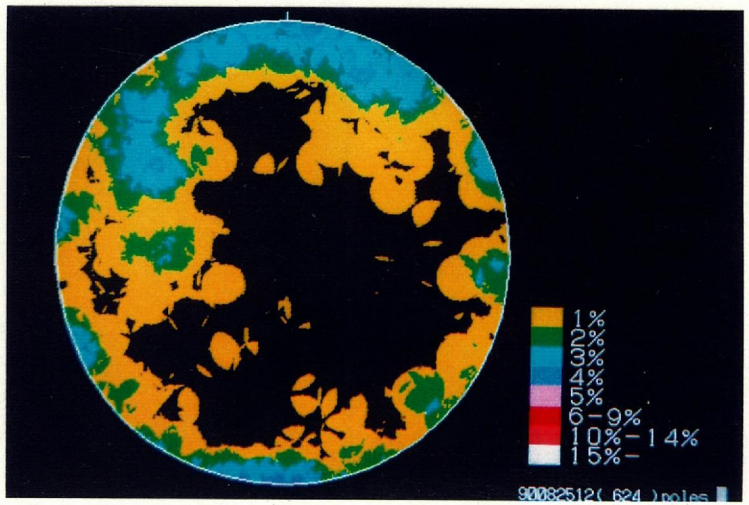

Fig. 58-13. Contour diagram of microscopic fluid inclusion planes of quartz at locality No. 13.
1 to 3:examined result on each thin section, S:synoptic (1, 2 and 3)

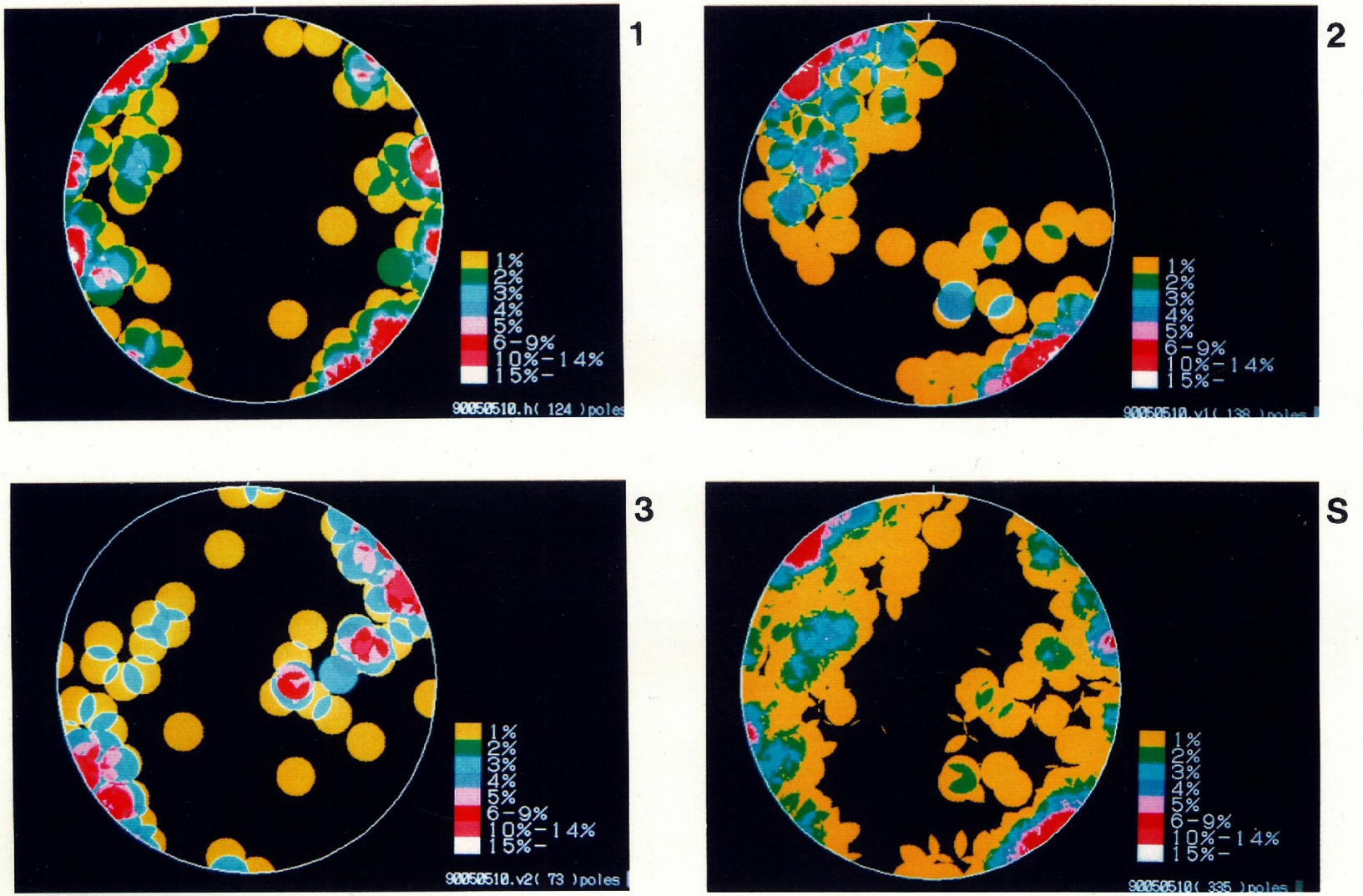

Fig. 58-14. Contour diagram of microscopic fluid inclusion planes of quartz at locality No. 14.
1 to 3:examined result on each thin section, S:synoptic (1, 2 and 3)

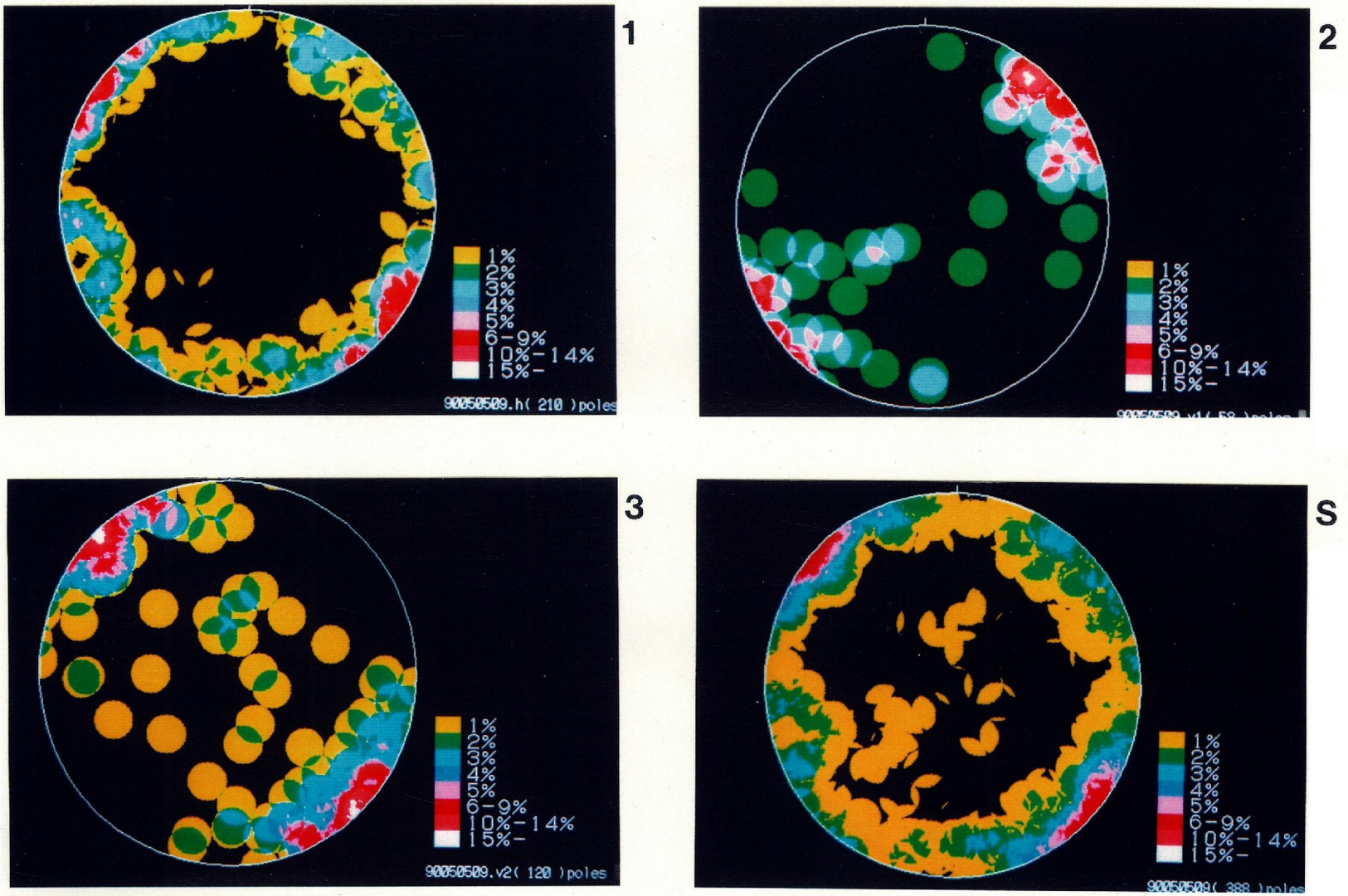

Fig. 58-15. Contour diagram of microscopic fluid inclusion planes of quartz at locality No. 15.
1 to 3:examined result on each thin section, S:synoptic (1, 2 and 3)

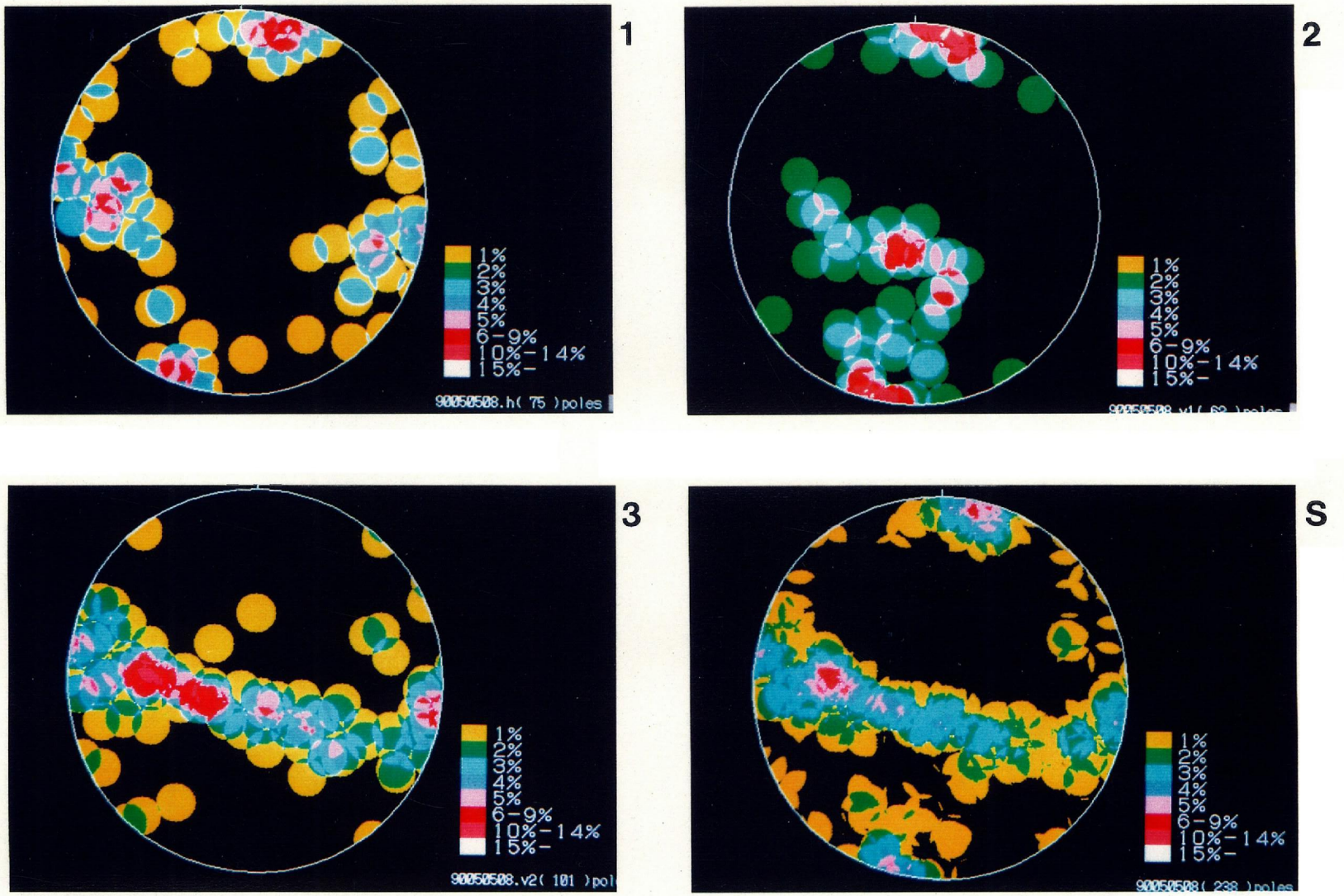

Fig. 58-16. Contour diagram of microscopic fluid inclusion planes of quartz at locality No. 16.
1 to 3:examined result on each thin section, S:synoptic (1, 2 and 3)

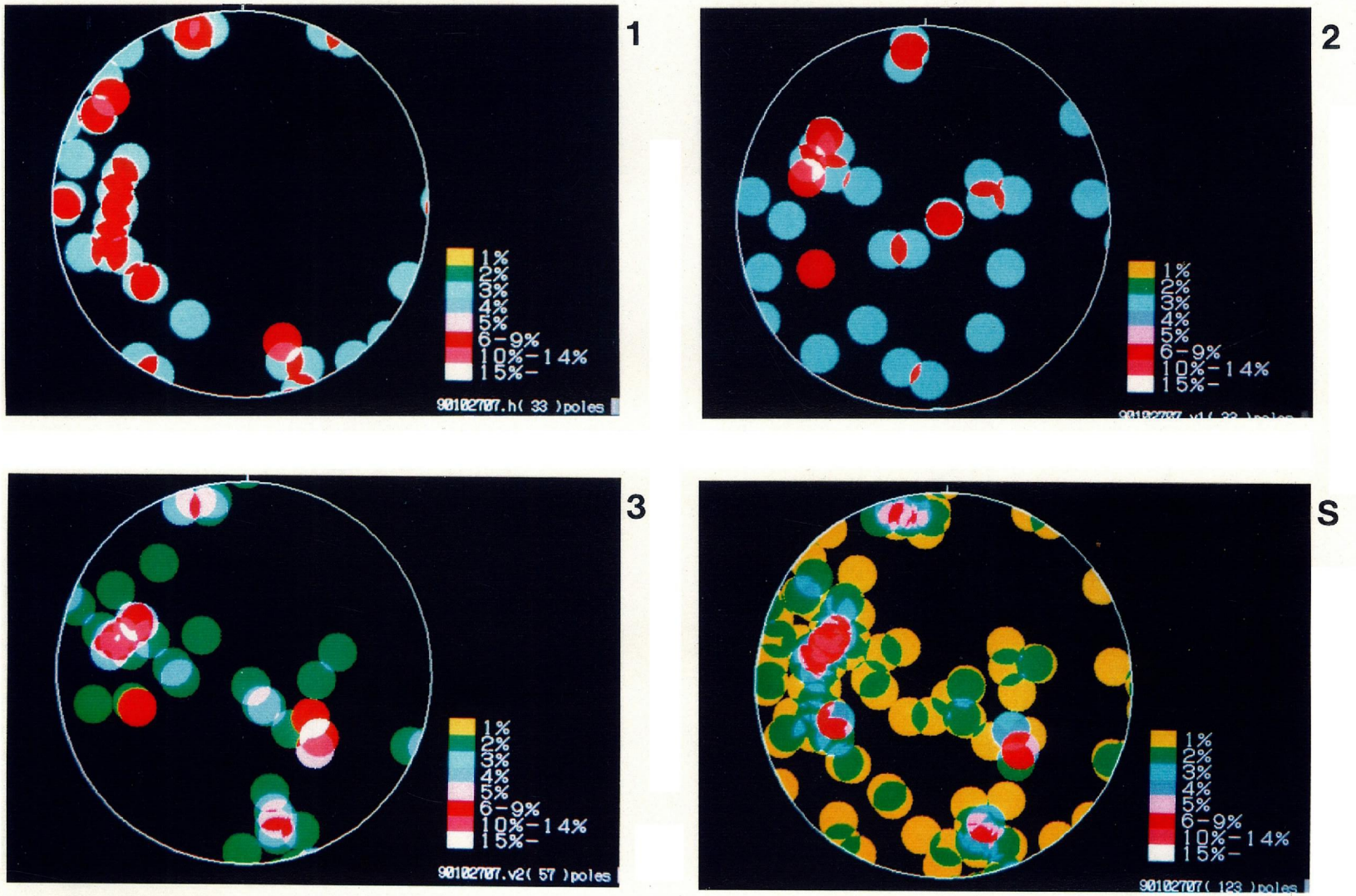

Fig. 58-17. Contour diagram of microscopic fluid inclusion planes of quartz at locality No. 17.
1 to 3:examined result on each thin section, S:synoptic (1, 2 and 3)

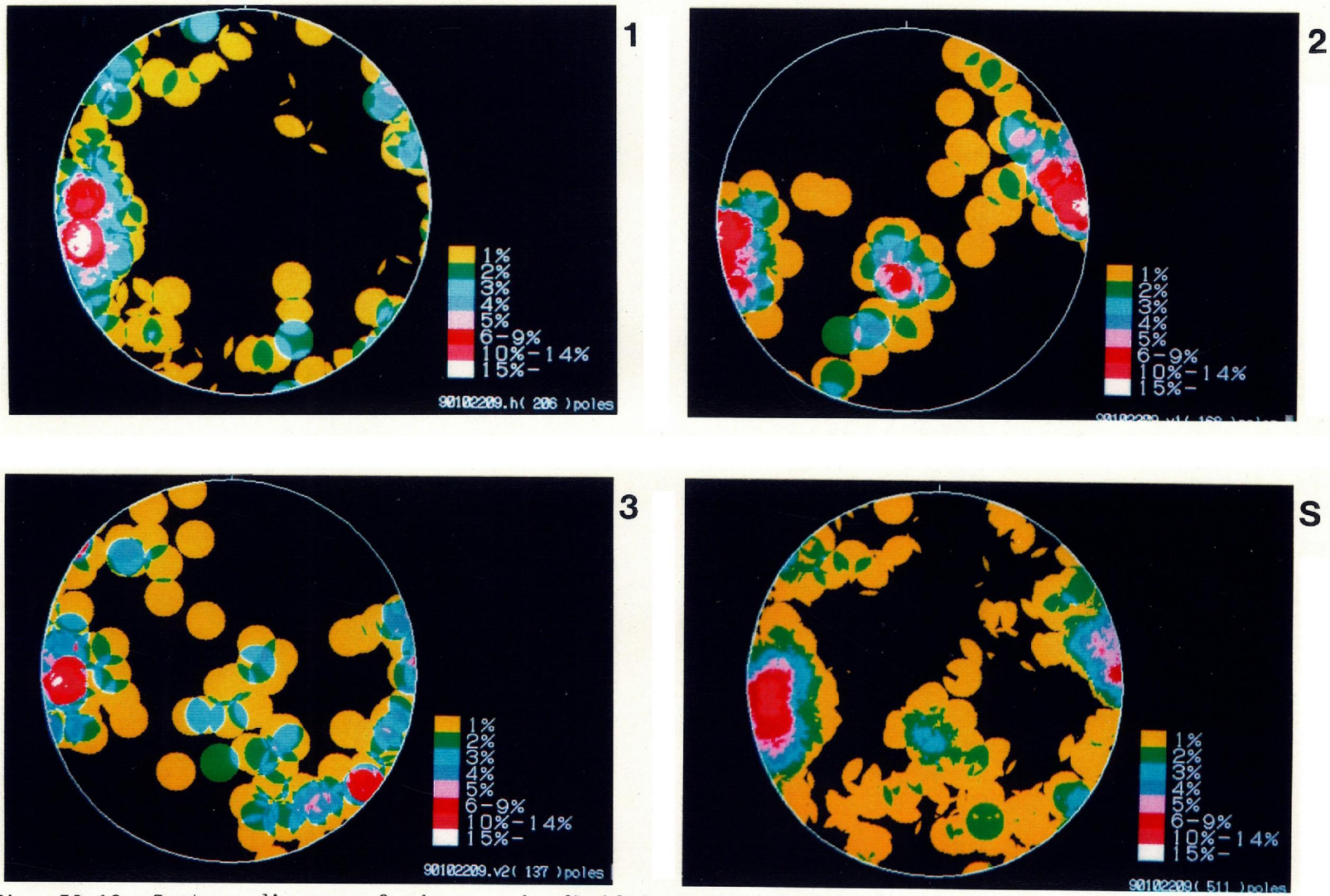

Fig. 58-18. Contour diagram of microscopic fluid inclusion planes of quartz at locality No. 18.
1 to 3:examined result on each thin section, S:synoptic (1, 2 and 3)

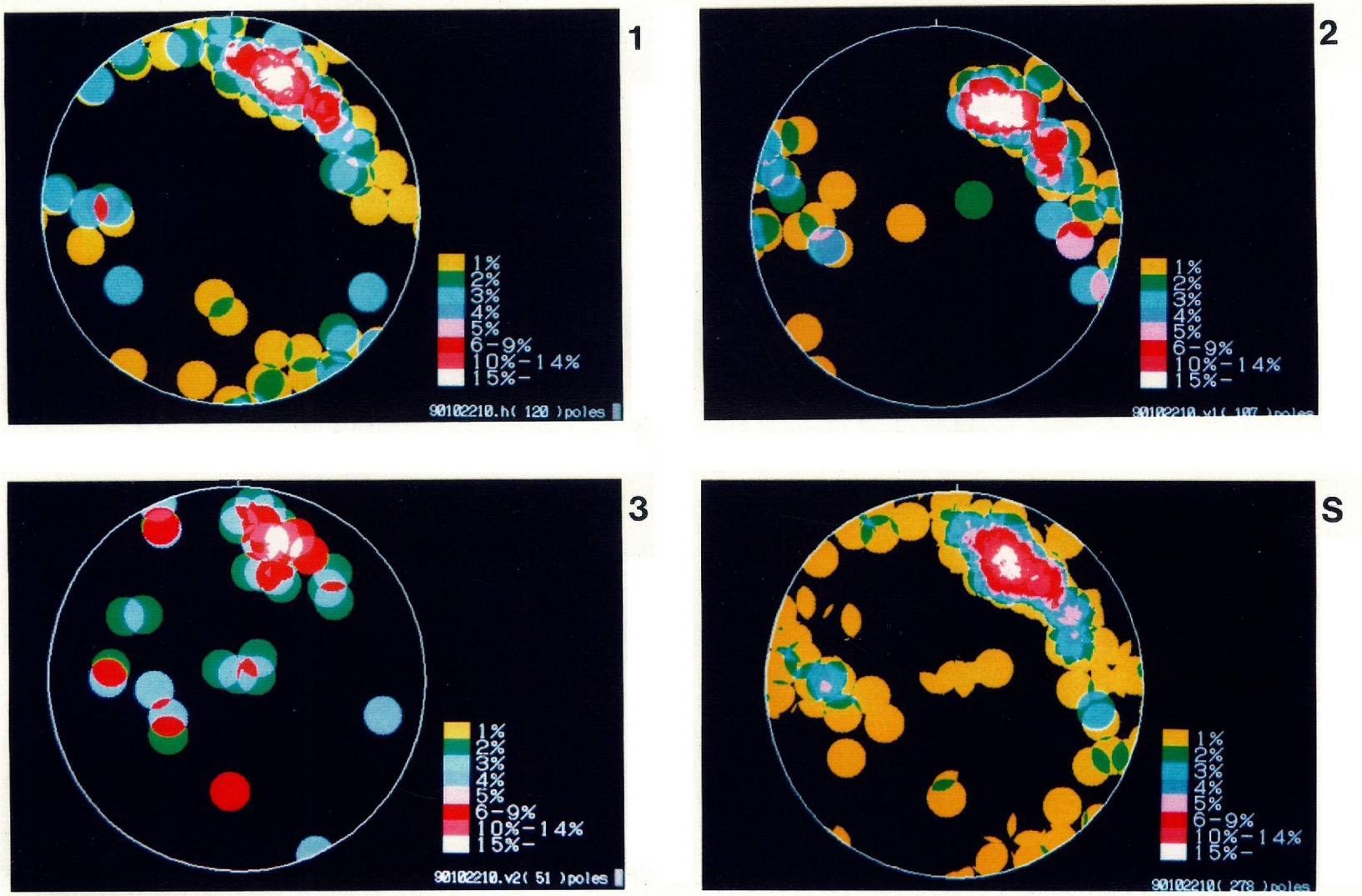

Fig. 58-19. Contour diagram of microscopic fluid inclusion planes of quartz at locality No. 19.
1 to 3:examined result on each thin section, S:synoptic (1, 2 and 3)

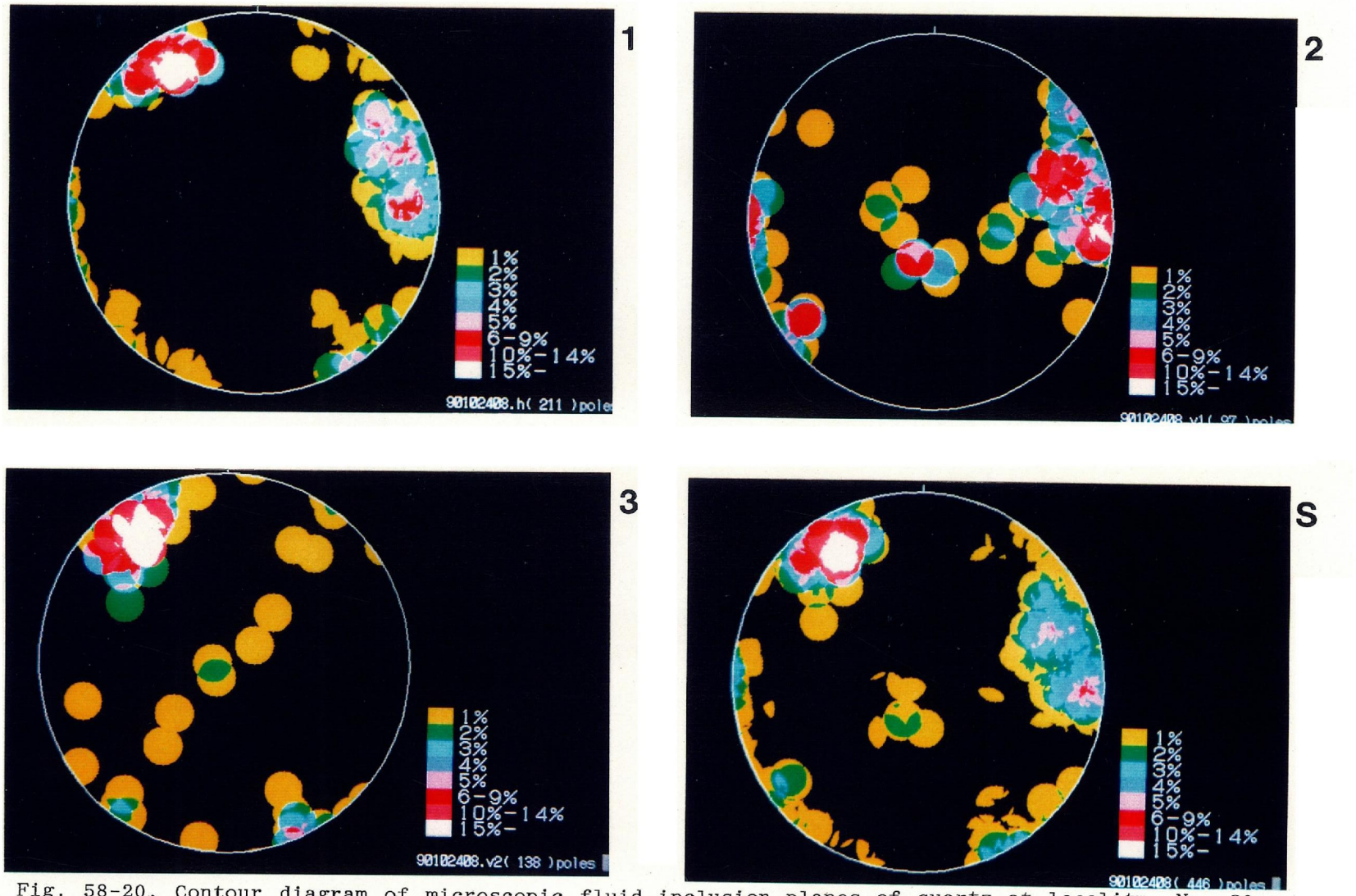

Fig. 58-20. Contour diagram of microscopic fluid inclusion planes of quartz at locality No. 20.
1 to 3:examined result on each thin section, S:synoptic (1, 2 and 3)

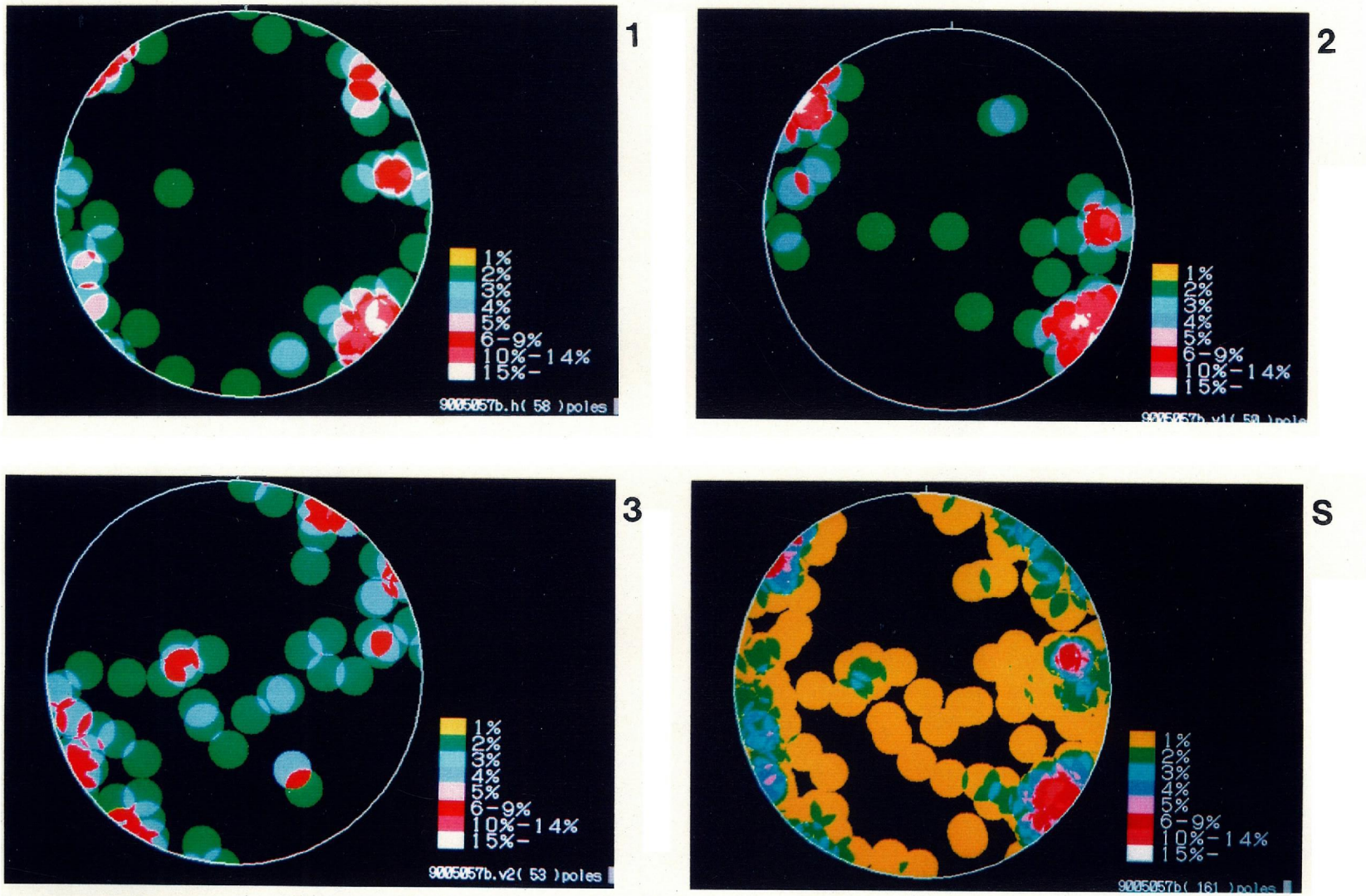

Fig. 58-21. Contour diagram of microscopic fluid inclusion planes of quartz at locality No. 21.
1 to 3:examined result on each thin section, S:synoptic (1, 2 and 3)

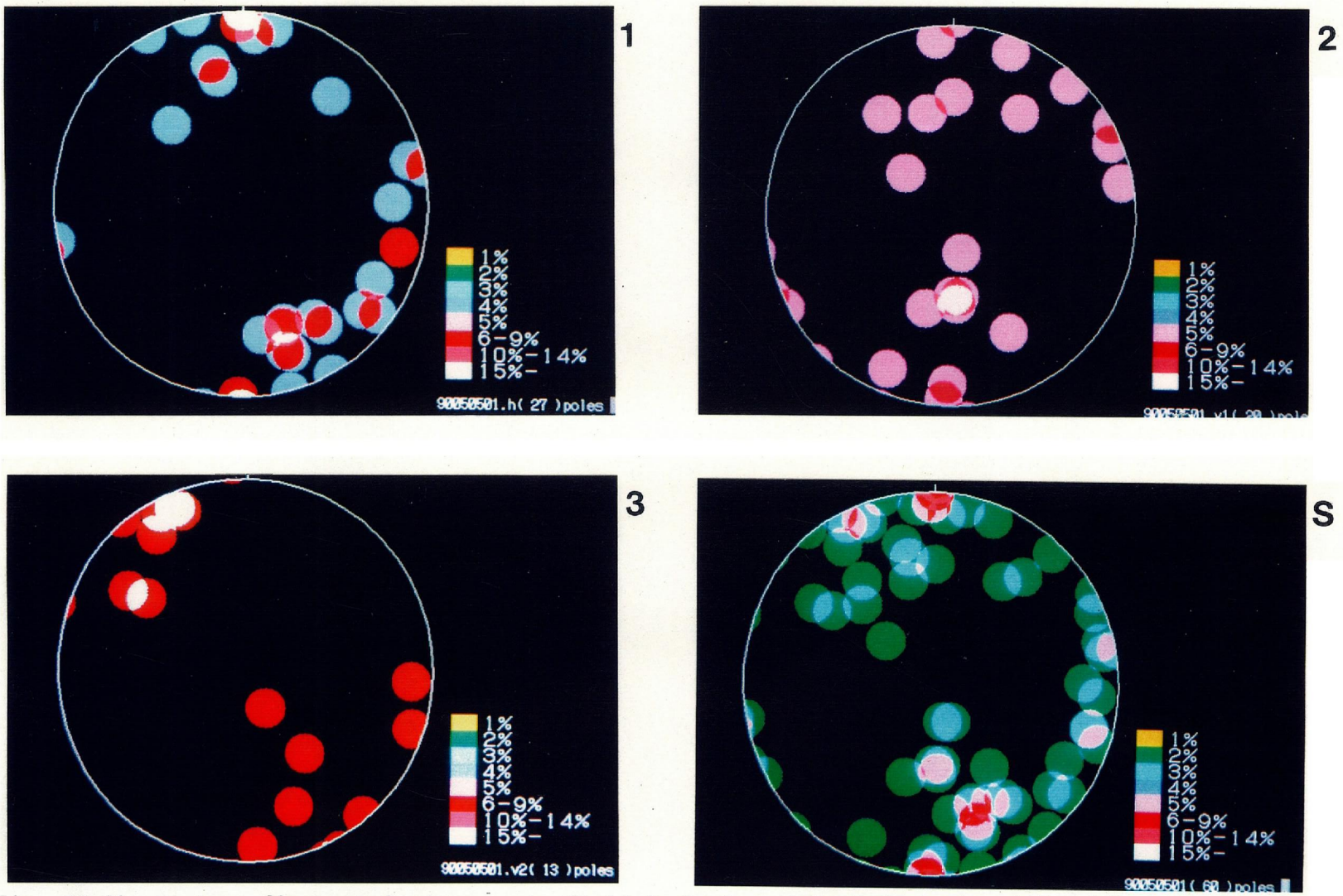

Fig. 58-22. Contour diagram of microscopic fluid inclusion planes of quartz at locality No. 22.
1 to 3:examined result on each thin section, S:synoptic (1, 2 and 3)

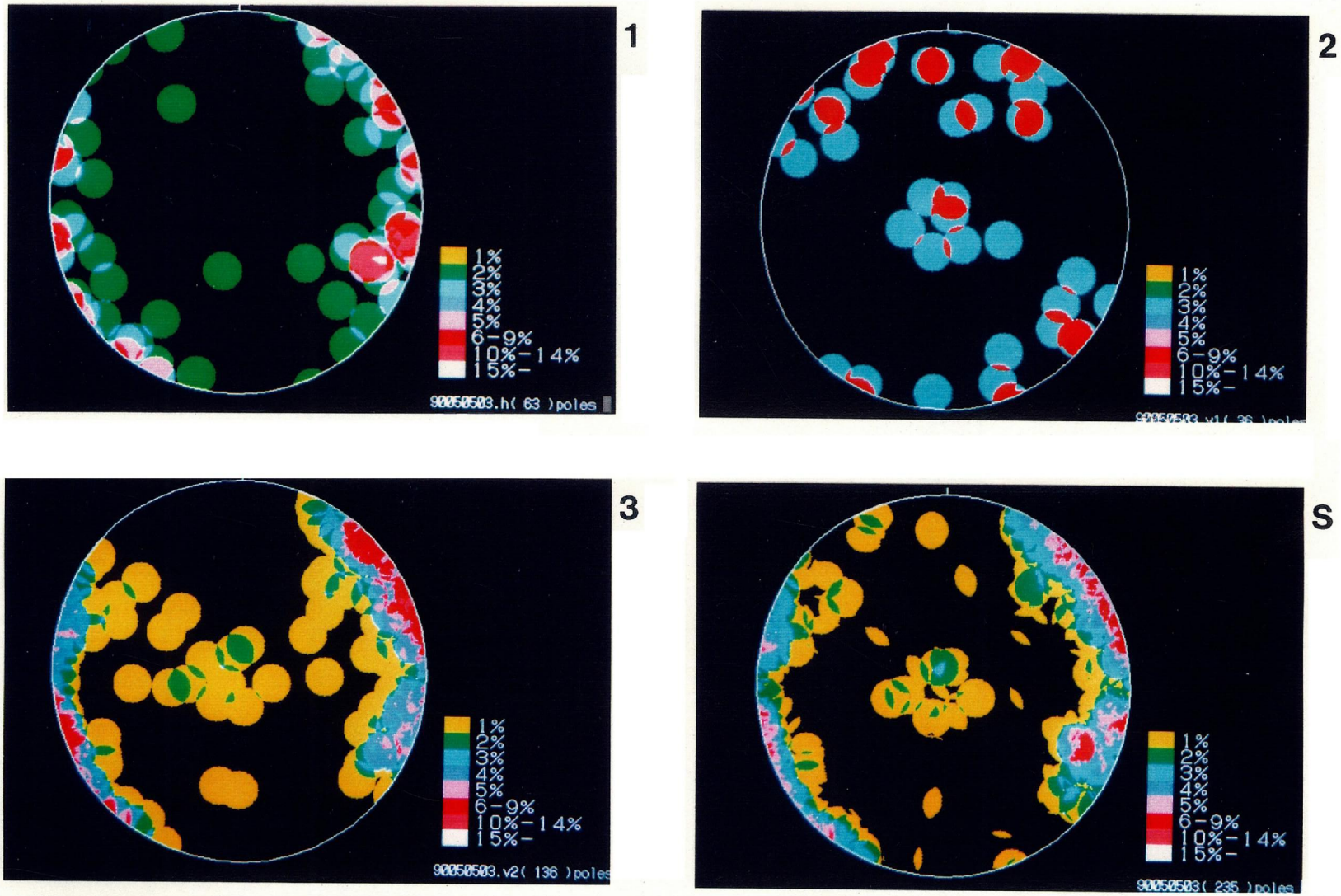

Fig. 58-23. Contour diagram of microscopic fluid inclusion planes of quartz at locality No. 23.
1 to 3:examined result on each thin section, S:synoptic (1, 2 and 3)

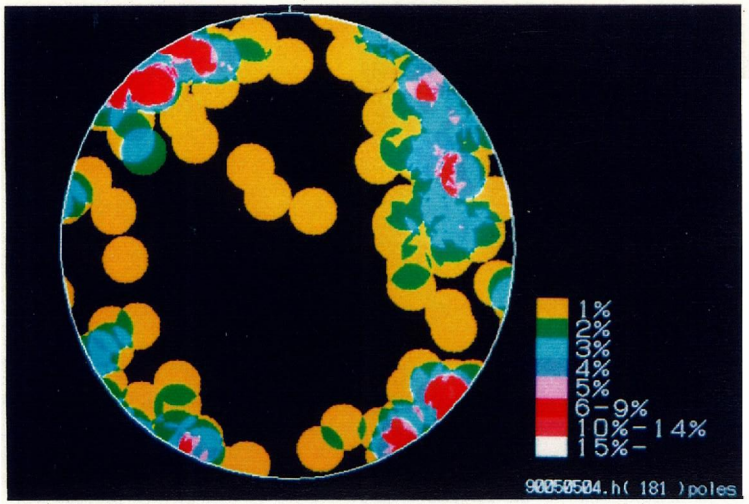

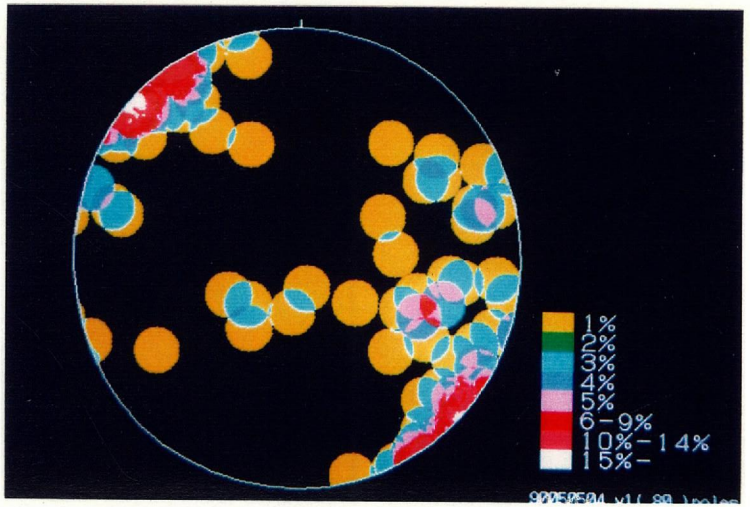

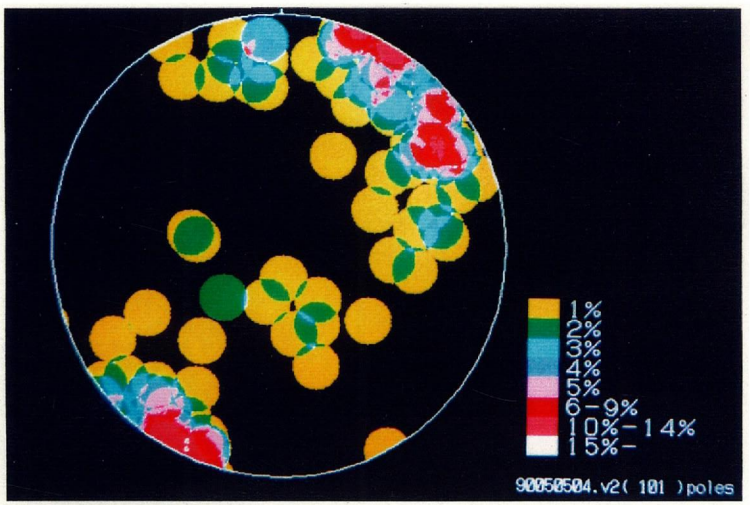

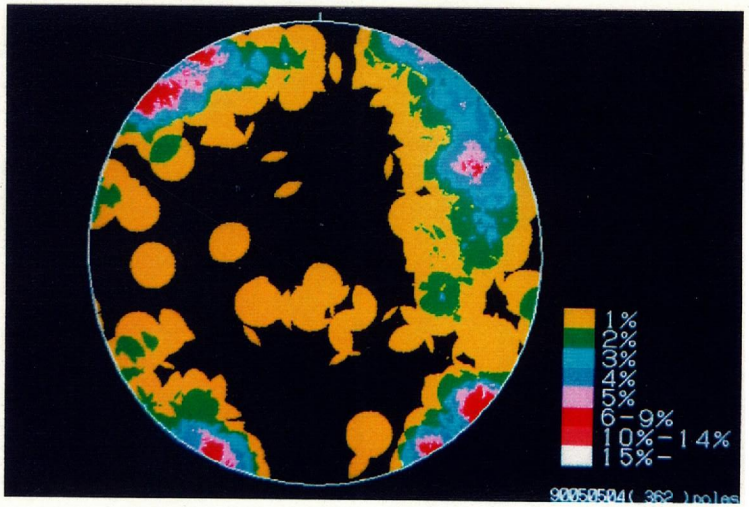

Fig. 58-24. Contour diagram of microscopic fluid inclusion planes of quartz at locality No. 24.
1 to 3:examined result on each thin section, S:synoptic (1, 2 and 3)

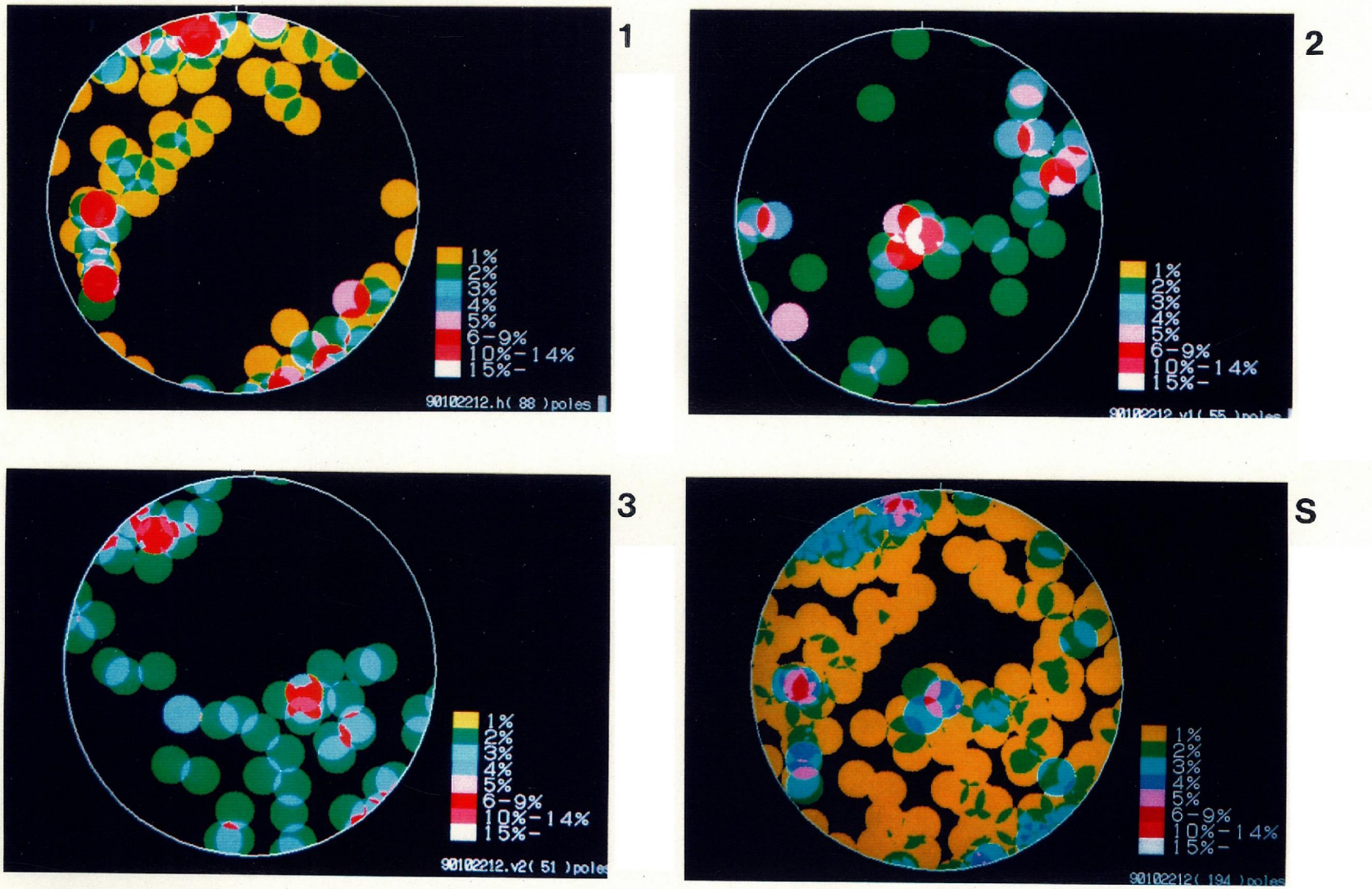

Fig. 58-25. Contour diagram of microscopic fluid inclusion planes of quartz at locality No. 25.
1 to 3:examined result on each thin section, S:synoptic (1, 2 and 3)

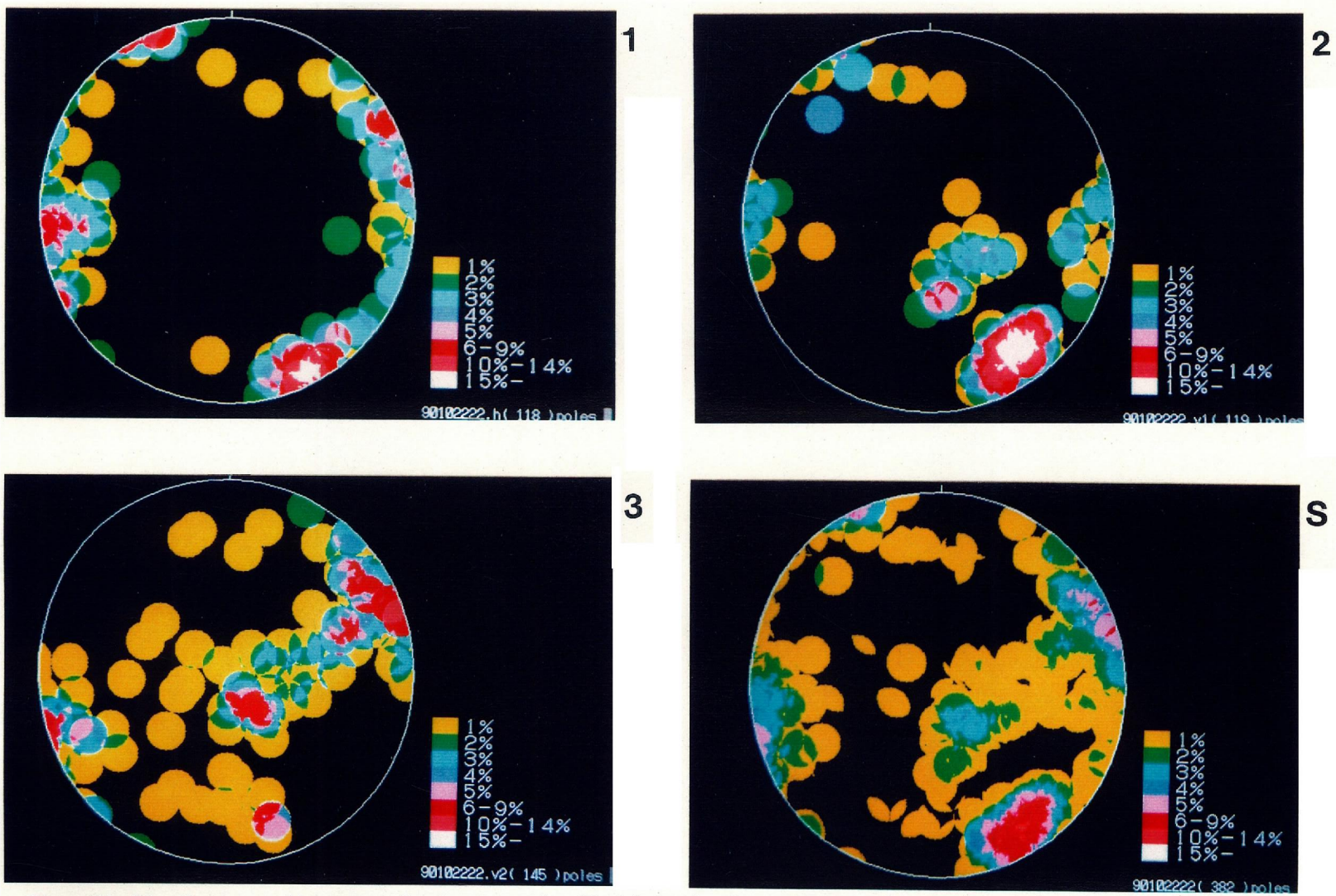

Fig. 58-26. Contour diagram of microscopic fluid inclusion planes of quartz at locality No. 26.
1 to 3:examined result on each thin section, S:synoptic (1, 2 and 3)

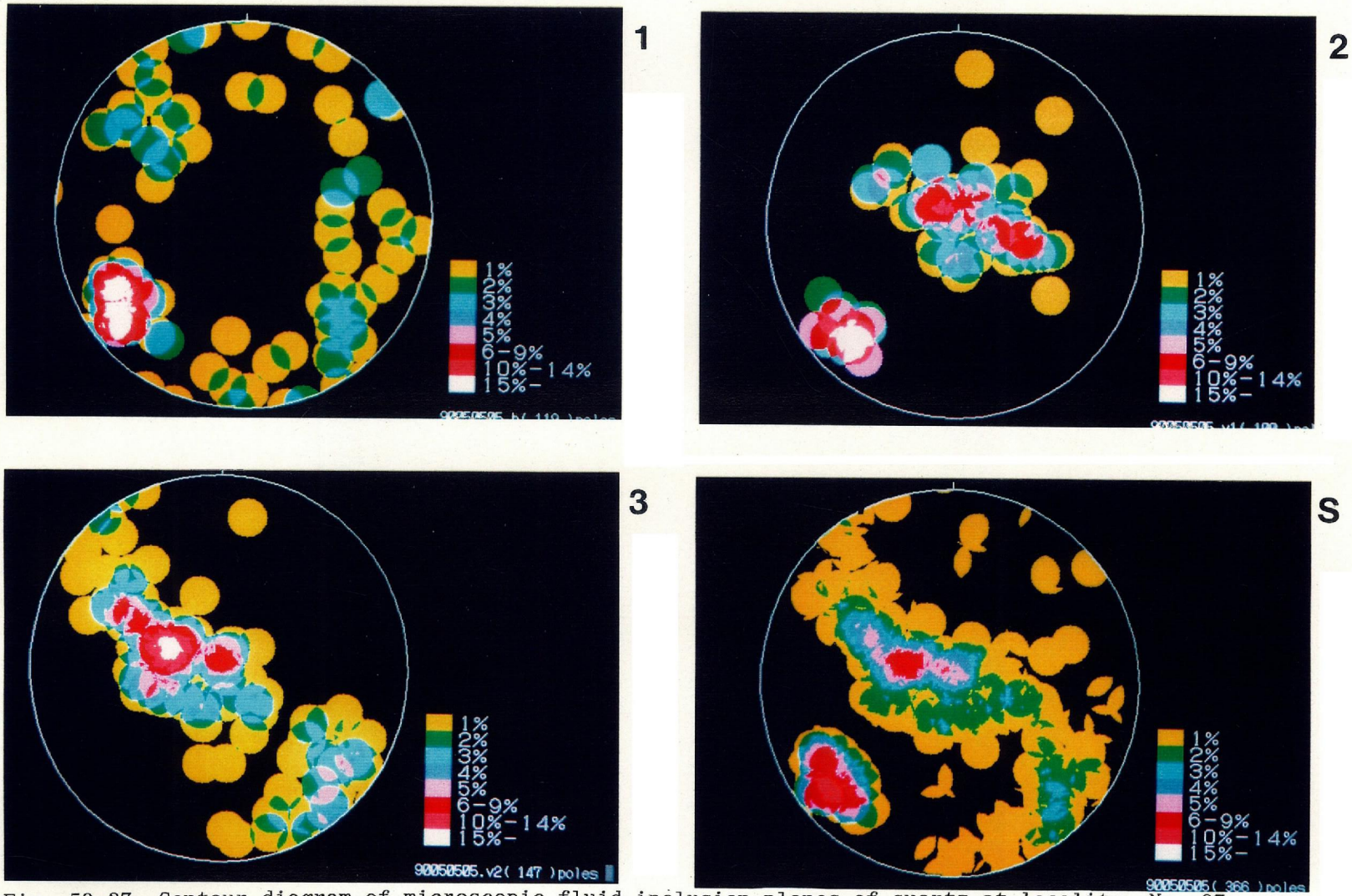

Fig. 58-27. Contour diagram of microscopic fluid inclusion planes of quartz at locality No. 27.
1 to 3:examined result on each thin section, S:synoptic (1, 2 and 3)

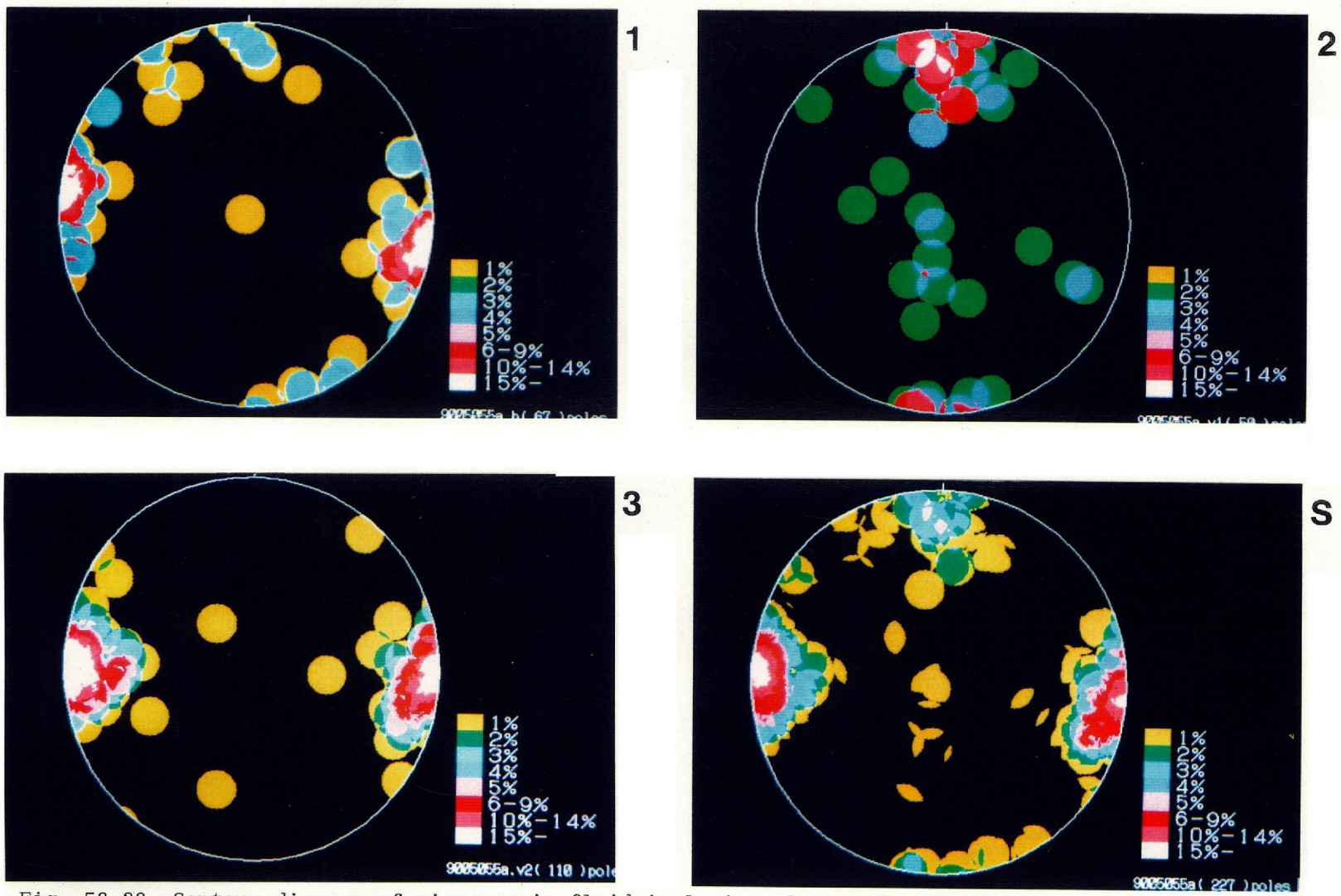

Fig. 58-28. Contour diagram of microscopic fluid inclusion planes of quartz at locality No. 28.
1 to 3:examined result on each thin section, S:synoptic (1, 2 and 3)

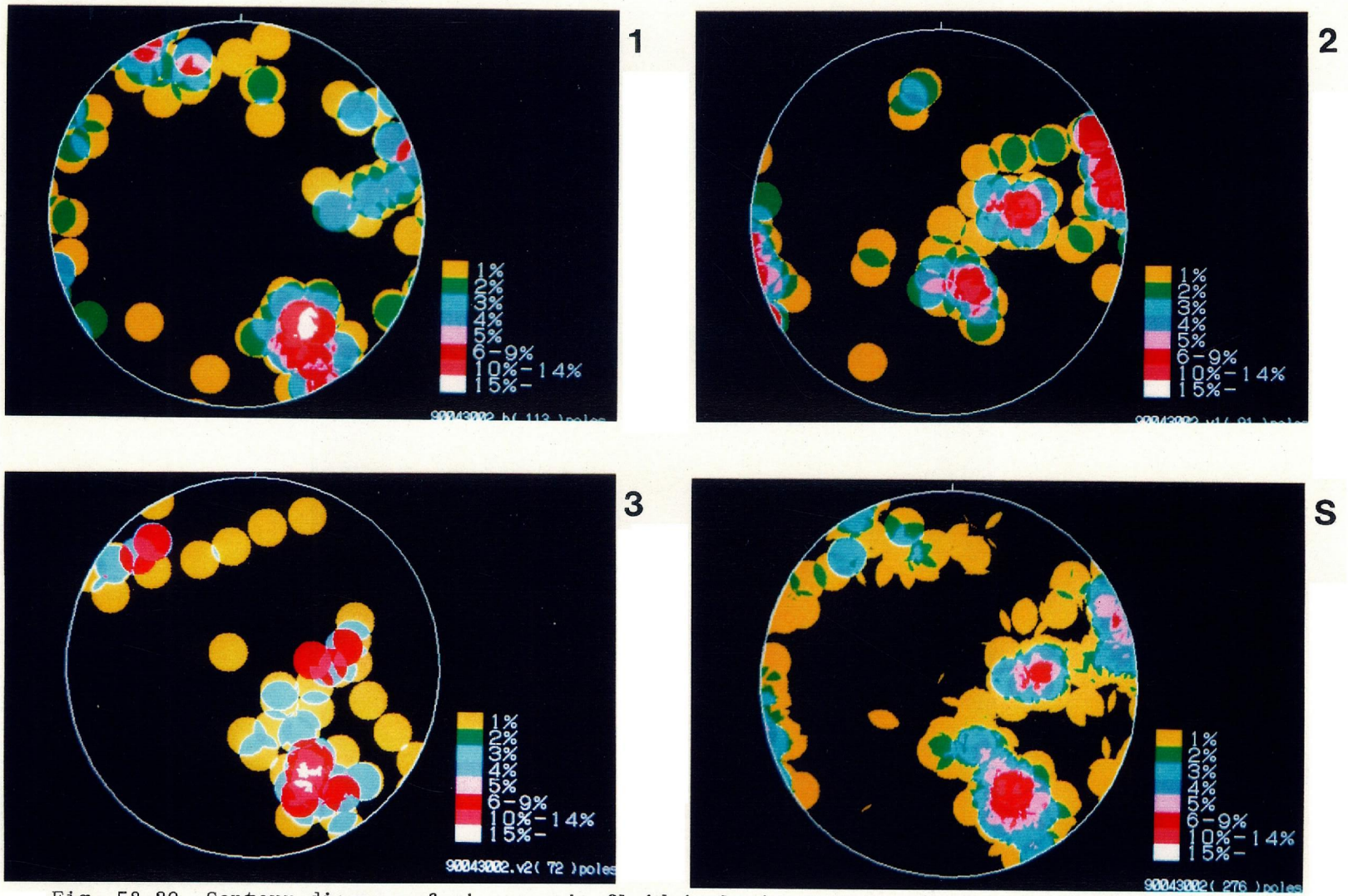

Fig. 58-29. Contour diagram of microscopic fluid inclusion planes of quartz at locality No. 29.
1 to 3:examined result on each thin section, S:synoptic (1, 2 and 3)

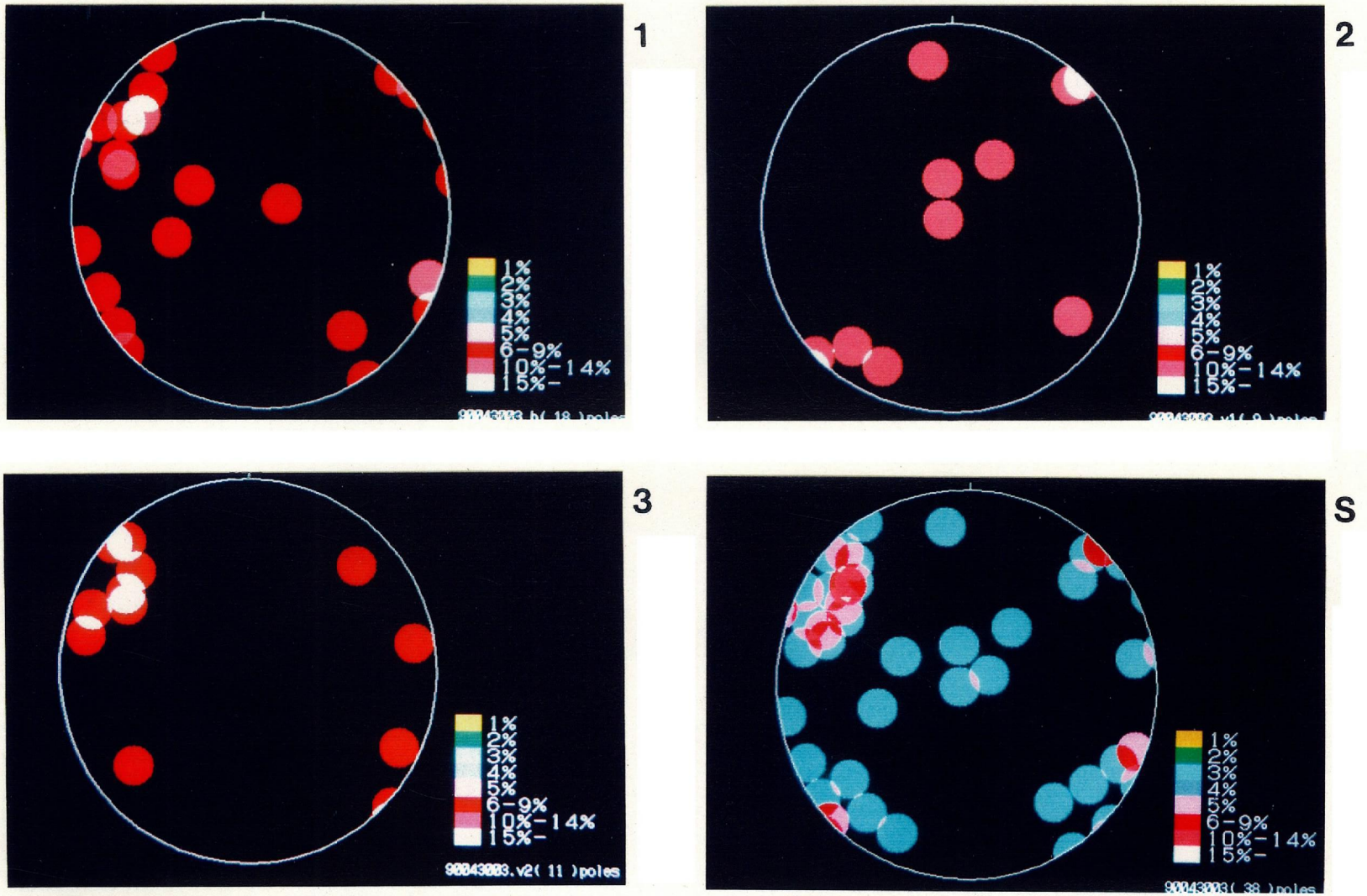

Fig. 58-30. Contour diagram of microscopic fluid inclusion planes of quartz at locality No. 30.
1 to 3:examined result on each thin section, S:synoptic (1, 2 and 3)

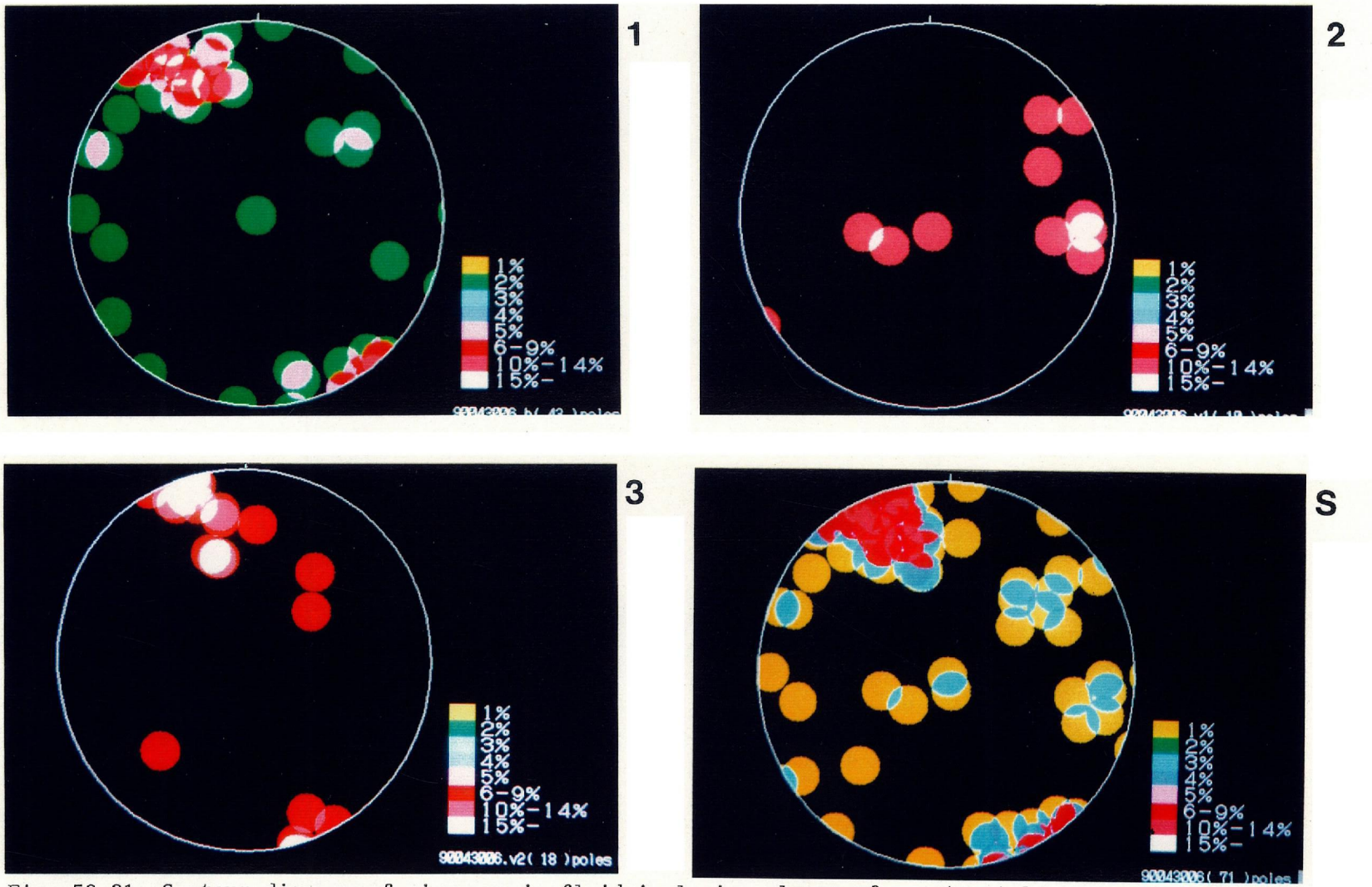

Fig. 58-31. Contour diagram of microscopic fluid inclusion planes of quartz at locality No. 31.
1 to 3:examined result on each thin section, S:synoptic (1, 2 and 3)

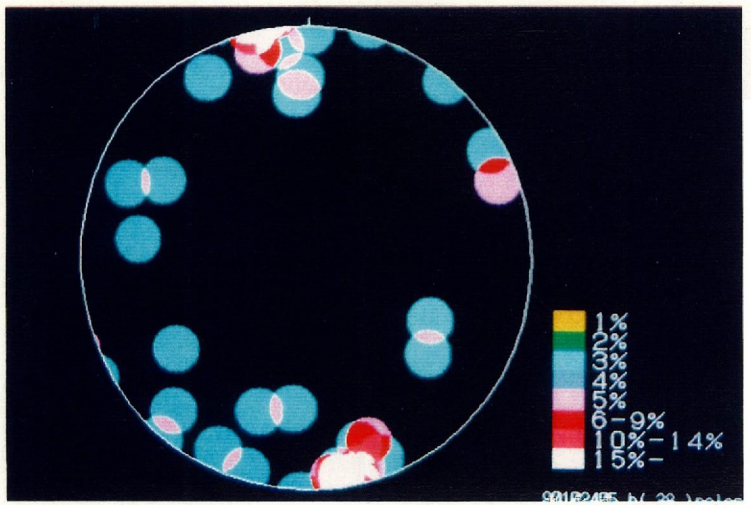

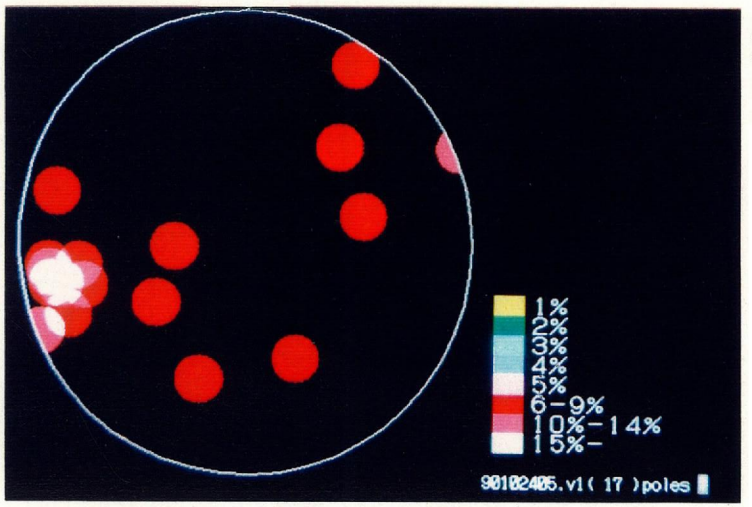

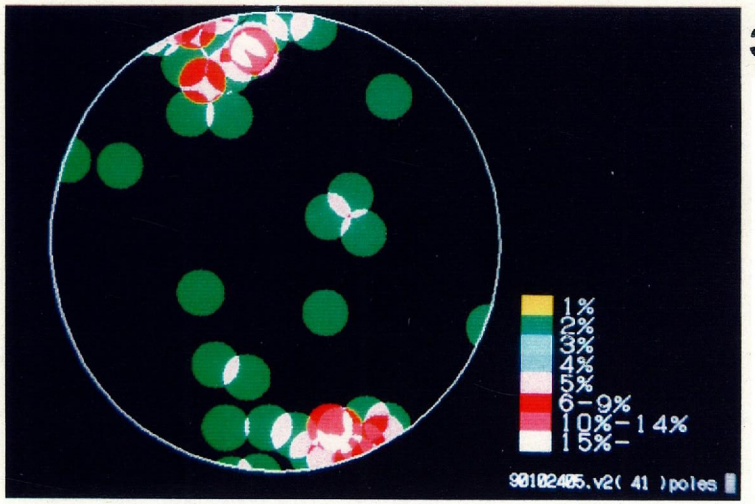

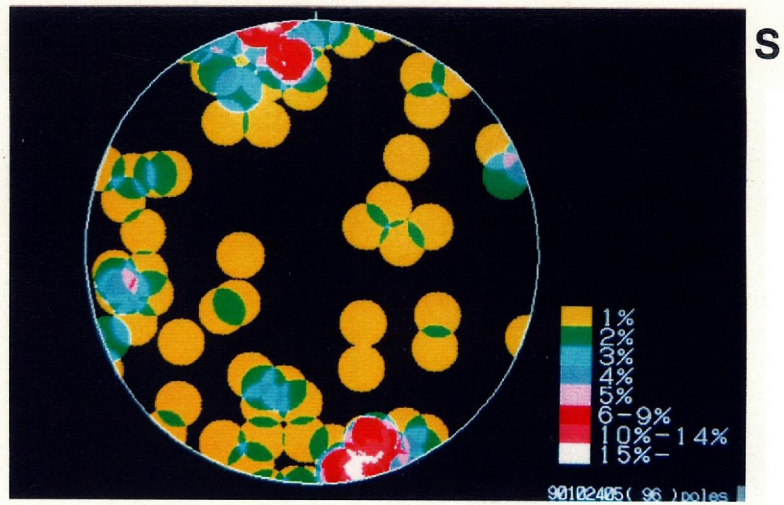

Fig. 58-32. Contour diagram of microscopic fluid inclusion planes of quartz at locality No. 32.
1 to 3:examined result on each thin section, S:synoptic (1, 2 and 3)

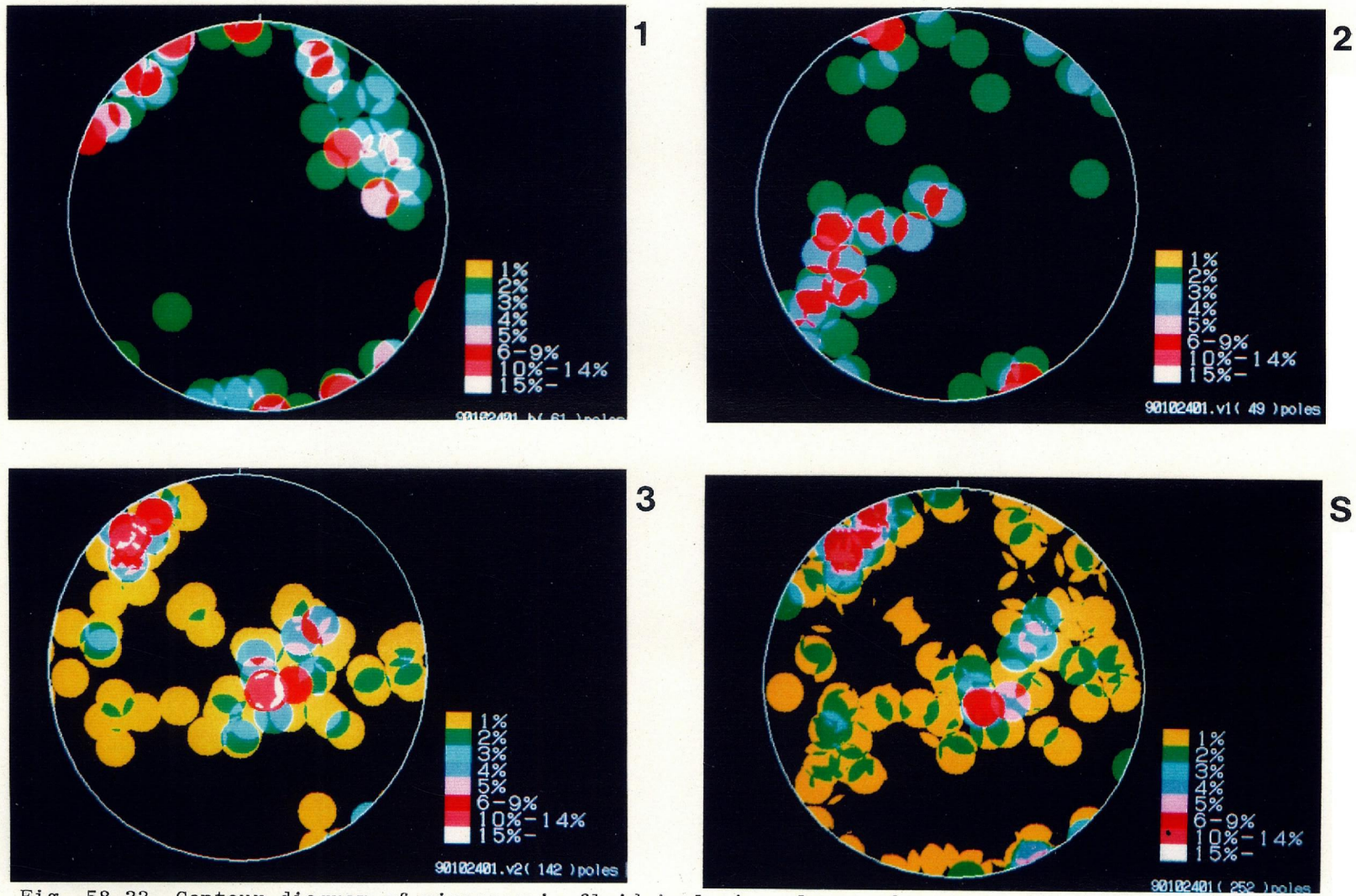

Fig. 58-33. Contour diagram of microscopic fluid inclusion planes of quartz at locality No. 33.
1 to 3:examined result on each thin section, S:synoptic (1, 2 and 3)

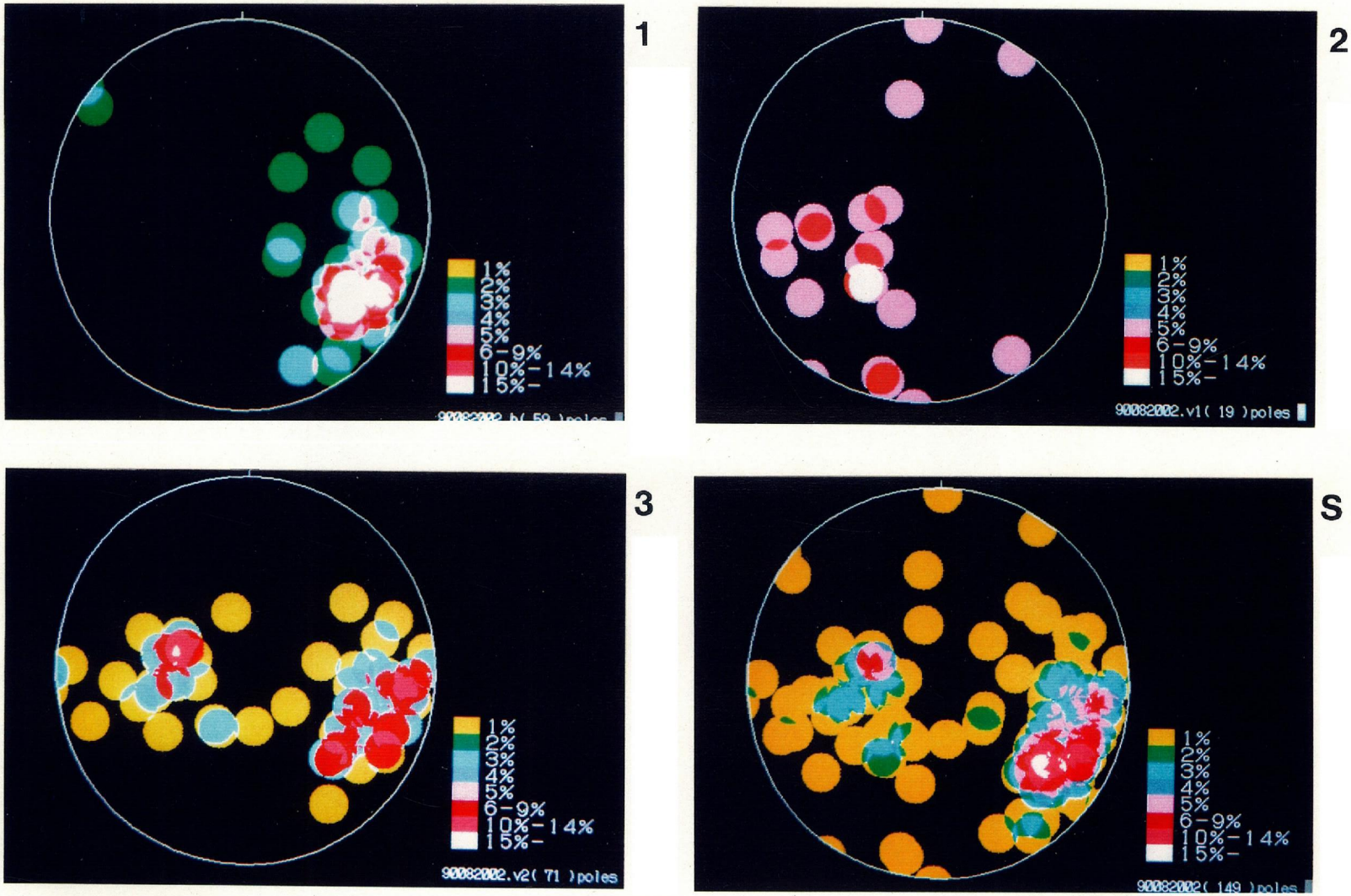

Fig. 58-34. Contour diagram of microscopic fluid inclusion planes of quartz at locality No. 34.
1 to 3:examined result on each thin section, S:synoptic (1, 2 and 3)

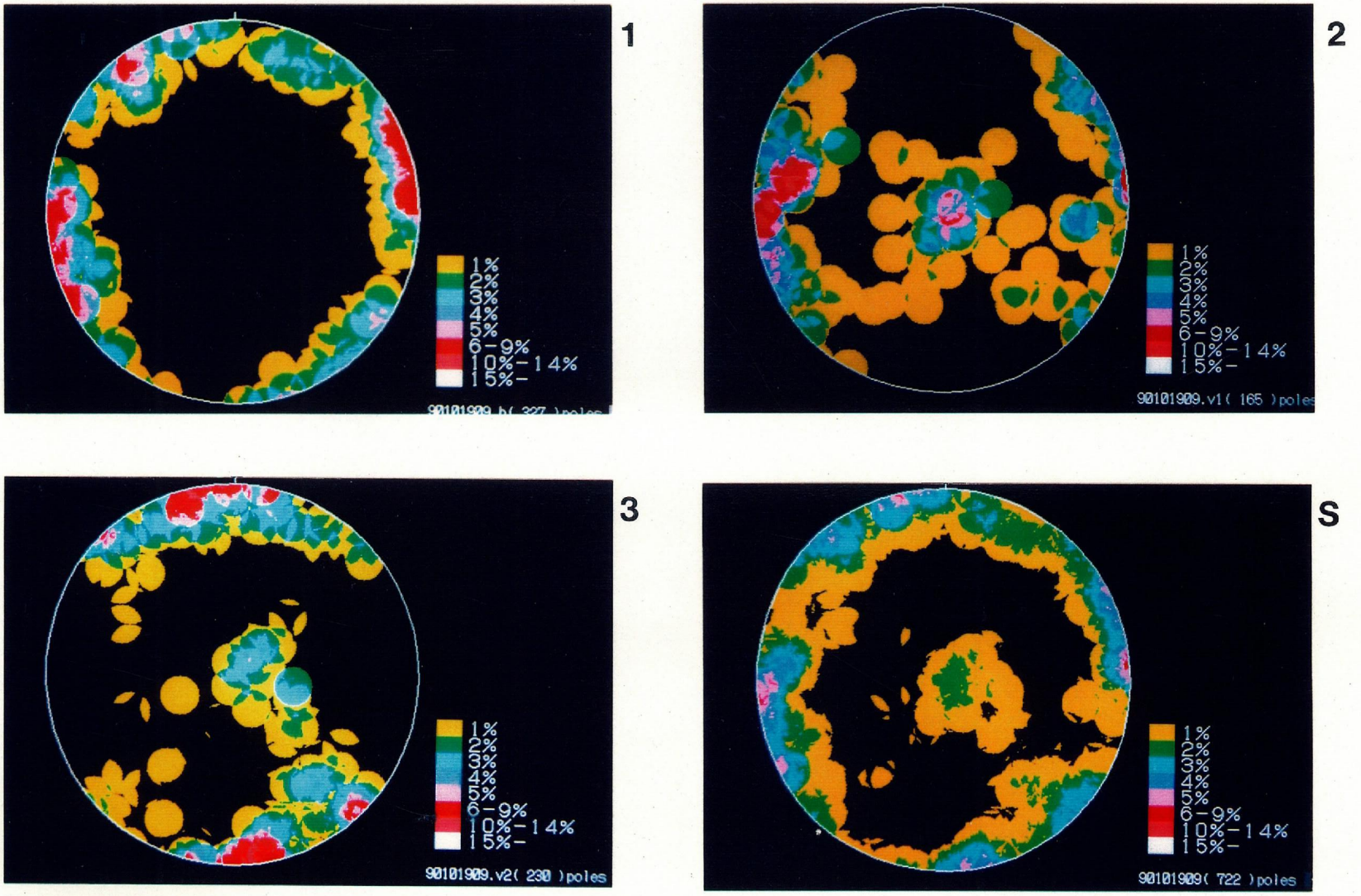

Fig. 58-35. Contour diagram of microscopic fluid inclusion planes of quartz at locality No. 35.
1 to 3:examined result on each thin section, S:synoptic (1, 2 and 3)

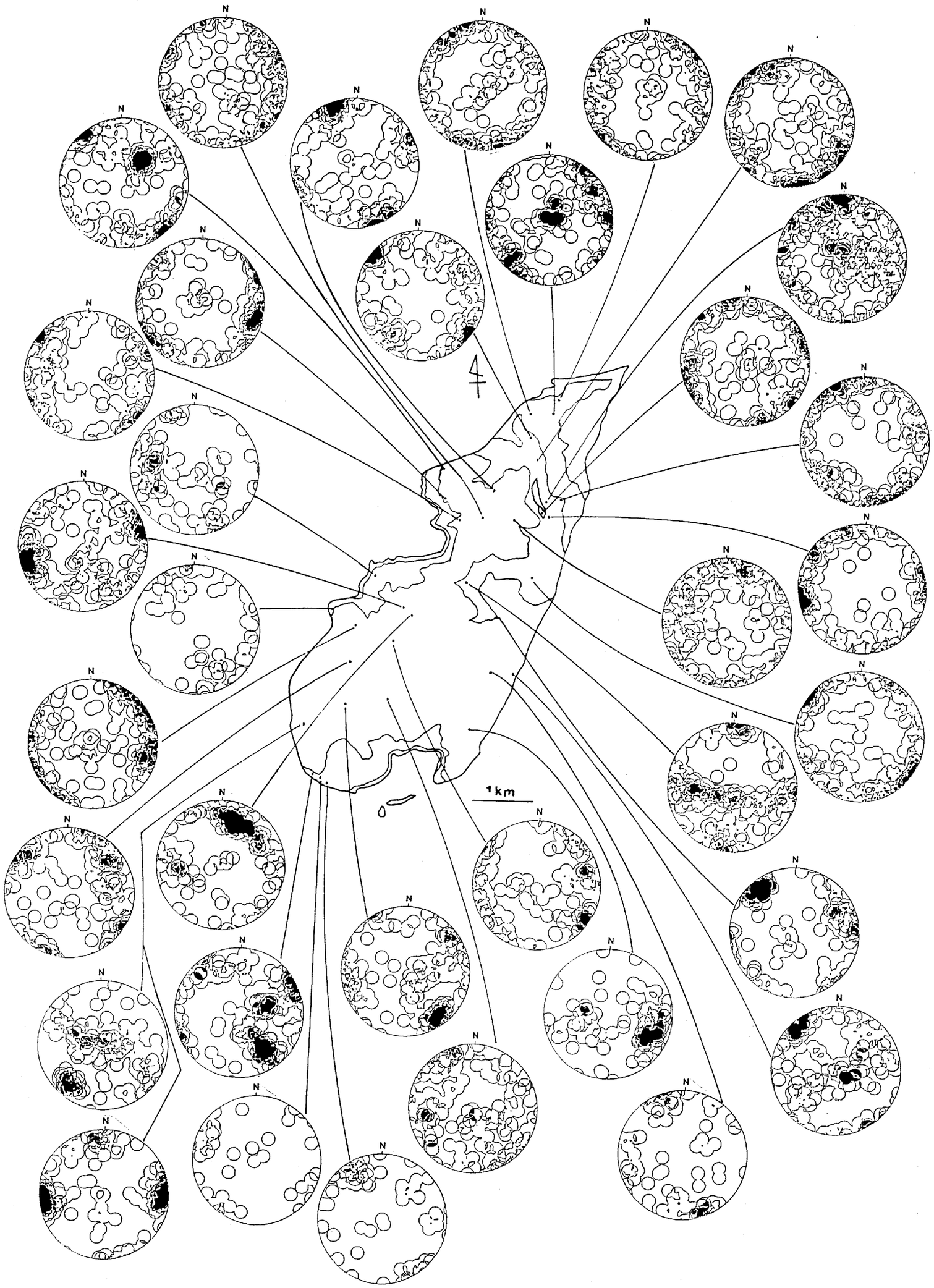

Fig. 59. Spatial variation of fabric (synoptic) of fluid inclusion planes in quartz of the granodiorite and medium–grained granite.

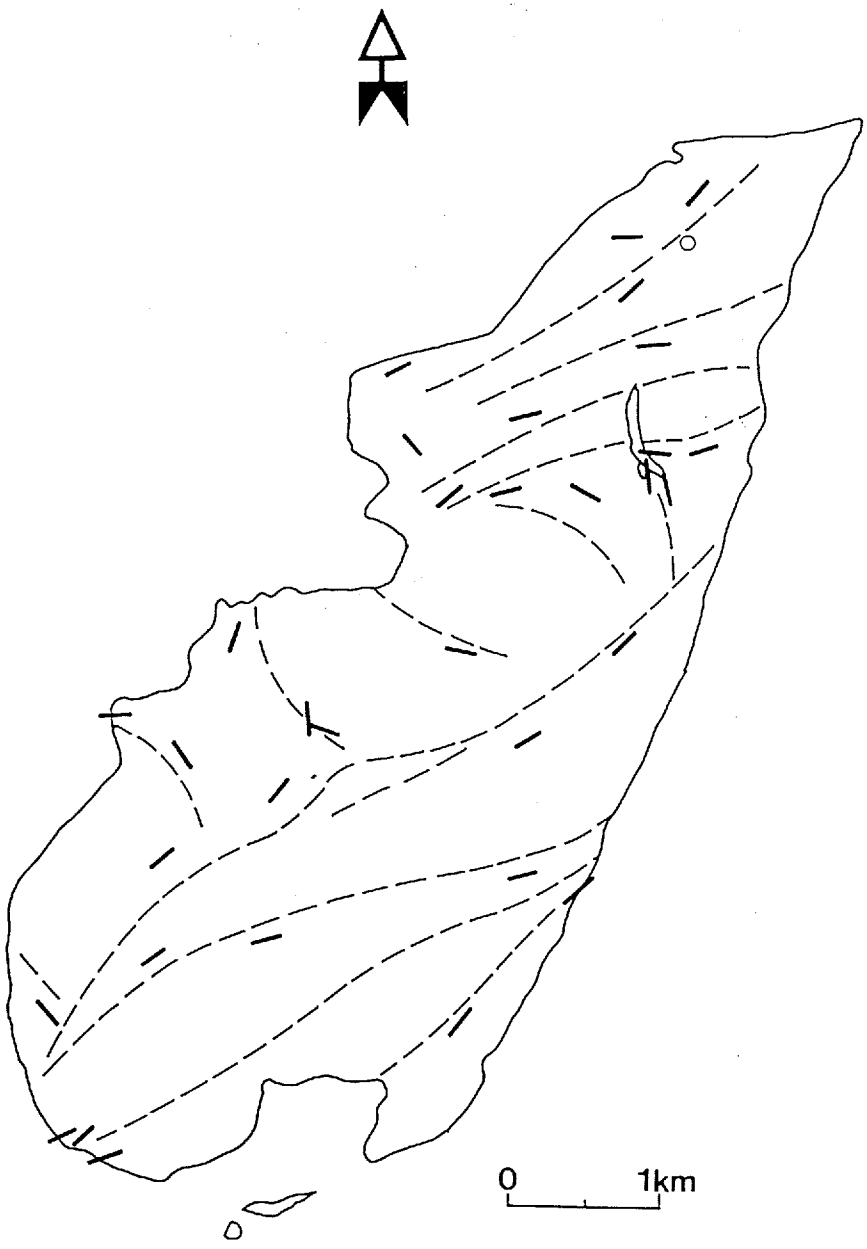

Fig. 60. Spatial variation of the orientation direction of the first order of fluid inclusion planes in quartz of the granodiorite and medium-grained granite.
Open circle: data for horizontal attitude.

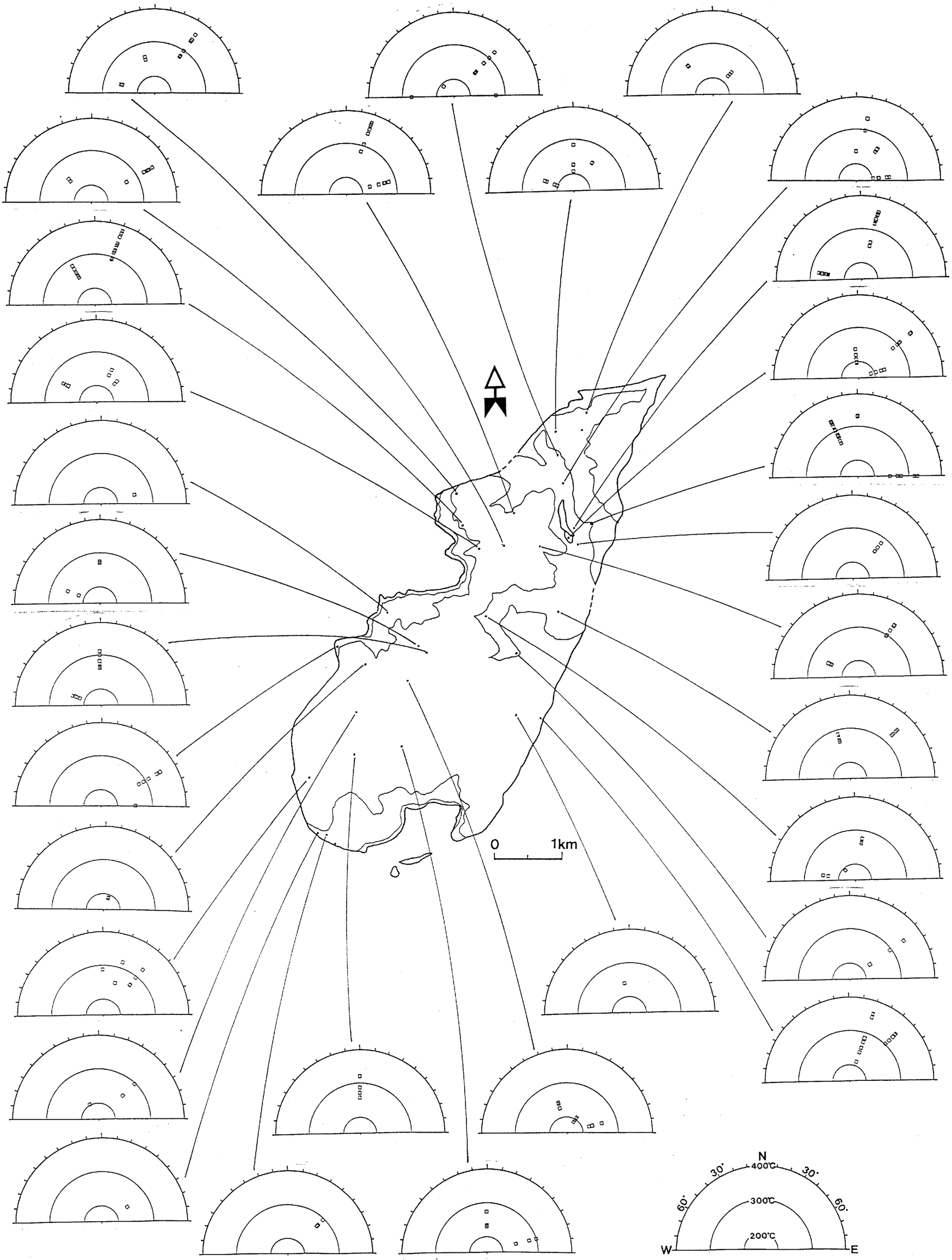

Fig. 61. Spatial variation of the orientation direction of fluid inclusion planes in quartz and their homogenization temperature in the granodiorite and medium-grained granite.

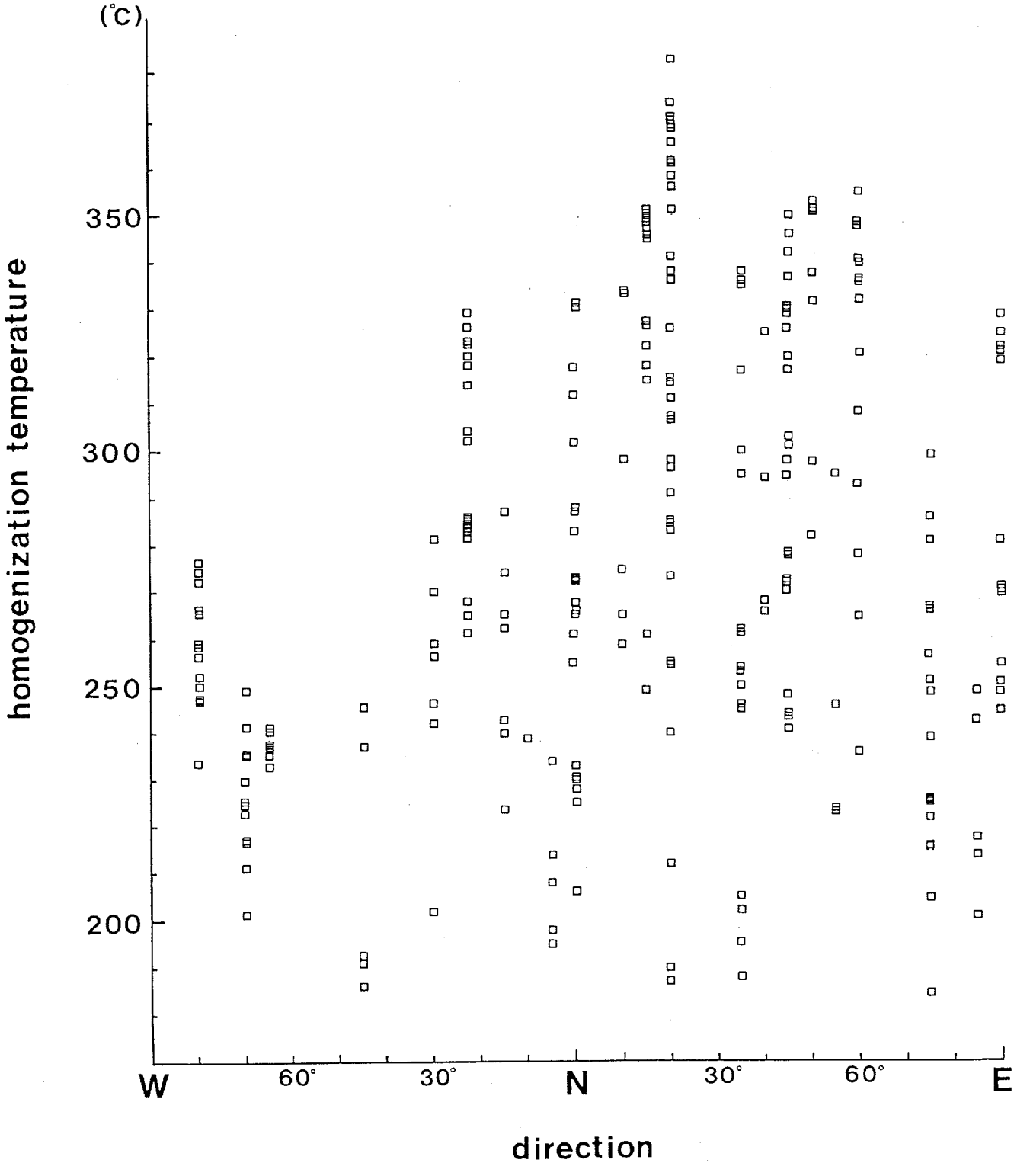

Fig. 62. Relationship between the orientation direction of fluid inclusion planes in quartz and homogenization temperature in the granodiorite and medium-grained granite.

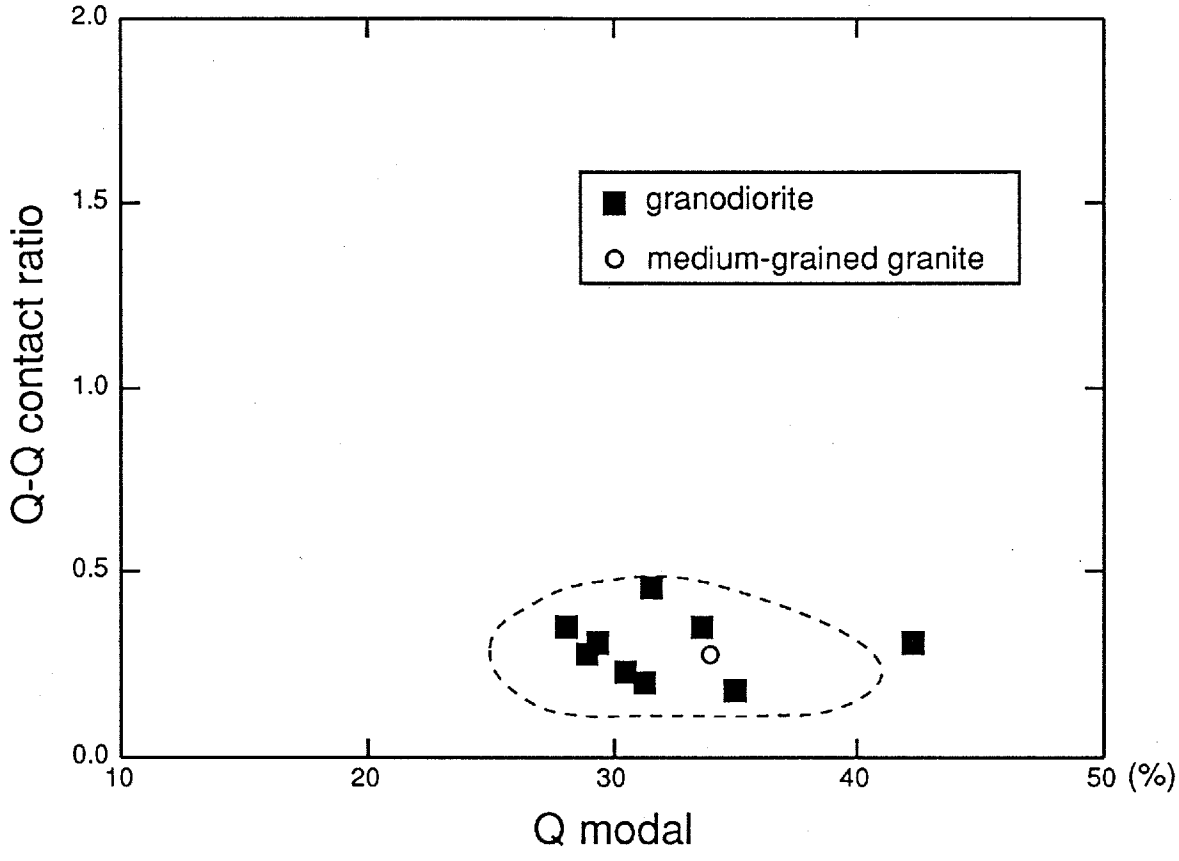

Fig. 63. Relationship between Q–Q contact ratio and modal Q.
Boken line shows the value range for the Ishizuchi granite by Sakurai and Hara (1979).

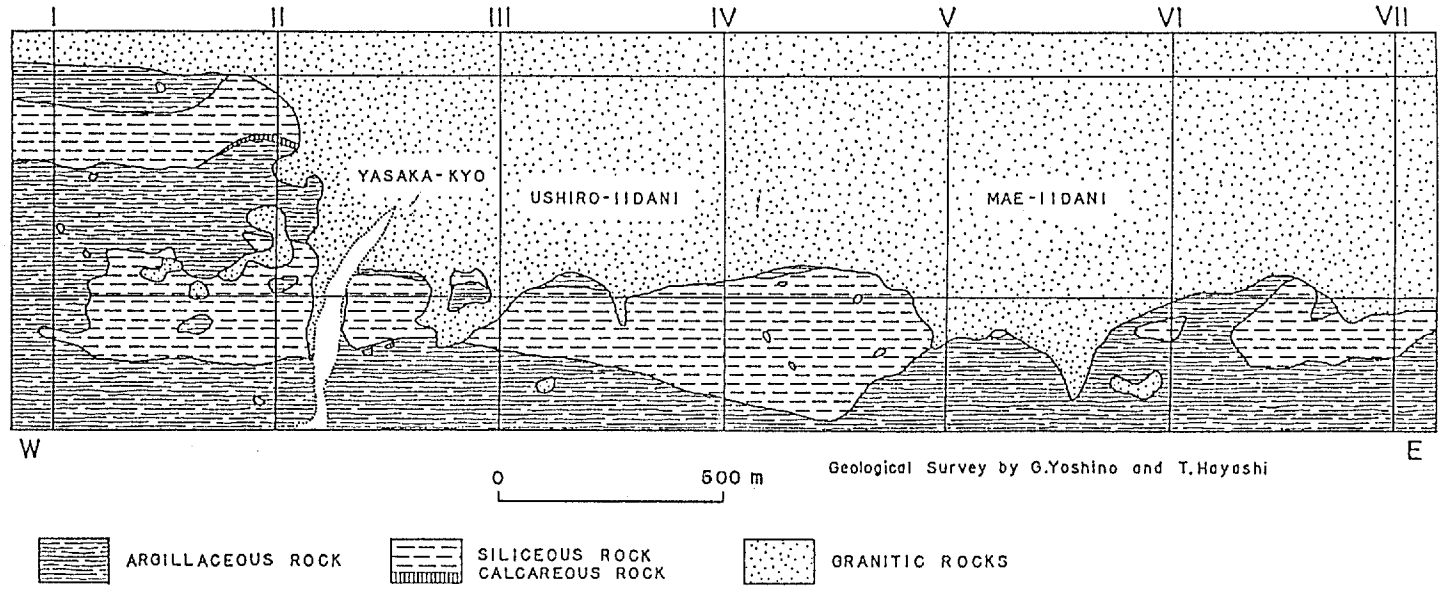

Fig. 64. Geological map of the Ozegawa area (after Yoshino and Hayashi, 1979).

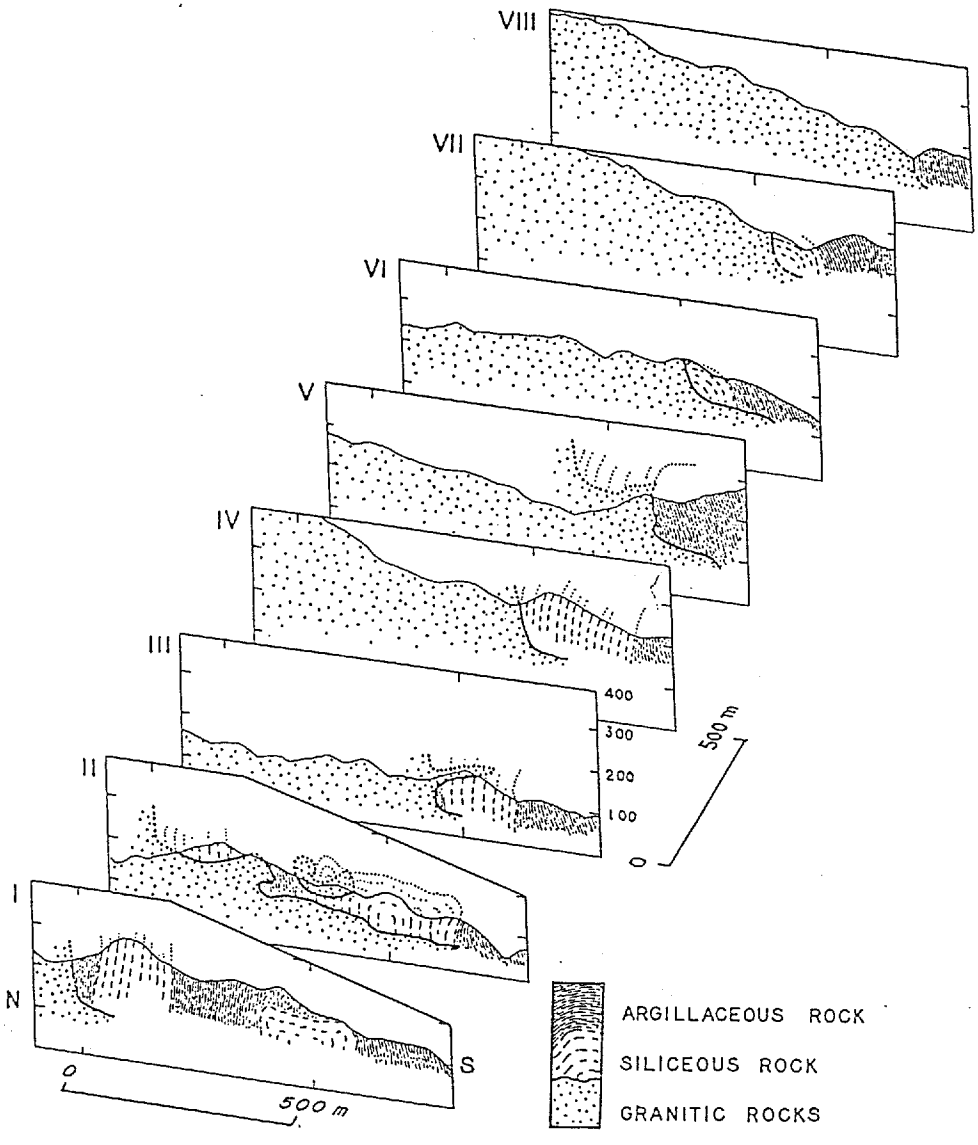

Fig. 65. Geological profiles the Ozegawa area (after Yoshino and Hayashi, 1979). See Fig. 64 for location of profile lines.

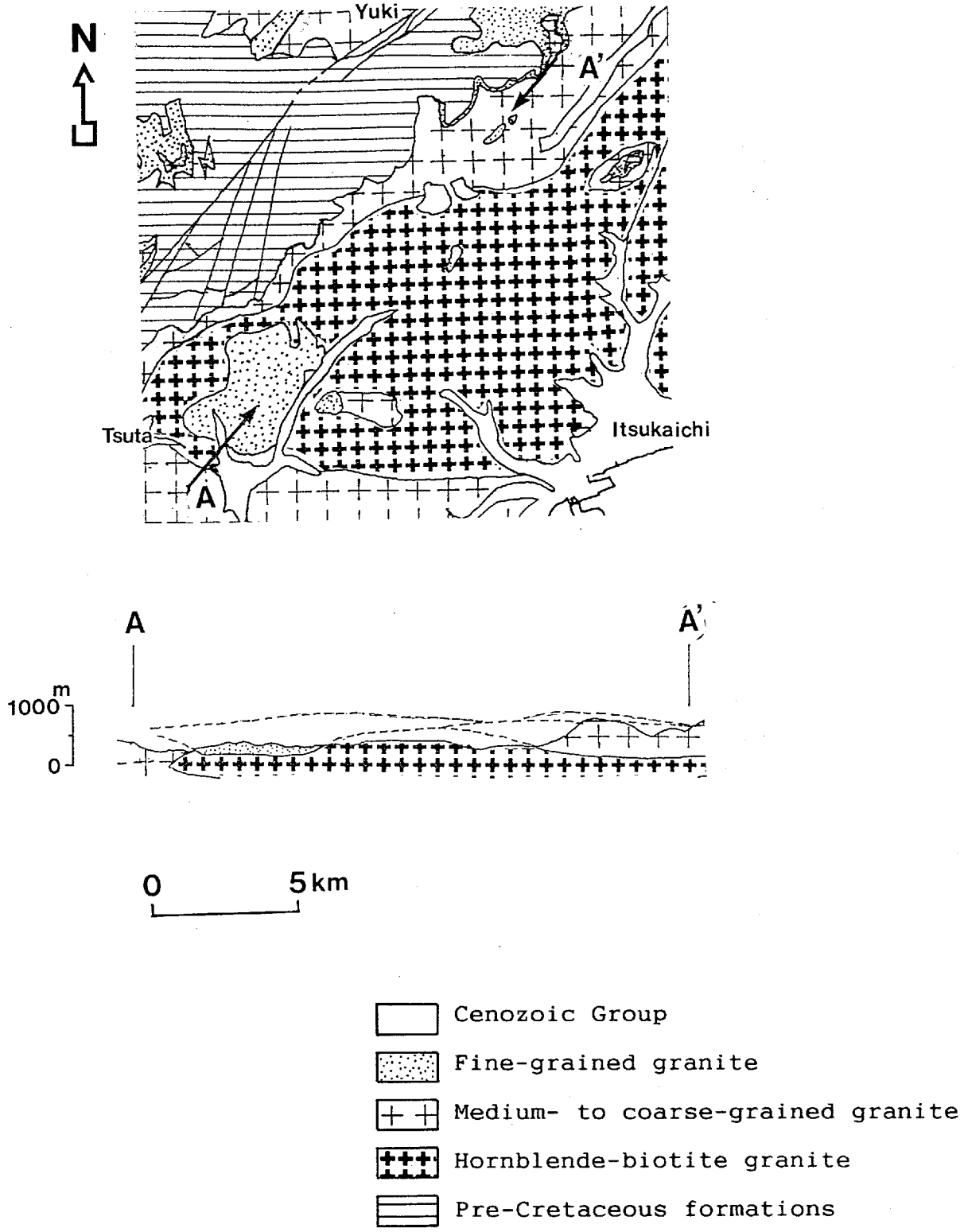

Fig. 66. Geological map of the Saeki area (compiled from Takahashi,Y. et al., 1989 and Takahashi,Y., 1991 and the present author's data).

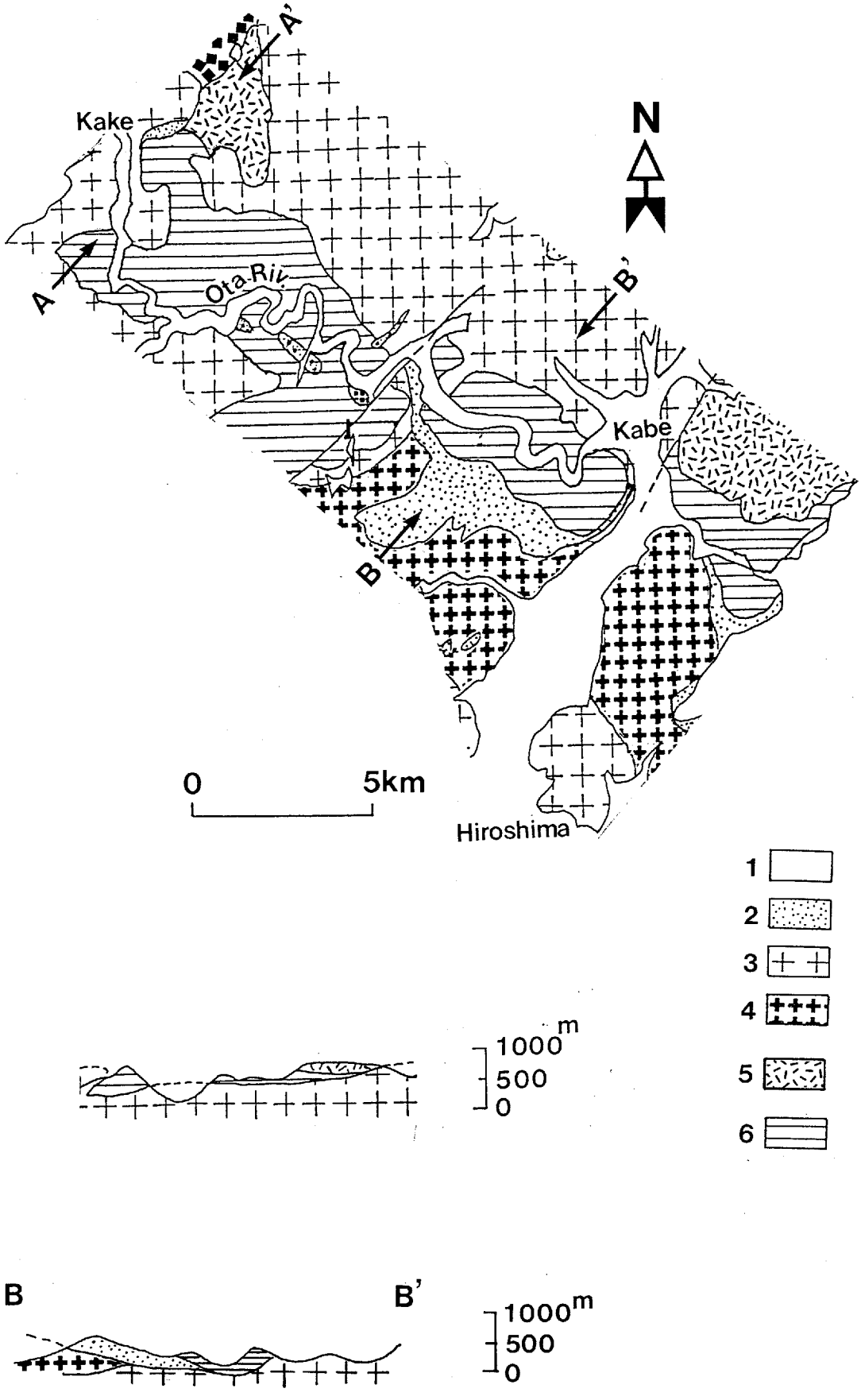

Fig. 67. Geological map of the Hiroshima–Kake area (compiled from Yamada et al., 1985 and the present author's data).
1:Cenozoic Group, 2:Fine–grained granite, 3:Medium– to coarse–grained granite, 4:Hornblende–biotite granite, 5:Rhyolitic rocks, 6:Pre–Cretaceous formations.

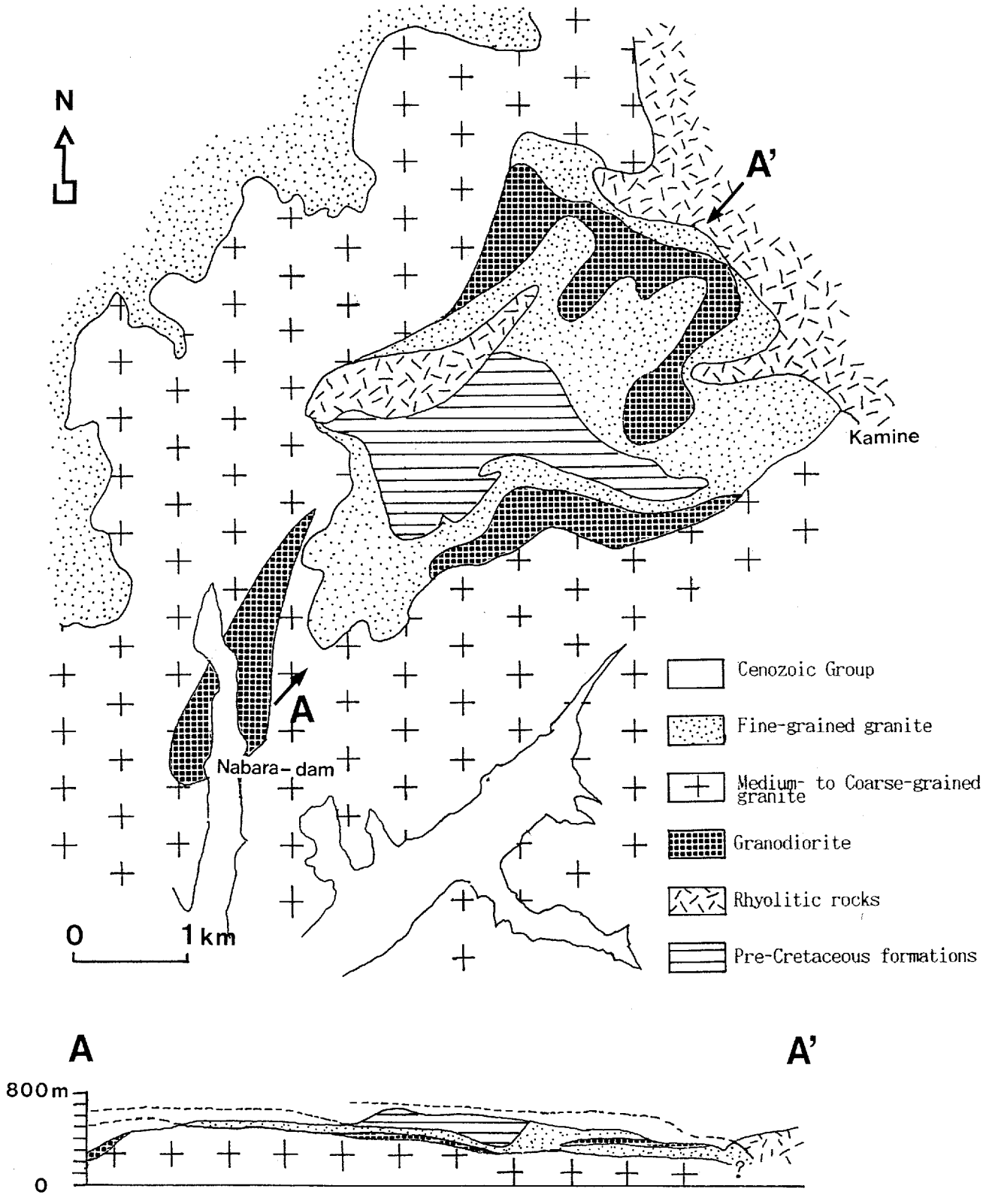

Fig. 68. Geological map of the Yachiyo area (compiled from Hara, 1955, Yamada et al., 1985 and the present author's data.

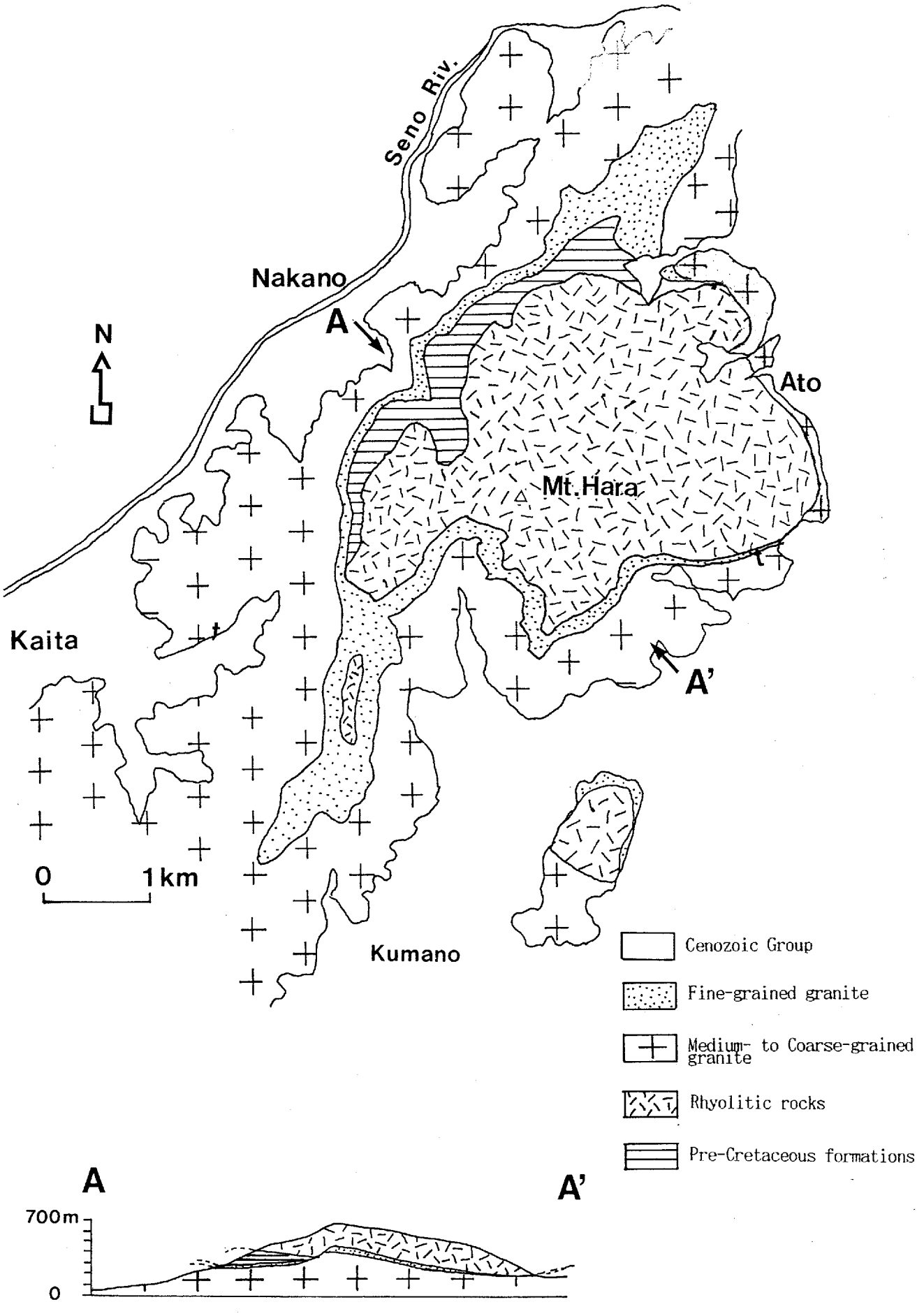

Fig. 69. Geological map of the Kumano area.

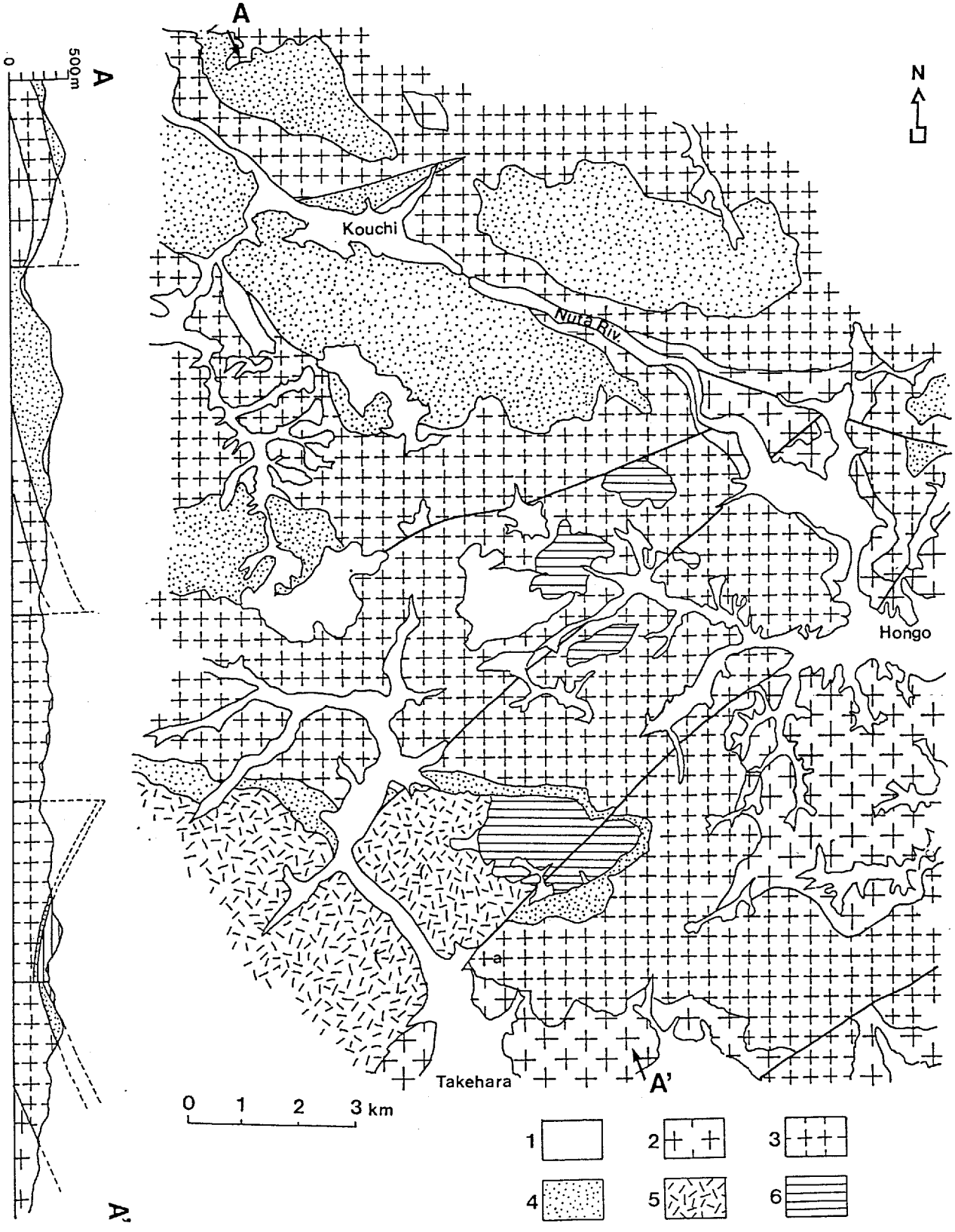

Fig. 70. Geological map of the Takehara area (compiled from Yoshida et al., 1985 and the present author's data).
1:Cenozoic Group, 2:Coarse-grained granite, 3:Medium-grained granite, 4:Fine-grained granite, 5:Rhyolitic rocks, 6:Pre-Cretaceous formation.

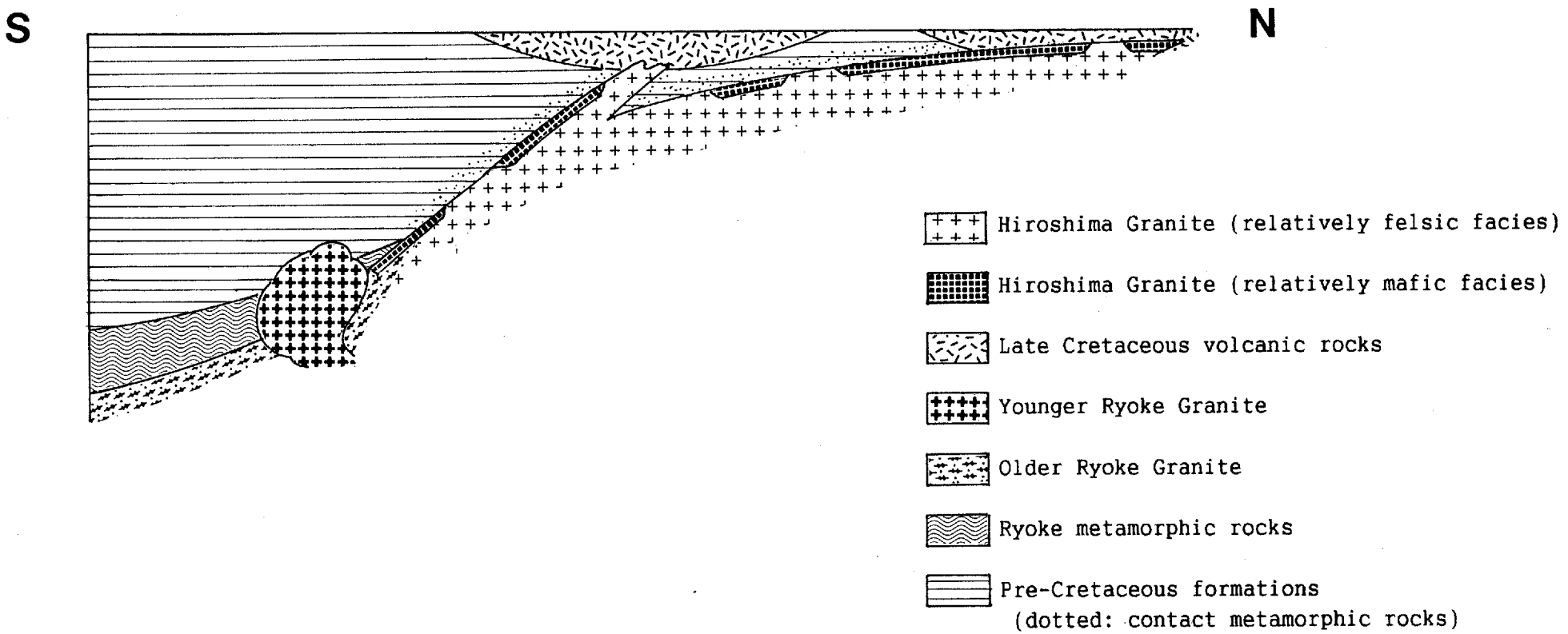

Fig. 71. Schematical geological profile of the Togouchi–Yuu–Takehara district.
Traversed from the northern margin of the Ryoke zone to the northern end of the San–yo zone.

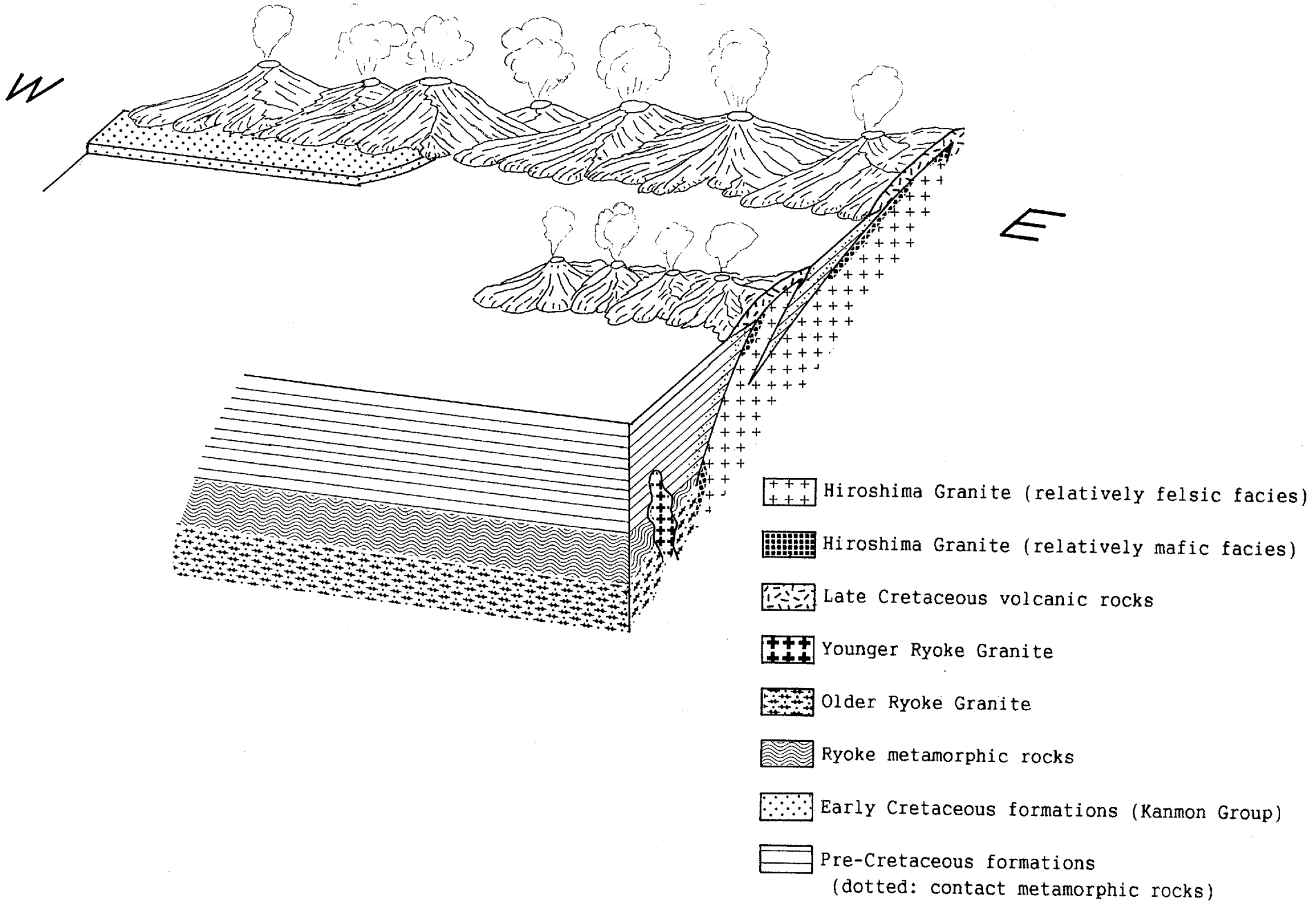

Fig. 72. Schematic diagram illustrating geologic events occurring in the central–western Chugoku Province during late Cretaceous period.

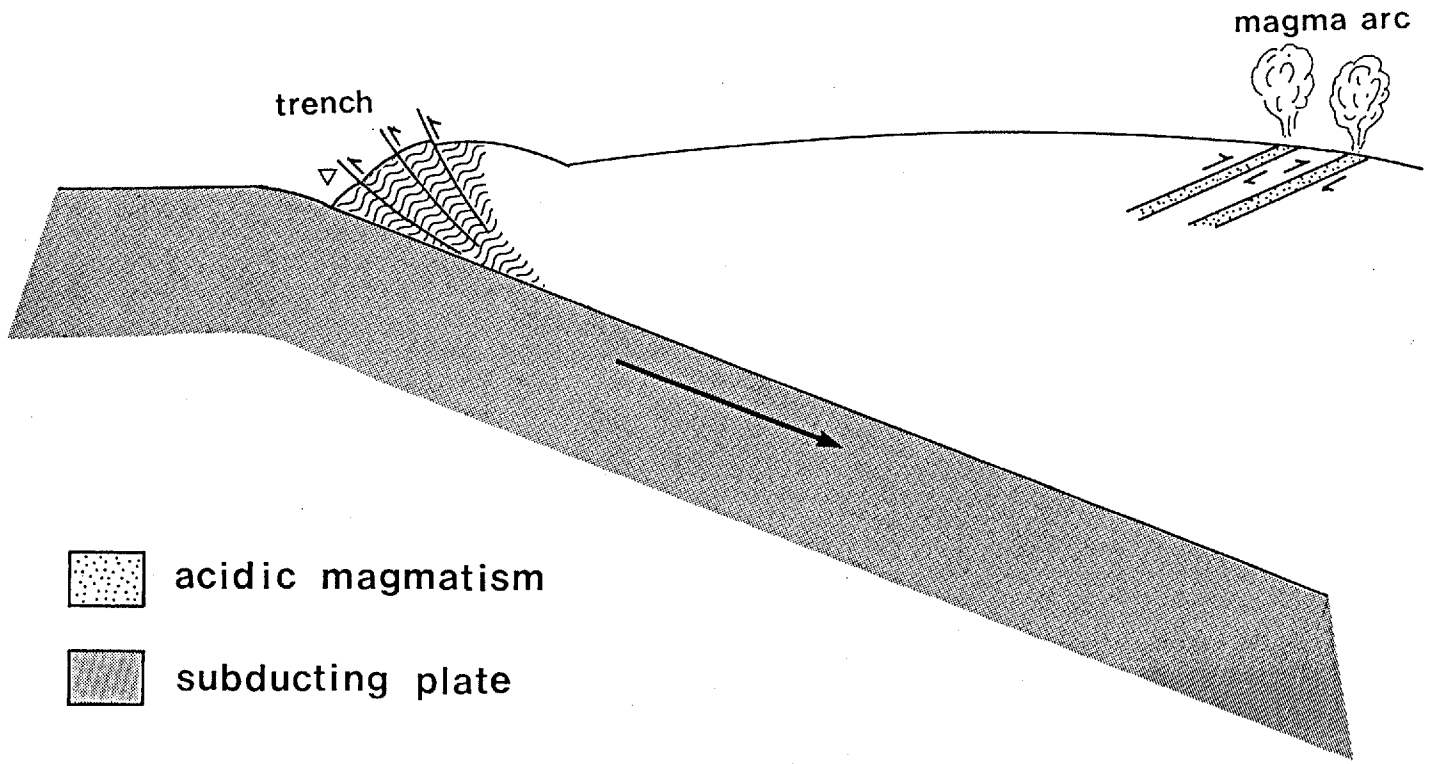

Fig. 73. Schematic diagram illustrating tectonic framework related with late Cretaceous igneous activities.

Chemical compositions of minerals

Table 1. Specimen numbers and analyzed minerals

No.	specimen No.	rock	Opx	Cpx	Cu	Amp	Bi	Gt	I.O	Pl	Kf
1	86081005	TL	○	○		○	○		○	○	
2	86090708	TL	○	○		○			○	○	
3	86121702	TL	○	○			○			○	
4	86121704	TL				○			○	○	
5	86121705	TL	○	○			○			○	
6	86122405	TL				○			○	○	
7	60111806	DI				○	○		○	○	
8	60120506	DI					○			○	
9	90050503	DI			○		○		○	○	○
10	9005055A	DI				○	○		○	○	○
11	90102408D	DI				○	○			○	
12	90102206	DI				○	○		○	○	○
13	90032511A	GD				○	○			○	
14	90043006	GD				○	○		○	○	○
15	90050505	GD				○	○		○	○	○
16	90050509	GD				○					
17	90082401	GD				○	○			○	○
18	90082513	GD				○	○		○	○	○
19	90102202	GD				○	○		○	○	○
20	90102209	GD				○	○		○	○	○
21	90102222	GD				○	○			○	○
22	90102401	GD				○	○		○	○	○
23	90102407	GD				○	○			○	○
24	90102408G	GD			○		○			○	
25	90102707	GD				○				○	
26	86120307	PG				○	○			○	○
27	87043004	PG					○			○	○
28	87052806	PG					○		○	○	○
29	87062801	PG					○		○	○	○
30	87122210	GR					○		○	○	○
31	87122502	GR					○		○	○	○
32	90101909	GR				○	○			○	○
33	90101906B	AP								○	○
34	85112607	RH						○		○	
35	86112803	RH					○			○	
36	86120106	RH					○		○	○	

TL:tonalite, DI:dark inclusion, GD:granodiorite, PG:porphyritic granite, GR:granite, Ap:aplite, RH:rhyolite.
Opx:orthopyroxene, Cpx:clinopyroxene, Cu:cummingtonite, Amp:calcic amphibole, Bi:biotite, Gt:garnet, I.O:iron-titan oxides, Pl:plagioclase, Kf:K-feldspar.

Table 2. Chemical compositions of orthopyroxene from tonalite.

specimen	86081005	86081005	86081005	86081005	86090708
grain	1	1	2	2	1
position	1	2	1	2	1
SiO_2	51.37	52.16	52.13	52.04	51.16
TiO_2	0.33	0.30	0.38	0.35	0.37
Al_2O_3	0.95	1.04	0.98	0.95	1.17
FeO	26.29	25.79	24.06	23.22	24.97
MnO	0.61	0.52	0.51	0.56	0.56
MgO	18.86	19.60	19.64	19.99	19.64
CaO	1.69	1.55	1.81	1.82	1.73
Na_2O	0.01	0.02	0.02	0.01	0.02
K_2O	0.00	0.00	0.00	0.00	0.01
Total	100.10	100.99	99.52	98.95	99.62
Si	3.918	3.924	3.951	3.955	3.900
Ti	0.019	0.017	0.021	0.020	0.021
Al	0.086	0.093	0.088	0.085	0.105
Fe	1.677	1.622	1.525	1.475	1.592
Mn	0.039	0.033	0.033	0.036	0.036
Mg	2.143	2.196	2.218	2.263	2.230
Ca	0.138	0.125	0.147	0.148	0.141
Na	0.001	0.002	0.003	0.002	0.003
K	0.000	0.000	0.000	0.000	0.001
Total	8.021	8.013	7.985	7.984	8.028
Wo	3.48	3.17	3.78	3.82	3.56
En	54.15	55.69	57.02	58.23	56.28
Fs	42.37	41.14	39.20	37.95	40.16

An analyzed position of each grain is presented as the following abbreviations.

C:core, M:mantle, R:rim

(Table 2. continued)

specimen	86090708	86121702	86121702	86121705	86121705
grain	1	1	1	1	1
position	2	1	2	1	2
SiO_2	50.07	52.25	53.30	52.40	52.93
TiO_2	0.23	0.27	0.37	0.37	0.38
Al_2O_3	0.61	2.38	0.95	0.92	0.98
FeO	32.19	16.33	18.99	22.84	21.79
MnO	0.85	0.28	0.48	0.51	0.52
MgO	14.42	24.83	24.09	21.00	21.43
CaO	1.67	1.74	1.49	1.49	1.65
Na_2O	0.03	0.03	0.01	0.02	0.03
K_2O	0.02	0.00	0.00	0.01	0.02
Total	100.10	98.11	99.68	99.56	99.73
Si	3.939	3.873	3.933	3.945	3.956
Ti	0.014	0.015	0.021	0.021	0.021
Al	0.057	0.208	0.083	0.082	0.086
Fe	2.118	1.012	1.172	1.437	1.362
Mn	0.057	0.018	0.030	0.033	0.033
Mg	1.690	2.742	2.648	2.355	2.386
Ca	0.141	0.138	0.118	0.120	0.132
Na	0.005	0.004	0.001	0.003	0.004
K	0.002	0.000	0.000	0.001	0.002
Total	8.022	8.010	8.005	7.996	7.983
Wo	3.57	3.55	2.99	3.07	3.40
En	42.80	70.45	67.25	60.19	61.50
Fs	53.63	26.00	29.76	36.74	35.10

(Table 2. continued)

specimen	86121705	86121705	86121705	86121705
grain	1	2	2	2
position	3(R)	1	2	3
SiO_2	51.63	53.32	52.03	51.79
TiO_2	0.44	0.31	0.32	0.25
Al_2O_3	0.96	0.68	0.82	0.80
FeO	25.52	21.96	26.25	26.89
MnO	0.59	0.53	0.53	0.63
MgO	18.86	21.85	18.54	17.94
CaO	1.65	1.17	1.62	1.47
Na_2O	0.02	0.01	0.01	0.02
K_2O	0.01	0.00	0.00	0.00
Total	99.68	99.83	100.12	99.79
Si	3.938	3.976	3.958	3.966
Ti	0.025	0.017	0.018	0.014
Al	0.086	0.060	0.074	0.072
Fe	1.627	1.369	1.669	1.722
Mn	0.038	0.033	0.034	0.041
Mg	2.143	2.427	2.101	2.046
Ca	0.135	0.093	0.132	0.121
Na	0.003	0.001	0.001	0.003
K	0.001	0.000	0.000	0.000
Total	7.996	7.977	7.988	7.985
Wo	3.45	2.40	3.38	3.10
En	54.87	62.40	53.84	52.63
Fs	41.67	35.20	42.78	44.27

Plate 3. Chemical compositions of clinopyroxene.(oxygen=12)

specimen	86081005	86081005	86081005	86081005	86090708
grain	1	1	2	2	1
position	1	2	1	2	1
SiO_2	51.03	51.25	50.92	51.70	50.62
TiO_2	0.39	0.77	0.67	0.35	0.07
Al_2O_3	2.39	1.70	1.87	1.50	0.35
FeO	14.58	12.85	12.28	14.92	17.61
MnO	0.33	0.36	0.25	0.43	0.53
MgO	13.13	13.92	14.01	15.36	9.22
CaO	18.45	19.41	19.71	14.99	20.51
Na_2O	0.18	0.17	0.18	0.16	0.20
K_2O	0.01	0.00	0.01	0.00	0.01
Total	100.50	100.43	99.89	99.41	99.12
Si	3.855	3.858	3.848	3.914	3.969
Ti	0.022	0.044	0.038	0.020	0.004
Al	0.213	0.151	0.167	0.134	0.032
Fe	0.921	0.809	0.776	0.944	1.154
Mn	0.021	0.023	0.016	0.028	0.035
Mg	1.478	1.560	1.577	1.732	1.077
Ca	1.493	1.565	1.596	1.216	1.723
Na	0.027	0.025	0.027	0.023	0.031
K	0.001	0.000	0.001	0.000	0.001
Total	8.031	8.035	8.045	8.011	8.026
Ab	38.36	39.77	40.41	31.24	43.57
An	37.97	39.67	39.94	44.50	27.24
Or	23.67	20.56	19.65	24.26	29.19

An analyzed position of each grain is presented as the following abbreviations.

C:core, M:mantle, R:rim

(Plate 3. continued)

specimen	86090708	86090708	86090708	86121702	86121702
grain	1	2	2	1	1
position	2	1	2	1	2
SiO_2	50.11	51.01	50.57	51.50	51.32
TiO_2	0.12	0.09	0.13	0.08	0.07
Al_2O_3	0.62	0.48	0.53	0.48	0.59
FeO	19.00	16.39	17.57	13.51	14.31
MnO	0.49	0.51	0.51	0.35	0.26
MgO	8.61	10.15	9.82	12.06	10.96
CaO	19.57	20.57	20.03	21.32	21.48
Na_2O	0.21	0.23	0.22	0.15	0.20
K_2O	0.01	0.01	0.00	0.00	0.00
Total	98.75	99.44	99.37	99.45	99.19
Si	3.961	3.961	3.949	3.949	3.960
Ti	0.007	0.005	0.008	0.005	0.004
Al	0.058	0.044	0.048	0.043	0.054
Fe	1.256	1.064	1.147	0.866	0.923
Mn	0.033	0.033	0.034	0.023	0.017
Mg	1.014	1.174	1.143	1.377	1.260
Ca	1.657	1.711	1.675	1.751	1.775
Na	0.032	0.035	0.033	0.022	0.030
K	0.001	0.001	0.000	0.000	0.000
Total	8.019	8.029	8.036	8.036	8.024
Wo	42.20	43.32	42.25	43.83	44.85
En	25.83	29.73	28.82	34.49	31.83
Fs	31.97	26.95	28.92	21.68	23.32

(Plate 3. continued)

specimen	86121702	86121702	86121705	86121705
grain	2	2	1	1
position	1	2	1	2
SiO_2	51.99	49.50	51.83	51.62
TiO_2	0.08	0.01	0.04	0.57
Al_2O_3	0.55	4.28	1.33	2.09
FeO	14.54	14.08	14.22	11.43
MnO	0.37	0.30	0.40	0.32
MgO	10.78	10.04	11.09	13.80
CaO	21.46	20.68	20.89	19.08
Na_2O	0.19	0.15	0.21	0.30
K_2O	0.01	0.02	0.02	0.04
Total	99.97	99.06	100.03	99.25
Si	3.980	3.811	3.951	3.898
Ti	0.005	0.001	0.002	0.032
Al	0.050	0.388	0.119	0.186
Fe	0.930	0.906	0.906	0.722
Mn	0.024	0.020	0.026	0.020
Mg	1.229	1.151	1.259	1.552
Ca	1.759	1.705	1.706	1.543
Na	0.028	0.022	0.031	0.044
K	0.001	0.002	0.002	0.004
Total	8.006	8.006	8.003	8.001
Wo	44.89	45.32	44.06	40.43
En	31.36	30.60	32.53	40.67
Fs	23.74	24.08	23.41	18.91

Plate 4. Chemical compositions of cummingtonite. (oxygen=23)

Plate 4–1. Chemical compositions of cummingtonite from dark inclusion.

specimen	90050503	90050503	90050503	90050503	90050503
grain	1	1	1	2	2
position	1	2	3	1	2
SiO_2	50.98	51.19	50.84	51.01	49.32
TiO_2	0.07	0.06	0.08	0.06	0.11
Al_2O_3	1.07	0.36	0.89	0.95	2.56
FeO	31.30	31.79	31.94	31.39	31.83
MnO	2.57	3.01	2.58	2.94	1.77
MgO	9.71	9.55	9.45	9.19	8.32
CaO	1.63	1.05	1.32	1.69	3.08
Na_2O	0.14	0.06	0.14	0.10	0.26
K_2O	0.03	0.00	0.02	0.14	0.17
Total	97.51	97.06	97.26	97.48	97.42
Si	7.886	7.975	7.906	7.916	7.692
Al	0.114	0.025	0.094	0.084	0.308
Al	0.082	0.042	0.069	0.089	0.162
Fe	2.971	2.736	2.732	2.779	2.893
Mg	2.238	2.216	2.190	2.125	1.932
Ti	0.009	0.007	0.009	0.007	0.012
Mn	0.000	0.000	0.000	0.000	0.000
Ca	0.270	0.175	0.220	0.282	0.510
Mn	0.337	0.397	0.340	0.386	0.234
Fe	1.376	1.405	1.421	1.293	1.256
Na	0.017	0.024	0.019	0.039	0.000
Ca	0.000	0.024	0.024	0.000	0.005
Na	0.042	0.018	0.047	0.030	0.078
K	0.007	0.000	0.004	0.028	0.033
(A)	0.049	0.042	0.069	0.058	0.116
mg	0.36	0.35	0.35	0.34	0.32

An analyzed position of each grain is presented as the following abbreviations.

C:core, M:mantle, R:rim

(Plate 4–1. continued)

specimen	90050503
grain	2
position	3
SiO_2	49.38
TiO_2	0.10
Al_2O_3	2.35
FeO	32.91
MnO	0.00
MgO	8.58
CaO	2.76
Na_2O	0.32
K_2O	0.14
Total	96.54
Si	7.742
Al	0.258
Al	0.175
Fe	2.810
Mg	2.004
Ti	0.012
Mn	0.000
Ca	0.463
Mn	0.000
Fe	1.504
Na	0.033
Ca	0.011
Na	0.098
K	0.029
(A)	0.138
mg	0.32

Plate 4–2. Chemical compositions of cummingtonite from granodiorite.

specimen	90102408G	90102408G	90102408G
grain	1	1	1
position	1	2	3
SiO_2	51.87	52.33	51.74
TiO_2	0.04	0.06	0.12
Al_2O_3	1.20	0.64	0.90
FeO	29.81	29.79	30.56
MnO	1.48	1.61	1.39
MgO	11.49	11.61	11.41
CaO	1.60	1.44	1.34
Na_2O	0.19	0.12	0.19
K_2O	0.06	0.04	0.04
Total	97.74	97.64	97.69
Si	7.893	7.964	7.901
Al	0.107	0.036	0.099
Al	0.108	0.079	0.063
Fe	2.283	2.282	2.328
Mg	2.604	2.632	2.595
Ti	0.005	0.007	0.014
Mn	0.000	0.000	0.000
Ca	0.261	0.235	0.219
Mn	0.191	0.207	0.180
Fe	1.510	1.508	1.573
Na	0.040	0.050	0.028
Ca	0.075	0.075	0.075
Na	0.056	0.035	0.056
K	0.012	0.008	0.008
(A)	0.143	0.119	0.139
mg	0.41	0.41	0.40

Table 5. Chemical compositions of calcic amphiboles. (oxygen=23)

Names of amphiboles after the nomenclature by Leake(1978) are presented in "remarks" as the following abbreviations.

AH: actinolitic hornblende, FAH: ferro-actinolitic hornblende, FEH: ferro-edenic hornblende, FH: ferro-hornblende, MH: magnesio-hornblende, MHH: magnesian hastingstic hornblende, TS: tschermakite, TSH: tschermakitic hornblende.

Table 5-1. Chemical compositions of calcic amphiboles from tonalite.

specimen	86081005	86081005	86081005	86081005	86090708
grain	1	1	2	2	1
position	1	2	1	2	1
SiO_2	46.04	46.15	46.73	46.44	43.80
TiO_2	1.46	1.49	1.33	1.37	1.78
Al_2O_3	7.34	7.31	6.61	7.02	7.74
FeO	19.25	18.62	18.94	19.00	21.60
MnO	0.23	0.16	0.26	0.22	0.28
MgO	10.84	11.19	11.25	10.91	9.06
CaO	11.04	11.06	11.10	11.01	10.83
Na_2O	1.26	1.23	1.18	1.24	1.47
K_2O	0.62	0.60	0.53	0.58	0.99
Total	98.05	97.79	97.93	97.78	97.54
Si	6.917	6.927	7.011	6.979	6.744
Al	1.083	1.073	0.989	1.021	1.256
Al	0.216	0.220	0.179	0.223	0.147
Fe	2.195	2.111	2.159	2.179	2.569
Mg	2.425	2.501	2.513	2.443	2.078
Ti	0.164	0.168	0.149	0.155	0.206
Mn	0.000	0.000	0.000	0.000	0.000
Ca	1.749	1.755	1.751	1.765	1.753
Mn	0.029	0.020	0.033	0.027	0.036
Fe	0.222	0.225	0.216	0.208	0.211
Na	0.000	0.000	0.000	0.000	0.000
Ca	0.028	0.023	0.033	0.008	0.032
Na	0.366	0.357	0.344	0.362	0.437
K	0.118	0.115	0.102	0.110	0.194
(A)	0.511	0.495	0.479	0.480	0.664
mg	0.50	0.52	0.51	0.51	0.43
remarks	MH	MH	MH	MH	MH

An analyzed position of each grain is presented as the following abbreviations.
C:core, M:mantle, R:rim

(Table 5–1. continued)

specimen	86090708	86090708	86090708	86121704	86121704
grain	1	2	2	1	1
position	2	1	2	1(C)	2(R)
SiO_2	44.73	44.21	43.25	45.28	45.76
TiO_2	1.67	1.43	1.41	1.50	1.57
Al_2O_3	7.17	7.97	8.77	7.53	7.37
FeO	21.08	22.38	21.73	19.78	20.67
MnO	0.27	0.27	0.25	0.24	0.27
MgO	9.31	8.30	8.52	10.12	9.71
CaO	10.89	10.92	10.78	11.01	11.09
Na_2O	1.35	1.35	1.34	1.39	1.32
K_2O	0.86	0.93	0.93	0.65	0.75
Total	97.34	97.77	96.99	97.50	98.50
Si	6.864	6.798	6.693	6.875	6.901
Al	1.136	1.202	1.307	1.125	1.099
Al	0.160	0.243	0.292	0.222	0.211
Fe	2.512	2.689	2.580	2.319	2.430
Mg	2.128	1.902	1.963	2.287	2.181
Ti	0.193	0.166	0.164	0.171	0.178
Mn	0.000	0.000	0.000	0.000	0.000
Ca	1.780	1.776	1.736	1.778	1.790
Mn	0.035	0.035	0.032	0.031	0.034
Fe	0.185	0.189	0.231	0.192	0.176
Na	0.000	0.000	0.000	0.000	0.000
Ca	0.009	0.022	0.049	0.013	0.001
Na	0.403	0.402	0.403	0.410	0.386
K	0.169	0.182	0.184	0.125	0.145
(A)	0.581	0.606	0.637	0.547	0.531
mg	0.44	0.40	0.41	0.48	0.46
remarks	MH	FH	MH	MH	MH

(Table 5-1. continued)

specimen	86121704	86121704	86121704	86121704	86121704
grain	2	2	2	2	3
position	1(C)	2(C)	3(R)	4(R)	1(C)
SiO_2	44.92	44.66	49.07	49.97	45.70
TiO_2	1.63	1.65	0.73	0.54	1.53
Al_2O_3	7.51	7.28	4.82	3.76	7.09
FeO	20.31	22.29	20.99	20.84	19.94
MnO	0.28	0.24	0.31	0.26	0.25
MgO	9.72	8.05	10.12	10.63	10.42
CaO	10.80	10.80	10.94	10.79	10.77
Na_2O	1.40	1.36	0.74	0.61	1.40
K_2O	0.71	0.81	0.35	0.32	0.66
Total	97.29	97.13	98.08	97.72	97.75
Si	6.858	6.899	7.362	7.500	6.917
Al	1.142	1.101	0.638	0.500	1.083
Al	0.210	0.224	0.215	0.166	0.183
Fe	2.393	2.733	2.441	2.397	2.294
Mg	2.210	1.852	2.262	2.376	2.350
Ti	0.188	0.191	0.082	0.061	0.174
Mn	0.000	0.000	0.000	0.000	0.000
Ca	1.764	1.787	1.757	1.735	1.739
Mn	0.036	0.031	0.039	0.033	0.032
Fe	0.200	0.146	0.192	0.218	0.229
Na	0.000	0.036	0.012	0.013	0.000
Ca	0.002	0.002	0.002	0.002	0.007
Na	0.414	0.408	0.216	0.178	0.411
K	0.138	0.159	0.067	0.060	0.127
(A)	0.555	0.569	0.285	0.240	0.546
mg	0.46	0.39	0.46	0.48	0.48
remarks	MH	FH	AH	AH	MH

(Table 5–1. continued)

specimen	86121704	86121704	86121704	86122405	86122405
grain	3	4	4	1	1
position	2(R)	1	2	1(C)	2(R)
SiO_2	45.86	45.73	45.80	47.70	48.65
TiO_2	1.56	1.58	1.53	1.33	1.19
Al_2O_3	7.28	7.06	7.11	6.63	5.78
FeO	19.76	19.62	19.68	15.43	15.11
MnO	0.21	0.22	0.32	0.23	0.26
MgO	10.34	10.03	10.10	13.13	13.62
CaO	10.74	10.95	10.78	11.34	11.34
Na_2O	1.28	1.50	1.52	1.13	0.90
K_2O	0.68	0.67	0.69	0.52	0.45
Total	97.70	97.36	97.53	97.43	97.31
Si	6.930	6.944	6.945	7.063	7.184
Al	1.070	1.056	1.055	0.937	0.816
Al	0.226	0.208	0.215	0.219	0.190
Fe	2.269	2.343	2.330	1.737	1.681
Mg	2.328	2.269	2.280	2.896	2.997
Ti	0.177	0.180	0.174	0.148	0.132
Mn	0.000	0.000	0.000	0.000	0.000
Ca	1.738	1.781	1.750	1.798	1.784
Mn	0.027	0.028	0.042	0.029	0.032
Fe	0.227	0.149	0.164	0.173	0.184
Na	0.007	0.042	0.045	0.000	0.000
Ca	0.007	0.000	0.000	0.001	0.010
Na	0.374	0.441	0.447	0.323	0.258
K	0.131	0.130	0.134	0.098	0.084
(A)	0.512	0.057	0.582	0.421	0.352
mg	0.48	0.48	0.48	0.60	0.62
remarks	MH	MH	MH	MH	MH

(Table 5-1. continued)

specimen	86122405
grain	2
position	1(R)
SiO_2	47.80
TiO_2	1.73
Al_2O_3	6.27
FeO	15.25
MnO	0.28
MgO	13.63
CaO	11.24
Na_2O	0.89
K_2O	0.46
Total	97.56
Si	7.058
Al	0.942
Al	0.149
Fe	1.662
Mg	2.997
Ti	0.192
Mn	0.000
Ca	1.744
Mn	0.036
Fe	0.220
Na	0.000
Ca	0.034
Na	0.254
K	0.087
(A)	0.376
mg	0.61
remarks	MH

Table 5–2. Chemical compositions of calcic amphiboles from dark inclusion.

specimen	60111806	60111806	9005055A	9005055A	90102206
grain	1	1	1	1	1
position	1	2	1	2	1
SiO_2	47.30	46.78	43.56	44.11	42.12
TiO_2	1.19	1.13	1.65	1.60	1.54
Al_2O_3	6.16	6.49	8.39	8.26	8.38
FeO	17.28	17.66	22.19	20.21	23.62
MnO	0.51	0.51	0.45	0.42	0.64
MgO	11.41	10.84	8.22	9.75	7.14
CaO	11.93	11.69	10.60	10.39	10.87
Na_2O	1.06	1.02	1.88	2.08	1.51
K_2O	0.42	0.50	0.71	0.59	0.77
Total		96.61	97.65	97.41	96.59
	97.25				
Si	7.101	7.084	6.714	6.740	6.640
Al	0.899	0.916	1.286	1.260	1.360
Al	0.191	0.241	0.238	0.228	0.197
Fe	2.124	2.185	2.685	2.370	2.944
Mg	2.551	2.445	1.886	2.219	1.677
Ti	0.135	0.128	0.191	0.183	0.183
Mn	0.000	0.000	0.000	0.000	0.000
Ca	1.891	1.884	1.750	1.700	1.744
Mn	0.065	0.065	0.059	0.054	0.086
Fe	0.044	0.051	0.174	0.213	0.170
Na	0.000	0.000	0.017	0.033	0.000
Ca	0.026	0.011	0.026	0.000	0.090
Na	0.307	0.300	0.561	0.617	0.461
K	0.080	0.096	0.139	0.115	0.156
(A)	0.413	0.407	0.727	0.732	0.707
mg	0.54	0.52	0.40	0.46	0.35
remarks	MH	MH	FH	MH	FH

(Table 5-2. continued)

specimen	90102206	90102408D	90102408D	90102408D	90102408D
grain	1	1	1	1	2
position	2	1	2	3	1
SiO_2	42.93	47.15	47.20	44.37	47.66
TiO_2	1.46	0.94	0.99	1.78	0.85
Al_2O_3	7.96	5.44	5.56	8.51	5.19
FeO	23.44	20.71	20.44	21.60	20.62
MnO	0.81	0.56	0.67	0.58	0.73
MgO	7.41	9.75	9.78	8.25	10.00
CaO	10.76	10.98	11.31	10.84	10.94
Na_2O	1.54	1.10	1.07	1.74	1.03
K_2O	0.57	0.47	0.53	0.55	0.51
Total	96.86	97.10			97.53
			97.55	98.22	
Si	6.725	7.193	7.169	6.761	7.232
Al	1.275	0.807	0.831	1.239	0.768
Al	0.194	0.171	0.164	0.289	0.161
Fe	2.905	2.506	2.510	2.635	2.482
Mg	1.728	2.216	2.213	1.873	2.260
Ti	0.172	0.108	0.113	0.204	0.097
Mn	0.000	0.000	0.000	0.000	0.000
Ca	1.728	1.792	1.828	1.769	1.772
Mn	0.108	0.072	0.086	0.075	0.094
Fe	0.164	0.136	0.086	0.117	0.134
Na	0.000	0.000	0.000	0.039	0.000
Ca	0.078	0.002	0.011	0.011	0.006
Na	0.467	0.325	0.315	0.514	0.303
K	0.114	0.091	0.103	0.107	0.099
(A)	0.659	0.419	0.429	0.632	0.407
mg	0.36	0.46	0.46	0.40	0.46
remarks	FH	MH	MH	FH	MH

(Table 5–2. continued)

specimen	90102408D	90102408D	90102408D
grain	2	2	2
position	2	3(R)	4
SiO_2	46.95	46.84	45.85
TiO_2	1.13	1.04	0.30
Al_2O_3	5.66	5.67	7.17
FeO	20.47	20.60	20.09
MnO	0.56	0.61	0.60
MgO	9.70	9.55	9.30
CaO	11.15	11.17	11.77
Na_2O	1.15	1.17	1.15
K_2O	0.53	0.56	0.68
Total	97.30	97.21	96.91
Si	7.150	7.150	7.024
Al	0.850	0.850	0.976
Al	0.165	0.169	0.318
Fe	2.505	2.540	2.525
Mg	2.200	2.171	2.122
Ti	0.129	0.119	0.035
Mn	0.000	0.000	0.000
Ca	1.818	1.826	1.874
Mn	0.072	0.079	0.078
Fe	0.101	0.089	0.048
Na	0.008	0.006	0.000
Ca	0.006	0.006	0.057
Na	0.339	0.346	0.341
K	0.103	0.109	0.133
(A)	0.448	0.461	0.133
mg	0.46	0.45	0.45
remarks	MH	MH	FH

Table 5–3. Chemical compositions of calcic amphiboles from granodiorite.

specimen	90032511A	90032511A	90043006	90043006	90050505
grain	1	1	1	1	1
position	1	2	1	2	1
SiO_2	46.36	45.16	43.26	43.18	47.25
TiO_2	1.13	1.50	1.72	1.60	1.11
Al_2O_3	6.63	7.36	8.70	8.59	5.73
FeO	20.97	21.43	22.21	21.61	18.36
MnO	0.61	0.63	0.70	0.59	0.71
MgO	9.38	8.87	7.97	8.45	11.48
CaO	11.32	11.17	10.46	10.51	10.98
Na_2O	1.25	1.37	2.09	2.15	1.44
K_2O	0.61	0.71	0.68	0.66	0.72
Total	98.26	98.18	97.77	97.32	97.79
Si	7.021	6.880	6.671	6.672	7.104
Al	0.979	1.120	1.329	1.328	0.896
Al	0.204	0.200	0.251	0.236	0.120
Fe	2.552	2.616	2.711	2.633	2.182
Mg	2.115	2.012	1.831	1.945	2.572
Ti	0.129	0.172	0.199	0.186	0.126
Mn	0.000	0.000	0.000	0.000	0.000
Ca	1.819	1.805	1.727	1.739	1.768
Mn	0.078	0.081	0.091	0.077	0.090
Fe	0.102	0.114	0.144	0.159	0.125
Na	0.000	0.000	0.039	0.026	0.017
Ca	0.016	0.017	0.026	0.011	0.024
Na	0.366	0.404	0.624	0.642	0.420
K	0.118	0.138	0.133	0.129	0.138
(A)	0.501	0.558	0.784	0.782	0.582
mg	0.44	0.42	0.39	0.41	0.53
remarks	MH	FH	FH	FH	MH

(Table 5–3. continued)

specimen	90050505	90050505	90050509	90050509	90082401
grain	1	1	1	1	1
position	2	3	1	2	1
SiO_2	46.59	46.43	41.40	41.28	45.65
TiO_2	1.15	0.70	1.43	1.33	0.58
Al_2O_3	5.97	6.45	14.07	14.53	6.17
FeO	20.52	19.77	20.17	20.28	23.57
MnO	0.72	0.72	0.68	0.66	0.86
MgO	9.99	10.77	7.87	7.80	8.87
CaO	10.68	10.79	9.93	9.83	9.53
Na_2O	1.50	1.47	1.44	1.31	1.48
K_2O	0.78	0.66	0.51	0.53	0.54
Total	97.91	97.76	97.49	97.53	97.25
Si	7.073	7.031	6.293	6.267	7.060
Al	0.927	0.969	1.707	1.733	0.940
Al	0.141	0.181	0.812	0.866	0.185
Fe	2.467	2.310	2.244	2.218	2.703
Mg	2.260	2.429	1.782	1.764	2.044
Ti	0.132	0.080	0.163	0.151	0.068
Mn	0.000	0.000	0.000	0.000	0.000
Ca	1.736	1.715	1.594	1.560	1.543
Mn	0.093	0.092	0.087	0.084	0.113
Fe	0.136	0.193	0.319	0.356	0.345
Na	0.035	0.000	0.000	0.000	0.000
Ca	0.000	0.035	0.024	0.038	0.035
Na	0.441	0.431	0.423	0.385	0.443
K	0.151	0.128	0.099	0.103	0.106
(A)	0.592	0.594	0.546	0.526	0.584
mg	0.46	0.49	0.41	0.41	0.40
remarks	MH	MH	TS	TS	MH

(Table 5–3. continued)

specimen	90082401	90082513	90082513	90082513	90102202
grain	1	1	1	2	1
position	2	1	2	1	1
SiO_2	45.08	42.27	43.08	45.08	44.65
TiO_2	0.56	2.19	2.02	1.10	1.43
Al_2O_3	6.10	9.99	9.27	6.71	7.67
FeO	24.11	21.60	21.31	21.33	21.68
MnO	0.92	0.29	0.34	0.43	0.55
MgO	8.34	8.27	8.66	9.19	9.11
CaO	9.79	10.32	10.30	11.07	10.28
Na_2O	1.55	2.50	2.28	1.57	1.75
K_2O	0.50	0.37	0.52	0.65	0.53
Total	96.94	97.79	97.78	97.12	97.65
Si	7.032	6.489	6.599	6.943	6.837
Al	0.968	1.511	1.401	1.057	1.163
Al	0.153	0.296	0.272	0.160	0.220
Fe	2.843	2.559	2.521	2.605	2.536
Mg	1.938	1.892	1.975	2.108	2.079
Ti	0.066	0.253	0.232	0.127	0.165
Mn	0.000	0.000	0.000	0.000	0.000
Ca	1.577	1.696	1.690	1.802	1.686
Mn	0.121	0.038	0.004	0.057	0.071
Fe	0.302	0.214	0.209	0.141	0.239
Na	0.000	0.052	0.057	0.000	0.004
Ca	0.058	0.026	0.011	0.024	0.022
Na	0.468	0.743	0.677	0.468	0.519
K	0.099	0.072	0.101	0.127	0.103
(A)	0.625	0.841	0.789	0.619	0.644
mg	0.38	0.41	0.42	0.43	0.43
remarks	MH	TSH	TSH	MH	MH

(Table 5–3. continued)

specimen	90102202	90102209	90102209	90102222	90102222
grain	1	1	1	1	1
position	2	1	2	1	2
SiO_2	44.57	44.23	43.38	48.93	49.24
TiO_2	1.51	1.57	1.76	0.46	0.42
Al_2O_3	7.82	8.15	8.63	3.27	2.94
FeO	19.99	19.68	18.96	23.29	22.93
MnO	0.38	0.40	0.44	1.05	1.04
MgO	10.04	9.16	8.54	8.49	8.70
CaO	10.31	10.83	10.85	10.91	11.04
Na_2O	1.88	1.94	1.82	0.65	0.60
K_2O	0.56	0.73	0.85	0.31	0.25
Total	97.05	96.69	95.22	97.35	97.16
Si	6.815	6.800	6.763	7.511	7.556
Al	1.185	1.200	1.237	0.489	0.444
Al	0.223	0.277	0.349	0.101	0.088
Fe	2.317	2.445	2.462	2.905	2.875
Mg	2.286	2.097	1.984	1.941	1.988
Ti	0.174	0.181	0.206	0.053	0.049
Mn	0.000	0.000	0.000	0.000	0.000
Ca	1.688	1.784	1.812	1.779	1.798
Mn	0.049	0.052	0.058	0.137	0.136
Fe	0.238	0.084	0.009	0.084	0.066
Na	0.025	0.080	0.121	0.000	0.000
Ca	0.049	0.000	0.005	0.014	0.016
Na	0.556	0.579	0.551	0.194	0.177
K	0.108	0.143	0.168	0.060	0.049
(A)	0.714	0.722	0.724	0.269	0.242
mg	0.47	0.45	0.45	0.39	0.40
remarks	MH	MH	FEH	FAH	FAH

(Table 5-3. continued)

specimen	90102401	90102401	90102401	90102407	90102407
grain	1	1	1	1	1
position	1	2	3	1(C)	2(R)
SiO_2	44.07	44.01	44.42	44.29	44.72
TiO_2	1.66	1.71	1.70	1.52	1.40
Al_2O_3	8.57	8.51	8.36	8.46	7.28
FeO	20.41	20.52	20.79	20.80	21.49
MnO	0.37	0.43	0.23	0.73	1.07
MgO	9.16	8.80	9.16	8.81	8.49
CaO	10.79	10.82	10.10	10.65	10.89
Na_2O	2.08	2.03	2.12	2.04	1.74
K_2O	0.69	0.79	0.78	0.65	0.62
Total	97.80	97.60	97.65	97.95	97.71
Si	6.720	6.735	6.777	6.757	6.871
Al	1.280	1.265	1.223	1.243	1.129
Al	0.261	0.269	0.280	0.279	0.190
Fe	2.468	2.529	2.444	2.544	2.705
Mg	2.081	2.005	2.081	2.003	1.943
Ti	0.190	0.197	0.195	0.174	0.162
Mn	0.000	0.000	0.000	0.000	0.000
Ca	1.762	1.773	1.651	1.741	1.792
Mn	0.047	0.055	0.030	0.094	0.139
Fe	0.135	0.096	0.208	0.109	0.055
Na	0.056	0.076	0.112	0.057	0.013
Ca	0.000	0.005	0.035	0.016	0.016
Na	0.616	0.601	0.626	0.602	0.519
K	0.134	0.154	0.151	0.127	0.121
(A)	0.750	0.760	0.811	0.745	0.657
mg	0.44	0.43	0.44	0.43	0.41
remarks	MH	FH	MH	MH	FH

(Table 5–3. continued)

specimen	90102707	90102707	90102707	90102707
grain	1	1	1	1
position	1	2(R)	3	4
SiO_2	44.19	45.23	44.75	44.11
TiO_2	1.76	1.56	1.67	1.68
Al_2O_3	8.53	8.10	8.25	8.88
FeO	20.89	20.52	20.96	20.76
MnO	0.34	0.32	0.32	0.27
MgO	9.03	9.61	9.06	9.11
CaO	10.77	10.68	10.62	10.56
Na_2O	1.66	1.61	1.63	1.79
K_2O	0.85	0.73	0.77	0.76
Total	98.02	98.36	98.03	97.92
Si	6.731	6.829	6.802	6.713
Al	1.269	1.171	1.198	1.287
Al	0.262	0.271	0.279	0.306
Fe	2.487	2.391	2.479	2.437
Mg	2.049	2.161	2.051	2.065
Ti	0.202	0.177	0.191	0.192
Mn	0.000	0.000	0.000	0.000
Ca	1.757	1.727	1.729	1.721
Mn	0.044	0.041	0.041	0.035
Fe	0.173	0.199	0.184	0.205
Na	0.026	0.033	0.046	0.040
Ca	0.075	0.075	0.075	0.075
Na	0.490	0.471	0.480	0.528
K	0.165	0.141	0.149	0.147
(A)	0.731	0.687	0.705	0.751
mg	0.44	0.45	0.44	0.44
remarks	MH	MH	MH	MH

Table 5–4. Chemical compositions of calcic amphiboles from porphyritic granite.

specimen	86120307	86120307	86120307	86120307	86120307
grain	1	1	1	1	1
position	1(C)	2(C)	3(R)	4(R)	5(R)
SiO_2	41.73	41.49	41.80	42.14	41.95
TiO_2	1.87	1.98	1.90	1.77	1.91
Al_2O_3	9.15	9.20	9.24	8.89	9.32
FeO	24.11	24.09	25.06	23.99	24.20
MnO	0.33	0.28	0.46	0.38	0.38
MgO	6.13	6.04	5.29	5.95	5.93
CaO	11.24	11.26	11.08	11.13	11.14
Na_2O	1.79	1.75	1.73	1.74	1.77
K_2O	1.09	1.12	1.06	1.02	1.08
Total	97.45	97.20	97.61	97.01	97.69
Si	6.552	6.533	6.575	6.631	6.565
Al	1.448	1.467	1.425	1.369	1.435
Al	0.245	0.240	0.288	0.280	0.284
Fe	3.099	3.108	3.248	3.115	3.110
Mg	1.434	1.417	1.239	1.395	1.381
Ti	0.221	0.235	0.224	0.210	0.225
Mn	0.000	0.000	0.000	0.000	0.000
Ca	1.889	1.899	1.866	1.876	1.868
Mn	0.043	0.037	0.061	0.051	0.050
Fe	0.066	0.063	0.047	0.041	0.056
Na	0.002	0.000	0.026	0.033	0.026
Ca	0.078	0.078	0.078	0.078	0.078
Na	0.545	0.534	0.528	0.531	0.538
K	0.219	0.224	0.212	0.204	0.216
(A)	0.842	0.836	0.817	0.813	0.831
mg	0.31	0.31	0.27	0.31	0.30
remarks	MHH	MHH	FEH	FEH	FEH

Table 5-5. Chemical compositions of calcic amphiboles from granite.

specimen	90101909	90101909	90101909
grain	1	1	1
position	1	2	3
SiO_2	44.18	44.35	44.50
TiO_2	1.25	0.33	0.29
Al_2O_3	7.37	6.83	7.68
FeO	25.33	25.91	26.01
MnO	1.14	1.21	0.80
MgO	6.14	6.02	5.41
CaO	10.12	9.94	11.37
Na_2O	1.95	1.61	1.05
K_2O	0.72	0.78	0.67
Total	98.20	96.98	97.78
Si	6.878	7.005	6.957
Al	1.122	0.995	1.043
Al	0.230	0.276	0.372
Fe	3.200	3.268	3.334
Mg	1.424	1.417	1.260
Ti	0.146	0.039	0.034
Mn	0.000	0.000	0.000
Ca	1.687	1.681	1.828
Mn	0.150	0.162	0.106
Fe	0.097	0.153	0.066
Na	0.066	0.004	0.000
Ca	0.000	0.000	0.075
Na	0.588	0.493	0.318
K	0.143	0.157	0.134
(A)	0.731	0.650	0.527
mg	0.30	0.29	0.27
remarks	FH	FH	FH

Table 6. Chemical compositions of biotite. (oxygen=22)

Table 6–1. Chemical compositions of biotite from tonalite.

specimen	86081005	86081005	86121705	86121705	86121705
grain	1	1	1	1	1
point	1	2	1	2	3
SiO_2	35.72	35.33	36.72	36.63	36.65
TiO_2	4.54	4.41	5.19	5.13	4.70
Al_2O_3	14.33	14.51	13.86	13.92	14.15
FeO	21.71	24.20	20.85	21.13	20.91
MnO	0.10	0.12	0.10	0.11	0.04
MgO	8.97	8.95	10.66	10.69	10.99
CaO	0.03	0.03	0.00	0.00	0.00
Na_2O	0.13	0.17	0.19	0.18	0.22
K_2O	8.57	7.99	9.10	9.28	9.07
Total	94.11	95.70	96.67	97.07	96.73
Si	5.580	5.478	5.567	5.544	5.551
Al	2.420	2.522	2.433	2.456	2.449
Al	0.218	0.129	0.043	0.027	0.076
Ti	0.533	0.514	0.591	0.584	0.535
Fe	2.836	3.138	2.643	2.674	2.648
Mn	0.014	0.015	0.013	0.014	0.005
Mg	2.087	2.067	2.407	2.410	2.479
Ca	0.005	0.005	0.000	0.000	0.000
Na	0.040	0.051	0.056	0.053	0.065
K	1.707	1.579	1.759	1.791	1.752
Total	15.441	15.498	15.511	15.553	15.560
mg	0.42	0.40	0.48	0.47	0.48

(Table 6–1. continued)

specimen	86121705
grain	1
point	4
SiO_2	35.76
TiO_2	4.25
Al_2O_3	14.47
FeO	21.23
MnO	0.10
MgO	11.46
CaO	0.00
Na_2O	0.24
K_2O	8.20
Total	95.71
Si	5.469
Al	2.531
Al	0.077
Ti	0.489
Fe	2.714
Mn	0.013
Mg	2.611
Ca	0.000
Na	0.071
K	1.599
Total	15.574
mg	0.49

Table 6–2. Chemical compositions of biotite from dark inclusion.

specimen	60111806	60111806	60120506	60120506	60120506
grain	1	1	1	1	2
point	1	2	1	2	1
SiO_2	36.37	36.63	35.69	35.51	35.35
TiO_2	3.67	3.55	4.01	4.03	3.93
Al_2O_3	14.25	13.92	13.56	13.54	13.83
FeO	21.31	21.68	25.65	26.20	26.36
MnO	0.23	0.25	0.27	0.24	0.27
MgO	10.81	10.91	7.08	7.25	7.11
CaO	0.02	0.02	0.02	0.03	0.04
Na_2O	0.07	0.06	0.08	0.08	0.08
K_2O	8.73	8.72	9.47	9.37	9.29
Total	95.47	95.74	95.83	96.24	96.27
Si	5.586	5.618	5.620	5.581	5.556
Al	2.414	2.382	2.380	2.419	2.444
Al	0.166	0.134	0.135	0.088	0.118
Ti	0.424	0.409	0.475	0.476	0.465
Fe	2.736	2.780	3.376	3.442	3.464
Mn	0.030	0.033	0.036	0.032	0.036
Mg	2.474	2.494	1.661	1.697	1.666
Ca	0.003	0.003	0.003	0.005	0.007
Na	0.020	0.019	0.024	0.024	0.024
K	1.710	1.706	1.901	1.877	1.862
Total	15.565	15.577	15.611	15.641	15.641
mg	0.47	0.47	0.33	0.33	0.32

(Table 6–2. continued)

specimen	60120506	90050503	90050503	90050503	9005055A
grain	2	1	1	1	1
point	2	1	2	3	1
SiO_2	35.38	34.90	35.36	35.31	35.29
TiO_2	3.91	4.54	4.55	4.42	3.70
Al_2O_3	13.95	13.84	13.60	13.43	13.61
FeO	26.43	26.02	25.27	25.25	27.29
MnO	0.29	0.40	0.35	0.34	0.28
MgO	7.17	6.89	7.26	7.39	6.85
CaO	0.03	0.02	0.00	0.00	0.00
Na_2O	0.09	0.06	0.04	0.08	0.09
K_2O	9.20	9.77	10.09	9.88	8.53
Total	96.43	96.43	96.52	96.11	95.64
Si	5.549	5.495	5.544	5.557	5.586
Al	2.451	2.505	2.456	2.443	2.414
Al	0.126	0.062	0.056	0.048	0.124
Ti	0.460	0.537	0.536	0.523	0.441
Fe	3.465	3.425	3.313	3.322	3.612
Mn	0.039	0.053	0.047	0.046	0.038
Mg	1.675	1.616	1.696	1.732	1.615
Ca	0.004	0.003	0.000	0.000	0.001
Na	0.027	0.017	0.013	0.025	0.026
K	1.840	1.962	2.017	1.983	1.721
Total	15.636	15.674	15.679	15.678	15.578
mg	0.33	0.32	0.34	0.34	0.31

(Table 6–2. continued)

specimen	9005055A	9005055A	90102206	90102206	90102408D
grain	2	2	1	1	1
point	1	2	1	2(R)	1
SiO_2	34.98	34.27	34.60	34.73	35.20
TiO_2	3.90	3.66	4.61	4.52	4.43
Al_2O_3	13.77	16.34	13.61	13.83	13.61
FeO	26.43	25.55	26.10	26.27	23.66
MnO	0.24	0.23	0.36	0.27	0.24
MgO	7.46	7.28	7.49	7.33	8.58
CaO	0.01	0.01	0.01	0.03	0.00
Na_2O	0.06	0.09	0.06	0.10	0.09
K_2O	8.28	8.25	8.96	8.78	9.42
Total	95.13	95.69	95.79	95.85	95.23
Si	5.540	5.358	5.467	5.476	5.532
Al	2.460	2.642	2.533	2.524	2.468
Al	0.109	0.370	0.000	0.045	0.053
Ti	0.464	0.431	0.548	0.536	0.523
Fe	3.499	3.340	3.447	3.464	3.109
Mn	0.032	0.031	0.048	0.036	0.032
Mg	1.761	1.696	1.763	1.721	2.009
Ca	0.002	0.002	0.002	0.005	0.000
Na	0.018	0.028	0.019	0.029	0.027
K	1.671	1.645	1.805	1.765	1.888
Total	15.556	15.542	15.631	15.601	15.642
mg	0.33	0.34	0.34	0.33	0.39

(Table 6–2. continued)

specimen	90102408D
grain	1
point	2
SiO_2	35.32
TiO_2	4.30
Al_2O_3	13.42
FeO	23.45
MnO	0.30
MgO	8.61
CaO	1.24
Na_2O	0.10
K_2O	8.79
Total	95.53
Si	5.529
Al	2.471
Al	0.004
Ti	0.506
Fe	3.069
Mn	0.040
Mg	2.008
Ca	0.208
Na	0.030
K	1.755
Total	15.620
mg	0.40

Table 6–3. Chemical compositions of biotite from granodiorite.

specimen	90032511A	90032511A	90043006	90043006	90043006
grain	1	1	1	1	2
point	1	2	1	2	1
SiO_2	35.18	35.00	36.04	36.12	35.93
TiO_2	4.28	4.24	1.95	1.51	1.78
Al_2O_3	13.62	14.03	13.33	13.30	13.39
FeO	24.78	25.34	26.40	26.00	27.68
MnO	0.28	0.26	0.35	0.35	0.36
MgO	8.09	8.03	8.66	9.04	7.65
CaO	0.01	0.02	0.00	0.09	0.05
Na_2O	0.13	0.09	0.14	0.14	0.07
K_2O	9.07	8.91	8.79	8.06	8.69
Total	95.43	95.92	95.66	94.60	95.59
Si	5.537	5.487	5.681	5.722	5.700
Al	2.463	2.513	2.319	2.278	2.300
Al	0.062	0.079	0.156	0.204	0.202
Ti	0.506	0.499	0.231	0.180	0.212
Fe	3.261	3.321	3.478	3.443	3.670
Mn	0.037	0.035	0.047	0.047	0.048
Mg	1.897	1.875	2.033	2.134	1.808
Ca	0.002	0.004	0.000	0.015	0.008
Na	0.039	0.027	0.042	0.043	0.020
K	1.821	1.782	1.766	1.629	1.757
Total	15.624	15.622	15.754	15.693	15.726
mg	0.37	0.36	0.37	0.38	0.33

(Table 6–3. continued)

specimen	90043006	90050505	90050505	90082401	90082401
grain	2	1	1	1	1
point	2	1	2	1	2
SiO_2	35.97	36.36	36.17	35.01	35.27
TiO_2	1.67	4.27	4.13	3.27	3.04
Al_2O_3	13.28	13.13	13.37	13.58	13.96
FeO	28.35	25.08	25.33	26.91	26.76
MnO	0.36	0.28	0.31	0.41	0.44
MgO	7.76	8.55	8.13	7.62	7.74
CaO	0.00	0.00	0.00	0.03	0.06
Na_2O	0.04	0.10	0.10	0.10	0.07
K_2O	8.68	10.03	9.93	8.33	8.18
Total	96.11	97.80	97.48	95.26	95.54
Si	5.690	5.602	5.598	5.558	5.566
Al	2.310	2.398	2.402	2.442	2.434
Al	0.166	–	0.036	0.099	0.162
Ti	0.198	0.495	0.481	0.390	0.361
Fe	3.750	3.231	3.277	3.572	3.530
Mn	0.048	0.037	0.041	0.056	0.059
Mg	1.830	1.962	1.874	1.803	1.819
Ca	0.000	0.000	0.000	0.004	0.010
Na	0.013	0.030	0.029	0.031	0.022
K	1.751	1.971	1.959	1.686	1.646
Total	15.756	15.712	15.697	15.640	15.609
mg	0.33	0.38	0.36	0.34	0.34

(Table 6–3. continued)

specimen	90082513	90082513	90102202	90102202	90102209
grain	1	1	1	1	1
point	1	2	1	2	1
SiO_2	35.22	35.08	35.31	35.31	36.23
TiO_2	3.88	3.73	3.91	3.82	3.65
Al_2O_3	13.19	13.32	13.59	13.79	13.23
FeO	26.78	27.00	25.45	25.86	23.95
MnO	0.39	0.36	0.47	0.43	0.36
MgO	7.27	7.36	8.33	7.95	8.67
CaO	0.00	0.00	0.00	0.00	0.00
Na_2O	0.09	0.09	0.13	0.10	0.06
K_2O	8.56	8.45	8.51	8.41	9.55
Total	95.38	95.37	95.69	95.69	95.70
Si	5.588	5.568	5.543	5.547	5.664
Al	2.412	2.432	2.457	2.453	2.336
Al	0.054	0.058	0.057	0.100	0.102
Ti	0.463	0.444	0.461	0.451	0.429
Fe	3.551	3.583	3.340	3.397	3.131
Mn	0.053	0.048	0.062	0.057	0.048
Mg	1.717	1.740	1.947	1.861	2.019
Ca	0.000	0.000	0.000	0.000	0.000
Na	0.027	0.026	0.038	0.032	0.017
K	1.731	1.711	1.702	1.686	1.903
Total	15.595	15.611	15.609	15.584	15.648
mg	0.33	0.33	0.37	0.35	0.39

(Table 6-3. continued)

specimen	90102209	90102222	90102222	90102222	90102222
grain	1	1	1	2	2
point	2	1	2	1	2
SiO_2	36.02	35.51	35.68	35.71	35.85
TiO_2	3.33	3.00	2.98	2.93	2.83
Al_2O_3	13.25	12.97	13.22	13.24	13.55
FeO	25.05	26.93	27.25	26.91	26.94
MnO	0.34	0.47	0.47	0.48	0.43
MgO	8.50	7.25	7.30	7.29	7.30
CaO	0.00	0.01	0.03	0.00	0.04
Na_2O	0.07	0.09	0.07	0.08	0.06
K_2O	9.53	9.23	9.32	9.21	9.04
Total	96.09	95.45	96.31	95.85	96.02
Si	5.640	5.655	5.635	5.654	5.653
Al	2.360	2.345	2.365	2.346	2.347
Al	0.085	0.088	0.095	0.124	0.171
Ti	0.392	0.359	0.354	0.349	0.335
Fe	3.279	3.585	3.598	3.562	3.551
Mn	0.045	0.064	0.063	0.065	0.057
Mg	1.982	1.720	1.718	1.720	1.714
Ca	0.000	0.001	0.004	0.000	0.006
Na	0.021	0.027	0.022	0.024	0.017
K	1.904	1.875	1.876	1.859	1.817
Total	15.708	15.720	15.730	15.703	15.670
mg	0.38	0.32	0.32	0.33	0.33

(Table 6–3. continued)

specimen	90102401	90102401	90102407	90102407	90102408G
grain	1	1	1	1	1
point	1	2	1	2	1
SiO_2	36.06	36.28	36.14	36.05	35.55
TiO_2	3.21	3.00	3.84	4.16	3.50
Al_2O_3	13.38	12.93	13.48	13.53	13.59
FeO	27.31	25.21	24.12	24.39	27.08
MnO	0.51	0.48	0.52	0.47	0.29
MgO	7.26	7.90	8.65	8.45	7.09
CaO	0.01	0.00	0.01	0.00	0.03
Na_2O	0.06	0.07	0.07	0.05	0.10
K_2O	9.18	9.08	9.42	9.36	9.35
Total	96.97	94.96	96.23	96.46	96.58
Si	5.643	5.741	5.622	5.599	5.590
Al	2.357	2.259	2.378	2.401	2.410
Al	0.110	0.152	0.092	0.075	0.108
Ti	0.378	0.357	0.449	0.485	0.414
Fe	3.572	3.335	3.136	3.167	3.560
Mn	0.067	0.064	0.069	0.062	0.039
Mg	1.691	1.862	2.003	1.954	1.661
Ca	0.002	0.001	0.001	0.001	0.005
Na	0.019	0.021	0.021	0.016	0.030
K	1.832	1.832	1.868	1.853	1.875
Total	15.672	15.623	15.639	15.612	15.690
mg	0.32	0.36	0.39	0.38	0.32

(Table 6–3. continued)

specimen	90102408G
grain	1
point	2
SiO_2	35.42
TiO_2	3.73
Al_2O_3	13.16
FeO	26.91
MnO	0.36
MgO	7.10
CaO	0.03
Na_2O	0.11
K_2O	9.34
Total	96.16
Si	5.599
Al	2.401
Al	0.050
Ti	0.443
Fe	3.556
Mn	0.048
Mg	1.672
Ca	0.005
Na	0.034
K	1.883
Total	15.691
mg	0.32

Table 6–4. Chemical compositions of biotite from porphyritic granite.

specimen	86120307	86120307	86120307	86120307	86120307
grain	1	1	1	1	1
point	1	2	3	4(R)	5(R)
SiO_2	34.77	34.88	34.81	35.60	34.67
TiO_2	3.90	4.00	4.00	3.05	2.81
Al_2O_3	13.76	13.65	13.86	13.97	14.28
FeO	27.48	28.03	27.61	26.95	27.84
MnO	0.40	0.45	0.50	0.41	0.47
MgO	5.79	5.79	5.64	6.35	5.99
CaO	0.03	0.00	0.01	0.03	0.07
Na_2O	0.14	0.14	0.13	0.06	0.06
K_2O	9.25	9.16	9.29	9.51	9.17
Total	95.51	96.09	95.85	95.93	95.35
Si	5.555	5.548	5.545	5.636	5.552
Al	2.445	2.452	2.455	2.364	2.448
Al	0.144	0.107	0.148	0.242	0.248
Ti	0.468	0.478	0.479	0.363	0.338
Fe	3.671	3.728	3.677	3.567	3.727
Mn	0.054	0.060	0.068	0.055	0.064
Mg	1.377	1.372	1.338	1.498	1.428
Ca	0.005	0.000	0.002	0.004	0.012
Na	0.044	0.042	0.039	0.018	0.019
K	1.885	1.858	1.886	1.920	1.873
Total	15.647	15.644	15.637	15.667	15.708
mg	0.27	0.27	0.27	0.30	0.28

(Table 6–4. continued)

specimen	87043004	87043004	87052806	87052806	87052806
grain	1	1	1	1	1
point	1	2	1	2	3(R)
SiO_2	35.18	34.38	33.69	33.92	34.03
TiO_2	4.53	3.92	4.08	3.86	3.10
Al_2O_3	13.65	14.67	13.57	13.87	14.12
FeO	27.04	26.91	29.18	28.81	29.39
MnO	0.25	0.28	0.48	0.50	0.40
MgO	6.73	6.39	5.41	5.47	5.50
CaO	0.00	0.09	0.02	0.03	0.02
Na_2O	0.16	0.13	0.07	0.06	0.06
K_2O	9.25	8.15	8.90	9.02	9.10
Total	96.79	94.91	95.41	95.54	95.71
Si	5.520	5.472	5.445	5.461	5.479
Al	2.480	2.528	2.555	2.539	2.521
Al	0.045	0.223	0.029	0.092	0.157
Ti	0.534	0.468	0.496	0.467	0.375
Fe	3.547	3.580	3.943	3.878	3.956
Mn	0.033	0.037	0.065	0.069	0.054
Mg	1.574	1.514	1.303	1.312	1.320
Ca	0.000	0.016	0.003	0.005	0.003
Na	0.049	0.039	0.023	0.018	0.018
K	1.852	1.655	1.834	1.851	1.867
Total	15.634	15.531	15.695	15.692	15.750
mg	0.31	0.30	0.25	0.25	0.25

(Table 6–4. continued)

specimen	87062801	87062801	87062801
grain	1	1	1
point	1	2	3
SiO_2	35.41	34.94	35.10
TiO_2	3.73	3.70	3.96
Al_2O_3	13.47	13.69	13.61
FeO	27.23	27.48	27.39
MnO	0.27	0.21	0.34
MgO	6.68	6.58	6.53
CaO	0.03	0.01	0.03
Na_2O	0.14	0.17	0.19
K_2O	9.10	9.01	9.26
Total	96.06	95.78	96.39
Si	5.598	5.550	5.547
Al	2.402	2.450	2.453
Al	0.108	0.112	0.080
Ti	0.444	0.442	0.470
Fe	3.600	3.649	3.618
Mn	0.036	0.028	0.045
Mg	1.573	1.556	1.537
Ca	0.005	0.001	0.005
Na	0.043	0.052	0.058
K	1.835	1.824	1.865
Total	15.642	15.665	15.678
mg	0.30	0.30	0.30

Table 6–5. Chemical compositions of biotite from granite.

specimen	87122210	87122210	87122502	87122502	87122502
grain	1	1	1	1	1
point	1	2	1	2	3
SiO_2	34.66	34.85	35.06	34.70	35.13
TiO_2	4.16	4.28	3.65	3.70	3.43
Al_2O_3	13.81	13.45	13.73	13.64	13.54
FeO	27.97	27.63	27.12	27.51	27.40
MnO	0.61	0.69	0.48	0.54	0.54
MgO	5.98	6.03	6.54	6.45	6.52
CaO	0.01	0.00	0.02	0.01	0.02
Na_2O	0.12	0.08	0.07	0.10	0.10
K_2O	8.96	9.34	9.44	9.27	9.30
Total	96.28	96.35	96.10	95.92	95.98
Si	5.501	5.532	5.557	5.526	5.581
Al	2.499	2.468	2.443	2.474	2.419
Al	0.083	0.048	0.121	0.086	0.116
Ti	0.496	0.511	0.435	0.443	0.410
Fe	3.711	3.666	3.594	3.663	3.640
Mn	0.082	0.093	0.065	0.073	0.073
Mg	1.413	1.425	1.544	1.529	1.542
Ca	0.002	0.001	0.003	0.002	0.003
Na	0.038	0.024	0.021	0.031	0.031
K	1.814	1.890	1.909	1.883	1.885
Total	15.638	15.656	15.691	15.709	15.700
mg	0.28	0.28	0.30	0.29	0.30

(Table 6–5. continued)

specimen	90101909	90101909	90101909	90101909
grain	1	1	1	1
point	1	2	3	4
SiO_2	35.21	35.81	36.39	36.02
TiO_2	3.53	3.59	2.83	3.28
Al_2O_3	13.65	13.05	13.22	13.34
FeO	27.51	27.21	27.30	27.56
MnO	0.59	0.53	0.50	0.52
MgO	6.32	6.52	7.09	6.43
CaO	0.00	0.01	0.00	0.00
Na_2O	0.09	0.08	0.08	0.09
K_2O	9.33	9.35	9.57	9.54
Total	96.23	96.15	96.98	96.78
Si	5.581	5.666	5.703	5.669
Al	2.419	2.334	2.297	2.331
Al	0.130	0.099	0.144	0.143
Ti	0.421	0.427	0.333	0.388
Fe	3.645	3.599	3.577	3.626
Mn	0.079	0.071	0.066	0.069
Mg	1.492	1.537	1.655	1.508
Ca	0.000	0.002	0.000	0.000
Na	0.028	0.025	0.024	0.027
K	1.886	1.886	1.912	1.915
Total	15.681	15.646	15.712	15.677
mg	0.29	0.30	0.32	0.29

Table 6–6. Chemical compositions of biotite from rhyolite.

specimen	86112803	86120106	86120106	86120106
grain	1	1	1	1
point	1	1	2	3
SiO_2	32.49	33.91	34.01	34.41
TiO_2	1.15	2.83	2.82	2.14
Al_2O_3	20.53	15.57	15.44	19.56
FeO	25.43	25.25	25.14	22.16
MnO	0.69	0.28	0.31	0.27
MgO	5.47	7.37	7.59	7.64
CaO	0.02	0.32	0.06	0.22
Na_2O	0.07	0.05	0.04	0.48
K_2O	9.02	9.09	9.17	8.43
Total	94.88	94.67	94.58	95.32
Si	5.148	5.402	5.418	5.300
Al	2.852	2.598	2.582	2.700
Al	0.982	0.324	0.318	0.850
Ti	0.137	0.338	0.337	0.248
Fe	3.369	3.363	3.349	2.854
Mn	0.092	0.037	0.042	0.035
Mg	1.292	1.749	1.801	1.754
Ca	0.003	0.055	0.010	0.035
Na	0.023	0.015	0.011	0.144
K	1.821	1.847	1.864	1.657
Total	15.720	15.730	15.732	15.577
mg	0.28	0.34	0.35	0.38

Table 7. Chemical compositions of garnet from rhyolites (in Sakane)

specimen	85112607	85112607	85112607	85112607	85112607
grain	1	1	1	1	2
position	1(C)	2(C)	3(R)	4(R)	1(C)
SiO_2	37.61	37.04	36.64	37.64	37.34
TiO_2	0.00	0.02	0.01	0.00	0.00
Al_2O_3	20.64	20.88	20.83	20.98	21.03
FeO	33.10	32.97	32.12	32.80	34.70
MnO	5.07	5.22	6.14	6.14	4.14
MgO	1.30	1.27	1.06	1.03	1.21
CaO	2.45	2.46	2.00	2.24	2.23
Na_2O	0.00	0.01	0.00	0.02	0.02
K_2O	0.02	0.00	0.00	0.02	0.02
Total	100.19	99.87	98.80	100.87	100.69
Si	6.089	6.025	6.028	6.065	6.031
Ti	0.000	0.002	0.001	0.000	0.000
Al	3.938	4.002	4.038	3.983	4.003
Fe	4.480	4.484	4.418	4.418	4.686
Mn	0.695	0.719	0.855	0.838	0.566
Mg	0.314	0.308	0.260	0.247	0.291
Ca	0.425	0.429	0.352	0.387	0.386
Na	0.000	0.003	0.000	0.006	0.006
K	0.004	0.000	0.000	0.004	0.004
Total	15.944	15.973	15.952	15.949	15.973
Alm	75.76	75.50	75.07	75.02	79.03
Sps	11.75	12.11	14.53	14.22	9.55
Pyr	5.30	5.18	4.41	4.20	4.91
Grs	7.18	7.22	5.99	6.56	6.51

Abbreviations of "C", "M" and "R" in "position" show core, middle and rim within a analyzed grain respectively.

C:core, M:mantle, R:rim

(Table.7 continued)

specimen	85112607
grain	2
position	2(R)
SiO_2	37.52
TiO_2	0.00
Al_2O_3	20.98
FeO	33.01
MnO	5.57
MgO	1.09
CaO	1.99
Na_2O	0.02
K_2O	0.04
Total	100.22
Si	6.075
Ti	0.000
Al	4.003
Fe	4.468
Mn	0.764
Mg	0.263
Ca	0.345
Na	0.006
K	0.008
Total	15.931
Alm	76.51
Sps	13.08
Pyr	4.50
Grs	5.91

Table 8. Chemical compositions of iron–titan oxides.

Ilmenite coexisting with magnetite within a specimen is presented in "remarks" as the abbreviation of "+MG"

Table 8–1. Chemical compositions of ilmenite from tonalite.

specimen	86081005	86081005	86090708	86090708	86090708
grain	1	1	1	1	1
position	1	2	1	2	3
SiO_2	0.03	0.09	0.04	0.08	0.06
TiO_2	48.98	50.13	50.43	50.32	50.58
Al_2O_3	0.17	1.25	0.45	0.75	0.11
FeO	48.52	47.55	47.14	47.24	46.92
MnO	1.06	1.04	1.35	1.47	1.40
MgO	0.17	0.14	0.09	0.08	0.07
CaO	0.03	0.05	0.07	0.07	0.06
Na_2O	0.00	0.00	0.00	0.01	0.00
K_2O	0.04	0.04	0.05	0.04	0.04
Total	99.00	100.29	99.60	100.05	99.24
recalculated					
Fe_2O_3	6.55	4.27	3.79	4.13	3.14
FeO	42.63	43.71	43.73	43.52	43.86
Total	99.62	100.68	99.93	100.41	99.54
mol. ratio					
ilmenite	93.49	94.14	95.74	95.00	96.59
Fe_2O_3	90.57	91.42	92.53	91.56	93.31
$MnTiO_3$	2.29	2.20	2.88	3.13	3.02
$MgTiO_3$	0.63	0.52	0.33	0.31	0.25
Hematite	6.51	5.86	4.26	5.00	3.41
remarks					

An analyzed position of each grain is presented as the following abbreviations.

C:core, M:mantle, R:rim

(Table 8–1. continued)

specimen	86121704	86121704	86122405	86122405	86122405
grain	1	1	1	1	2
position	1	2	1	2	1
SiO_2	0.06	0.13	0.05	0.08	0.05
TiO_2	52.81	52.48	48.28	48.03	48.40
Al_2O_3	0.15	1.31	0.00	0.03	0.00
FeO	43.45	42.22	48.29	48.30	47.69
MnO	2.80	2.79	2.67	2.62	2.62
MgO	0.04	0.04	0.10	0.09	0.08
CaO	0.07	0.06	0.06	0.08	0.08
Na_2O	0.02	0.03	0.00	0.03	0.01
K_2O	0.04	0.04	0.06	0.03	0.04
Total	99.44	99.10	99.51	99.29	98.97
recalculated					
Fe_2O_3	–	–	8.71	8.93	7.86
FeO	44.49	44.21	40.45	40.27	40.62
Total	99.26	98.81	100.32	100.12	99.71
mol. ratio					
ilmenite	100.88	100.16	91.72	91.45	92.49
Fe_2O_3	94.69	94.00	85.62	85.48	86.53
$MnTiO_3$	6.04	6.01	5.72	5.63	5.65
$MgTiO_3$	0.15	0.15	0.38	0.34	0.30
Hematite	–	–	8.28	8.55	7.51
remarks					

Table 8–2. Chemical compositions of ilmenite from dark inclusion.

specimen	60111806	60111806	9005055A	9005055A	90102206
grain	1	1	1	1	1
position	1	2	1	2	1(C)
SiO_2	0.05	0.06	0.11	0.11	0.03
TiO_2	53.13	52.80	5.79	22.49	50.37
Al_2O_3	0.01	0.14	0.16	0.15	0.00
FeO	43.02	44.07	83.40	71.24	43.69
MnO	3.44	2.85	0.60	1.39	4.85
MgO	0.08	0.07	0.00	0.02	0.00
CaO	0.08	0.08	0.08	0.06	0.06
Na_2O	0.00	0.01	0.00	0.00	0.00
K_2O	0.04	0.04	0.05	0.04	0.01
Total	99.85	100.12	90.18	95.51	99.01
recalculated					
Fe_2O_3	–	–	87.69	58.39	3.77
FeO	44.06	44.36	4.50	18.71	40.30
Total	99.96	100.04	98.92	101.31	99.38
mol. ratio					
ilmenite	101.08	100.10	11.62	43.40	96.39
Fe_2O_3	93.42	93.72	10.25	40.29	85.92
$MnTiO_3$	7.38	6.10	1.38	3.03	10.47
$MgTiO_3$	0.28	0.27	0.00	0.08	0.00
Hematite	–	–	88.38	56.60	3.61
remarks					+MG

(Table 8–2. continued)

specimen	90102206
grain	1
position	2(R)
SiO_2	0.36
TiO_2	51.25
Al_2O_3	0.14
FeO	41.86
MnO	5.41
MgO	0.01
CaO	0.43
Na_2O	0.00
K_2O	0.01
Total	99.47
recalculated	
Fe_2O_3	2.03
FeO	40.03
Total	99.66
mol. ratio	
ilmenite	97.85
Fe_2O_3	86.04
$MnTiO_3$	11.77
$MgTiO_3$	0.04
Hematite	2.15
remarks	+MG

Table 8–3. Chemical compositions of ilmenite from granodiorite.

specimen	90043006	90043006	90050505	90050505	90082513
grain	1	1	1	1	1
position	1	2	1	2	1
SiO_2	0.05	0.05	0.11	0.04	0.04
TiO_2	53.04	53.13	5.32	52.09	50.59
Al_2O_3	0.00	0.01	0.49	0.03	0.01
FeO	43.01	42.33	85.59	43.92	43.82
MnO	3.03	3.18	0.62	4.28	5.08
MgO	0.01	0.02	0.02	0.02	0.02
CaO	0.04	0.04	0.08	0.05	0.08
Na_2O	0.01	0.00	0.01	0.02	0.00
K_2O	0.05	0.05	0.04	0.02	0.04
Total	99.23	98.80	92.29	100.47	99.69
recalculated					
Fe_2O_3	–	–	90.65	1.69	4.03
FeO	44.56	44.47	4.03	42.40	40.42
Total	99.00	98.52	101.32	100.60	100.05
mol. ratio					
ilmenite	101.64	102.28	10.43	98.37	96.15
Fe_2O_3	95.05	95.30	8.96	89.15	85.16
$MnTiO_3$	6.54	6.90	1.40	9.12	10.91
$MgTiO_3$	0.05	0.08	0.07	0.09	0.09
Hematite	–	–	89.57	1.63	3.85
remarks			+MG	+MG	

(Table 8–3. continued)

specimen	90082513	90082513	90082513	90102202	90102202
grain	1	2	2	1	1
position	2	1	2	1	2
SiO_2	0.04	0.04	0.05	0.04	0.03
TiO_2	50.34	50.83	50.69	50.88	50.90
Al_2O_3	0.02	0.00	0.01	0.01	0.01
FeO	43.75	43.51	43.53	45.01	45.03
MnO	5.29	4.90	4.85	4.25	4.40
MgO	0.03	0.05	0.05	0.06	0.05
CaO	0.07	0.08	0.07	0.06	0.06
Na_2O	0.00	0.00	0.00	0.01	0.00
K_2O	0.03	0.04	0.03	0.05	0.05
Total	99.57	99.46	99.28	100.36	100.54
recalculated					
Fe_2O_3	4.43	3.30	3.37	4.17	4.32
FeO	39.77	40.54	40.50	41.25	41.14
Total	99.98	99.75	99.59	100.73	100.92
mol. ratio					
ilmenite	95.76	96.85	96.76	96.05	95.91
Fe_2O_3	84.30	86.12	86.14	86.77	86.36
$MnTiO_3$	11.36	10.55	10.45	9.06	9.35
$MgTiO_3$	0.11	0.19	0.17	0.22	0.20
Hematite	4.24	3.15	3.24	3.95	4.09
remarks					

(Table 8–3. continued)

specimen	90102401
grain	1
position	2
SiO_2	0.10
TiO_2	51.88
Al_2O_3	0.04
FeO	41.65
MnO	6.03
MgO	0.04
CaO	0.10
Na_2O	0.00
K_2O	0.05
Total	99.89
recalculated	
Fe_2O_3	1.45
FeO	40.34
Total	99.98
mol. ratio	
ilmenite	98.55
Fe_2O_3	85.48
$MnTiO_3$	12.94
$MgTiO_3$	0.14
Hematite	1.45
remarks	+MG

Table 8–4. Chemical compositions of ilmenite from porphyritic granite.

specimen	87052806	87052806	87062801	87062801
grain	1	1	1	1
position	1	2	1	2
SiO_2	0.02	0.06	0.01	0.00
TiO_2	51.65	51.19	50.95	50.87
Al_2O_3	0.02	0.68	0.00	0.01
FeO	40.40	39.90	23.91	23.49
MnO	6.80	6.53	23.22	23.32
MgO	0.01	0.01	0.03	0.02
CaO	0.09	0.05	0.04	0.04
Na_2O	0.01	0.04	0.01	0.01
K_2O	0.04	0.01	0.02	0.04
Total	99.04	98.47	98.19	97.80
recalculated				
Fe_2O_3	1.09	0.63	1.91	1.62
FeO	39.42	39.33	22.19	22.04
Total	99.10	98.48	98.35	97.91
mol. ratio				
ilmenite	98.93	98.37	98.16	98.42
Fe_2O_3	84.18	84.18	47.60	47.47
$MnTiO_3$	14.71	14.15	50.44	50.87
$MgTiO_3$	0.04	0.04	0.11	0.08
Hematite	1.07	1.63	1.84	1.58
remarks				

Table 8–5. Chemical compositions of ilmenite from granite.

specimen	87122502	87122502	87122502
grain	1	1	1
position	1	2	3
SiO_2	0.00	0.00	0.01
TiO_2	50.61	50.45	50.55
Al_2O_3	0.01	0.01	0.00
FeO	43.63	43.51	43.62
MnO	4.08	4.07	4.21
MgO	0.05	0.04	0.03
CaO	0.01	0.01	0.06
Na_2O	0.02	0.00	0.01
K_2O	0.00	0.00	0.00
Total	98.41	98.09	98.49
recalculated			
Fe_2O_3	2.62	2.62	2.85
FeO	41.27	41.16	41.06
Total	98.65	98.35	98.77
mol. ratio			
ilmenite	97.46	97.46	97.26
Fe_2O_3	88.42	88.44	88.00
$MnTiO_3$	8.85	8.86	9.14
$MgTiO_3$	0.19	0.15	0.11
Hematite	2.54	2.54	2.74
remarks			

Table 8–6. Chemical compositions of ilmenite from rhyolite.

specimen	86120106	86120106
grain	1	1
position	1	2
SiO_2	4.23	8.41
TiO_2	48.28	47.37
Al_2O_3	3.46	0.24
FeO	39.98	38.83
MnO	3.85	3.96
MgO	0.02	0.01
CaO	0.05	0.10
Na_2O	0.04	0.00
K_2O	0.03	0.01
Total	99.94	98.93
recalculated		
Fe_2O_3	0.63	0.44
FeO	39.41	38.44
Total	99.93	98.96
mol. ratio		
ilmenite	94.10	99.15
Fe_2O_3	85.56	89.74
$MnTiO_3$	8.46	9.36
$MgTiO_3$	0.08	0.04
Hematite	5.90	0.85
remarks		

Table 8–7. Chemical compositions of magnetite from dark inclusion.

specimen	90050503	90050503	90102206	90102206	90102206
grain	1	1	2	3	3
position	1	2	1	1(C)	2(R)
SiO_2	0.17	0.10	0.06	0.06	0.09
TiO_2	5.38	5.02	0.62	0.79	0.34
Al_2O_3	0.25	0.12	0.09	0.08	0.09
FeO	85.69	86.35	91.13	91.10	91.31
MnO	1.05	0.94	0.16	0.22	0.08
MgO	0.05	0.00	0.00	0.00	0.00
CaO	0.06	0.06	0.05	0.08	0.10
Na_2O	0.00	0.00	0.00	0.00	0.00
K_2O	0.06	0.06	0.01	0.01	0.01
Total	92.70	92.64	92.12	92.34	92.02
recalculated					
Fe2O3	57.10	57.99	66.81	66.64	67.31
FeO	34.31	34.17	31.01	31.13	30.75
Total	98.36	98.40	98.80	99.01	98.75
mol. ratio					
USP	5.24	4.90	0.61	0.77	0.33
SP	94.76	95.10	99.39	99.23	99.67

Table 8–8. Chemical compositions of magnetite from granodiorite.

specimen	90050505	90050505	90102209	90102209	90102209
grain	2	2	1	1	2
position	1	2	1	2	1
SiO_2	0.10	0.11	0.08	0.09	0.16
TiO_2	4.55	5.35	1.65	1.91	1.52
Al_2O_3	0.18	0.50	0.19	0.17	0.13
FeO	87.15	86.69	91.37	90.07	90.96
MnO	0.54	0.54	0.36	0.45	0.32
MgO	0.01	0.02	0.01	0.02	0.04
CaO	0.07	0.06	0.08	0.08	0.06
Na_2O	0.01	0.01	0.00	0.00	0.00
K_2O	0.05	0.04	0.06	0.07	0.06
Total	92.65	93.32	93.79	92.87	93.24
recalculated					
Fe2O3	58.90	57.33	65.76	64.53	65.64
FeO	34.15	35.11	32.20	32.00	31.90
Total	98.49	99.01	100.32	99.27	99.76
mol. ratio					
USP	4.43	5.17	1.58	1.85	1.47
SP	95.57	94.83	98.42	98.15	98.53

(Table 8–8. continued)

specimen	90102209	90102401
grain	2	1
position	2	1
SiO_2	0.09	0.29
TiO_2	3.11	6.82
Al_2O_3	0.17	0.24
FeO	88.35	84.92
MnO	0.47	0.95
MgO	0.02	0.07
CaO	0.07	0.08
Na_2O	0.00	0.00
K_2O	0.07	0.07
Total	92.35	93.43
recalculated		
Fe2O3	61.68	54.60
FeO	32.85	35.80
Total	98.46	98.84
mol. ratio		
USP	3.04	6.60
SP	96.96	93.40

Table 8–9. Chemical compositions of magnetite from granite.

specimen	87122210	87122210
grain	1	1
position	1	2
SiO_2	0.08	0.08
TiO_2	0.41	0.40
Al_2O_3	0.33	0.28
FeO	90.13	89.31
MnO	0.08	0.04
MgO	0.01	0.00
CaO	0.06	0.06
Na_2O	0.00	0.00
K_2O	0.01	0.03
Total	91.11	90.20
recalculated		
Fe2O3	66.19	65.58
FeO	30.57	30.30
Total	97.73	96.74
mol. ratio		
USP	0.40	0.40
SP	99.60	99.60

Table. 9. Chemical compositions of plagioclase. (oxygen=32)

F in remarks: fine-grained, C in remarks: coarse-grained

Table 9-1. Chemical compositions of plagioclase from the tonalite.

specimen	86081005	86081005	86081005	86081005	86081005
grain	1	1	1	1	2
position	1(C)	2(M)	3(M)	4(R)	1(C)
SiO_2	52.23	48.31	52.68	54.57	52.71
TiO_2	0.03	0.05	0.04	0.00	0.02
Al_2O_3	29.87	32.53	29.59	28.31	29.80
FeO	0.25	0.34	0.22	0.26	0.25
MnO	0.02	0.02	0.02	0.04	0.01
MgO	0.02	0.01	0.01	0.01	0.01
CaO	11.83	15.81	12.67	10.89	12.36
Na_2O	4.27	2.50	4.24	5.22	4.35
K_2O	0.24	0.10	0.23	0.23	0.23
Total	98.75	99.68	99.69	99.53	99.73
Si	9.578	8.888	9.593	9.904	9.586
Ti	0.004	0.007	0.005	0.000	0.003
Al	6.454	7.052	6.348	6.055	6.387
Fe	0.039	0.053	0.034	0.039	0.038
Mn	0.004	0.004	0.002	0.005	0.001
Mg	0.005	0.003	0.003	0.003	0.002
Ca	2.323	3.115	2.470	2.117	2.407
Na	1.516	0.892	1.495	1.837	1.534
K	0.055	0.024	0.053	0.052	0.053
Total	19.977	20.037	20.002	20.013	20.011
Ab	38.46	21.80	36.85	45.32	38.02
An	60.15	77.61	61.84	53.39	60.67
Or	1.40	0.59	1.31	1.28	1.31
remarks	C	C	C	C	F

An analyzed position of each grain is presented as the following abbreviations.

C:core, M:mantle, R:rim

(Plate 9–1 continued)

specimen	86081005	86081005	86090708	86090708	86090708
grain	2	2	1	1	1
position	2(M)	3(R)	1(C)	2(M)	3(R)
SiO_2	52.94	53.78	58.12	47.29	52.79
TiO_2	0.08	0.02	0.00	0.00	0.00
Al_2O_3	29.39	28.71	25.83	32.99	29.33
FeO	0.49	0.26	0.17	0.27	0.29
MnO	0.01	0.01	0.00	0.00	0.00
MgO	0.01	0.01	0.00	0.00	0.01
CaO	12.32	11.31	7.60	15.82	11.71
Na_2O	4.23	4.75	7.04	2.28	4.67
K_2O	0.23	0.24	0.14	0.06	0.19
Total	99.72	99.08	98.90	98.70	99.00
Si	9.635	9.810	10.503	8.783	9.660
Ti	0.011	0.002	0.000	0.000	0.000
Al	6.303	6.170	5.499	7.219	6.325
Fe	0.074	0.039	0.026	0.041	0.044
Mn	0.002	0.001	0.000	0.000	0.000
Mg	0.004	0.004	0.000	0.000	0.001
Ca	2.401	2.209	1.471	3.147	2.295
Na	1.491	1.678	2.466	0.821	1.657
K	0.054	0.056	0.031	0.015	0.044
Total	19.975	19.969	19.996	20.025	20.028
Ab	37.03	42.09	61.74	20.40	41.00
An	61.62	56.51	37.48	79.22	57.91
Or	1.34	1.40	0.78	0.37	1.09
remarks	F	F	C	C	C

(Plate 9–1 continued)

specimen	86121702	86121702	86121702	86121702	86121702
grain	1	1	1	2	2
position	1(C)	2(M)	3(R)	1(C)	2(M)
SiO_2	45.41	43.81	49.76	43.18	43.30
TiO_2	0.00	0.03	0.03	0.05	0.00
Al_2O_3	35.40	37.48	32.68	36.78	36.51
FeO	0.28	0.28	0.23	0.20	0.24
MnO	0.00	0.00	0.00	0.00	0.00
MgO	0.00	0.01	0.02	0.00	0.01
CaO	15.47	13.88	11.03	17.92	17.74
Na_2O	2.10	2.47	4.37	0.93	1.05
K_2O	0.10	0.15	0.32	0.06	0.04
Total	98.76	98.11	98.44	99.12	98.89
Si	8.434	8.174	9.162	8.046	8.085
Ti	0.000	0.004	0.004	0.007	0.000
Al	7.748	8.240	7.090	8.075	8.032
Fe	0.043	0.044	0.035	0.031	0.037
Mn	0.000	0.000	0.000	0.000	0.000
Mg	0.000	0.003	0.005	0.000	0.003
Ca	3.077	2.773	2.175	3.576	3.547
Na	0.756	0.893	1.559	0.336	0.380
K	0.024	0.036	0.075	0.014	0.010
Total	20.082	20.166	20.106	20.085	20.094
Ab	19.38	23.82	40.50	8.49	9.55
An	80.00	75.22	57.55	91.15	90.19
Or	0.62	0.96	1.95	0.35	0.25
remarks	C	C	C	C	C

(Plate 9–1 continued)

specimen	86121702	86121704	86121704	86121704	86121704
grain	2	1	1	1	2
position	3(R)	1(C)	2(M)	3(R)	1(C)
SiO_2	49.58	48.39	56.06	58.07	55.91
TiO_2	0.02	0.02	0.00	0.00	0.02
Al_2O_3	33.28	32.41	27.44	26.14	27.80
FeO	0.19	0.29	0.32	0.24	0.29
MnO	0.00	0.00	0.01	0.00	0.00
MgO	0.01	0.01	0.00	0.00	0.02
CaO	10.51	15.94	10.23	8.49	10.14
Na_2O	4.41	2.44	5.67	6.67	5.52
K_2O	0.29	0.06	0.20	0.18	0.24
Total	98.29	99.56	99.93	99.80	99.94
Si	9.123	8.908	10.108	10.427	10.073
Ti	0.003	0.003	0.000	0.000	0.002
Al	7.216	7.030	5.830	5.531	5.903
Fe	0.029	0.045	0.047	0.036	0.043
Mn	0.000	0.000	0.001	0.000	0.000
Mg	0.003	0.002	0.001	0.000	0.005
Ca	2.071	3.143	1.974	1.633	1.956
Na	1.572	0.872	1.982	2.320	1.928
K	0.068	0.014	0.046	0.040	0.055
Total	20.086	20.017	19.990	19.988	19.965
Ab	42.00	21.39	48.93	57.58	48.36
An	56.18	78.26	49.94	41.42	50.26
Or	1.82	0.34	1.14	0.99	1.38
remarks	C	F	F	F	C

(Plate 9–1 continued)

specimen	86121704	86121704	86121704	86121705	86121705
grain	2	2	2	1	1
position	2(M)	3(M)	4(R)	1(C)	2(M)
SiO_2	45.22	49.51	60.63	49.11	53.30
TiO_2	0.01	0.02	0.00	0.04	0.04
Al_2O_3	34.74	31.77	24.58	31.93	29.03
FeO	0.38	0.47	0.11	0.35	0.26
MnO	0.00	0.00	0.00	0.00	0.02
MgO	0.04	0.04	0.00	0.02	0.03
CaO	18.94	14.87	6.29	15.49	12.05
Na_2O	0.86	2.84	7.86	2.67	4.54
K_2O	0.01	0.14	0.26	0.11	0.26
Total	100.22	99.66	99.73	99.72	99.53
Si	8.345	9.084	10.820	9.017	9.706
Ti	0.001	0.003	0.000	0.006	0.005
Al	7.555	6.869	5.168	6.908	6.229
Fe	0.059	0.072	0.017	0.054	0.040
Mn	0.000	0.000	0.000	0.000	0.003
Mg	0.011	0.010	0.001	0.005	0.008
Ca	3.751	2.921	1.203	3.046	2.350
Na	0.306	1.010	2.717	0.950	1.602
K	0.002	0.032	0.058	0.026	0.060
Total	20.030	20.000	19.984	20.011	20.005
Ab	7.41	24.97	67.99	23.28	39.43
An	92.54	74.24	30.56	76.08	59.09
Or	0.05	0.79	1.45	0.64	1.48
remarks	C	C	C	C	C

(Plate 9–1 continued)

specimen	86121705	86121705	86121705	86121705	86121705
grain	1	2	2	2	3
position	3(R)	1(C)	2(M)	3(R)	1(C)
SiO_2	55.15	48.88	49.83	55.42	48.64
TiO_2	0.00	0.03	0.03	0.01	0.00
Al_2O_3	27.95	32.19	31.62	27.56	32.39
FeO	0.28	0.27	0.31	0.25	0.26
MnO	0.04	0.02	0.00	0.00	0.00
MgO	0.02	0.01	0.03	0.02	0.01
CaO	10.76	15.66	14.89	9.90	16.05
Na_2O	5.11	2.78	2.76	5.61	2.50
K_2O	0.32	0.11	0.14	0.35	0.09
Total	99.63	99.95	99.61	99.12	99.94
Si	9.989	8.964	9.132	10.073	8.923
Ti	0.000	0.004	0.004	0.001	0.000
Al	5.965	6.956	6.828	5.902	7.002
Fe	0.042	0.041	0.047	0.038	0.040
Mn	0.006	0.003	0.000	0.000	0.000
Mg	0.005	0.003	0.008	0.005	0.003
Ca	2.087	3.076	2.923	1.927	3.153
Na	1.793	0.988	0.980	1.976	0.889
K	0.074	0.026	0.033	0.081	0.021
Total	19.962	20.061	19.956	20.003	20.031
Ab	44.75	23.88	24.56	49.07	21.65
An	53.41	75.49	74.62	48.92	77.84
Or	1.85	0.63	0.83	2.01	0.51
remarks	C	C	C	C	C

(Plate 9–1 continued)

specimen	86121705	86122405	86122405	86122405	86122405
grain	3	1	1	1	2
position	2(C)	1(C)	2(M)	3(R)	1(C)
SiO_2	49.21	48.44	47.02	54.50	47.54
TiO_2	0.00	0.01	0.02	0.01	0.01
Al_2O_3	32.38	32.54	33.56	28.91	33.45
FeO	0.39	0.39	0.40	0.40	0.37
MnO	0.00	0.00	0.00	0.00	0.00
MgO	0.00	0.02	0.01	0.02	0.02
CaO	15.70	16.55	17.69	11.88	17.35
Na_2O	2.56	2.14	1.49	4.73	1.79
K_2O	0.09	0.07	0.04	0.12	0.04
Total	100.33	100.16	100.22	100.56	100.56
Si	8.981	8.877	8.641	9.806	8.699
Ti	0.000	0.002	0.002	0.001	0.002
Al	6.964	7.027	7.266	6.130	7.211
Fe	0.060	0.060	0.061	0.060	0.056
Mn	0.000	0.000	0.000	0.000	0.000
Mg	0.000	0.004	0.003	0.004	0.005
Ca	3.069	3.248	3.481	2.290	3.399
Na	0.905	0.761	0.529	1.647	0.635
K	0.021	0.016	0.009	0.027	0.009
Total	20.000	19.996	19.992	19.966	20.016
Ab	22.32	18.61	12.96	40.89	15.47
An	77.16	81.00	86.82	58.44	84.31
Or	0.52	0.39	0.22	0.67	0.22
remarks	C	F	F	F	C

(Plate 9–1 continued)

specimen	86122405	86122405	86122405
grain	2	2	2
position	2(M)	3(R)	4(R)
SiO_2	47.91	46.84	53.98
TiO_2	0.05	0.03	0.02
Al_2O_3	33.06	33.70	29.22
FeO	0.34	0.41	0.33
MnO	0.00	0.00	0.00
MgO	0.00	0.01	0.02
CaO	16.67	17.56	12.01
Na_2O	2.10	1.60	4.65
K_2O	0.07	0.04	0.18
Total	100.20	100.19	100.40
Si	8.783	8.612	9.736
Ti	0.007	0.004	0.003
Al	7.141	7.302	6.210
Fe	0.052	0.063	0.050
Mn	0.000	0.000	0.000
Mg	0.001	0.003	0.005
Ca	3.274	3.459	2.320
Na	0.745	0.570	1.624
K	0.016	0.010	0.041
Total	20.020	20.023	19.989
Ab	18.22	13.89	40.20
An	81.38	85.87	58.79
Or	0.39	0.24	1.01
remarks	C	C	C

Plate 9–2. Chemical compositions of plagioclase from the dark inclusion.

specimen	60111806	60111806	60111806	60111806	60111806
grain	1	1	1	1	2
position	1(C)	2(M)	3(R)	4(VEIN)	1(C)
SiO_2	44.65	48.23	54.93	61.49	55.52
TiO_2	0.00	0.01	0.00	0.00	0.00
Al_2O_3	34.34	32.02	27.44	23.25	27.21
FeO	0.30	0.41	0.10	0.08	0.14
MnO	0.00	0.01	0.01	0.00	0.00
MgO	0.06	0.02	0.00	0.00	0.00
CaO	18.19	15.02	9.39	4.48	9.37
Na_2O	1.11	2.66	5.96	8.89	6.14
K_2O	0.03	0.06	0.12	0.20	0.12
Total	98.68	98.43	97.95	98.39	98.50
Si	8.359	8.965	10.081	11.075	10.134
Ti	0.000	0.002	0.000	0.000	0.000
Al	7.577	7.013	5.934	4.933	5.853
Fe	0.047	0.064	0.016	0.012	0.021
Mn	0.000	0.002	0.002	0.000	0.000
Mg	0.016	0.005	0.001	0.000	0.000
Ca	3.648	2.990	1.845	0.865	1.831
Na	0.402	0.957	2.120	3.103	2.171
K	0.007	0.013	0.028	0.045	0.027
Total	20.056	20.012	20.026	20.033	20.038
Ab	9.76	23.74	52.84	77.09	53.60
An	90.07	75.94	46.46	21.79	45.73
Or	0.17	0.32	0.70	1.12	0.67
remarks	C	C	C	C	F

(Plate 9–2 continued)

specimen	60111806	60111806	60120506	60120506	60120506
grain	2	2	1	1	1
position	2(M)	3(R)	1(C)	2(C)	3(M)
SiO_2	51.06	56.64	47.78	51.63	59.93
TiO_2	0.04	0.00	0.01	0.01	0.00
Al_2O_3	30.33	26.80	33.43	30.27	24.76
FeO	0.39	0.17	0.20	0.14	0.11
MnO	0.00	0.00	0.00	0.00	0.02
MgO	0.00	0.00	0.00	0.00	0.00
CaO	13.14	8.39	15.72	13.56	6.65
Na_2O	3.95	6.47	2.36	3.82	7.45
K_2O	0.08	0.16	0.05	0.09	0.34
Total	98.99	98.64	99.54	99.52	99.26
Si	9.387	10.289	8.788	9.431	10.757
Ti	0.005	0.000	0.002	0.002	0.000
Al	6.570	5.737	7.244	6.515	5.236
Fe	0.060	0.026	0.030	0.022	0.016
Mn	0.000	0.000	0.000	0.000	0.002
Mg	0.000	0.000	0.001	0.000	0.000
Ca	2.587	1.632	3.096	2.653	1.279
Na	1.407	2.277	0.842	1.352	2.591
K	0.019	0.037	0.011	0.020	0.078
Total	20.035	19.999	20.014	19.995	19.960
Ab	34.54	57.33	21.16	33.41	65.33
An	64.99	41.74	78.57	66.10	32.70
Or	0.47	0.93	0.28	0.49	1.97
remarks	F	F	C	C	C

(Plate 9–2 continued)

specimen	60120506	60120506	60120506	60120506	60120506
grain	1	2	2	2	3
position	4(R)	1(C)	2(M)	3(R)	1(C)
SiO_2	60.21	53.98	54.05	65.36	56.08
TiO_2	0.00	0.04	0.01	0.00	0.00
Al_2O_3	25.02	28.71	29.26	21.26	27.27
FeO	0.09	0.25	0.12	0.10	0.24
MnO	0.00	0.02	0.03	0.00	0.01
MgO	0.00	0.01	0.00	0.00	0.00
CaO	6.75	11.43	11.05	3.70	9.30
Na_2O	7.58	5.00	5.21	8.43	6.18
K_2O	0.27	0.15	0.12	0.34	0.17
Total	99.91	99.59	99.84	99.19	99.26
Si	10.736	9.804	9.777	11.573	10.159
Ti	0.000	0.006	0.001	0.000	0.000
Al	5.257	6.144	6.236	4.435	5.822
Fe	0.013	0.038	0.017	0.015	0.037
Mn	0.000	0.003	0.004	0.000	0.001
Mg	0.000	0.004	0.000	0.000	0.001
Ca	1.289	2.224	2.141	0.702	1.805
Na	2.619	1.760	1.826	2.893	2.170
K	0.060	0.035	0.027	0.077	0.039
Total	19.975	20.016	20.031	19.695	20.034
Ab	65.79	43.31	45.48	78.46	53.54
An	32.71	55.83	53.85	19.45	45.50
Or	1.51	0.86	0.67	2.09	0.96
remarks	C	F	F	F	F

(Plate 9–2 continued)

specimen	60120506	60120506	60120506	60120506	60120506
grain	3	4	4	4	5
position	2(M)	1(C)	2(M)	3(R)	1(C)
SiO_2	59.13	58.66	59.22	57.91	58.25
TiO_2	0.00	0.00	0.00	0.00	0.01
Al_2O_3	26.65	25.47	24.73	26.26	25.06
FeO	0.10	0.11	0.15	0.17	0.16
MnO	0.01	0.00	0.01	0.02	0.02
MgO	0.00	0.00	0.00	0.00	0.00
CaO	4.09	7.41	6.94	8.54	7.00
Na_2O	8.31	7.23	7.42	6.63	7.37
K_2O	0.33	0.26	0.32	0.17	0.33
Total	98.61	99.14	98.79	99.69	98.19
Si	10.624	10.573	10.700	10.407	10.603
Ti	0.000	0.000	0.000	0.000	0.001
Al	5.643	5.410	5.265	5.560	5.374
Fe	0.015	0.016	0.022	0.026	0.025
Mn	0.001	0.000	0.001	0.003	0.003
Mg	0.000	0.000	0.000	0.000	0.000
Ca	0.786	1.430	1.343	1.644	1.364
Na	2.893	2.526	2.596	2.307	2.600
K	0.076	0.060	0.074	0.038	0.075
Total	20.039	20.015	20.002	19.985	20.046
Ab	76.72	62.65	64.32	57.42	63.93
An	21.27	35.86	33.85	41.64	34.23
Or	2.02	1.49	1.83	0.95	1.84
remarks	F	C	C	C	C

(Plate 9–2 continued)

specimen	60120506	60120506	90050503	90050503	90050503
grain	5	5	1	1	2
position	2(M)	3(R)	1(C)	2(R)	1(C)
SiO_2	58.34	54.09	57.76	59.94	58.02
TiO_2	0.00	0.00	0.00	0.00	0.02
Al_2O_3	25.19	28.49	26.21	24.69	26.10
FeO	0.14	0.06	0.00	0.00	0.00
MnO	0.00	0.02	0.00	0.00	0.00
MgO	0.00	0.00	0.00	0.00	0.00
CaO	7.23	10.54	7.81	6.46	8.01
Na_2O	7.26	5.41	6.90	7.83	6.86
K_2O	0.24	0.13	0.20	0.20	0.28
Total	98.40	98.74	98.88	99.12	99.29
Si	10.592	9.878	10.441	10.766	10.454
Ti	0.000	0.000	0.000	0.000	0.002
Al	5.388	6.132	5.583	5.227	5.541
Fe	0.021	0.009	0.000	0.000	0.000
Mn	0.000	0.003	0.000	0.000	0.000
Mg	0.001	0.000	0.000	0.000	0.000
Ca	1.405	2.061	1.512	1.244	1.545
Na	2.555	1.916	2.418	2.725	2.396
K	0.056	0.031	0.046	0.045	0.064
Total	20.019	20.029	19.999	20.006	20.003
Ab	63.27	47.66	60.81	67.89	59.83
An	35.34	51.57	38.03	30.99	38.58
Or	1.39	0.77	1.16	1.12	1.60
remarks	C	C	F	F	C

(Plate 9–2 continued)

specimen	90050503	90050503	9005055A	9005055A	9005055A
grain	2	2	1	1	1
position	2(M)	3(R)	1(C)	2(M)	3(R)
SiO_2	58.81	62.25	52.23	48.76	53.68
TiO_2	0.00	0.00	0.03	0.02	0.01
Al_2O_3	25.47	22.98	32.06	35.77	31.50
FeO	0.00	0.00	0.15	0.16	0.16
MnO	0.00	0.00	0.00	0.00	0.00
MgO	0.00	0.00	0.01	0.00	0.00
CaO	7.25	4.12	6.47	6.21	3.42
Na_2O	7.02	9.00	6.34	5.83	7.69
K_2O	0.28	0.21	0.25	0.21	0.28
Total	98.84	98.56	97.54	96.95	96.74
Si	10.609	11.166	9.576	9.002	9.845
Ti	0.000	0.001	0.004	0.002	0.002
Al	5.415	4.858	6.925	7.781	6.807
Fe	0.000	0.000	0.022	0.025	0.024
Mn	0.000	0.000	0.000	0.000	0.000
Mg	0.000	0.000	0.003	0.000	0.000
Ca	1.400	0.791	1.271	1.227	0.672
Na	2.454	3.128	2.254	2.085	2.734
K	0.065	0.049	0.059	0.049	0.065
Total	19.943	19.992	20.114	20.172	20.149
Ab	62.62	78.83	62.45	61.58	78.23
An	35.72	19.93	35.91	36.98	19.91
Or	1.66	1.23	1.63	1.45	1.86
remarks	C	C	C	C	C

(Plate 9–2 continued)

specimen	9005055A	9005055A	9005055A	9005055A	9005055A
grain	2	2	2	3	3
position	1(C)	2(M)	3(R)	1(C)	2(R)
SiO_2	52.26	53.67	51.36	52.46	64.09
TiO_2	0.03	0.05	0.04	0.04	0.02
Al_2O_3	31.35	30.30	34.21	30.89	22.10
FeO	0.16	0.11	0.16	0.12	0.23
MnO	0.00	0.00	0.00	0.00	0.00
MgO	0.00	0.00	0.00	0.00	0.00
CaO	6.92	7.04	3.06	7.28	2.74
Na_2O	6.23	6.44	7.62	6.18	9.83
K_2O	0.15	0.14	0.23	0.15	0.15
Total	97.10	97.76	96.67	97.12	99.15
Si	9.631	9.817	9.435	9.672	11.393
Ti	0.004	0.007	0.005	0.006	0.003
Al	6.807	6.531	7.405	6.711	4.628
Fe	0.025	0.017	0.025	0.018	0.034
Mn	0.000	0.000	0.000	0.000	0.000
Mg	0.001	0.001	0.001	0.001	0.000
Ca	1.366	1.380	0.602	1.437	0.521
Na	2.223	2.282	2.712	2.207	3.387
K	0.035	0.032	0.055	0.034	0.033
Total	20.091	20.067	20.240	20.086	20.000
Ab	60.90	61.48	79.88	59.70	85.21
An	38.14	37.66	18.50	39.38	13.96
Or	0.96	0.86	1.62	0.92	0.83
remarks	F	F	F	F	F

(Plate 9–2 continued)

specimen	9005055A	9005055A	90102206	90102206	90102408D
grain	4	4	1	1	1
position	1(C)	2(R)	1(C)	2(M)	1(C)
SiO_2	58.14	63.21	61.27	58.90	59.76
TiO_2	0.04	0.02	0.00	0.00	0.00
Al_2O_3	26.08	22.33	24.18	25.60	24.90
FeO	0.13	0.14	0.18	0.15	0.14
MnO	0.00	0.00	0.00	0.00	0.04
MgO	0.00	0.00	0.00	0.00	0.00
CaO	7.58	3.36	5.68	7.42	6.97
Na_2O	7.16	9.45	8.04	7.27	7.29
K_2O	0.15	0.24	0.23	0.14	0.45
Total	99.28	98.74	99.58	99.47	99.55
Si	10.469	11.304	10.926	10.574	10.713
Ti	0.006	0.002	0.000	0.000	0.000
Al	5.535	4.705	5.081	5.415	5.260
Fe	0.019	0.021	0.026	0.022	0.021
Mn	0.000	0.000	0.000	0.000	0.006
Mg	0.001	0.001	0.000	0.000	0.000
Ca	1.461	0.643	1.084	1.426	1.338
Na	2.499	3.274	2.780	2.529	2.532
K	0.035	0.054	0.051	0.032	0.103
Total	20.025	20.005	19.949	19.999	19.974
Ab	62.24	81.99	70.54	63.08	63.30
An	36.89	16.65	28.17	36.12	34.13
Or	0.87	1.35	1.29	0.80	2.58
remarks	F	F	F	F	C

(Plate 9-2 continued)

specimen	90102408D	90102408D	90102408D	90102408D	90102408D
grain	1	1	2	2	3
position	2(M)	3(R)	1(C)	2(R)	1(C)
SiO_2	58.73	62.53	54.11	61.76	53.71
TiO_2	0.04	0.04	0.04	0.02	0.04
Al_2O_3	25.35	22.82	28.42	23.63	29.09
FeO	0.14	0.13	0.11	0.09	0.12
MnO	0.00	0.00	0.00	0.00	0.01
MgO	0.00	0.01	0.01	0.00	0.01
CaO	7.29	4.33	10.96	5.04	11.89
Na_2O	7.09	8.72	5.19	8.54	4.79
K_2O	0.43	0.36	0.15	0.19	0.12
Total	99.07	98.94	98.99	99.27	99.78
Si	10.594	11.185	9.867	11.030	9.739
Ti	0.005	0.005	0.005	0.003	0.005
Al	5.388	4.810	6.107	4.973	6.216
Fe	0.021	0.019	0.017	0.013	0.018
Mn	0.000	0.000	0.000	0.000	0.002
Mg	0.000	0.003	0.003	0.000	0.003
Ca	1.408	0.830	2.140	0.964	2.309
Na	2.478	3.022	1.834	2.955	1.683
K	0.099	0.082	0.035	0.043	0.028
Total	19.995	19.957	20.008	19.981	20.003
Ab	61.86	76.39	45.52	74.34	41.63
An	35.67	21.54	53.61	24.58	57.68
Or	2.47	2.07	0.87	1.08	0.69
remarks	C	C	F	F	F

(Plate 9–2 continued)

specimen	90102408D	90102408D	90102408D
grain	3	4	4
position	2(R)	1(C)	2(R)
SiO_2	56.96	54.57	62.23
TiO_2	0.02	0.04	0.01
Al_2O_3	26.87	28.34	23.23
FeO	0.15	0.14	0.16
MnO	0.00	0.00	0.00
MgO	0.01	0.00	0.00
CaO	9.11	10.91	4.71
Na_2O	6.25	5.40	8.76
K_2O	0.14	0.16	0.32
Total	99.51	99.56	99.42
Si	10.270	9.898	11.100
Ti	0.003	0.005	0.001
Al	5.709	6.057	4.882
Fe	0.023	0.021	0.024
Mn	0.000	0.000	0.000
Mg	0.003	0.000	0.000
Ca	1.759	2.119	0.900
Na	2.184	1.898	3.028
K	0.032	0.037	0.073
Total	19.981	20.036	20.008
Ab	54.59	46.58	75.23
An	44.61	52.52	22.96
Or	0.80	0.91	1.81
remarks	F	F	F

Plate 9–3. Chemical compositions of plagioclase from granodiorite.

specimen	90032511A	90032511A	90032511A	90043006	90043006
grain	1	1	1	1	1
position	1(C)	2(M)	3(R)	1(C)	2(M)
SiO_2	57.34	58.72	61.42	61.10	59.48
TiO_2	0.00	0.00	0.00	0.03	0.04
Al_2O_3	26.58	25.34	23.57	24.12	25.19
FeO	0.15	0.10	0.15	0.13	0.14
MnO	0.00	0.00	0.00	0.00	0.00
MgO	0.01	0.00	0.00	0.01	0.00
CaO	8.41	6.92	4.71	5.61	6.79
Na_2O	6.71	7.20	8.59	8.03	7.52
K_2O	0.22	0.22	0.21	0.30	0.23
Total	99.40	98.49	98.65	99.33	99.38
Si	10.341	10.626	11.034	10.924	10.671
Ti	0.000	0.000	0.000	0.004	0.005
Al	5.648	5.403	4.989	5.082	5.325
Fe	0.022	0.015	0.023	0.020	0.021
Mn	0.000	0.000	0.001	0.000	0.000
Mg	0.001	0.000	0.000	0.001	0.001
Ca	1.625	1.341	0.906	1.075	1.304
Na	2.344	2.525	2.989	2.782	2.615
K	0.049	0.051	0.048	0.067	0.053
Total	20.031	19.961	19.990	19.955	19.996
Ab	58.01	64.22	75.35	70.52	65.47
An	40.78	34.49	23.44	27.78	33.20
Or	1.21	1.30	1.21	1.70	1.33
remarks	F	F	F	C	C

(Plate 9–3 continued)

specimen	90043006	90043006	90043006	90043006	90050505
grain	1	2	2	2	1
position	3(R)	1(C)	2(M)	3(R)	1(C)
SiO_2	63.48	58.98	62.33	63.10	58.09
TiO_2	0.02	0.05	0.02	0.02	0.00
Al_2O_3	22.66	24.93	23.19	22.29	26.23
FeO	0.08	0.11	0.16	0.13	0.00
MnO	0.00	0.00	0.00	0.00	0.00
MgO	0.00	0.00	0.00	0.00	0.00
CaO	3.66	6.53	4.26	3.41	8.16
Na_2O	9.23	7.66	8.90	9.34	6.76
K_2O	0.41	0.20	0.30	0.38	0.32
Total	99.55	98.44	99.15	98.66	99.55
Si	11.270	10.680	11.131	11.301	10.441
Ti	0.002	0.007	0.003	0.002	0.000
Al	4.741	5.319	4.881	4.705	5.556
Fe	0.012	0.017	0.023	0.019	0.000
Mn	0.000	0.000	0.000	0.000	0.000
Mg	0.000	0.000	0.000	0.000	0.001
Ca	0.697	1.266	0.815	0.653	1.570
Na	3.176	2.686	3.079	3.243	2.355
K	0.092	0.045	0.068	0.086	0.072
Total	19.991	20.020	19.999	20.009	19.995
Ab	79.86	66.92	77.26	81.05	58.90
An	17.83	31.96	21.03	16.80	39.29
Or	2.31	1.12	1.71	2.15	1.80
remarks	C	F	F	F	C

(Plate 9–3 continued)

specimen	90050505	90050505	90050505	90050505	90050505
grain	1	1	1	2	2
position	2(M)	3(R)	4(R)	1(C)	2(R)
SiO_2	57.35	55.95	65.17	54.65	61.97
TiO_2	0.00	0.00	0.00	0.01	0.00
Al_2O_3	26.48	27.26	21.53	28.70	23.32
FeO	0.00	0.00	0.00	0.00	0.00
MnO	0.00	0.00	0.00	0.00	0.00
MgO	0.01	0.01	0.00	0.02	0.00
CaO	8.49	9.52	2.54	11.04	4.64
Na_2O	6.57	6.21	10.10	5.41	8.72
K_2O	0.29	0.17	0.31	0.10	0.24
Total	99.19	99.12	99.65	99.93	98.89
Si	10.359	10.150	11.516	9.869	11.095
Ti	0.000	0.000	0.000	0.001	0.000
Al	5.637	5.826	4.483	6.108	4.920
Fe	0.000	0.000	0.000	0.000	0.000
Mn	0.000	0.000	0.000	0.000	0.000
Mg	0.003	0.001	0.000	0.005	0.000
Ca	1.642	1.850	0.481	2.136	0.890
Na	2.299	2.183	3.456	1.894	3.024
K	0.067	0.038	0.069	0.023	0.055
Total	20.006	20.048	20.005	20.035	19.984
Ab	57.32	53.61	86.27	46.67	76.19
An	41.01	45.46	12.01	52.76	22.42
Or	1.67	0.93	1.72	0.57	1.39
remarks	C	C	C	F	F

(Plate 9–3 continued)

specimen	90050505	90050505	90050505	90050505	90082401
grain	3	3	3	3	1
position	1(C)	2(M)	3(R)	4(R)	1(C)
SiO_2	46.49	58.44	57.58	61.03	61.64
TiO_2	0.05	0.01	0.01	0.00	0.00
Al_2O_3	33.77	25.85	26.22	24.08	23.45
FeO	0.00	0.00	0.00	0.00	0.16
MnO	0.00	0.00	0.00	0.00	0.00
MgO	0.01	0.00	0.01	0.00	0.00
CaO	17.59	7.37	8.24	5.34	4.65
Na_2O	1.33	7.19	6.91	8.33	8.44
K_2O	0.03	0.21	0.18	0.22	0.53
Total	99.28	99.07	99.14	99.00	98.87
Si	8.603	10.532	10.401	10.938	11.059
Ti	0.008	0.001	0.001	0.000	0.000
Al	7.364	5.488	5.581	5.085	4.958
Fe	0.000	0.000	0.000	0.000	0.024
Mn	0.000	0.000	0.000	0.000	0.000
Mg	0.003	0.000	0.002	0.000	0.000
Ca	3.487	1.423	1.594	1.025	0.893
Na	0.477	2.510	2.417	2.893	2.935
K	0.007	0.049	0.041	0.049	0.120
Total	19.949	20.003	20.037	19.991	19.989
Ab	12.00	63.03	59.62	72.93	73.89
An	87.82	35.74	39.37	25.84	23.09
Or	0.18	1.23	1.01	1.24	3.02
remarks	C	C	C	C	C

(Plate 9-3 continued)

specimen	90082401	90082401	90082401	90082401	90082401
grain	1	1	2	2	2
position	2(M)	3(R)	1(C)	2(M)	3(R)
SiO_2	57.91	61.60	61.31	57.50	61.71
TiO_2	0.00	0.00	0.00	0.00	0.00
Al_2O_3	25.89	23.35	23.79	26.20	23.34
FeO	0.21	0.13	0.25	0.20	0.12
MnO	0.01	0.00	0.02	0.00	0.01
MgO	0.00	0.00	0.01	0.00	0.00
CaO	7.56	4.72	5.02	8.04	4.82
Na_2O	6.98	8.67	8.38	6.90	8.59
K_2O	0.27	0.38	0.41	0.24	0.40
Total	98.83	98.85	99.19	99.10	98.99
Si	10.482	11.057	10.981	10.400	11.061
Ti	0.000	0.000	0.000	0.000	0.000
Al	5.521	4.939	5.021	5.583	4.930
Fe	0.032	0.020	0.038	0.031	0.018
Mn	0.001	0.000	0.002	0.000	0.001
Mg	0.001	0.000	0.002	0.000	0.000
Ca	1.466	0.907	0.963	1.558	0.925
Na	2.448	3.015	2.907	2.419	2.984
K	0.062	0.086	0.094	0.056	0.092
Total	20.013	20.024	20.009	20.046	20.012
Ab	61.05	74.85	72.57	59.52	74.23
An	37.41	23.01	25.09	39.10	23.48
Or	1.55	2.14	2.35	1.38	2.29
remarks	C	C	C	C	C

(Plate 9–3 continued)

specimen	90082401	90082401	90082401	90082513	90082513
grain	3	3	3	1	1
position	1(C)	2(M)	3(R)	1(C)	2(M)
SiO_2	50.64	57.29	63.08	58.54	59.75
TiO_2	0.00	0.00	0.00	0.04	0.04
Al_2O_3	30.94	26.16	22.73	25.94	24.91
FeO	0.23	0.18	0.13	0.15	0.17
MnO	0.00	0.00	0.00	0.00	0.00
MgO	0.00	0.00	0.00	0.00	0.00
CaO	13.50	7.52	3.72	7.50	5.95
Na_2O	3.74	6.96	9.25	7.23	7.91
K_2O	0.13	0.25	0.33	0.16	0.27
Total	99.17	98.36	99.24	99.55	99.00
Si	9.296	10.421	11.240	10.509	10.745
Ti	0.000	0.000	0.000	0.005	0.006
Al	6.692	5.607	4.772	5.487	5.280
Fe	0.036	0.028	0.020	0.022	0.025
Mn	0.000	0.000	0.000	0.000	0.000
Mg	0.000	0.000	0.000	0.001	0.000
Ca	2.654	1.465	0.709	1.443	1.146
Na	1.330	2.453	3.192	2.513	2.756
K	0.029	0.058	0.074	0.037	0.062
Total	20.037	20.031	20.008	20.018	20.019
Ab	32.85	61.26	79.90	62.57	69.09
An	66.44	37.29	18.25	36.50	29.36
Or	0.72	1.45	1.85	0.92	1.55
remarks	C	C	C	F	F

(Plate 9–3 continued)

specimen	90082513	90082513	90082513	90082513	90102202
grain	1	2	2	2	1
position	3(R)	1(C)	2(M)	3(R)	1(C)
SiO_2	62.64	58.22	58.48	62.74	59.16
TiO_2	0.03	0.02	0.04	0.05	0.00
Al_2O_3	22.83	25.22	25.34	22.44	24.99
FeO	0.14	0.20	0.18	0.00	0.21
MnO	0.00	0.00	0.00	0.00	0.00
MgO	0.00	0.01	0.01	0.00	0.00
CaO	3.48	6.66	6.92	3.30	6.81
Na_2O	9.30	7.29	7.37	9.56	7.21
K_2O	0.34	0.28	0.25	0.30	0.35
Total	98.74	97.91	98.58	98.38	98.73
Si	11.216	10.609	10.593	11.267	10.685
Ti	0.003	0.003	0.005	0.007	0.000
Al	4.815	5.414	5.407	4.747	5.319
Fe	0.021	0.031	0.027	0.000	0.031
Mn	0.000	0.000	0.000	0.000	0.000
Mg	0.000	0.002	0.001	0.000	0.000
Ca	0.667	1.301	1.342	0.635	1.318
Na	3.225	2.574	2.586	3.325	2.523
K	0.077	0.065	0.057	0.068	0.082
Total	20.024	20.000	20.020	20.049	19.958
Ab	80.83	64.79	64.44	82.55	63.81
An	17.24	33.58	34.14	15.76	34.12
Or	1.93	1.64	1.42	1.69	2.07
remarks	F	C	C	C	C

(Plate 9–3 continued)

specimen	90102202	90102202	90102202	90102202	90102202
grain	1	1	2	2	2
position	2(M)	3(R)	1(C)	2(M)	3(R)
SiO_2	58.30	63.63	57.04	58.28	61.11
TiO_2	0.00	0.00	0.00	0.00	0.00
Al_2O_3	25.57	22.21	26.15	25.88	24.08
FeO	0.16	0.10	0.13	0.16	0.14
MnO	0.00	0.00	0.00	0.00	0.02
MgO	0.00	0.00	0.00	0.00	0.00
CaO	7.35	3.46	8.31	7.77	5.48
Na_2O	7.09	9.65	6.82	6.95	8.33
K_2O	0.28	0.18	0.19	0.18	0.23
Total	98.74	99.23	98.65	99.21	99.38
Si	10.549	11.327	10.368	10.500	10.925
Ti	0.000	0.000	0.000	0.000	0.000
Al	5.452	4.658	5.602	5.496	5.072
Fe	0.024	0.015	0.020	0.023	0.020
Mn	0.000	0.000	0.000	0.000	0.003
Mg	0.000	0.000	0.000	0.000	0.000
Ca	1.425	0.660	1.618	1.499	1.049
Na	2.485	3.329	2.404	2.425	2.887
K	0.065	0.040	0.043	0.042	0.052
Total	20.000	20.029	20.055	19.985	20.008
Ab	62.14	82.32	58.85	60.79	71.98
An	36.23	16.69	40.10	38.15	26.73
Or	1.63	0.99	1.05	1.05	1.30
remarks	C	C	F	F	F

(Plate 9–3 continued)

specimen	90102209	90102209	90102209	90102209	90102209
grain	1	1	1	2	2
position	1(C)	2(M)	3(R)	1(C)	2(M)
SiO_2	58.32	59.60	61.86	62.73	61.57
TiO_2	0.01	0.00	0.00	0.00	0.00
Al_2O_3	26.06	25.02	23.44	22.79	23.76
FeO	0.19	0.19	0.11	0.10	0.17
MnO	0.00	0.00	0.00	0.00	0.00
MgO	0.00	0.00	0.00	0.00	0.00
CaO	7.67	6.81	4.35	4.07	5.28
Na_2O	7.02	7.52	8.75	9.22	8.40
K_2O	0.23	0.36	0.32	0.19	0.32
Total	99.50	99.50	98.83	99.10	99.49
Si	10.482	10.691	11.084	11.199	10.990
Ti	0.002	0.000	0.000	0.000	0.000
Al	5.519	5.288	4.949	4.795	4.997
Fe	0.028	0.029	0.017	0.015	0.025
Mn	0.000	0.000	0.000	0.000	0.000
Mg	0.000	0.001	0.001	0.001	0.000
Ca	1.476	1.309	0.835	0.778	1.010
Na	2.446	2.614	3.038	3.189	2.904
K	0.052	0.083	0.073	0.043	0.073
Total	20.005	20.014	19.997	20.020	20.000
Ab	61.12	64.77	76.64	79.21	72.38
An	37.58	33.18	21.52	19.72	25.80
Or	1.30	2.06	1.84	1.07	1.82
remarks	C	C	C	F	F

(Plate 9–3 continued)

specimen	90102209	90102209	90102209	90102209	90102222
grain	2	3	3	3	1
position	3(R)	1(C)	2(M)	3(R)	1(C)
SiO_2	62.76	58.63	59.43	63.49	59.16
TiO_2	0.00	0.02	0.01	0.00	0.00
Al_2O_3	22.67	25.57	24.94	22.17	24.57
FeO	0.09	0.17	0.17	0.13	0.15
MnO	0.00	0.02	0.01	0.00	0.00
MgO	0.00	0.01	0.00	0.00	0.00
CaO	4.02	7.72	6.75	3.49	6.34
Na_2O	8.99	7.12	7.58	9.69	7.72
K_2O	0.21	0.22	0.29	0.20	0.45
Total	98.75	99.47	99.17	99.16	98.38
Si	11.231	10.543	10.693	11.317	10.731
Ti	0.000	0.003	0.001	0.000	0.000
Al	4.779	5.417	5.286	4.656	5.251
Fe	0.014	0.026	0.025	0.019	0.022
Mn	0.001	0.003	0.002	0.000	0.000
Mg	0.001	0.001	0.001	0.000	0.000
Ca	0.770	1.486	1.301	0.666	1.232
Na	3.118	2.481	2.643	3.348	2.713
K	0.047	0.050	0.067	0.045	0.103
Total	19.962	20.011	20.018	20.051	20.052
Ab	78.92	61.30	65.44	82.10	66.66
An	19.89	37.46	32.90	16.80	30.81
Or	1.19	1.24	1.66	1.10	2.53
remarks	F	C	C	C	C

(Plate 9–3 continued)

specimen	90102222	90102222	90102222	90102222	90102222
grain	1	1	2	2	2
position	2(M)	3(R)	1(C)	2(M)	3(R)
SiO_2	59.94	64.36	59.83	57.10	63.94
TiO_2	0.00	0.00	0.00	0.00	0.00
Al_2O_3	25.17	22.16	25.15	26.25	22.15
FeO	0.12	0.07	0.04	0.18	0.09
MnO	0.01	0.02	0.00	0.00	0.01
MgO	0.00	0.00	0.00	0.01	0.00
CaO	6.67	3.37	6.79	8.41	3.33
Na_2O	7.50	9.51	7.51	6.59	9.48
K_2O	0.36	0.31	0.21	0.16	0.36
Total	99.76	99.80	99.51	98.69	99.36
Si	10.709	11.379	10.707	10.368	11.362
Ti	0.000	0.000	0.000	0.000	0.000
Al	5.299	4.617	5.303	5.615	4.637
Fe	0.018	0.011	0.006	0.028	0.014
Mn	0.001	0.003	0.000	0.000	0.002
Mg	0.001	0.000	0.000	0.002	0.000
Ca	1.275	0.639	1.301	1.635	0.633
Na	2.596	3.259	2.603	2.319	3.264
K	0.081	0.069	0.047	0.036	0.081
Total	19.980	19.976	19.966	20.003	19.992
Ab	65.36	81.86	65.78	57.69	81.72
An	32.60	16.40	33.03	41.42	16.25
Or	2.04	1.73	1.19	0.90	2.03
remarks	C	C	F	F	F

(Plate 9–3 continued)

specimen	90102401	90102401	90102401	90102401	90102401
grain	1	1	1	2	2
position	1(C)	2(M)	3(R)	1(C)	2(M)
SiO_2	59.06	59.11	65.11	58.70	64.10
TiO_2	0.00	0.00	0.00	0.04	0.01
Al_2O_3	25.36	25.58	21.54	25.57	22.36
FeO	0.17	0.15	0.15	0.15	0.11
MnO	0.00	0.00	0.00	0.00	0.02
MgO	0.00	0.00	0.00	0.00	0.00
CaO	7.22	7.37	2.69	7.46	3.32
Na_2O	7.31	7.35	9.94	7.22	9.38
K_2O	0.29	0.23	0.21	0.18	0.37
Total	99.41	99.80	99.65	99.32	99.68
Si	10.612	10.583	11.507	10.560	11.350
Ti	0.000	0.000	0.000	0.005	0.001
Al	5.369	5.397	4.485	5.419	4.665
Fe	0.026	0.022	0.022	0.022	0.016
Mn	0.000	0.000	0.000	0.000	0.003
Mg	0.001	0.000	0.001	0.001	0.001
Ca	1.390	1.413	0.510	1.437	0.629
Na	2.546	2.551	3.402	2.517	3.219
K	0.066	0.053	0.047	0.042	0.084
Total	20.009	20.020	19.975	20.004	19.969
Ab	63.19	63.16	85.43	62.63	81.45
An	35.17	35.53	13.39	36.33	16.42
Or	1.64	1.31	1.18	1.05	2.13
remarks	C	C	C	F	F

(Plate 9–3 continued)

specimen	90102401	90102407	90102407	90102407	90102407
grain	2	1	1	1	1
position	3(R)	1(C)	2(C)	3(M)	4(M)
SiO_2	64.28	59.33	61.30	59.28	60.91
TiO_2	0.00	0.00	0.00	0.00	0.00
Al_2O_3	22.21	24.93	24.15	24.94	23.84
FeO	0.11	0.11	0.12	0.12	0.13
MnO	0.00	0.02	0.02	0.01	0.00
MgO	0.00	0.00	0.00	0.00	0.00
CaO	3.28	6.88	5.85	6.90	5.74
Na_2O	9.65	7.63	8.00	7.34	7.87
K_2O	0.15	0.22	0.29	0.39	0.68
Total	99.69	99.11	99.73	98.99	99.17
Si	11.373	10.683	10.922	10.687	10.933
Ti	0.000	0.000	0.000	0.000	0.000
Al	4.629	5.289	5.070	5.298	5.043
Fe	0.017	0.016	0.018	0.018	0.020
Mn	0.000	0.003	0.003	0.002	0.000
Mg	0.000	0.000	0.000	0.000	0.000
Ca	0.621	1.327	1.115	1.332	1.102
Na	3.310	2.662	2.763	2.565	2.738
K	0.034	0.049	0.065	0.091	0.155
Total	19.984	20.029	19.957	19.992	19.992
Ab	83.12	65.61	69.70	64.00	68.19
An	16.02	33.18	28.66	33.73	27.95
Or	0.85	1.21	1.64	2.27	3.86
remarks	F	C	C	C	C

(Plate 9–3 continued)

specimen	90102407	90102407	90102407	90102407	90102408G
grain	1	2	2	2	1
position	5(R)	1(C)	2(M)	3(R)	1(C)
SiO_2	64.21	59.89	59.82	63.85	58.40
TiO_2	0.00	0.00	0.00	0.00	0.02
Al_2O_3	21.38	24.16	24.55	21.90	25.39
FeO	0.08	0.17	0.13	0.09	0.10
MnO	0.02	0.00	0.02	0.00	0.00
MgO	0.00	0.00	0.00	0.00	0.00
CaO	2.80	6.03	6.42	3.22	7.47
Na_2O	9.64	7.98	7.50	9.59	7.02
K_2O	0.45	0.30	0.36	0.32	0.40
Total	98.59	98.52	98.79	98.97	98.80
Si	11.484	10.828	10.783	11.387	10.567
Ti	0.000	0.000	0.000	0.000	0.003
Al	4.506	5.147	5.214	4.603	5.414
Fe	0.012	0.026	0.020	0.013	0.015
Mn	0.003	0.000	0.003	0.000	0.000
Mg	0.000	0.000	0.000	0.000	0.000
Ca	0.536	1.168	1.239	0.614	1.448
Na	3.342	2.794	2.618	3.313	2.461
K	0.104	0.068	0.082	0.073	0.092
Total	19.986	20.030	19.959	20.004	20.000
Ab	83.61	68.89	66.08	82.56	61.28
An	13.79	29.44	31.85	15.62	36.43
Or	2.60	1.68	2.07	1.82	2.29
remarks	C	F	F	F	C

(Plate 9–3 continued)

specimen	90102408G	90102408G	90102707	90102707	90102707
grain	1	1	1	1	1
position	2(M)	3(R)	1(C)	2(M)	3(M)
SiO_2	58.78	62.25	60.29	60.71	59.73
TiO_2	0.02	0.00	0.00	0.00	0.00
Al_2O_3	25.49	22.98	24.32	24.21	24.58
FeO	0.12	0.10	0.20	0.15	0.14
MnO	0.00	0.00	0.00	0.00	0.00
MgO	0.00	0.01	0.00	0.01	0.01
CaO	7.30	4.56	6.79	6.35	6.88
Na_2O	7.15	9.03	7.18	7.41	7.12
K_2O	0.20	0.27	0.65	0.65	0.60
Total	99.06	99.20	99.43	99.49	99.06
Si	10.590	11.127	10.816	10.869	10.757
Ti	0.003	0.000	0.000	0.000	0.000
Al	5.411	4.840	5.141	5.107	5.216
Fe	0.018	0.015	0.030	0.022	0.021
Mn	0.000	0.000	0.000	0.000	0.000
Mg	0.000	0.003	0.000	0.003	0.003
Ca	1.409	0.873	1.305	1.217	1.327
Na	2.496	3.128	2.496	2.571	2.485
K	0.046	0.062	0.149	0.148	0.138
Total	19.973	20.047	19.936	19.937	19.946
Ab	62.89	76.65	62.71	64.91	62.53
An	35.95	21.83	33.54	31.36	34.00
Or	1.16	1.52	3.74	3.74	3.47
remarks	C	C	C	C	C

(Plate 9–3 continued)

specimen	90102707	90102707	90102707	90102707	90102707
grain	1	1	2	2	2
position	4(R)	5(R)	1(C)	2(M)	3(M)
SiO_2	58.69	62.55	60.29	58.37	60.75
TiO_2	0.00	0.00	0.00	0.00	0.01
Al_2O_3	25.33	23.01	24.60	25.79	24.38
FeO	0.18	0.13	0.20	0.20	0.13
MnO	0.00	0.00	0.01	0.00	0.01
MgO	0.01	0.00	0.02	0.01	0.01
CaO	7.69	4.67	6.78	8.32	6.53
Na_2O	6.71	8.90	7.26	6.50	7.34
K_2O	0.56	0.11	0.60	0.46	0.62
Total	99.17	99.37	99.76	99.65	99.78
Si	10.586	11.146	10.781	10.493	10.846
Ti	0.000	0.000	0.000	0.000	0.001
Al	5.384	4.832	5.184	5.463	5.129
Fe	0.027	0.019	0.030	0.030	0.019
Mn	0.000	0.000	0.002	0.000	0.002
Mg	0.003	0.000	0.005	0.003	0.003
Ca	1.486	0.891	1.298	1.602	1.249
Na	2.345	3.073	2.516	2.264	2.539
K	0.129	0.025	0.137	0.105	0.141
Total	19.959	19.987	19.953	19.960	19.929
Ab	58.77	76.67	63.09	56.54	64.23
An	37.99	22.70	33.48	40.83	32.20
Or	3.23	0.62	3.44	2.62	3.57
remarks	C	C	C	C	C

(Plate 9–3 continued)

specimen	90102707
grain	2
position	4(R)
SiO_2	59.29
TiO_2	0.00
Al_2O_3	25.08
FeO	0.14
MnO	0.01
MgO	0.01
CaO	7.42
Na_2O	7.13
K_2O	0.56
Total	99.64
Si	10.643
Ti	0.000
Al	5.305
Fe	0.021
Mn	0.002
Mg	0.003
Ca	1.427
Na	2.480
K	0.128
Total	20.008
Ab	61.07
An	35.78
Or	3.15
remarks	C

Plate 9–4. Chemical compositions of plagiocalse from porphyritic granite.

specimen	86120307	86120307	86120307	86120307	86120307
grain	1	1	1	2	2
position	1(C)	2(M)	3(M)	1(C)	2(R)
SiO_2	57.45	60.40	60.35	62.16	62.54
TiO_2	0.02	0.02	0.02	0.00	0.01
Al_2O_3	26.38	24.68	24.60	23.72	22.90
FeO	0.11	0.13	0.18	0.05	0.10
MnO	0.02	0.01	0.00	0.03	0.04
MgO	0.00	0.01	0.00	0.00	0.00
CaO	8.67	6.56	6.46	5.37	4.60
Na_2O	6.35	7.60	7.38	8.23	8.33
K_2O	0.27	0.30	0.39	0.45	0.60
Total	99.26	99.71	99.38	100.02	99.11
Si	10.371	10.788	10.808	11.031	11.176
Ti	0.003	0.003	0.003	0.000	0.001
Al	5.611	5.194	5.191	4.960	4.823
Fe	0.016	0.019	0.027	0.008	0.015
Mn	0.003	0.001	0.000	0.005	0.006
Mg	0.001	0.002	0.000	0.000	0.000
Ca	1.676	1.254	1.239	1.021	0.880
Na	2.222	2.632	2.562	2.831	2.884
K	0.061	0.069	0.089	0.101	0.136
Total	19.963	19.962	19.919	19.955	19.921
Ab	55.84	66.18	65.41	71.38	73.55
An	42.62	32.08	32.32	26.07	22.98
Or	1.53	1.73	2.27	2.55	3.47
remarks	C	C	C	F	F

(Plate 9–4 continued)

specimen	86120307	86120307	87043004	87043004	87043004
grain	3	3	1	1	1
position	1(C)	2(R)	1(C)	2(M)	3(R)
SiO_2	56.10	61.25	59.76	60.25	63.85
TiO_2	0.00	0.00	0.01	0.00	0.00
Al_2O_3	27.33	23.95	24.91	25.34	22.72
FeO	0.19	0.09	0.16	0.18	0.08
MnO	0.02	0.00	0.00	0.00	0.00
MgO	0.00	0.00	0.00	0.01	0.00
CaO	9.63	5.79	6.95	7.10	4.19
Na_2O	5.81	7.89	7.05	7.21	8.97
K_2O	0.19	0.43	0.56	0.46	0.25
Total	99.27	99.40	99.39	100.54	100.07
Si	10.156	10.948	10.724	10.692	11.272
Ti	0.001	0.000	0.001	0.000	0.001
Al	5.830	5.044	5.268	5.298	4.726
Fe	0.029	0.013	0.025	0.027	0.012
Mn	0.003	0.000	0.000	0.000	0.000
Mg	0.000	0.000	0.000	0.002	0.000
Ca	1.868	1.109	1.336	1.350	0.792
Na	2.039	2.734	2.450	2.478	3.068
K	0.043	0.097	0.128	0.103	0.056
Total	19.969	19.946	19.931	19.950	19.926
Ab	51.21	69.16	62.20	62.58	78.11
An	47.71	28.38	34.55	34.82	20.47
Or	1.08	2.45	3.25	2.60	1.43
remarks	F	F	C	C	C

(Plate 9–4 continued)

specimen	87043004	87043004	87043004	87043004	87043004
grain	2	2	3	3	3
position	1(C)	2(R)	1(C)	2(M)	3(R)
SiO_2	62.51	65.16	58.88	60.90	61.46
TiO_2	0.00	0.00	0.00	0.00	0.00
Al_2O_3	23.32	22.23	26.14	24.10	24.13
FeO	0.10	0.12	0.12	0.19	0.16
MnO	0.00	0.00	0.00	0.00	0.00
MgO	0.00	0.00	0.01	0.00	0.00
CaO	5.09	3.54	7.91	5.76	5.54
Na_2O	8.41	9.18	6.65	7.65	7.86
K_2O	0.53	0.37	0.45	0.68	0.40
Total	99.95	100.59	100.15	99.28	99.56
Si	11.097	11.418	10.510	10.913	10.956
Ti	0.000	0.000	0.000	0.000	0.000
Al	4.877	4.589	5.498	5.089	5.069
Fe	0.015	0.017	0.018	0.028	0.024
Mn	0.000	0.000	0.000	0.000	0.000
Mg	0.000	0.000	0.001	0.001	0.000
Ca	0.968	0.664	1.513	1.106	1.057
Na	2.894	3.116	2.299	2.656	2.716
K	0.120	0.083	0.103	0.154	0.090
Total	19.970	19.887	19.941	19.947	19.913
Ab	72.40	80.31	58.44	67.33	69.87
An	24.59	17.55	38.94	28.77	27.81
Or	3.00	2.14	2.62	3.90	2.32
remarks	F	F	C	C	C

(Plate 9–4 continued)

specimen	87052806	87052806	87052806	87052806	87052806
grain	1	1	1	1	2
position	1(C)	2(M)	3(M)	4(R)	1(C)
SiO_2	59.62	59.69	58.72	63.76	59.58
TiO_2	0.00	0.00	0.02	0.00	0.03
Al_2O_3	25.36	24.93	25.00	22.69	25.09
FeO	0.23	0.24	0.20	0.15	0.21
MnO	0.00	0.00	0.00	0.00	0.00
MgO	0.01	0.01	0.00	0.00	0.01
CaO	6.96	6.96	6.97	3.94	6.79
Na_2O	7.48	7.35	7.49	9.45	7.44
K_2O	0.26	0.51	0.35	0.33	0.45
Total	99.93	99.70	98.76	100.31	99.59
Si	10.649	10.696	10.629	11.252	10.682
Ti	0.000	0.000	0.002	0.000	0.004
Al	5.337	5.264	5.333	4.718	5.299
Fe	0.035	0.035	0.031	0.022	0.031
Mn	0.000	0.000	0.000	0.000	0.000
Mg	0.004	0.003	0.001	0.001	0.003
Ca	1.332	1.336	1.351	0.744	1.304
Na	2.589	2.554	2.627	3.230	2.583
K	0.060	0.117	0.080	0.074	0.102
Total	20.006	20.007	20.055	20.042	20.007
Ab	64.40	63.14	64.23	79.34	64.21
An	34.10	33.97	33.81	18.84	33.26
Or	1.49	2.89	1.96	1.82	2.54
remarks	C	C	C	C	C

(Plate 9–4 continued)

specimen	87052806	87052806	87052806	87062801	87062801
grain	2	2	2	1	1
position	2(M)	3(M)	4(R)	1(C)	2(M)
SiO_2	58.89	64.82	66.39	58.59	57.97
TiO_2	0.00	0.00	0.00	0.00	0.01
Al_2O_3	25.41	21.40	20.69	24.91	25.69
FeO	0.25	0.20	0.20	0.19	0.19
MnO	0.00	0.00	0.00	0.02	0.02
MgO	0.01	0.00	0.00	0.01	0.01
CaO	6.99	2.58	1.51	6.75	7.33
Na_2O	7.42	9.73	10.65	7.13	6.86
K_2O	0.19	0.37	0.10	0.48	0.38
Total	99.16	99.11	99.54	98.07	98.45
Si	10.605	11.519	11.704	10.663	10.523
Ti	0.000	0.000	0.000	0.000	0.001
Al	5.392	4.481	4.298	5.343	5.495
Fe	0.037	0.029	0.029	0.028	0.029
Mn	0.000	0.000	0.000	0.003	0.003
Mg	0.002	0.001	0.000	0.001	0.004
Ca	1.348	0.491	0.286	1.315	1.425
Na	2.588	3.352	3.638	2.513	2.412
K	0.044	0.084	0.022	0.111	0.087
Total	20.015	19.958	19.978	19.977	19.978
Ab	64.39	84.71	91.52	63.28	60.91
An	34.51	13.17	7.92	33.92	36.89
Or	1.09	2.12	0.55	2.80	2.20
remarks	C	C	C	C	C

(Plate 9–4 continued)

specimen	87062801	87062801	87062801	87062801	87062801
grain	1	2	2	3	3
position	3(R)	1(C)	2(M)	1(C)	2(M)
SiO_2	62.28	61.87	62.25	62.59	62.95
TiO_2	0.00	0.00	0.00	0.00	0.00
Al_2O_3	22.77	22.90	22.96	22.57	22.28
FeO	0.16	0.19	0.10	0.10	0.04
MnO	0.00	0.00	0.03	0.05	0.01
MgO	0.00	0.00	0.01	0.00	0.00
CaO	4.27	4.08	4.25	3.64	3.43
Na_2O	8.76	8.60	8.97	9.24	9.20
K_2O	0.43	0.60	0.41	0.25	0.48
Total	98.67	98.23	98.96	98.44	98.39
Si	11.179	11.157	11.148	11.239	11.302
Ti	0.000	0.000	0.000	0.000	0.000
Al	4.817	4.866	4.845	4.775	4.715
Fe	0.024	0.028	0.014	0.015	0.006
Mn	0.000	0.000	0.004	0.008	0.001
Mg	0.000	0.000	0.002	0.001	0.001
Ca	0.821	0.787	0.814	0.700	0.660
Na	3.048	3.004	3.112	3.216	3.201
K	0.097	0.138	0.093	0.057	0.109
Total	19.986	19.981	20.032	20.010	19.995
Ab	76.39	75.92	77.05	80.46	80.47
An	21.18	20.60	20.65	18.11	16.79
Or	2.43	3.49	2.30	1.43	2.74
remarks	C	F	F	F	F

Plate 9–5. Chemical compositions of plagioclase from granite.

specimen	87122210	87122210	87122210	87122210	87122210
grain	1	1	1	2	2
position	1(C)	2(M)	3(R)	1(C)	2(C)
SiO_2	58.13	60.67	62.35	57.96	60.34
TiO_2	0.00	0.00	0.00	0.00	0.00
Al_2O_3	25.64	23.96	23.08	25.56	24.16
FeO	0.19	0.11	0.12	0.23	0.16
MnO	0.00	0.00	0.00	0.00	0.01
MgO	0.01	0.00	0.00	0.02	0.01
CaO	7.54	5.34	4.32	7.19	5.62
Na_2O	6.80	8.14	8.80	7.00	7.91
K_2O	0.45	0.36	0.28	0.32	0.40
Total	98.76	98.57	98.96	98.27	98.60
Si	10.527	10.931	11.150	10.539	10.881
Ti	0.000	0.000	0.001	0.000	0.000
Al	5.471	5.086	4.863	5.477	5.133
Fe	0.029	0.017	0.019	0.035	0.025
Mn	0.000	0.000	0.000	0.000	0.002
Mg	0.003	0.000	0.001	0.004	0.002
Ca	1.462	1.030	0.828	1.399	1.084
Na	2.387	2.841	3.050	2.465	2.763
K	0.104	0.082	0.065	0.075	0.091
Total	19.982	19.987	19.975	19.993	19.980
Ab	59.90	71.56	76.96	61.97	69.65
An	37.49	26.37	21.40	36.15	28.06
Or	2.61	2.07	1.64	1.89	2.29

(Plate 9–5. continued)

specimen	87122210	87122502	87122502	87122502	87122502
grain	2	1	1	1	2
position	3(R)	1(C)	2(M)	3(R)	1(C)
SiO_2	62.01	62.90	60.89	65.01	62.43
TiO_2	0.00	0.00	0.01	0.00	0.01
Al_2O_3	23.16	23.14	24.19	21.76	23.33
FeO	0.08	0.06	0.12	0.03	0.16
MnO	0.00	0.02	0.05	0.02	0.04
MgO	0.01	0.00	0.01	0.00	0.00
CaO	4.32	4.63	5.93	3.04	4.87
Na_2O	8.85	8.71	7.97	9.64	8.32
K_2O	0.22	0.17	0.30	0.35	0.39
Total	98.65	99.63	99.47	99.86	99.56
Si	11.125	11.166	10.888	11.471	11.110
Ti	0.000	0.000	0.001	0.000	0.002
Al	4.896	4.839	5.097	4.524	4.893
Fe	0.012	0.008	0.018	0.005	0.024
Mn	0.000	0.003	0.007	0.004	0.006
Mg	0.002	0.000	0.002	0.000	0.000
Ca	0.829	0.881	1.136	0.575	0.928
Na	3.076	2.996	2.761	3.295	2.870
K	0.050	0.038	0.068	0.079	0.088
Total	19.990	19.932	19.977	19.953	19.921
Ab	77.50	76.31	69.16	83.25	73.29
An	21.24	22.72	29.13	14.75	24.46
Or	1.26	0.97	1.70	2.00	2.25

(Plate 9–5. continued)

specimen	87122502	87122502	90101909	90101909	90101909
grain	2	2	1	1	1
position	2(M)	3(R)	1(C)	2(M)	3(M)
SiO_2	61.20	63.34	58.86	58.26	61.49
TiO_2	0.02	0.01	0.00	0.03	0.00
Al_2O_3	24.32	22.57	25.25	25.67	23.71
FeO	0.12	0.10	0.08	0.07	0.13
MnO	0.01	0.00	0.02	0.00	0.01
MgO	0.00	0.00	0.00	0.00	0.00
CaO	5.76	3.97	7.43	7.95	5.49
Na_2O	7.88	9.02	7.32	6.95	8.23
K_2O	0.44	0.23	0.33	0.28	0.39
Total	99.75	99.23	99.29	99.21	99.45
Si	10.903	11.273	10.600	10.508	10.986
Ti	0.002	0.001	0.000	0.004	0.000
Al	5.106	4.733	5.358	5.456	4.992
Fe	0.018	0.015	0.012	0.011	0.019
Mn	0.002	0.000	0.003	0.000	0.002
Mg	0.001	0.000	0.000	0.000	0.000
Ca	1.100	0.756	1.433	1.536	1.050
Na	2.721	3.112	2.554	2.429	2.849
K	0.099	0.052	0.076	0.064	0.089
Total	19.952	19.941	20.036	20.007	19.987
Ab	69.04	79.09	62.63	60.12	71.07
An	28.44	19.59	35.51	38.29	26.71
Or	2.51	1.32	1.86	1.58	2.22

(Plate 9–5. continued)

specimen	90101909
grain	1
position	4(R)
SiO_2	63.55
TiO_2	0.00
Al_2O_3	22.54
FeO	0.11
MnO	0.01
MgO	0.00
CaO	3.98
Na_2O	9.09
K_2O	0.41
Total	99.69
Si	11.275
Ti	0.000
Al	4.712
Fe	0.016
Mn	0.002
Mg	0.000
Ca	0.756
Na	3.125
K	0.093
Total	19.978
Ab	78.28
An	19.39
Or	2.33

Plate 9–6. Chemical compositions of plagioclase from aplite.

specimen	90101906B	90101906B	90101906B	90101906B	90101906B
grain	1	1	1	1	2
position	1(C)	2(M)	3(R)	4(R)	1(C)
SiO_2	65.56	64.96	65.24	67.68	65.81
TiO_2	0.00	0.00	0.00	0.00	0.00
Al_2O_3	21.43	21.48	21.23	19.60	21.21
FeO	0.04	0.08	0.05	0.02	0.09
MnO	0.00	0.00	0.01	0.00	0.00
MgO	0.00	0.00	0.00	0.00	0.00
CaO	2.26	2.47	2.06	0.23	1.90
Na_2O	10.23	10.14	10.35	11.49	10.18
K_2O	0.10	0.39	0.37	0.14	0.71
Total	99.62	99.52	99.31	99.16	99.91
Si	11.563	11.506	11.565	11.933	11.601
Ti	0.000	0.000	0.000	0.000	0.000
Al	4.455	4.483	4.433	4.072	4.405
Fe	0.006	0.012	0.008	0.002	0.013
Mn	0.000	0.000	0.002	0.000	0.000
Mg	0.000	0.000	0.000	0.000	0.000
Ca	0.426	0.468	0.391	0.044	0.359
Na	3.497	3.478	3.556	3.925	3.478
K	0.023	0.088	0.083	0.032	0.160
Total	19.970	20.035	20.038	20.009	20.016
Ab	88.49	85.96	88.02	98.05	86.73
An	10.93	11.86	9.93	1.15	9.28
Or	0.58	2.17	2.05	0.80	3.99

(Plate 9–6. continued)

specimen	90101906B	90101906B
grain	2	2
position	2(M)	3(R)
SiO_2	66.15	65.34
TiO_2	0.00	0.00
Al_2O_3	20.89	21.49
FeO	0.06	0.00
MnO	0.00	0.00
MgO	0.00	0.00
CaO	1.79	1.64
Na_2O	10.28	10.48
K_2O	0.72	0.23
Total	99.88	99.18
Si	11.656	11.570
Ti	0.000	0.000
Al	4.337	4.483
Fe	0.009	0.000
Mn	0.000	0.000
Mg	0.000	0.000
Ca	0.337	0.311
Na	3.510	3.595
K	0.161	0.052
Total	20.011	20.012
Ab	87.38	90.83
An	8.61	7.86
Or	4.01	1.31

Plate 9–7. Chemical compositions of plagioclase from rhyolite.

specimen	85112607	85112607	85112607	85112607	86112803
grain	1	1	1	1	1
position	1(C)	2(C)	3(C)	4(R)	1(C)
SiO_2	61.63	61.03	61.49	61.72	59.35
TiO_2	0.00	0.00	0.00	0.00	0.01
Al_2O_3	23.57	23.90	23.75	23.76	25.26
FeO	0.03	0.02	0.04	0.01	0.08
MnO	0.00	0.00	0.00	0.00	0.00
MgO	0.00	0.00	0.00	0.00	0.00
CaO	5.22	5.11	5.51	4.99	6.97
Na_2O	8.64	8.49	8.51	8.30	7.36
K_2O	0.14	0.17	0.20	0.44	0.24
Total	99.23	98.72	99.50	99.22	99.27
Si	11.018	10.964	10.976	11.027	10.658
Ti	0.000	0.000	0.000	0.000	0.002
Al	4.965	5.059	4.996	5.002	5.346
Fe	0.004	0.003	0.006	0.001	0.011
Mn	0.000	0.000	0.000	0.000	0.000
Mg	0.000	0.000	0.000	0.000	0.000
Ca	0.999	0.983	1.053	0.955	1.340
Na	2.993	2.955	2.944	2.873	2.562
K	0.032	0.039	0.046	0.100	0.055
Total	20.012	20.004	20.020	19.959	19.975
Ab	74.30	74.25	72.71	73.12	64.57
An	24.90	24.77	26.15	24.33	34.05
Or	0.79	0.98	1.14	2.55	1.39

(Plate 9–7. continued)

specimen	86112803	86112803	86120106	86120106
grain	1	1	1	1
position	2(M)	3(R)	1(C)	3(R)
SiO_2	58.79	58.72	66.03	64.80
TiO_2	0.00	0.02	0.00	0.00
Al_2O_3	25.69	25.68	20.61	21.56
FeO	0.05	0.08	0.07	0.06
MnO	0.00	0.01	0.02	0.00
MgO	0.00	0.00	0.00	0.00
CaO	7.37	7.40	1.21	1.86
Na_2O	7.30	7.07	10.85	10.18
K_2O	0.22	0.21	0.20	0.15
Total	99.41	99.18	99.00	98.60
Si	10.561	10.567	11.706	11.539
Ti	0.000	0.002	0.000	0.000
Al	5.438	5.445	4.305	4.523
Fe	0.007	0.011	0.011	0.009
Mn	0.000	0.001	0.003	0.000
Mg	0.001	0.000	0.000	0.000
Ca	1.418	1.426	0.229	0.355
Na	2.539	2.465	3.728	3.512
K	0.051	0.047	0.046	0.035
Total	20.015	19.964	20.029	19.973
Ab	63.22	62.41	92.81	89.80
An	35.51	36.41	6.05	9.31
Or	1.27	1.19	1.15	0.89

Table 10. Chemical compositions of K–feldspar. (oxygen=32)

Table 10–1. Chemical compositions of K–feldspar from dark inclusion.

specimen	90050503	90050503	90050503	90050503	9005055A
grain	1	1	2	2	1
position	1	2	1	2	1
SiO_2	64.24	64.15	64.19	64.06	63.25
TiO_2	0.01	0.02	0.01	0.00	0.06
Al_2O_3	18.41	18.50	18.46	18.21	19.70
FeO	0.00	0.00	0.00	0.00	0.08
MnO	0.00	0.00	0.00	0.00	0.00
MgO	0.01	0.01	0.01	0.01	0.00
CaO	0.03	0.15	0.06	0.04	0.02
Na_2O	0.81	1.35	1.02	1.03	1.14
K_2O	16.42	15.31	16.01	16.03	14.13
Total	99.92	99.48	99.76	99.36	98.38
Si	11.929	11.917	11.921	11.948	11.794
Ti	0.001	0.003	0.002	0.000	0.008
Al	4.029	4.049	4.040	4.002	4.329
Fe	0.000	0.000	0.000	0.000	0.012
Mn	0.000	0.000	0.000	0.000	0.000
Mg	0.001	0.002	0.002	0.002	0.000
Ca	0.006	0.030	0.012	0.007	0.003
Na	0.290	0.485	0.367	0.372	0.413
K	3.887	3.627	3.793	3.812	3.360
Total	20.144	20.112	20.137	20.143	19.920
Ab	6.94	11.70	8.80	8.87	10.91
An	0.18	0.78	0.33	0.21	0.41
Or	92.89	87.52	90.87	90.92	88.68

(Table 10–1. continued)

specimen	9005055A	9005055A	9005055A	90102206
grain	1	1	2	1
position	2	3	1	1
SiO_2	49.04	52.31	52.19	62.87
TiO_2	0.05	0.05	0.05	0.00
Al_2O_3	33.58	30.56	31.08	18.65
FeO	0.08	0.07	0.04	0.43
MnO	0.00	0.02	0.00	0.00
MgO	0.01	0.01	0.00	0.00
CaO	0.04	0.02	0.08	0.00
Na_2O	0.94	0.71	0.87	0.86
K_2O	11.38	12.37	11.28	14.95
Total	95.11	96.11	95.58	97.75
Si	9.465	10.000	9.968	11.875
Ti	0.008	0.007	0.007	0.000
Al	7.637	6.884	6.994	4.150
Fe	0.013	0.011	0.006	0.067
Mn	0.000	0.003	0.000	0.000
Mg	0.002	0.003	0.001	0.000
Ca	0.008	0.005	0.017	0.000
Na	0.352	0.263	0.321	0.315
K	2.800	3.015	2.747	3.600
Total	20.285	20.191	20.061	20.008
Ab	11.08	7.98	10.37	7.92
An	0.73	0.66	0.76	1.69
Or	88.19	91.36	88.87	90.39

Table 10–2. Chemical compositions of K–feldspar from granodiorite.

specimen	90043006	90043006	90050505	90050505	90082401
grain	1	1	1	1	1
position	1	2	1	2	1
SiO_2	88.89	64.24	64.87	64.44	64.25
TiO_2	0.02	0.05	0.02	0.06	0.01
Al_2O_3	5.78	18.47	18.42	18.55	18.44
FeO	0.02	0.06	0.00	0.00	0.10
MnO	0.00	0.00	0.00	0.00	0.00
MgO	0.00	0.00	0.00	0.00	0.00
CaO	0.03	0.03	0.03	0.01	0.03
Na_2O	0.66	0.52	1.08	1.44	1.07
K_2O	3.88	15.20	15.59	15.25	14.25
Total	99.28	98.56	100.00	99.74	98.16
Si	14.878	11.989	11.976	11.928	11.999
Ti	0.002	0.007	0.002	0.008	0.002
Al	1.141	4.062	4.006	4.046	4.057
Fe	0.002	0.009	0.000	0.000	0.015
Mn	0.000	0.000	0.000	0.000	0.000
Mg	0.001	0.000	0.000	0.000	0.000
Ca	0.005	0.005	0.006	0.002	0.007
Na	0.213	0.188	0.387	0.516	0.388
K	0.828	3.617	3.670	3.599	3.394
Total	17.070	19.876	20.047	20.099	19.862
Ab	20.28	4.92	9.52	12.54	10.20
An	0.77	0.37	0.15	0.05	0.57
Or	78.95	94.72	90.33	87.41	89.23

(Table 10–2. continued)

specimen	90082401	90082401	90082401	90082513	90082513
grain	1	2	2	1	1
position	2	1	2	1	2
SiO_2	61.88	64.54	63.81	64.15	63.49
TiO_2	0.00	0.00	0.00	0.06	0.05
Al_2O_3	20.05	18.46	18.25	18.46	18.66
FeO	0.09	0.11	0.11	0.10	0.12
MnO	0.00	0.00	0.00	0.00	0.00
MgO	0.00	0.00	0.00	0.00	0.00
CaO	0.07	0.13	0.06	0.02	0.03
Na_2O	0.99	2.71	1.21	0.77	0.77
K_2O	14.04	12.53	13.91	14.58	14.60
Total	97.12	98.47	97.34	98.13	97.72
Si	11.699	11.970	12.007	11.993	11.935
Ti	0.000	0.000	0.000	0.009	0.007
Al	4.466	4.034	4.046	4.067	4.134
Fe	0.014	0.016	0.017	0.015	0.018
Mn	0.000	0.000	0.000	0.000	0.000
Mg	0.000	0.000	0.000	0.000	0.000
Ca	0.014	0.025	0.013	0.004	0.005
Na	0.362	0.972	0.440	0.278	0.282
K	3.385	2.964	3.336	3.476	3.500
Total	19.941	19.981	19.859	19.842	19.881
Ab	9.59	24.45	11.57	7.36	7.41
An	0.75	1.04	0.77	0.50	0.62
Or	89.66	74.51	87.66	92.14	91.97

(Table 10–2. continued)

specimen	90082513	90082513	90082513	90102202	90102202
grain	2	2	2	1	1
position	1	2	3	1	2
SiO_2	64.51	64.05	63.84	64.83	64.69
TiO_2	0.01	0.03	0.06	0.00	0.00
Al_2O_3	18.31	18.49	18.63	18.39	18.40
FeO	0.00	0.00	0.00	0.06	0.09
MnO	0.00	0.00	0.00	0.01	0.02
MgO	0.01	0.00	0.01	0.00	0.00
CaO	0.00	0.03	0.05	0.04	0.04
Na_2O	0.82	0.82	0.74	1.09	1.45
K_2O	14.57	14.50	14.59	14.26	13.62
Total	98.24	97.92	97.92	98.68	98.32
Si	12.036	11.993	11.962	12.032	12.026
Ti	0.002	0.005	0.009	0.001	0.000
Al	4.025	4.079	4.112	4.023	4.031
Fe	0.000	0.000	0.000	0.009	0.014
Mn	0.000	0.000	0.000	0.002	0.003
Mg	0.004	0.000	0.003	0.000	0.000
Ca	0.000	0.006	0.010	0.007	0.008
Na	0.298	0.296	0.267	0.391	0.523
K	3.468	3.461	3.485	3.375	3.230
Total	19.832	19.841	19.849	19.839	19.834
Ab	7.90	7.88	7.10	10.32	13.84
An	0.10	0.17	0.34	0.48	0.67
Or	91.99	91.95	92.56	89.19	85.50

(Table 10–2. continued)

specimen	90102202	90102202	90102209	90102209	90102209
grain	2	2	1	1	2
position	1	2	1	2	1
SiO_2	64.40	63.86	64.44	64.35	64.53
TiO_2	0.05	0.03	0.02	0.00	0.03
Al_2O_3	19.05	18.62	18.41	18.25	18.27
FeO	0.08	0.09	0.11	0.07	0.12
MnO	0.02	0.00	0.01	0.00	0.01
MgO	0.00	0.00	0.00	0.00	0.01
CaO	0.31	0.03	0.01	0.02	0.05
Na_2O	3.64	1.04	0.96	1.02	1.17
K_2O	11.05	14.13	15.54	15.55	15.10
Total	98.61	97.78	99.49	99.26	99.27
Si	11.876	11.966	11.962	11.977	11.984
Ti	0.007	0.004	0.003	0.000	0.004
Al	4.139	4.110	4.026	4.001	3.998
Fe	0.013	0.014	0.016	0.011	0.018
Mn	0.003	0.000	0.002	0.000	0.001
Mg	0.000	0.000	0.001	0.000	0.002
Ca	0.060	0.005	0.002	0.003	0.009
Na	1.301	0.378	0.344	0.369	0.421
K	2.599	3.376	3.677	3.690	3.576
Total	19.998	19.852	20.033	20.052	20.012
Ab	32.72	10.01	8.51	9.06	10.45
An	1.91	0.51	0.52	0.35	0.74
Or	65.36	89.48	90.96	90.59	88.81

(Table 10–2. continued)

specimen	90102209	90102222	90102222	90102401	90102401
grain	2	1	1	1	1
position	2	1	2	1	2
SiO_2	63.60	62.60	63.14	64.73	63.97
TiO_2	0.07	0.06	0.05	0.02	0.06
Al_2O_3	18.27	18.64	18.72	18.44	18.51
FeO	0.10	0.05	0.01	0.07	0.07
MnO	0.02	0.02	0.04	0.04	0.02
MgO	0.01	0.00	0.00	0.00	0.00
CaO	0.06	0.03	0.04	0.06	0.02
Na_2O	1.14	1.10	1.95	1.34	1.13
K_2O	14.88	14.95	13.52	14.40	15.21
Total	98.15	97.45	97.46	99.09	98.98
Si	11.946	11.859	11.883	11.993	11.928
Ti	0.010	0.009	0.007	0.003	0.008
Al	4.044	4.160	4.151	4.027	4.066
Fe	0.015	0.009	0.002	0.011	0.012
Mn	0.004	0.003	0.006	0.006	0.002
Mg	0.001	0.000	0.000	0.000	0.001
Ca	0.012	0.005	0.009	0.012	0.003
Na	0.415	0.403	0.710	0.480	0.407
K	3.565	3.611	3.245	3.402	3.615
Total	20.012	20.059	20.012	19.933	20.042
Ab	10.34	10.00	17.89	12.28	10.08
An	0.80	0.41	0.42	0.73	0.43
Or	88.85	89.59	81.69	86.98	89.49

(Table 10–2 continued)

specimen	90102401	90102401	90102407	90102407	90102407
grain	2	2	1	1	2
position	1	2	1	2	1
SiO_2	64.69	64.67	63.98	64.15	63.47
TiO_2	0.00	0.03	0.01	0.00	0.02
Al_2O_3	18.45	18.49	18.27	18.23	18.24
FeO	0.06	0.11	0.08	0.05	0.00
MnO	0.01	0.00	0.00	0.04	0.06
MgO	0.01	0.01	0.00	0.00	0.00
CaO	0.01	0.04	0.02	0.00	0.00
Na_2O	1.00	1.11	1.02	0.74	0.39
K_2O	15.60	15.10	15.31	15.82	16.25
Total	99.83	99.57	98.69	99.02	98.43
Si	11.968	11.968	11.965	11.977	11.948
Ti	0.000	0.005	0.002	0.000	0.002
Al	4.021	4.031	4.027	4.010	4.045
Fe	0.010	0.017	0.013	0.008	0.000
Mn	0.001	0.000	0.000	0.006	0.009
Mg	0.001	0.002	0.000	0.000	0.000
Ca	0.002	0.008	0.003	0.000	0.000
Na	0.358	0.399	0.371	0.267	0.143
K	3.680	3.564	3.651	3.766	3.900
Total	20.041	19.993	20.031	20.034	20.048
Ab	8.83	10.00	9.19	6.59	3.53
An	0.36	0.66	0.39	0.36	0.23
Or	90.81	89.33	90.42	93.06	96.24

Table 10–3. Chemical compositions of K–feldspar from porphyritic granite.

specimen	86120307	86120307	87043004	87043004	87043004
grain	1	1	1	1	2
position	1	2	1	2	1
SiO_2	64.09	64.66	65.54	65.28	65.67
TiO_2	0.02	0.03	0.01	0.01	0.00
Al_2O_3	18.27	18.36	18.45	18.39	18.50
FeO	0.00	0.00	0.05	0.08	0.06
MnO	0.08	0.02	0.00	0.00	0.00
MgO	0.00	0.01	0.00	0.00	0.00
CaO	0.01	0.00	0.07	0.05	0.07
Na_2O	0.47	0.59	2.10	0.97	3.42
K_2O	15.84	15.84	14.67	16.33	12.87
Total	98.79	99.50	100.89	101.10	100.59
Si	11.984	11.995	11.970	11.969	11.962
Ti	0.003	0.004	0.002	0.001	0.000
Al	4.025	4.012	3.971	3.973	3.971
Fe	0.000	0.000	0.008	0.012	0.009
Mn	0.012	0.003	0.000	0.000	0.000
Mg	0.001	0.002	0.000	0.000	0.000
Ca	0.002	0.000	0.013	0.009	0.013
Na	0.171	0.210	0.744	0.346	1.206
K	3.778	3.747	3.416	3.817	2.990
Total	19.975	19.973	20.123	20.125	20.151
Ab	4.31	5.31	17.80	8.26	28.59
An	0.39	0.13	0.50	0.50	0.54
Or	95.30	94.57	81.71	91.24	70.87

(Table 10–3. continued)

specimen	87043004	87052806	87052806	87062801	87062801
grain	2	1	1	1	1
position	2	1	2	1	2
SiO_2	65.19	64.78	64.63	63.24	63.84
TiO_2	0.02	0.03	0.04	0.04	0.00
Al_2O_3	18.27	18.51	18.50	18.50	18.30
FeO	0.08	0.12	0.09	0.02	0.04
MnO	0.00	0.00	0.00	0.00	0.01
MgO	0.00	0.01	0.00	0.01	0.01
CaO	0.05	0.08	0.06	0.02	0.01
Na_2O	0.81	1.18	1.05	0.30	0.45
K_2O	16.28	15.10	15.14	15.50	15.23
Total	100.70	99.82	99.51	97.64	97.89
Si	11.990	11.962	11.967	11.941	12.000
Ti	0.003	0.004	0.006	0.006	0.000
Al	3.959	4.028	4.035	4.117	4.054
Fe	0.012	0.019	0.014	0.004	0.007
Mn	0.000	0.000	0.000	0.000	0.001
Mg	0.000	0.003	0.000	0.003	0.002
Ca	0.011	0.015	0.012	0.003	0.002
Na	0.290	0.424	0.375	0.110	0.165
K	3.818	3.556	3.575	3.733	3.650
Total	20.082	20.010	19.984	19.916	19.881
Ab	7.02	10.55	9.44	2.85	4.32
An	0.54	0.92	0.66	0.27	0.29
Or	92.44	88.53	89.90	96.88	95.38

Table 10–4. Chemical compositions of K–feldspar from granite.

specimen	87122210	87122210	87122210	87122210	87122502
grain	1	1	2	2	1
position	1	2	1	2	1
SiO_2	63.62	64.23	64.22	64.21	64.83
TiO_2	0.02	0.02	0.01	0.01	0.01
Al_2O_3	18.53	18.54	18.49	18.51	18.14
FeO	0.08	0.07	0.07	0.08	0.08
MnO	0.03	0.00	0.00	0.00	0.00
MgO	0.01	0.00	0.01	0.00	0.00
CaO	0.08	0.04	0.07	0.05	0.04
Na_2O	1.94	1.61	2.14	1.59	0.94
K_2O	13.49	13.73	13.14	13.81	15.53
Total	97.79	98.25	98.13	98.27	99.57
Si	11.928	11.973	11.968	11.972	12.015
Ti	0.002	0.002	0.001	0.002	0.001
Al	4.094	4.071	4.061	4.067	3.962
Fe	0.013	0.010	0.010	0.013	0.013
Mn	0.005	0.000	0.000	0.000	0.000
Mg	0.002	0.001	0.001	0.000	0.000
Ca	0.016	0.009	0.014	0.009	0.008
Na	0.704	0.583	0.771	0.576	0.336
K	3.225	3.264	3.122	3.284	3.671
Total	19.988	19.913	19.948	19.923	20.006
Ab	17.76	15.07	19.68	14.83	8.34
An	0.89	0.51	0.64	0.56	0.52
Or	81.35	84.41	79.67	84.61	91.14

(Table 10-4. continued)

specimen	87122502	90101909	90101909	90101909
grain	1	1	1	1
position	2	1	2	3
SiO_2	63.47	63.55	64.20	63.43
TiO_2	0.08	0.04	0.01	0.04
Al_2O_3	18.41	18.43	18.41	17.94
FeO	0.09	0.01	0.07	0.21
MnO	0.08	0.05	0.00	0.00
MgO	0.01	0.01	0.01	0.00
CaO	0.07	0.10	0.10	0.03
Na_2O	0.99	1.94	2.02	0.75
K_2O	14.85	13.64	13.91	15.94
Total	98.04	97.77	98.73	98.34
Si	11.930	11.928	11.947	11.959
Ti	0.011	0.006	0.001	0.006
Al	4.077	4.076	4.037	3.986
Fe	0.014	0.002	0.011	0.033
Mn	0.013	0.008	0.000	0.000
Mg	0.002	0.003	0.003	0.000
Ca	0.014	0.020	0.020	0.006
Na	0.361	0.706	0.728	0.274
K	3.559	3.265	3.301	3.832
Total	19.981	20.013	20.048	20.096
Ab	9.10	17.63	17.93	6.61
An	1.08	0.50	0.49	0.15
Or	89.82	81.56	81.24	92.45

Table 10–5. Chemical compositions of K–feldspar from aplite.

specimen	90101906B	90101906B	90101906B	90101906B	90101906B
grain	1	1	1	2	2
position	1	2	3	1	2
SiO_2	64.54	64.00	64.31	64.93	64.58
TiO_2	0.00	0.00	0.01	0.00	0.02
Al_2O_3	18.49	18.28	18.41	18.69	18.70
FeO	0.05	0.08	0.13	0.00	0.00
MnO	0.01	0.06	0.03	0.00	0.00
MgO	0.00	0.01	0.01	0.00	0.01
CaO	0.05	0.06	0.08	0.11	0.13
Na_2O	1.63	1.12	1.66	2.68	2.54
K_2O	15.25	16.18	15.15	13.51	13.54
Total	100.01	99.78	99.79	99.92	99.52
Si	11.927	11.914	11.917	11.926	11.912
Ti	0.000	0.000	0.002	0.000	0.003
Al	4.027	4.010	4.021	4.045	4.065
Fe	0.008	0.012	0.020	0.000	0.000
Mn	0.001	0.009	0.005	0.000	0.000
Mg	0.000	0.002	0.003	0.001	0.002
Ca	0.010	0.012	0.015	0.021	0.025
Na	0.582	0.405	0.596	0.953	0.906
K	3.593	3.840	3.580	3.165	3.185
Total	20.147	20.203	20.159	20.111	20.098
Ab	13.88	9.46	14.13	23.02	22.01
An	0.44	0.79	1.02	0.54	0.66
Or	85.68	89.75	84.84	76.44	77.33

Table 11. Crystallization temperature of pyroxenes deduced from two pyroxene geothermometer after Wells(1977).

sample No.	temperature
86081005	
	1015 (℃)
	1006
	1167
	1013
	997
	1002
	1162
	1101
	995
	1162
(average)	1053
86121702	
core	850
	788
rim	824
	782
86121705	
core	977
rim	850

Table 12. Observation number of fluid inclusion planes and orientation direction of the first, the second and the third orders.

loc. No.	specimem No.	number of the poles	order of concentration		
			1st	2nd	3rd
1	90082508	399	N40E80E	N40W90	N15W90
2	90082506	322	horizon	N35W70N	N10E80W
3	90082501	449	N85E90	N65E90S	N70W80N
4	90082511	957	N45E90	N45W65N	
5	90082401	545	N85E80N	N35E80N	
6	90101904	1138	N60E90	N45W35W	
7	90101901	553	N30W80E	N20E80W	
8	90101903	429	N75E85S	N20W85W	
9	90082403	344	N80W80S		
10	90082408	482	N70E90	EW 80N	
11	90082404	572	N10W10E	N80E85S	N40E80E
12	90082513	475	N75E90	N15W90	N35E90
13	90082512	624	N65W75S	N35E55E	N85W90
14	90050510	335	N45E90	N15W90	N25E50E
15	90050509	388	N45E90	N55W90	
16	90050508	238	N80W90	N10E50E	
17	90102707	123	N20E55E	N75E80S	
18	90102209	511	N 5W80E	N35E85N	EW 20N
19	90102210	278	N70W60S	NS 60E	
20	90102408	446	N55E70S	NS 80W	N25W65W
21	9005057B	161	N35E75N	N15W70W	N30W80E
22	90050501	60	EW 90	N70E60N	
23	90050503	235	N30W90	N20E70W	
24	90050504	362	N45E85S	N30W70W	N65W85N
25	90102212	194	N75E85S	NS 65E	horizon
26	90102222	382	N55E75N	N20W85W	
27	90050505	366	N40W70N	N20E20E	
28	9005055A	227	NS 90	EW 75S	
29	90043002	276	N60E50N	N20W85W	N10W40W
30	90043003	38	N45E70E	N45W90	
31	90043006	71	N65E70E		
32	90102405	96	N75E80N	N10W70E	
33	90102401	252	N45E80N	N20E20W	
34	90082002	149	N35E55S	N20E30E	N30W40W
35	90101909	722	N 5W90	N50E85S	N75E90

Table 13. Grain contact ratios for quartz(Q), K-feldspar(Kf), plagioclase(PL) and mafic minerals(M) in the granodiorite.
For locality numbers see Fig. 57. H-Gr:specimen from medium-grained granite near Mt.Nabe.

2 : 90082506 (B-5-H)

	Q	K F	P L	M
Q	0.18	2.65	0.47	2.36
K F	1.98	0.21	0.45	1.89
P L	0.96	1.23	0.68	2.46
M	1.00	1.08	0.51	4.01
MODAL	35.00	24.60	35.10	5.10

4 : 90082511 (B-6-H)

	Q	K F	P L	M
Q	0.35	2.23	0.81	1.92
K F	1.81	0.39	0.49	1.40
P L	1.41	1.06	0.51	1.53
M	1.09	0.98	0.50	2.95
MODAL	33.70	17.30	39.80	9.00

13 : 90082512 (B-4-H)

	Q	K F	P L	M
Q	0.46	2.16	0.86	1.70
K F	1.57	0.45	0.52	2.12
P L	1.16	0.96	0.69	1.94
M	0.73	1.25	0.62	3.21
MODAL	31.60	14.00	44.20	10.00

15 : 90050509

	Q	K F	P L	M
Q	0.28	2.08	0.83	2.15
K F	1.27	0.23	0.88	1.83
P L	1.02	1.78	0.64	1.40
M	1.14	1.59	0.60	1.51
MODAL	29.00	14.60	45.10	11.10

19 : 90102210 (C-1-1)

	Q	K F	P L	M
Q	0.23	3.46	0.66	1.59
K F	2.20	0.28	0.46	1.28
P L	1.26	1.37	0.65	1.77
M	1.07	1.35	0.63	3.33
MODAL	30.50	15.20	49.30	4.80

20 : 90102408 (C-2-1)

	Q	K F	P L	M
Q	0.28	1.05	1.52	1.53
K F	1.82	0.24	0.86	0.25
P L	1.70	0.56	0.42	1.65
M	1.20	0.12	1.16	1.62
MODAL	34.00	20.60	35.80	9.40

(Table 13 continued)

2 1 : 9005057B

	Q	K F	P L	M
Q	0.31	3.83	0.47	1.55
K F	2.30	0.46	0.32	1.37
P L	1.10	1.23	0.58	2.82
M	0.80	1.19	0.62	3.80
MODAL	29.40	14.70	48.40	7.60

2 4 : 90050504

	Q	K F	P L	M
Q	0.20	2.28	0.76	1.35
K F	2.17	0.35	0.47	0.86
P L	1.47	0.96	0.55	1.55
M	0.99	0.66	0.59	4.80
MODAL	31.30	24.80	37.40	6.40

2 5 : 90102212(C-3-1)

	Q	K F	P L	M
Q	0.31	1.83	1.10	2.13
K F	1.15	0.53	0.86	2.51
P L	0.87	1.09	0.80	2.54
M	0.61	1.15	0.92	3.52
MODAL	42.30	24.20	27.60	5.90

3 5 : 90101909

	Q	K F	P L	M
Q	0.35	2.28	0.65	2.68
K F	2.10	0.64	0.44	1.55
P L	1.48	1.09	0.61	1.67
M	1.66	1.04	0.45	2.41
MODAL	28.10	21.20	45.90	4.40

H − G r (87122502)

	Q	K F	P L	M
Q	0.38	2.45	0.65	1.62
K F	1.53	0.69	0.55	1.56
P L	0.99	1.36	0.64	1.96
M	0.86	1.33	0.68	2.90
MODAL	37.81	22.43	34.97	4.79

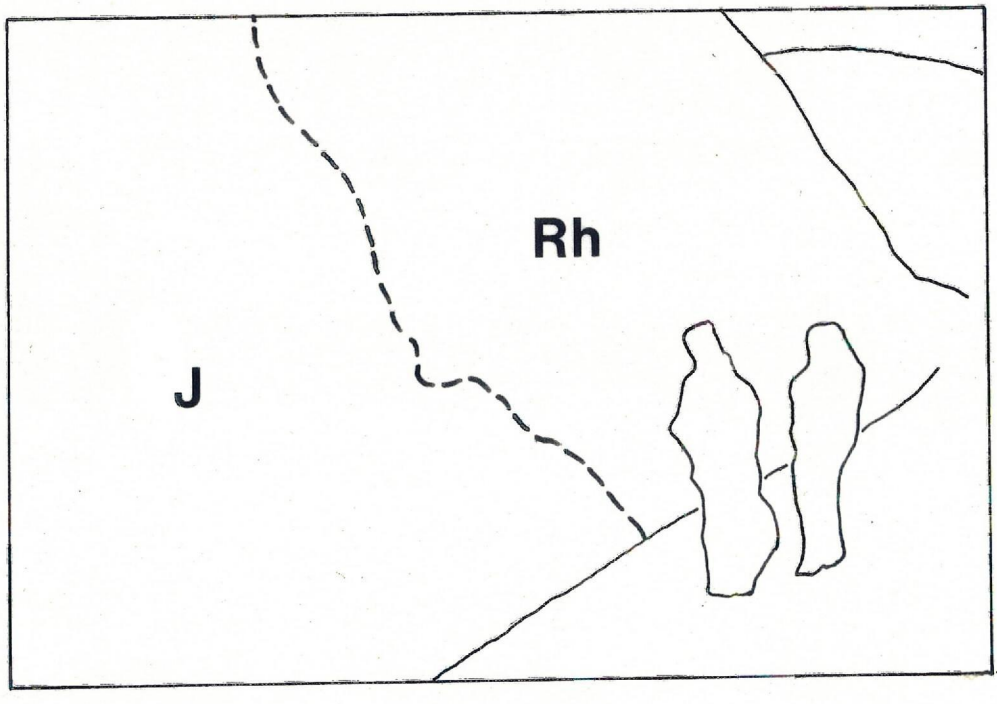

Plate 1. Contact between the rhyolitic rock (Rh) and mudstone of the Jurassic accretionary complex (J) to the west of Tabuki, Togouchi.
Broken line in the sketch shows the boundary between these rocks.

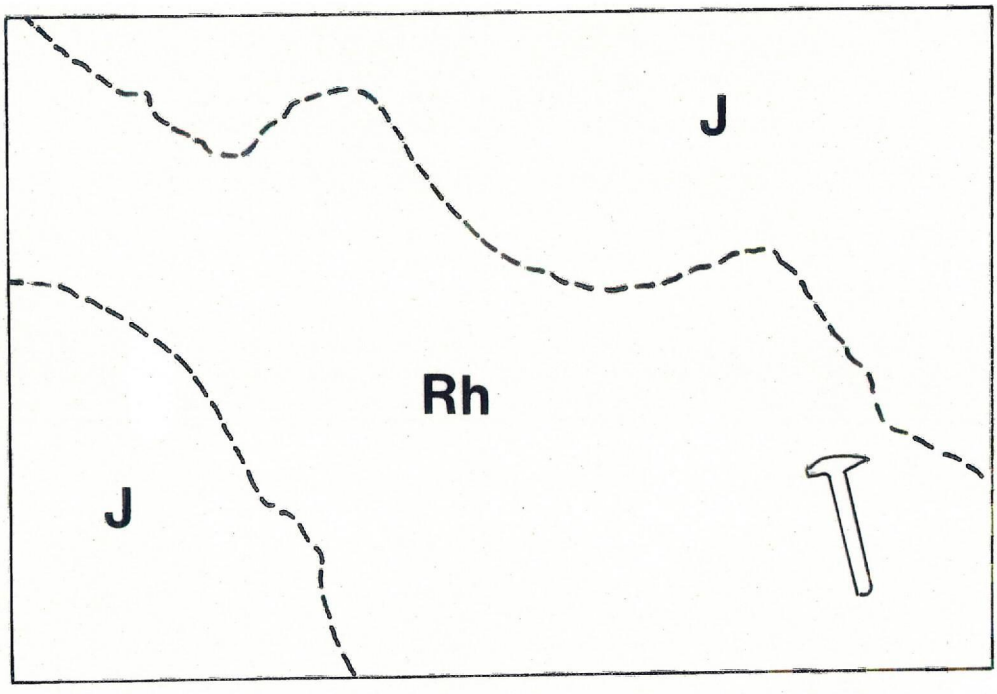

Plate 2. A dike of rhyolitic rock (Rh) obliquely intruded into the Jurassic accretionary complex (J). Note that the rhyolitic rock contains various sized and angular rock fragments from the Jurassic accretionary complex, to the north of Sakahara, Tsutsuga.

Plate 3. Fine-grained granite exposed on the river bed of the River Shiwagi on the north of Togouchi Hongou, Togouchi.

Plate 4. Subhorizontal dikes of the fine-grained granite intruded into the granodiorite, near Togouchi Hongou, Togouchi.

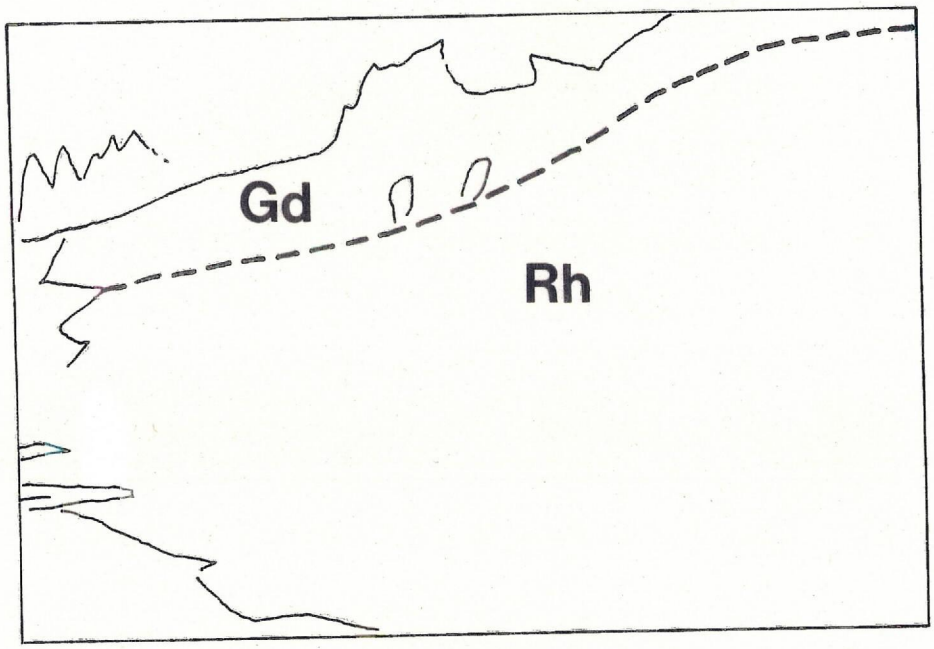

Plate 5. The granodiorite subhorizontally underlain by the rhyolitic rocks, in Kajinoki, Togouchi. Broken line in the sketch shows the boundary between the granodiorite (Gd) and the rhyolitic rocks (Rh).

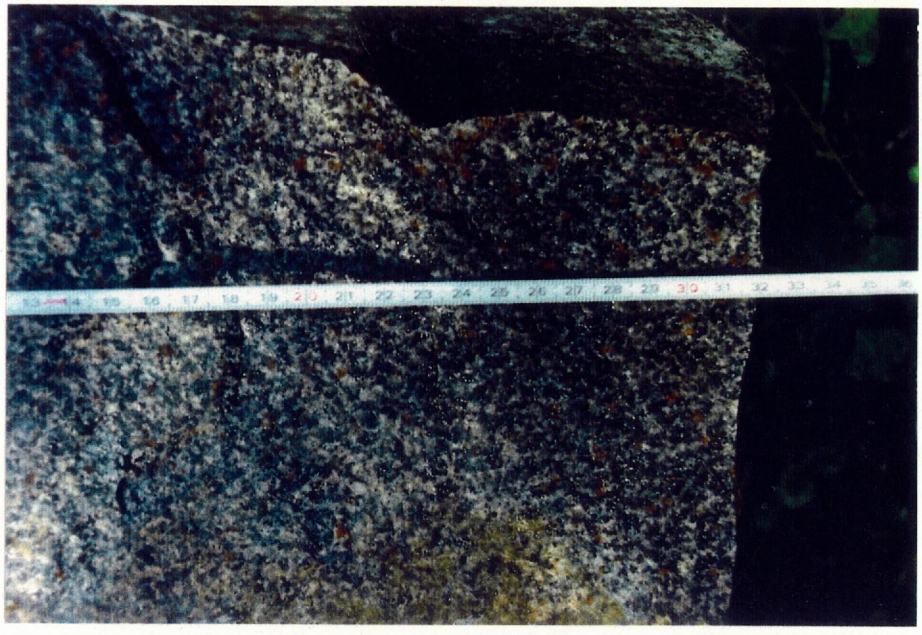

Plate 6. Field occurrence of the tonalite, near Dani, Yoshiwa.

Plate 7. Photomicrographs of the tonalite, near Dani, Yoshiwa.

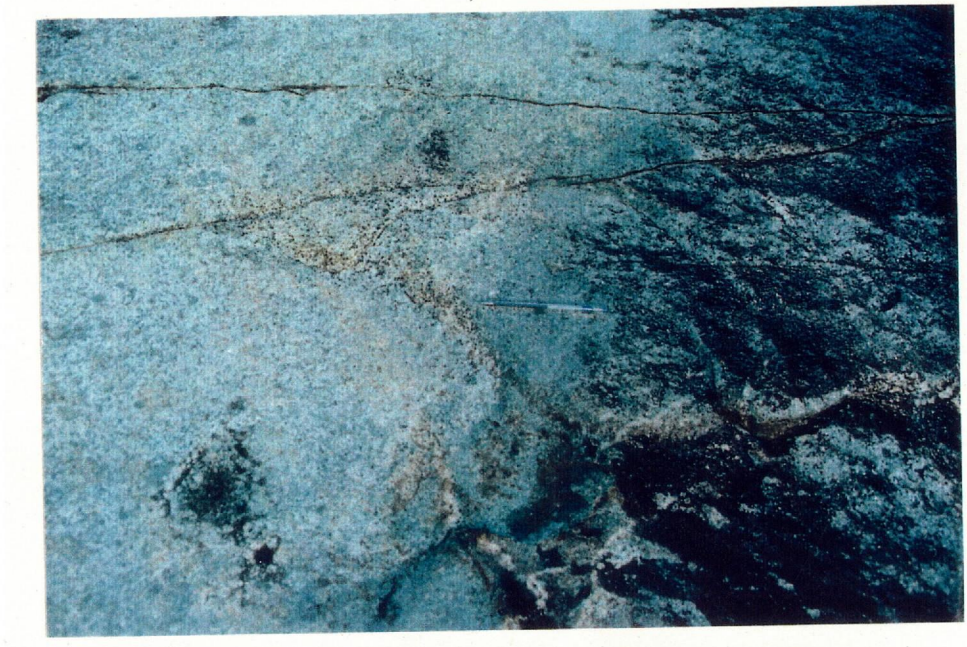

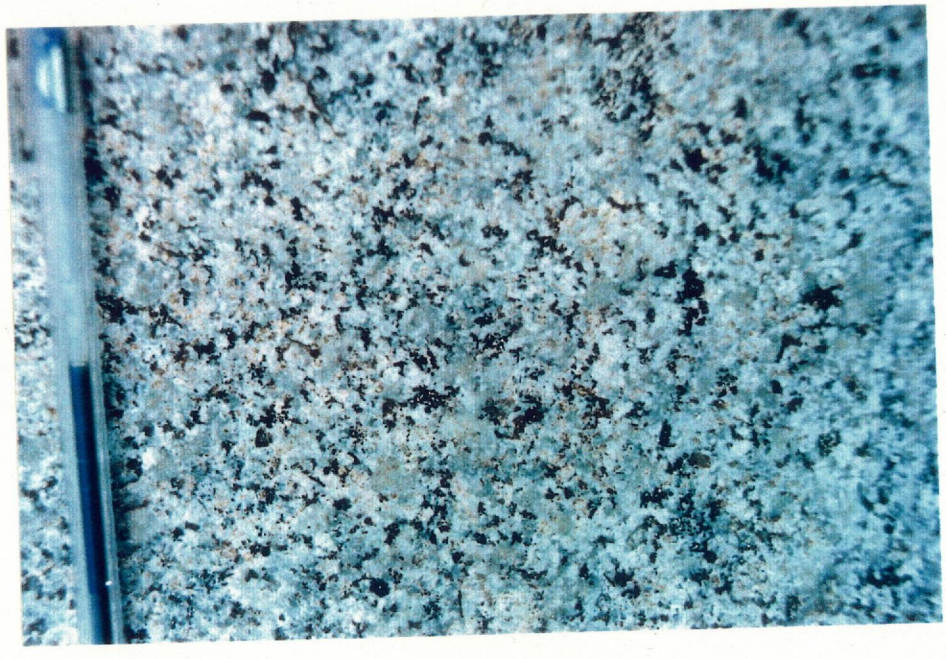

Plate 8. Field occurrence (upper) and hand specimen (lower) of the lower lithofacies of the granodiorite, near Togouchi Hongo, Togouchi.

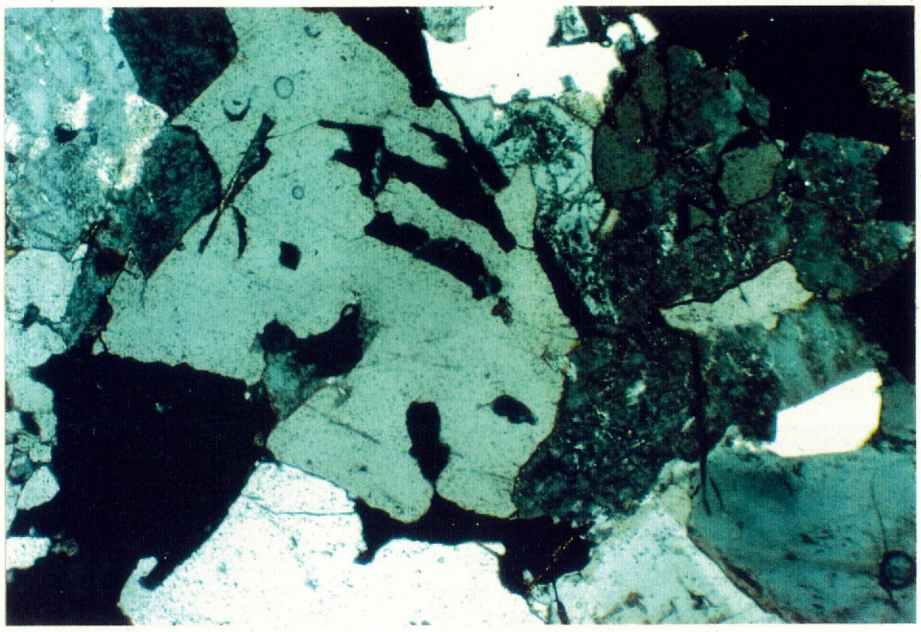

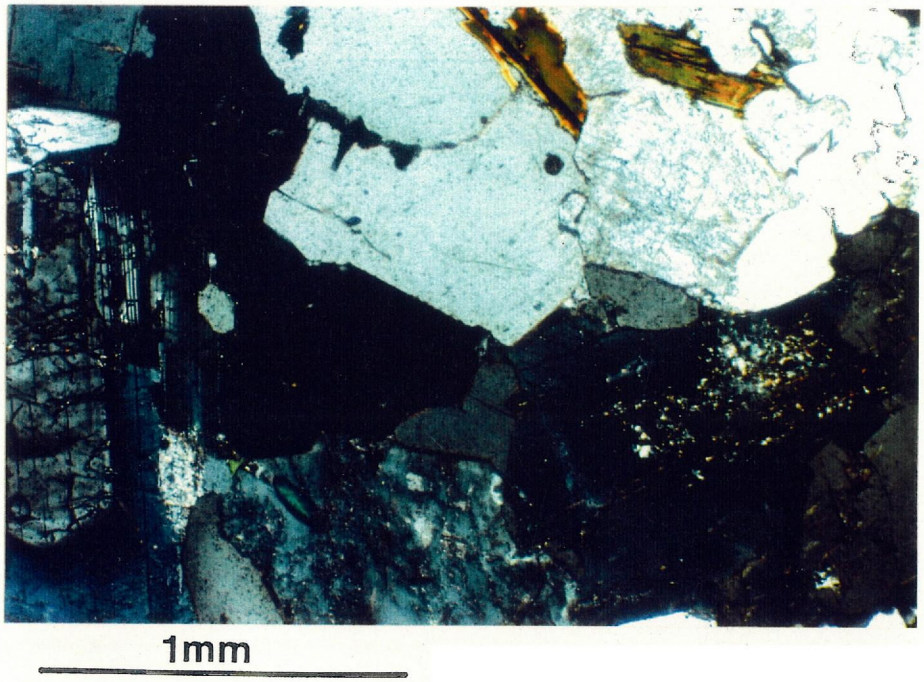

Plate 9. Photomicrographs of the lower lithofacies of the granodiorite, near Togouchi Hongou, Togouchi.

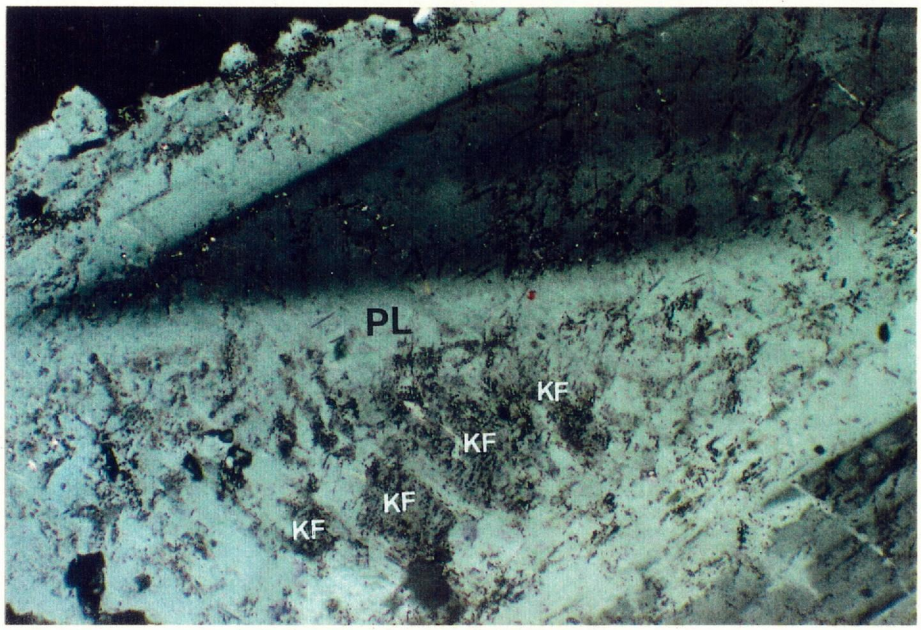

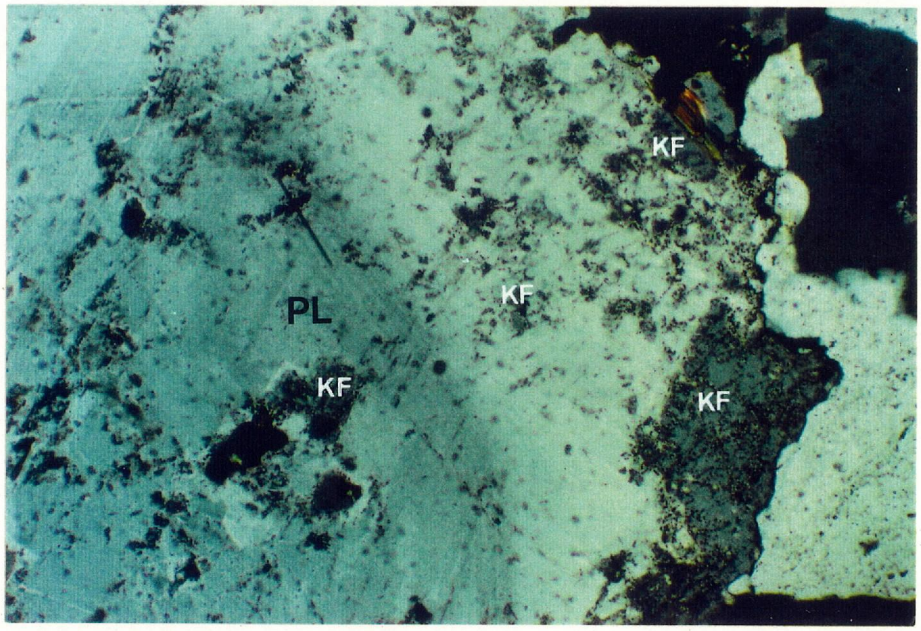

Plate 10. Photomicrographs of K-feldspar (KF) in plagioclase (PL) from the lower lithofacies of the granodiorite, near Togouchi Hongou, Togouchi.

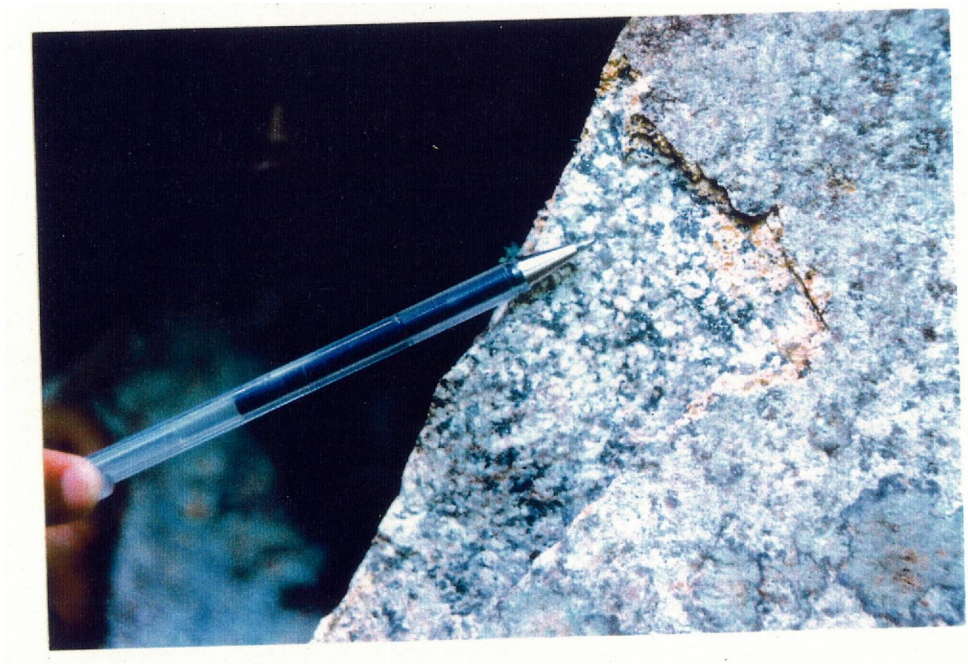

Plate 11. Field occurrence (upper) and hand specimen (lower) of the middle lithofacies of the granodiorite, on the northwestern slope of Mt.Ichima, Togouchi.

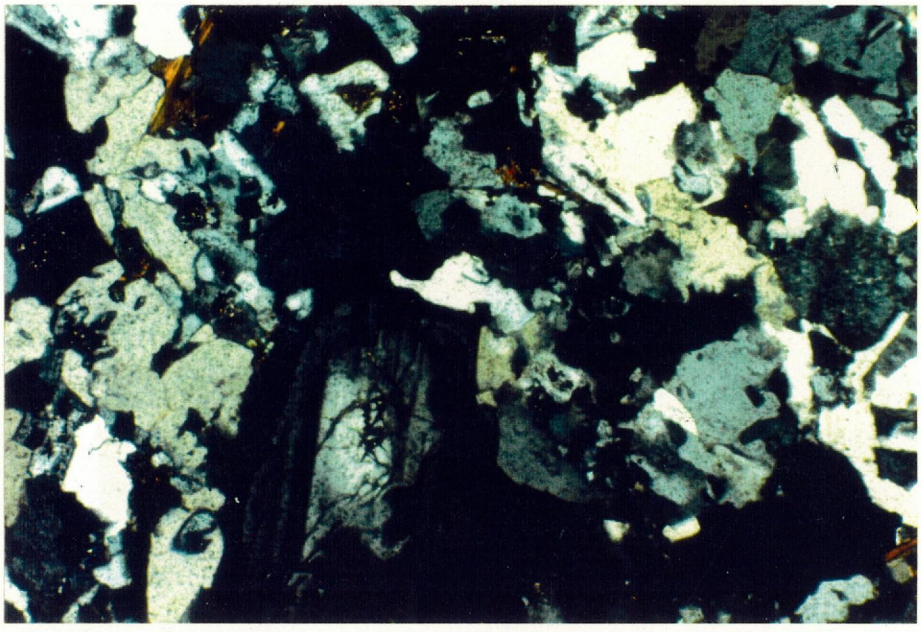

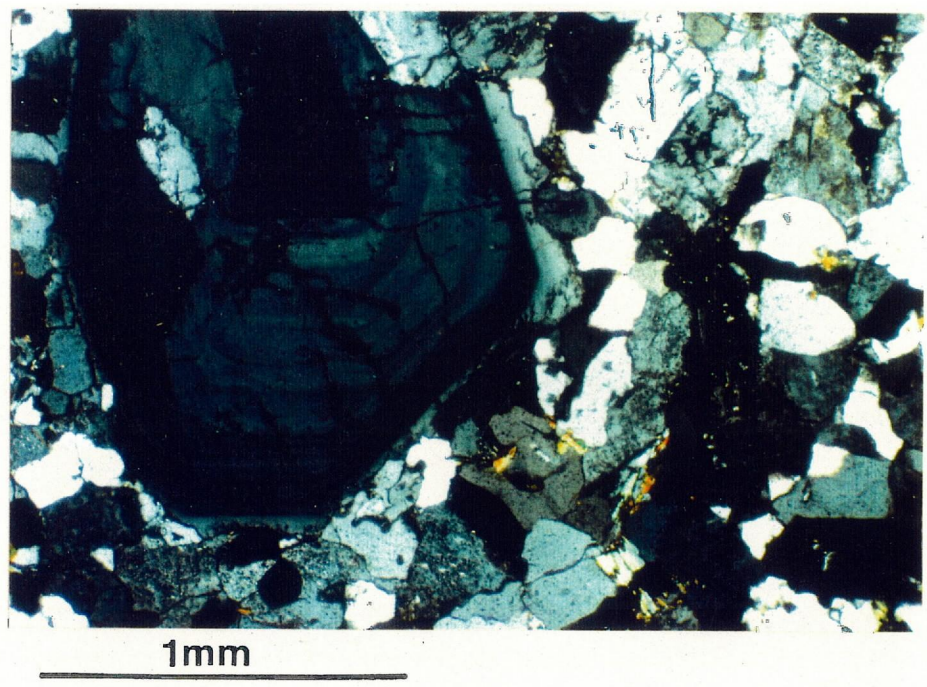

Plate 12. Photomicrographs of the middle lithofacies of the granodiorite, on the northwestern slope of Mt.Ichima, Togouchi.

Plate 13. Field occurrence (upper) and hand specimen (lower) of the upper lithofacies of the granodiorite, on the northwestern slope of Mt.Ichima, Togouchi.

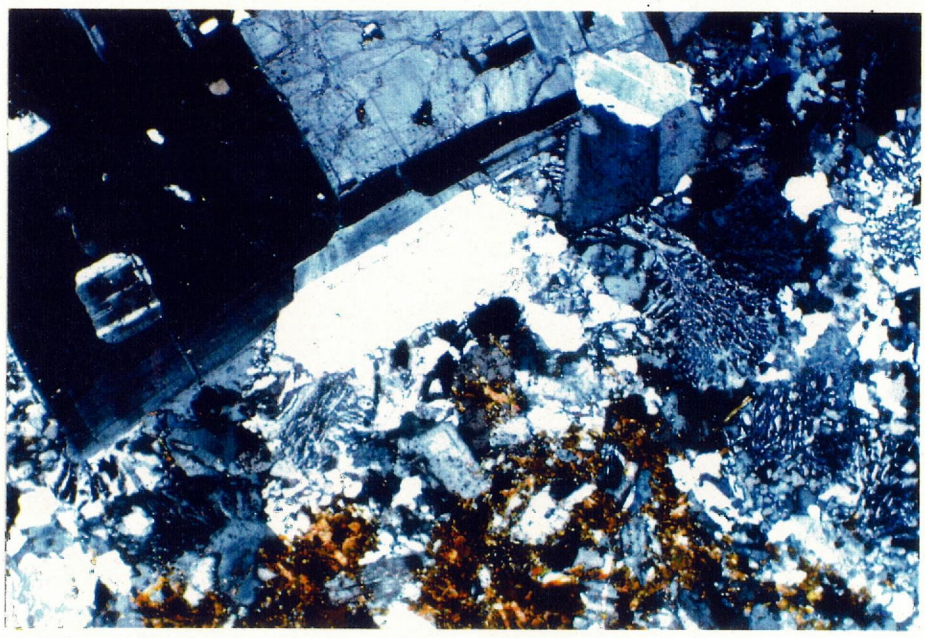

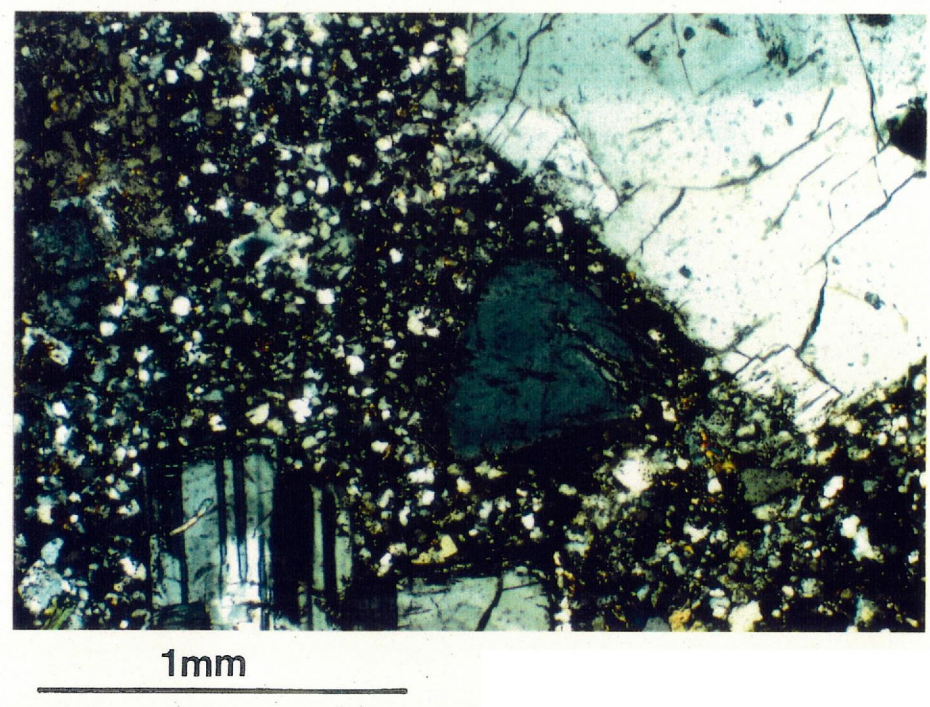

Plate 14. Photomicrographs of the upper lithofacies of the granodiorite on the northwestern slope of Mt.Ichima (upper) and near Nasu (lower), Togouchi.

Plate 15. Field occurrence (upper) and hand specimen (lower) of the dark inclusion in the lower lithofacies of granodiorite, near Togouchi Hongou, Togouchi.

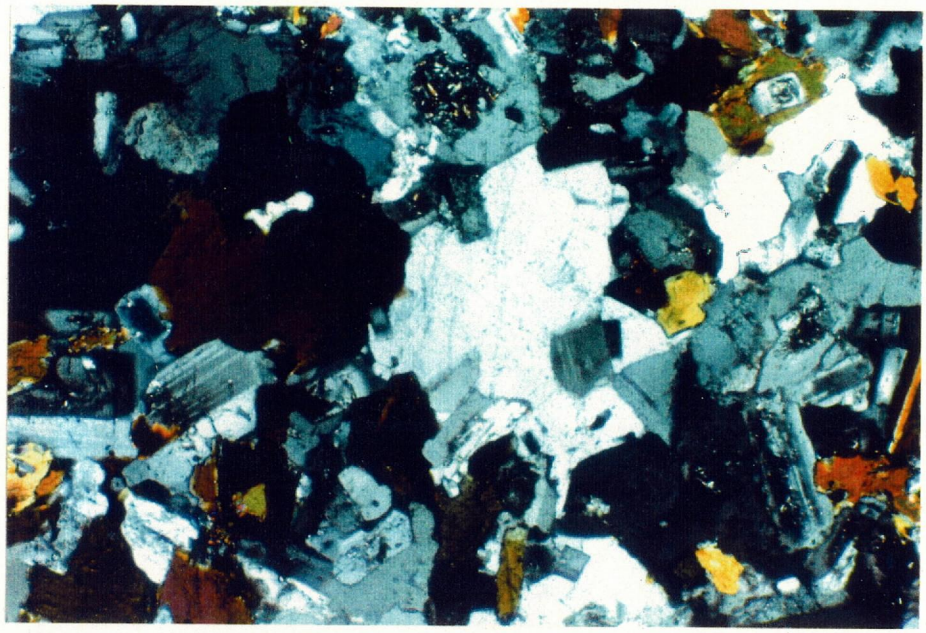

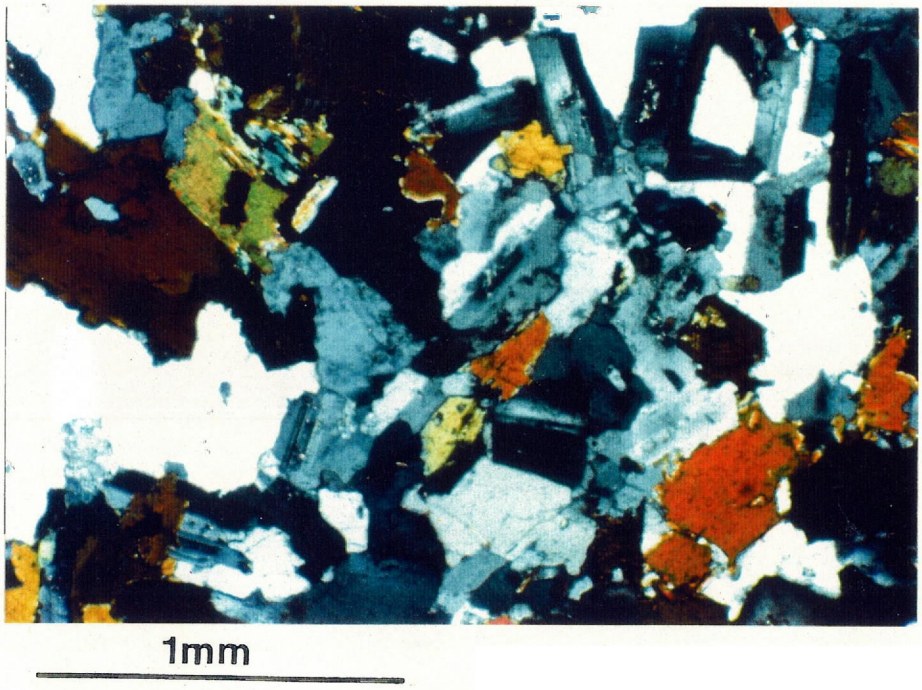

Plate 16. Photomicrographs of the dark inclusion in the lower lithofacies of the granodiorite, near Togouchi Hongou, Togouchi.

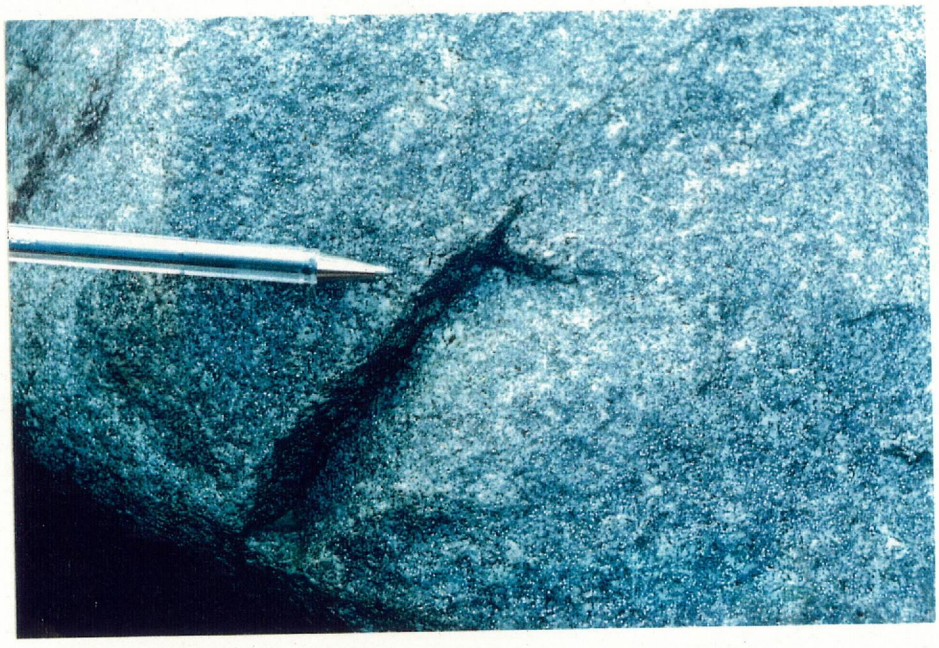

Plate 17. Field occurrence (upper) and hand specimen (lower) of the dark inclusion in the middle lithofacies of the granodiorite in the northwestern slope of Mt.Ichima, Togouchi.

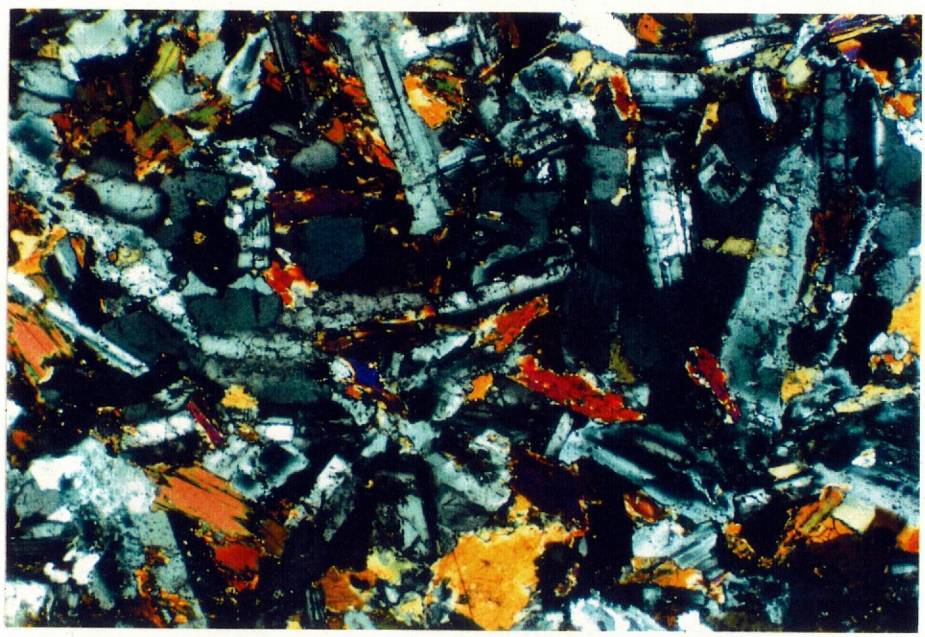

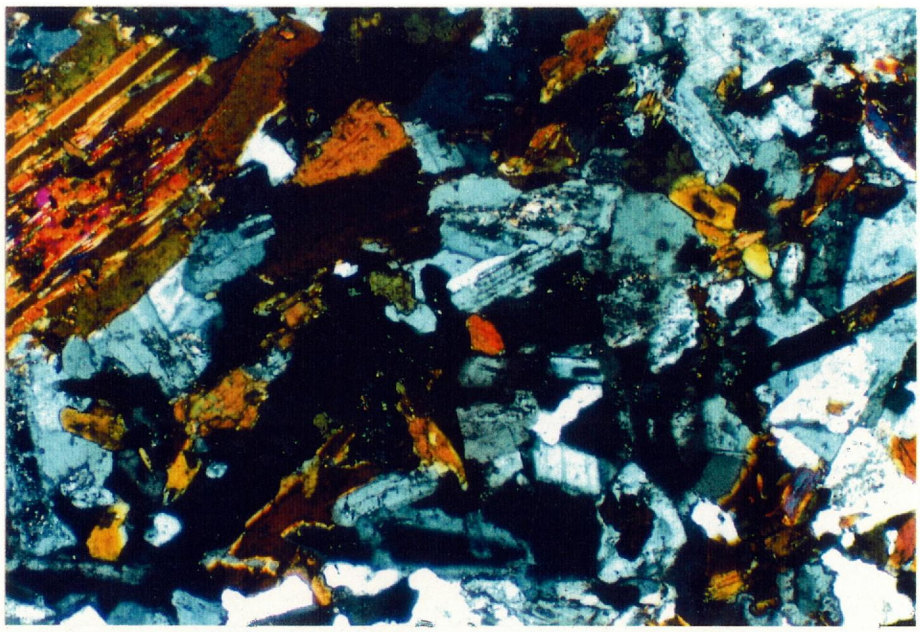

Plate 18. Photomicrographs of the dark inclusion in the middle lithofacies of granodiorite in the northwestern slope of Mt.Ichima, Togouchi.

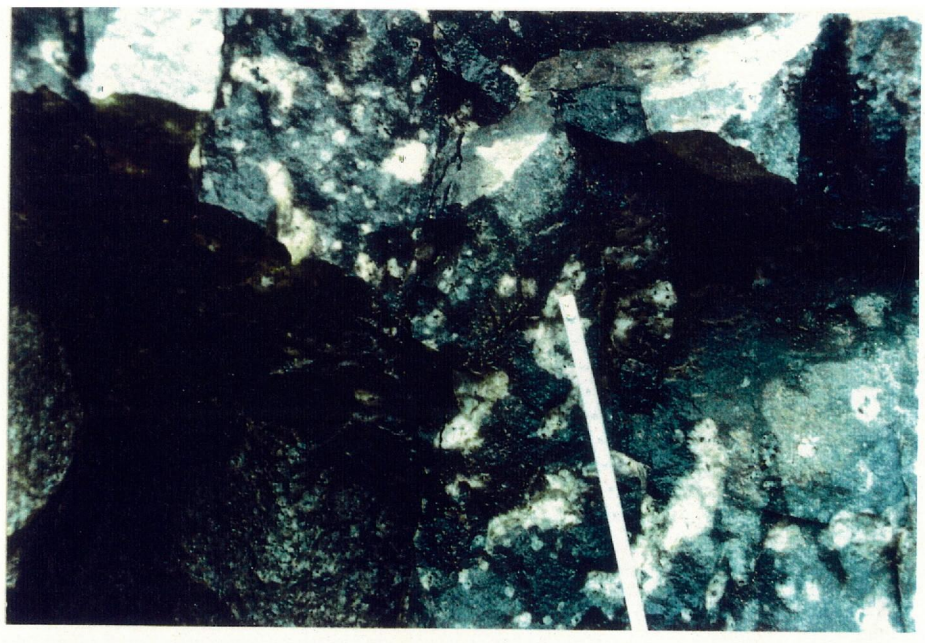

Plate 19. Field occurrence of leucocratic spheres in the dark inclusion in the northwestern slope of Mt.Ichima, Togouchi.

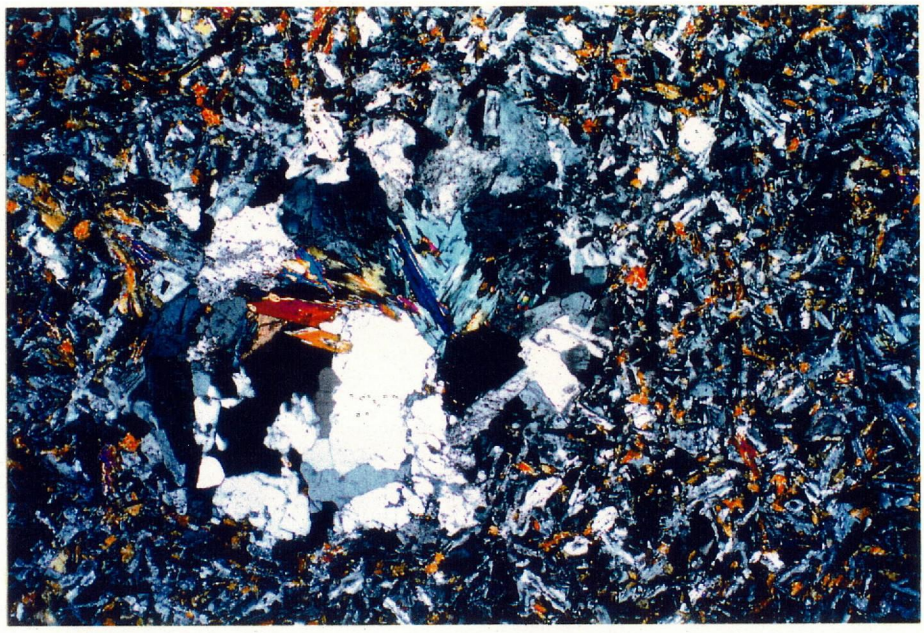

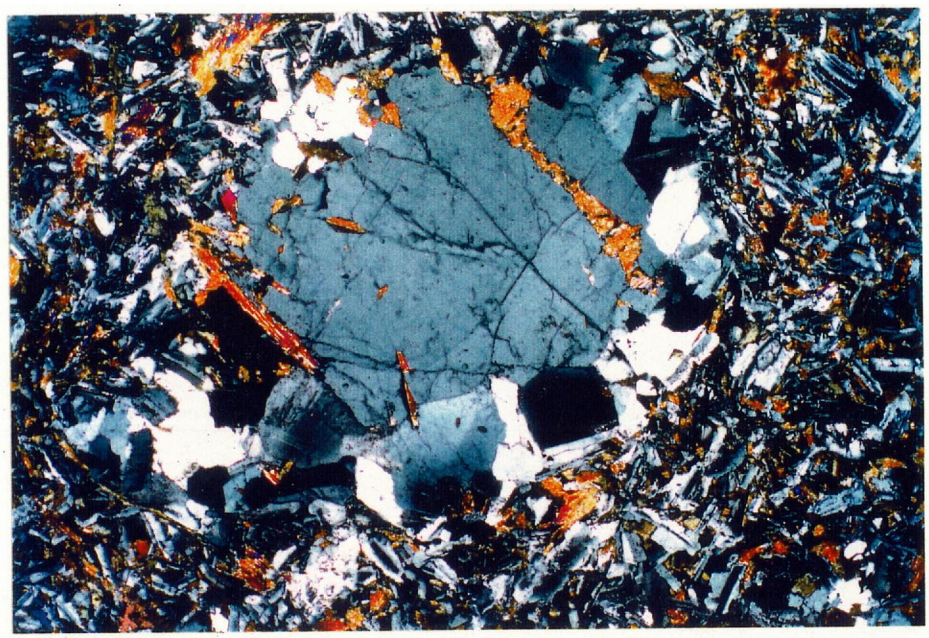

Plate 20. Photomicrographs of leucocratic spheres in the dark inclusion in the northwestern slope of Mt.Ichima, Togouchi.

Plate 21. Field occurrence (upper) and hand specimen (lower) of the dark inclusion in the upper lithofacies of the granodiorite, near Nasu, Togouchi.

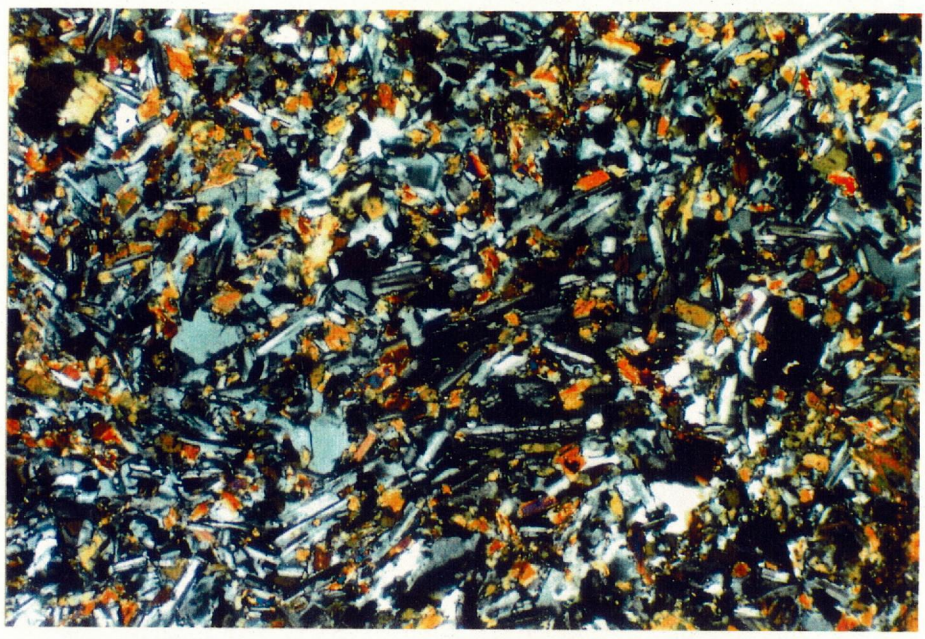

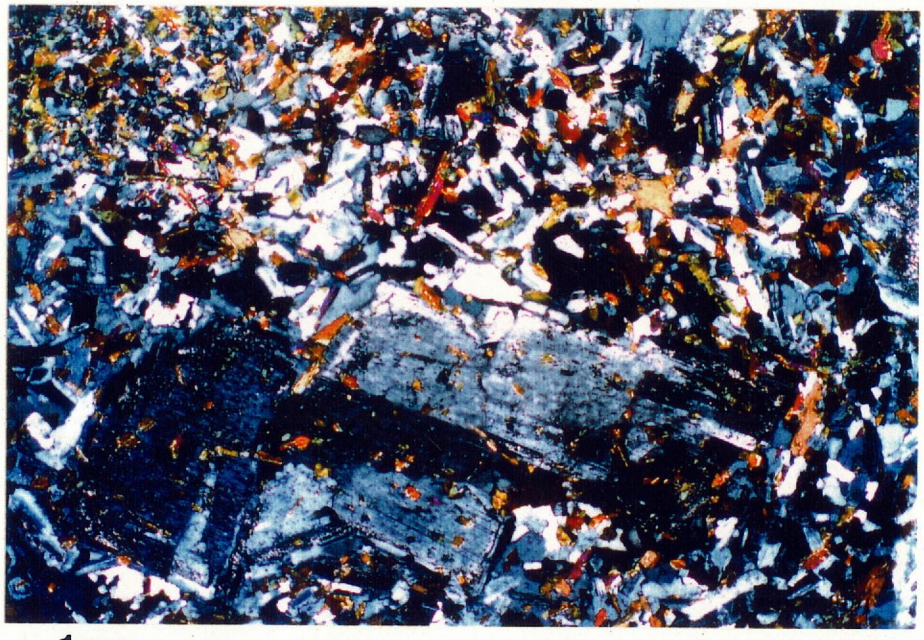

Plate 22. Photomicrographs of dark inclusion in the upper lithofacies of the granodiorite in the northwestern slope of Mt.Ichima, Togouchi.

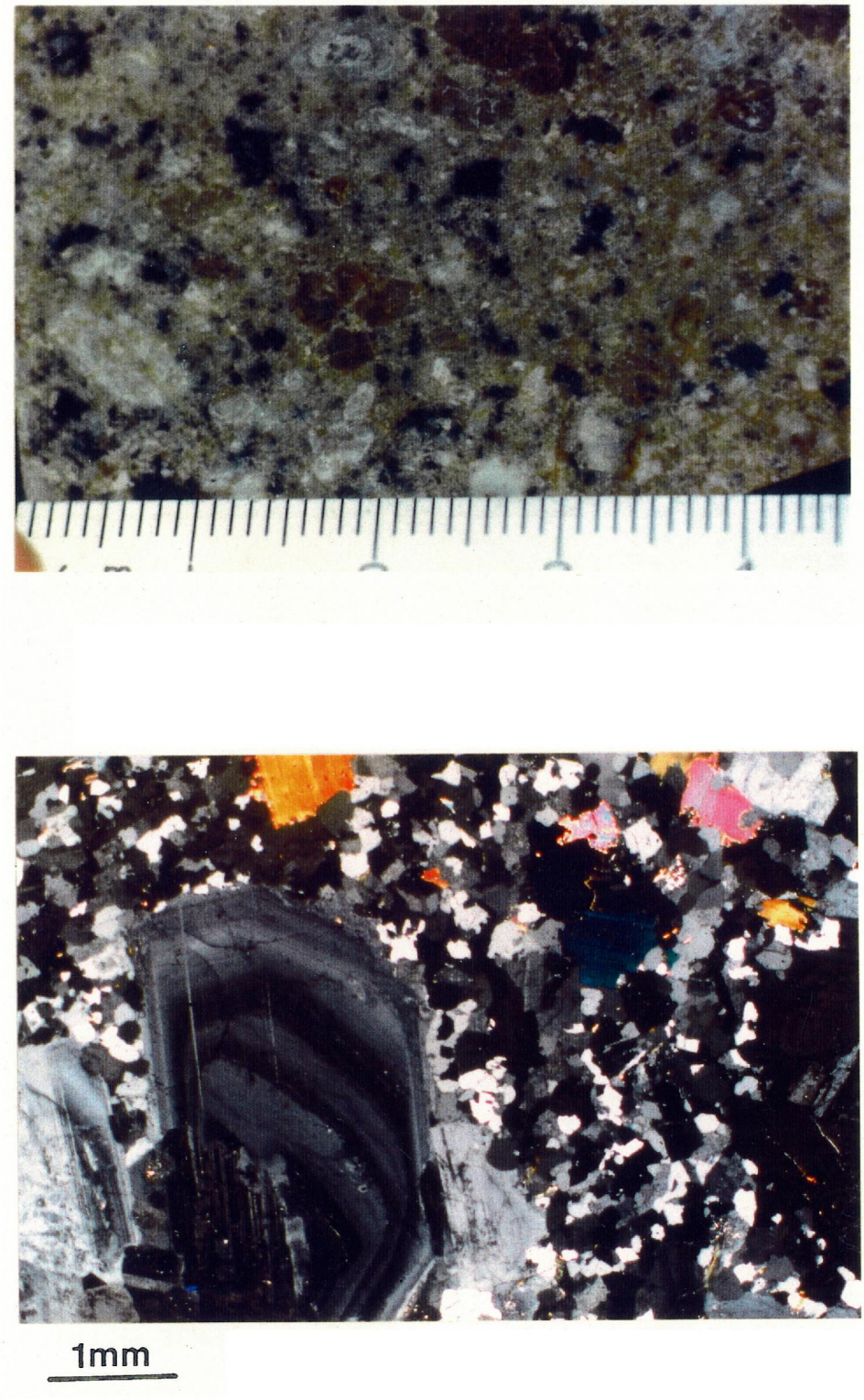

Plate 23. Hand specimen (upper) and photomicrograph (lower) of the porphyritic granite, more distinctive porphyritic type (P–type).

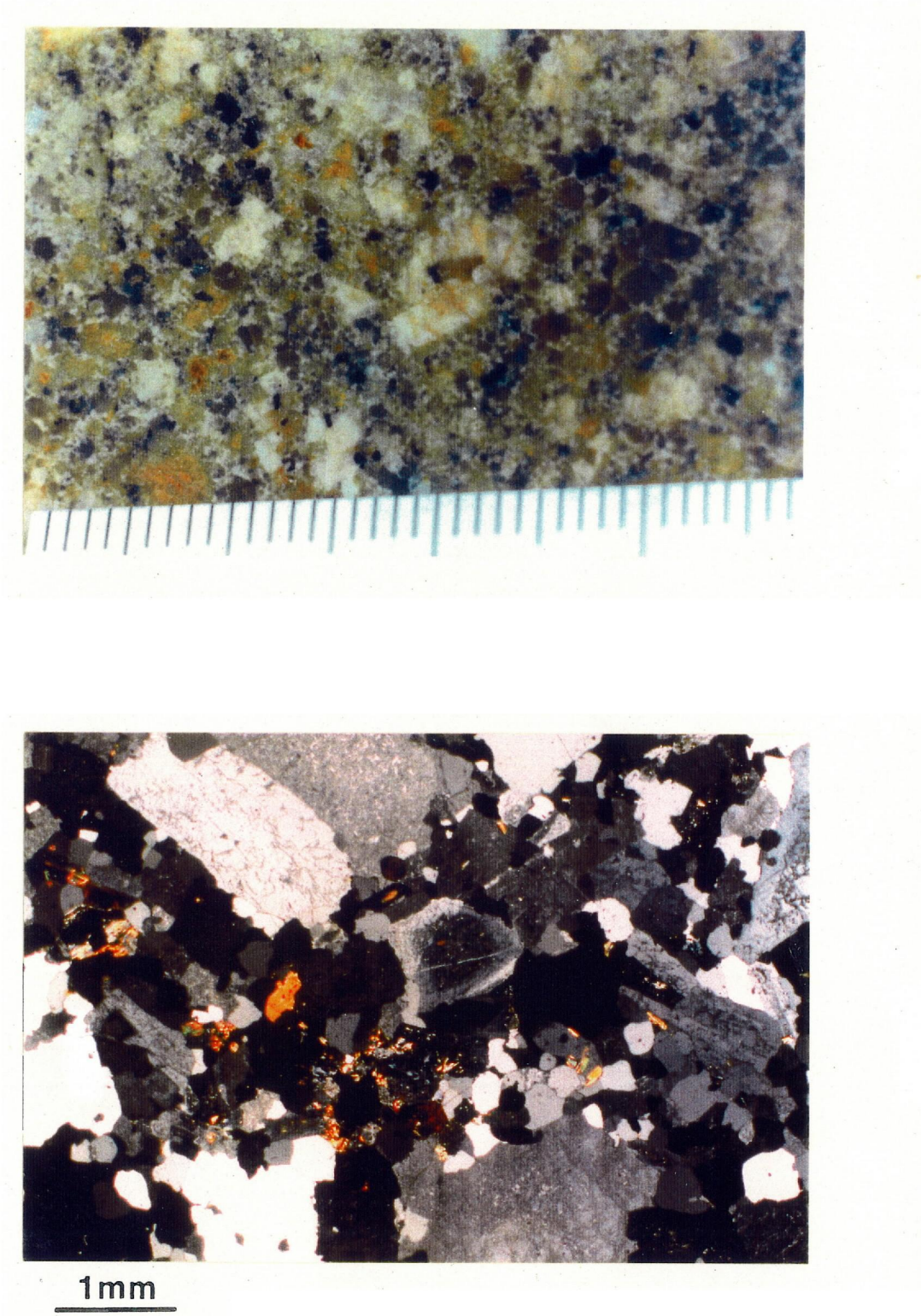

Plate 24. Hand specimen (upper) and photomicrograph (lower) of the porphyritic granite, less distinctive porphyritic type (E–type).

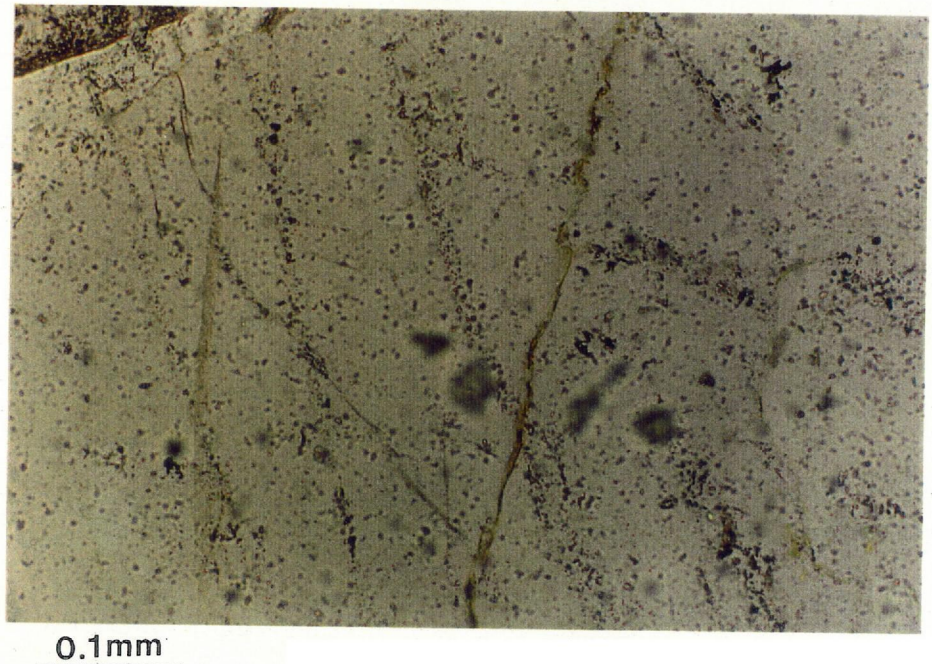

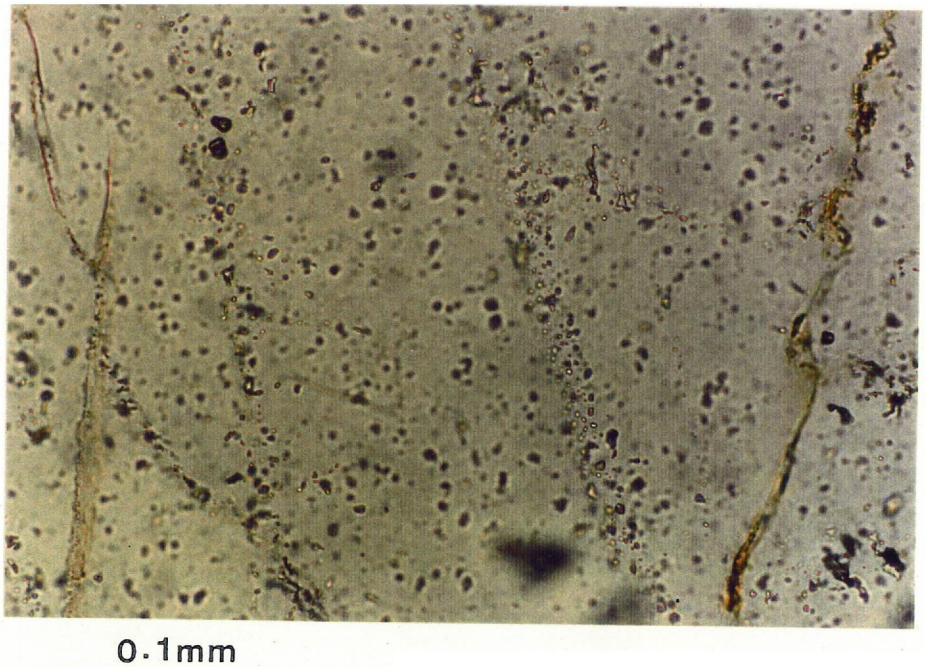

Plate 25. Photomicrographs of fluid inclusion in quartz in the granodiorite.

Plate 26. Subhorizontal dikes of fine-grained granite intruded into the Kuga Group in Hacchodani to the west of Otake.

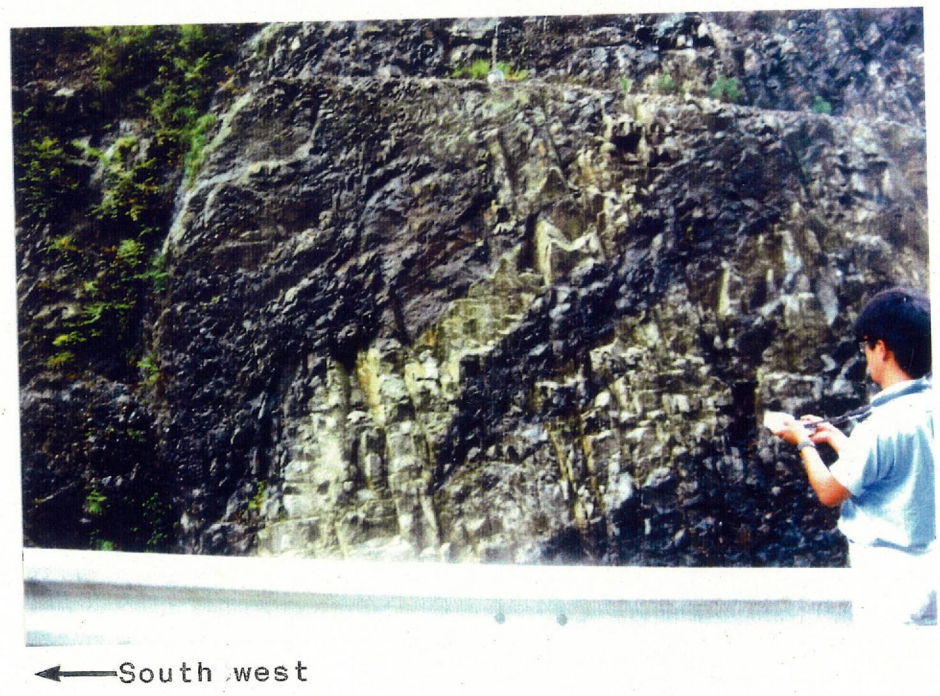

Plate 27. Dikes of fine-grained granite intruded into the Kuga Group in the south of Kake.